University of Alberta

Observations of Flow Distributions and River Breakup
in the Mackenzie Delta, NWT

by

Janelle Kristina Astrid Morley

A thesis submitted to the Faculty of Graduate Studies and Research
in partial fulfillment of the requirements for the degree of

Master of Science

in

Water Resources Engineering

Department of Civil and Environmental Engineering

Abstract

This study was part the Canadian International Polar Year (IPY) project entitled Study of Canadian Arctic River-delta Fluxes (IPY-SCARF), aimed at quantifying fluxes from the Mackenzie Delta channels towards the Beaufort Sea. The flow and water level data collected during the study period from 2006 to 2010 are presented. In addition, river breakup observations during each year of the study are shown, including oblique photos and satellite imagery that was used to document breakup progression. In support of the development of the Mackenzie Delta Hydrodynamic Model, a one-dimensional model was used to calibrate channel geometry and, in particular, channel bed slope for the seven primary channels of the Mackenzie Delta. The result and limitations of this modeling effort and suggestions for future data collection are presented.

Acknowledgments

The author would like to thank her supervisor, Dr. Faye Hicks, for all her help and guidance throughout this process and for her encouragement to pursue graduate studies. Thank you to Dr. Mark Loewen and Dr. Suzanne Kresta for being part of the oral examining committee.

The efforts of IPY-SCARF partners made this study possible. Thank you to Roger Piling, Randy Wedel and the field staff at the WSC for providing unpublished detailed records and collecting additional flow data to support this modeling effort. Thank you also to Phillip Marsh and Spyros Beltaos at Environment Canada for the cross-sections data collected. Thank you to Joost van der Sanden and Hugo Drouin from NRCan for processing satellite images, and collecting and processing ice thickness data. Breakup reports compiled by both Angus Pippy and the late Steve Solomon and the numerous oblique breakup photos provided by IPY-SCARF partners were extremely valuable. Thank you.

The support of both the Government of Canada's International Polar Year (IPY) program administered by Aboriginal Affairs and Northern Development Canada (AANDC) and the Natural Sciences and Engineering Research Council of Canada (NSERC) is gratefully acknowledged. Their funding is greatly appreciated. In addition, thank you to Aurora Research Institute for their support.

The author would like to thank the members of the river ice group at the University of Alberta, including Robyn Andrishak, Mike Brayall, Agata Hall, Vince MacFarlane, Josh Maxwell, Nadia Kovachis, David Watson, Liming Zhao and, in particular, Jennifer Nafziger. Thank you for all your assistance with this project and for your great company and organization during fieldwork.

For all their love and support, the author would like to especially like to thank her close friends, her family and her fiancé, Ben. Your support was so valuable. Without each of you this was not possible.

Table of Contents

List of Tables

List of Figures

List of Symbols

α_1, α_2	velocity weighting coefficient
A	flow area of cross-section (m^2)
C	expansion or contraction loss coefficient
g	gravitational acceleration (m/s^2)
h_e	energy head loss (m)
L	discharge weighted reach length (m)
n	Manning's roughness coefficient
Q_a	Assumed flow (m^3/s)
Q_c	Calculated flow (m^3/s)
Q_m	Manually measured flow (m^3/s)
Q_r	Average of hourly reported flows derived from the rating curve over a period at a specified station (m^3/s)
$Q_{r\ (range)}$	Range of hourly reported flows derived from the rating curve over a specified period (m^3/s)
Q_{ri}	Average of hourly reported inflow to the Delta over a specified period (m^3/s)
$Q_{ri(range)}$	Range of hourly inflow to the Delta over a specified period (m^3/s)
R	hydraulic radius for channel (m) (A/wetted perimeter)
$\bar{S}_f$	representative friction slope between two sections
V_1, V_2	average velocities (m^3/s) (total discharge/ total flow area)
Y_1, Y_2	depth of water at cross section (m)
Z_1, Z_2	elevation of the main channel inverts (m)

1.0 Introduction

The Mackenzie Delta is a rich area of Canada's north that is susceptible to and greatly affected by changes in river ice breakup and sea level increase (Lesack and Marsh, 2007). Each year, as a result of snowmelt runoff and ice jamming, spring breakup typically results in peak water levels. These peak water levels control the transfer of nutrients to lakes that are perched above normal channel water levels (Marsh and Hey, 1989). To address flooding susceptibility of the lakes and channels of the Mackenzie Delta due to changes in river ice, an understanding of the river ice regime, including ice jamming, must be developed. This study focuses on defining the available water level and flow data during both the open water and ice-affected season and synthesis of breakup data collected as part of this study. This data was then used in a hydraulic model to calibrate a geometry and slope for the important Delta channels.

1.1 Study Reach

The Mackenzie River basin, shown in Figure 1.1, stretches from northern Alberta in the south to the Beaufort Sea in the north and is bordered by the continental divide in the west and the Northwest Territories (NWT) border in the east (Woo and Thorne, 2003; Bélanger, 2010), such that it encompasses 20% of the land area of Canada (Mackay, 1963). It consists of 6 sub-basins: the Athabasca, the Peace, the Liard, the Peel, the Great Slave and the Mackenzie –Great Bear (Mackenzie River Basin Board (MRBB), 2010; Kerr and Miyagawa, 1996), which are each influenced to varying degrees by snowmelt runoff, glacier melt, regulation and storage effects of large lakes (Woo and Thorne, 2003).

The Mackenzie Delta, shown in Figure 1.2[1], is located at the mouth of the Mackenzie River basin. The Mackenzie Delta consists of nearly 50,000 inter-connected lakes (Emmerton *et al.*, 2007) and anastomosing channels (i.e. with vegetated islands greater than channels three times the channel width) (Mackay, 1963) which flow north though a permafrost influenced (Bigras, 1990) low gradient silt-sand plain (Lapointe, 1984; Nafziger *et al.*, 2009) towards the Beaufort Sea. As it covers an area of over 13,000 km^3 (Emmerton *et al.*, 2007; Fassnacht, 1997), it is the second largest arctic river Delta in the world after the Lena Delta in Russia. This study focuses on the channels of the Mackenzie Delta, including classification, water levels, flow patterns and modeling. Classification of the numerous Mackenzie Delta channels for the purposes of modeling and understanding flow is discussed in the following section.

1.1.1 Primary, Secondary and Tertiary Channels

As the Mackenzie Delta contains hundreds of channel reaches, the channels with the most hydraulic significance were identified. These channels were broken into three categories of hydraulic modeling importance: primary, secondary and tertiary. Figure 1.2 shows a map identifying the primary, secondary and tertiary channels, as well as the settlements located in the Delta. The channel network was selected based on the width, depth, known flow characteristics and location of

[1] The base image used in this figure is a Landsat 7 composite satellite image with a resolution of 15 m that was retrieved from Industry Tourism and Investment, NWT at http://geomatics.gov.nt.ca/ in 2009.

gauging stations operated by the WSC, as described by Nafziger *et al.* (2009).

The primary network includes seven channels: the Middle Channel/Kumak Channel (referred to as the Middle Channel), the East Channel, the Peel River/Peel Channel/West Channel (referred to as the West Channel), an unnamed channel that connects the West and Middle channels (referred to as the West-Middle Connection Channel), the Napoiak Channel, the Neklek Channel and the Reindeer Channel. Table 1.1 summarizes the seven primary channels, including their lengths and average widths. This table also defines the stationing for each channel which is used to reference locations along each of the channels and is denoted in terms of kilometers (km) downstream from one of the two inflow boundaries: the *Mackenzie River at Arctic Red River* (10LC014) or the *Peel River above Fort McPherson* (10MC002), which are shown in Figure 1.2. The gauging stations operated by the WSC are discussed further in Section 2.1.

The Middle Channel inflow station is at the *Mackenzie River at Arctic Red River* (10LC014) gauge, which is located at the community of Tsiigehtchic. The Middle Channel is the largest Delta channel, with numerous distributary channels that branch along its reach. The furthest upstream reach of the Middle Channel, up to Point Separation at *km* 25, is often referred to as the Mackenzie River, but is included as part of the Middle Channel in this study. North of Point Separation, the East Channel leaves the Middle Channel on the right bank (at *km* 48.2), and the Middle Channel receives flow from the West-Middle Channel at *km* 62.5. The "Turtle" is the adopted name used by members of this study group to describe the area between Point Separation and the West-Middle Connector Channel. The

Napoiak Channel branches from the Middle Channel on the left bank at *km* 140.8. The Neklek Channel and Reindeer Channels also distribute flow from the Middle Channel in the area informally referred to as the "Quadrapus" by members of this study group. The Middle Channel continues to distribute flow into secondary and tertiary channels, as it flows between Ellice and Richards Island towards the Beaufort Sea at *km* 293.5. At *km* 281, over ~90% of the flow in the Middle Channel flows into the Kumak Channel (Fassnacht, 1994; Traynor and Dallimore, 1992). As a result, in this study, the Kumak Channel is included as part of the Middle Channel, from *km* 281 to *km* 293.5. Overall, the Middle Channel ranges in width from 300 m to 3200 m, with an average width of 1225 m and is nearly two times (on average) wider than any of the other channels in Mackenzie Delta.

The East Channel branches from the Middle Channel on the right bank at *km* 48.2, just downstream of Point Separation at the Turtle. It meanders downstream past the community of Inuvik and continues along the east edge of the Delta. Flow from the Neklek Channel enters the East Channel at *km* 232.2. This flow runs north and splits into numerous channels at it approaches Kittigazuit Bay on the northeastern edge of the Delta, close to Tuktoyaktuk. The East Channel is significantly smaller in width than the Middle Channel, with an average with of ~550 m. Sections of the East and West Channels have a similar, regular, meander plan form (Lapointe, 1984).

The West Channel inflow boundary is the WSC station on the *Peel River above Fort McPherson* (10MC002). The upper reach of the West Channel from *km* 0 to *km* 64.8 is also referred as the Peel River. In this study, this reach is included as the upper reach of the West Channel. At *km* 64.8, the West-Middle Connector Channel splits from the West Channel and conveys water along the north side of the Turtle towards the Middle Channel. The West-Middle Connector Channel is 30 km in length and joins the Middle Channel at *km* 94.8. Downstream of *km* 64.8 along the West Channel is often named the Peel Channel, but is also referred to as the West Channel in this study. The West Channel continues to meander north from *km* 64.8 along the west side of the Delta, past the community of Aklavik and reaches the south shore of Shallow Bay at *km* 282. The West Channel is not as wide as the East and Middle Channels, with an average width of ~370 m.

The final three primary channels are the Napoiak, Neklek and Reindeer Channels, all of which branch from the Middle Channel. The Napoiak Channels stems from the Middle Channel at *km* 140.8 along the left bank. This channel extends northwest towards the south-east tip of Shallow Bay at *km* 204.3. It forms the shortest Delta flow route from *Mackenzie River at Arctic Red River (10LC014)* to the Beaufort Sea. This channel is similar in width to the West Channel with an average width of 444 m. At *km* 221 the Neklek Channel branches from the Middle Channel on the right bank. The water entering the Neklek Channel flows north-east towards the East Channel, where it joins the flow in East Channel at *km* 232.2 (along the East Channel). From this point, flow heads north towards Kittigazuit Bay. The final primary channel, the Reindeer Channel, is a distributary of the Middle Channel at *km* 223. The Reindeer Channel extends north-west from the Middle Channel, where it terminates along the north shore of

Shallow Bay at *km* 289 (see Figure 2.2). With the exception of the Middle Channel, it is the widest channel with an average with of 755 m.

The secondary channels were chosen as they carry significant flows especially at certain times of the year and contribute to significant flow changes in the primary channels. There are a total of 28 secondary channels. The important named secondary channels are shown in Figure 1.3. The tertiary class of channels was also identified based on relative importance. In comparison to the other channels, tertiary channels have small widths and depths and many are unnamed, with flow that is either unknown or small. Many of the secondary and tertiary channels, especially those with small widths, exhibit a tortuous meandering plan form (Lapointe, 1984). Altogether, 65 channel reaches are included in the classification network. There are also numerous additional flow paths in the Delta that are not identified as part of either the primary, secondary or tertiary network. These flow paths include channels with small widths and depths and flow travelling from lake to lake without forming a proper channel (Mackay, 1963; Emmerton *et al.*, 2007).

Table 1.1 Summary of the characteristics of the primary channels in the Mackenzie Delta.

Channel	**Abbrieviation**	**Length** (km)	**Average Width** (m)	**Origin***	**Upstream Boundary**		**Downstream Boundary**	
					Location	**Station**** (km)	**Location**	**Station**** (km)
Middle Channel	M	293.5	1225	1	Mackenzie River	0	Beaufort Sea	293.5
East Channel	E	236	556	1	Middle Channel	48.2	Kittigazut Bay	284.2
West Channel	W	282	369	2	Peel River	0	Shallow Bay	282
West-Middle Connection Channel	WM	30	712	2	West Channel	64.8	Middle Channel at station 62.5	94.8
Napoiak Channel	NP	63.5	444	1	Middle Channel	140.8	Shallow Bay	204.3
Neklek Channel	NL	12	396	1	Middle Channel	221	East Channel at station 232.2	233
Reindeer Channel	RD	66	755	1	Middle Channel	223	Shallow Bay	289

*Origin refers to the inflow boundary from which stationing is measured downstream

1 - *Mackenzie River at Arctic Red River* (10LC014)

2 - *Peel River above Fort McPherson* (10MC002)

**Station refers to distance along channel from origin

1.2 Previous Studies

The Delta, and the freshwater influenced coastline of the Beaufort Sea, are a haven for diverse populations of microorganisms, plants, fish, waterfowl, and wildlife (Carmack *et al.*, 2004). As lakes cover ~25% of the Delta area at low water times (Emmerton *et al.*, 2007), they are very significant to the overall Delta ecosystem (Marsh, 1986). The frequency with which these lakes are flooded is dependent on both the channel water levels and the sill height of the lakes (Marsh, 1986; Marsh and Hey, 1988), as permafrost limits subsurface drainage. Mackay (1963) first classified the lakes of the Mackenzie Delta into three categories: low closure lakes (which are connected to the channels infrequently), high closure lakes (which are connected to the channels annually) and no-closure lakes (which are always connected to channels). The description of each classification has been refined in recent studies (Marsh and Hey, 1989; Marsh and Hey, 1988), but the same three groupings are still used.

Though some lakes are also inundated during summer flood events, the most consistent and severe flooding of Delta lakes, especially those in the mid and upper Delta (Bigras, 1990), occurs as a result of ice jams during spring breakup (Marsh *et al.*, 1993). The Mackenzie Delta most often experiences a dynamic breakup (for which ice breaks and jams), as opposed to a thermal breakup (where intact ice deteriorates and melts in place). Dynamic breakup is characteristic of many north flowing river systems, as breakup commences first in the upper (southern) part of the basin, sending a snowmelt runoff wave and broken ice downstream into stronger, undeteriorated ice further downstream. As a result, ice jams usually occur. Ice jams cause significant flow obstructions resulting in rising upstream water levels and often a significant backwater effect. In the Delta, breakup begins in mid to late May when stage increases due to the arrival of snowmelt runoff and concludes when all channel are free of ice, typically by mid-June (Bigras, 1990; Terroux *et al.*, 1981).

As channel banks range from 10 m high in the upper Delta to 2 m in the lower Delta (Terroux *et al.*, 1981), ice jams are more common in the upper Delta, since the ice becomes constrained by the channel walls. In particular, as water levels on the Mackenzie River increase ice jams commonly form north of Point Separation at the Turtle and north towards Horseshoe Bay, creating a substantial backwater effect that potentially changes flow distributions. This contributes to the overall off- channel storage of Delta lakes, ranging from 26 to 31 km^3 during flooding (Emmerton *et al.*, 2007). As a result, ice jams can also have significant effects on sediment transport (Fassnacht, 1994; Goulding *et al.*, 2009) and nutrient transfer towards the Beaufort Sea (Emmerton *et al.*, 2008). In the outer Delta, breakup is further complicated by the overtopping of bottom fast ice as stage increases (Bélanger, 2010).

Recent studies have suggested the possibility of changing breakup and flooding patterns on the Mackenzie Delta (e.g. Rouse *et al.*, 1997). Through analysis of the water level records between 1976 and 2006, Goulding *et al.* (2008) showed a trend towards breakup occurring earlier in recent years, with peak water levels occurring ~1.5 days earlier per decade. Lesack and Marsh (2007) reported that the connection duration between the river and lakes with higher sill elevations, may be decreasing due to a decrease in ice jamming frequency or severity, while rising sea levels may be causing an increase in the number of connection days for lakes with lower sill levels. As a result of its widespread effect on Delta processes and changes observed in recent decades, a better understanding of river ice breakup in the Mackenzie Delta is critical.

1.2.1 IPY-SCARF

This study was part of the Canadian International Polar Year (IPY) project entitled "Study of Canadian Arctic River-delta Fluxes (IPY-SCARF)", aimed at quantifying water and nutrient fluxes in the Mackenzie Delta. In addition, the goal was to bring together researchers from different specializations to increase knowledge regarding the hydrology of the Delta and the effects of lake storage on flow distributions, particularly during breakup. As part of IPY-SCARF, the Mackenzie Delta Hydrodynamic Model (MDHM) is being developed, using a comprehensive one-dimensional platform that supports reversing flows, storm surges, ice jams and storage effects, all of which are typical of the Mackenzie Delta system (Nafziger *et al.*, 2009). Data limitations, particularly in regards to channel slope, have been the major constraint in the development of that model (Nafziger *et al.*, 2009).

In addition to the data collected by the author during spring breakup in 2010, many partners provided their detailed measurements of flow, water level and ice thickness for this study. These partners included the Water Survey of Canada (WSC), Natural Resources Canada (NRCan) and Environment Canada. IPY-

SCARF funding enabled the WSC to increase their field program in the Delta to include additional manual flow measurements and monitoring of winter water levels at many existing gauging stations. NRCan supported this study through the Canada Centre for Remote Sensing. Their contributions included detailed measurements of ice thickness, mapping of groundfast ice during winter, and mapping of ice and flood conditions during breakup. Environment Canada's efforts in this study included surveying of cross-section geometry, and documenting breakup (including measurements of ice jams and water levels at various locations in the Delta). Also, many IPY-SCARF members provided their oblique flight photos documenting ice conditions during breakup during this study. The contributions and contact info of each of the IPY-SCARF partners that provided data for this study are listed in Appendix A. This study involved the collation of the raw data provided by these partners.

1.3 Study Objectives

The goals of this study were two-fold:

- To collate all available data describing the Delta geometry, ice processes and flow distributions with particular emphasis on the data collected as part of the collaborative IPY-SCARF project.
- To use this data, in conjunction with hydraulic modeling, to calibrate an analogous channel geometry that could be used as input to a one-dimensional network model, the MDHM, of the Delta.

Chapter two describes data provided by the WSC, including both flow and water level data. The locations of each of the WSC gauges in relation to the primary channels are discussed. The increase in monitoring efforts during the study period from 2006 to 2010 is also presented. In particular, the manual flow measurements conducted during the IPY period are examined and compared. Typical ranges and average flows are deduced from the available channel flow measurements.

The third chapter presents the available data collected during the ice-affected seasons. In particular winter measurements of ice thickness are presented, including mapping of groundfast ice conditions. Spring breakup is the focus of the second half of the chapter and the sequence of breakup (which was deduced from oblique angle photo taken from aircraft, breakup reports and satellite imagery) is presented for each year during the study period (from 2006 to 2010).

Chapter four describes the steps taken to form a hydraulic model for calibration of primary channel slope and elevation, which could ultimately be used as geometric input into the MDHM. As this model has been limited by a lack of geometry information, particularly in regards to channel slope, the modeling efforts in this study focused upon calibration of channel geometry. In particular, this geometry was calibrated for summer open water conditions, during periods when flows in the Delta are the least complicated by storm surges.

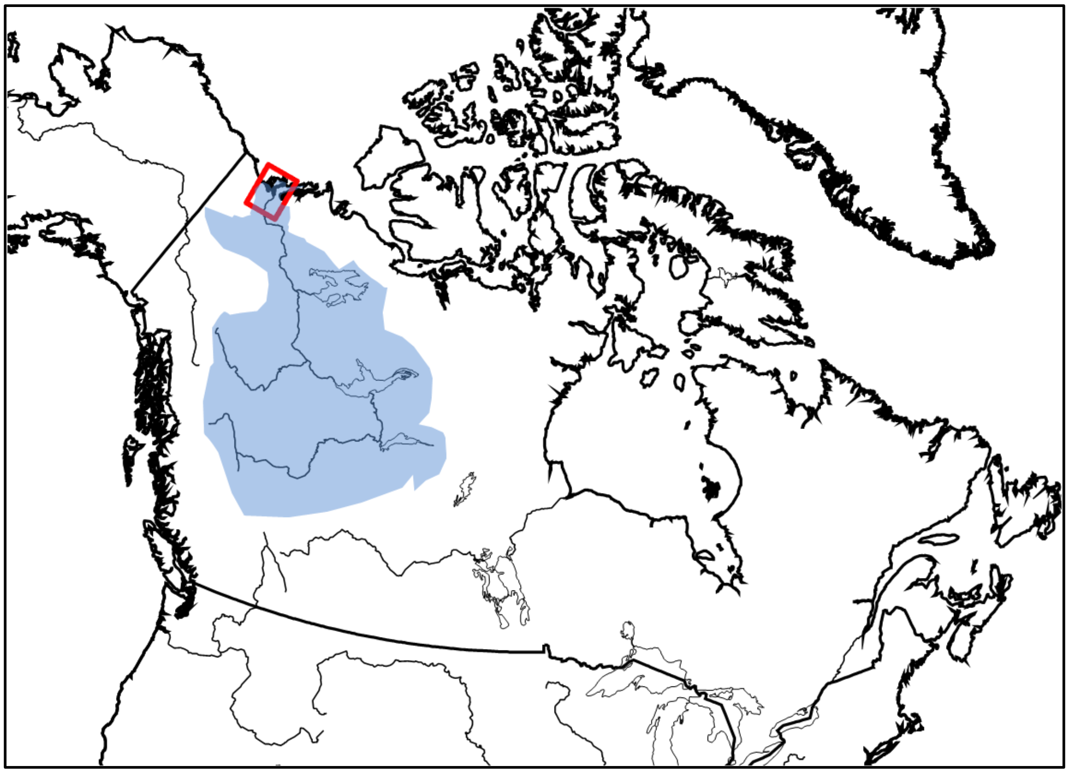

Figure 1.1 Location map of the Mackenzie River Basin in northwest Canada (adapted from Nafziger *et al*. (2009)).
(Base image source: ArcMap basemaps).

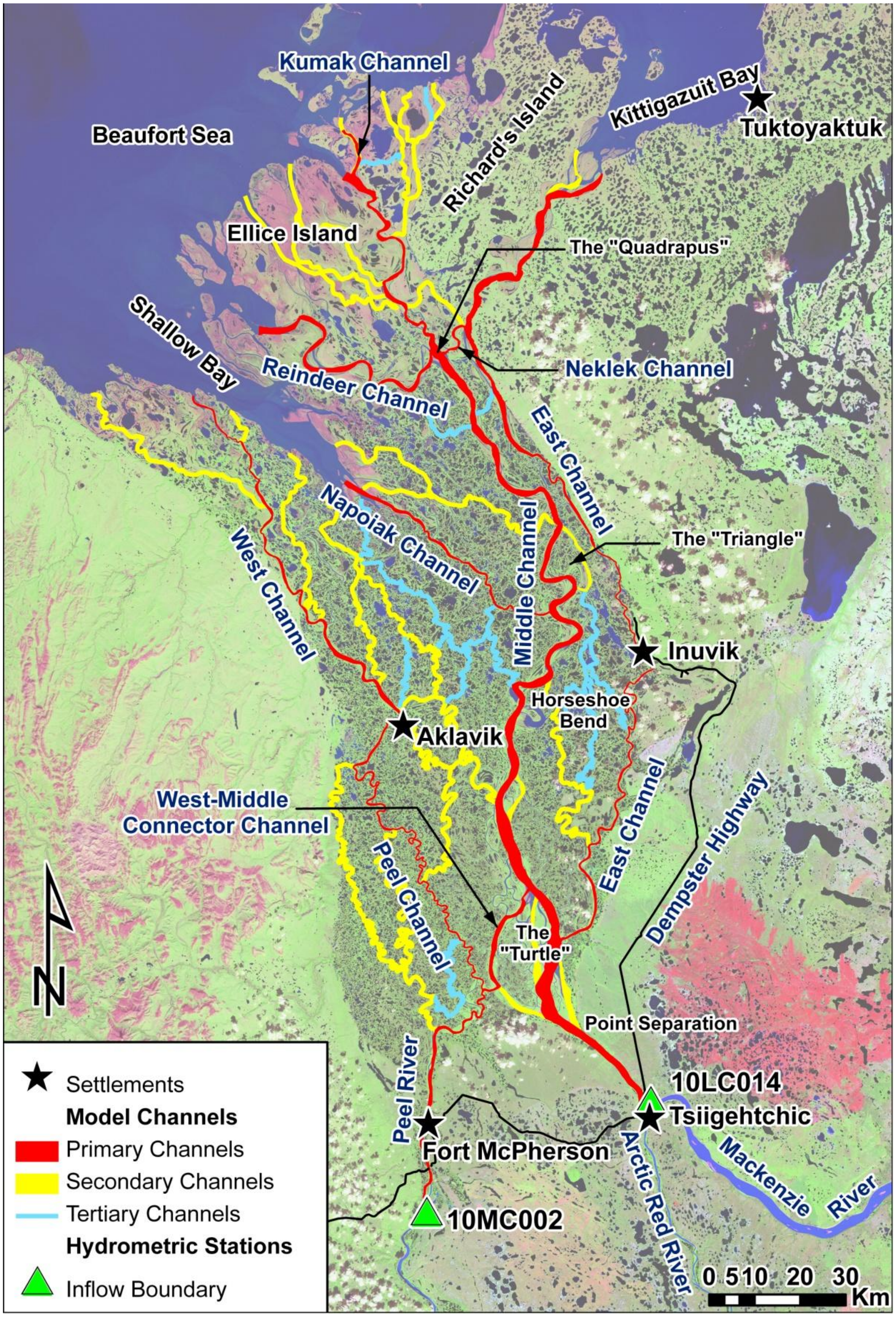

Figure 1.2 Location map of the Mackenzie Delta, including communities in the Mackenzie Delta and the primary channel inflow boundaries (adapted from Nafziger *et al.*(2009)).
(base image source: Industry Tourism and Investment, NWT).

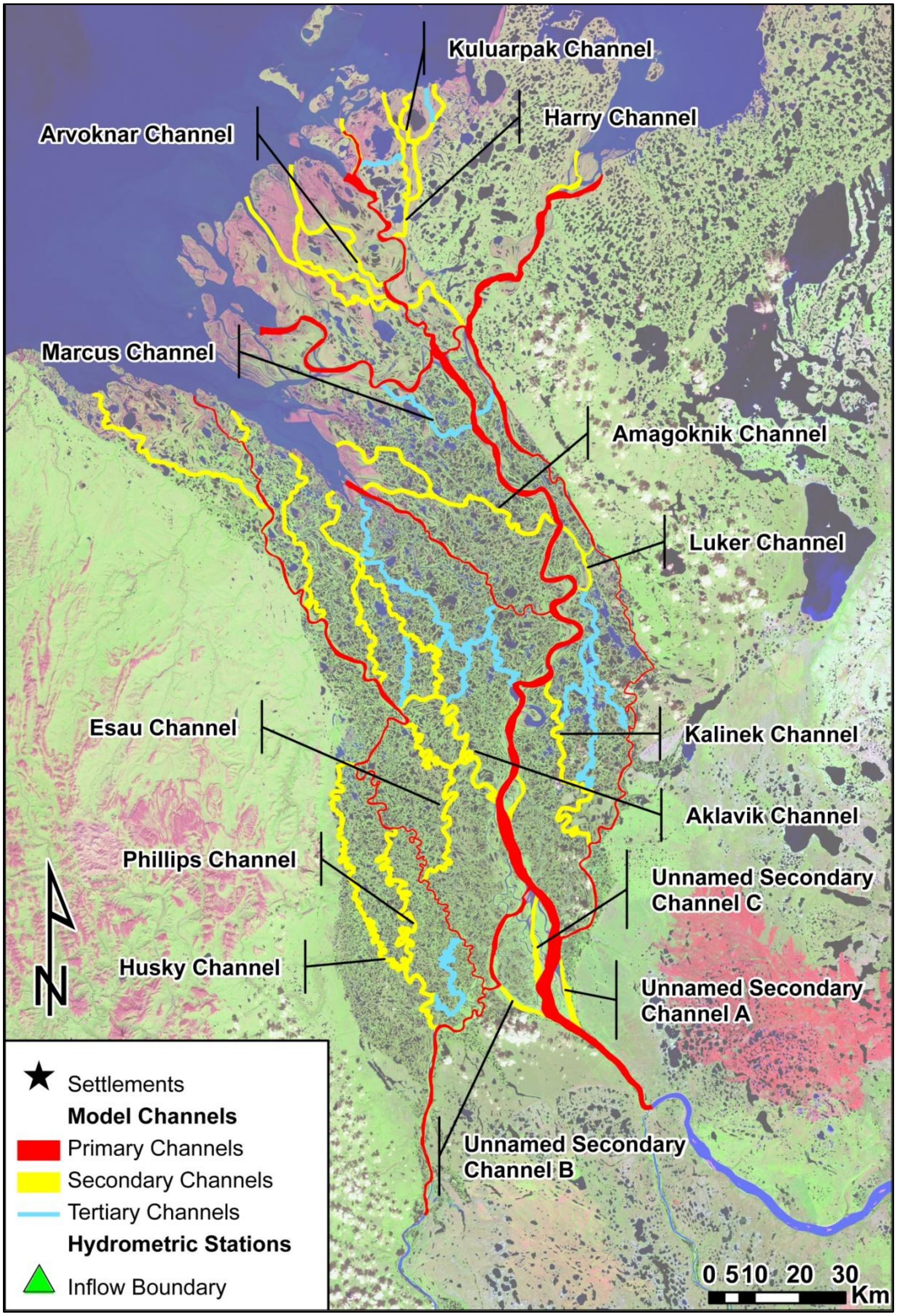

Figure 1.3 Names of secondary and tertiary channels in the Mackenzie Delta. (base image source: Industry Tourism and Investment, NWT).

2.0 Water Level and Flow Measurements in the Mackenzie Delta

The WSC collects water levels at 14 gauging station in the Mackenzie Delta, including water levels on the two inflow channels. As part of the IPY-SCARF effort, the WSC extended operations at some gauges to include the ice-affected months. In addition, the WSC manually measured flow at each gauging station at least twice over the study period. Additional flow measurements were also conducted by the WSC over the study period. This chapter presents the WSC data collected during the study period of 2006 to 2010. Magnitudes and percentages of flow in the primary channels are compared and mapped.

2.1 Location of the WSC Canada Gauging Stations

There are twelve WSC gauging stations along channels in the Mackenzie Delta and two upstream on the Mackenzie River and Peel Rivers. Each station reports water level on a river channel. In addition, a lake level measurement station is located on *Big Lake at Taglu Island* (10LC020). Table 2.1 lists the station numbers, names and Universal Transverse Mercator (UTM) coordinates for each gauging station. A map of the Mackenzie Delta with the location of each of the gauging stations is shown in Figure 2.1. Note that all of the WSC gauge names are italicized to aid in the clarity of this discussion.

Table 2.1 Water Survey of Canada gauging stations in the Mackenzie Delta.

Station Number	Station Name	UTM Zone 8W (NAD83)
10LC002	*Mackenzie River (East Channel) at Inuvik*	550802 7585121
10LC012	*Mackenzie River (Middle Channel) at Tununuk Point*	512293 7655477
10LC013	*Mackenzie River (East Channel) above Kittigazuit Bay*	543418 7686748
10LC014	*Mackenzie River at Arctic Red River*	554036 7482778
10LC015	*Mackenzie River at Confluence East Channel*	536657 7520174
10LC019	*Mackenzie River (Kumak Channel) Below Middle Channel*	490399 7690042
10LC020	*Big Lake at Taglu Island*	499391 7701545
10LC021	*Mackenzie River at Kuluarpak Channel*	504796 7458418
10MC002	*Peel River above Fort McPherson*	495396 7565538
10MC003	*Mackenzie River (Peel Channel) above Aklavik*	523848 7575650
10MC008	*Mackenzie River (Middle Channel) below Raymond Channel*	494566 7663630
10MC010	*Mackenzie River (Outflow Middle Channel) below Langley Island*	479531 7656491
10MC011	*Mackenzie River (Reindeer Channel) at Ellice Island*	514909 7502182
10MC022	*Peel River at Frog Creek*	500655 7613726
10MC023	*Mackenzie River (Napoiak Channel) above Shallow Bay*	501222 5697757

Including the inflow stations, 13 of the WSC monitoring stations collect water levels either on channels or within 4 km of channels that are part of the primary network:

- five stations along the Middle Channel,
- four stations along the East Channel,
- three stations along the West Channel,
- one station on the Napoiak Channel and
- one station on the Reindeer Channel.

Table 2.2 summarizes the locations of each of the stations along the primary channels. The remaining station, *Mackenzie River at Kuluarpak Channel* (10LC021), is located on the Kuluarpak Channel, which is part of the secondary network. The station at *Big Lake at Taglu Island* (10LC020) collects water level at Big Lake, which is very close to the Kuluarpak Channel station.

Table 2.2 Location of water level gauging stations operated by the WSC, which are along the primary channels of the Mackenzie Delta.

Channel	**Station Number**	**Station at WL measurement** (km)
Middle Channel	10LC014	0.0
	10LC015	48.2
	10MC008	110.5
	10MC010	245.0
	10LC019	285.0
East Channel	10LC015	52.2
	10LC002	144.2
	10LC012	232.2
	10LC013	283.2
West Channel	10MC002	0.0
	10MC022	53.0
	10MC003	173.0
Napoiak Channel	10MC023	188.8
Reindeer Channel	10MC011	276.5

Five gauging stations operated by the WSC provide water levels along the Middle Channel. The upstream inflow to the Middle Channel is located at *Mackenzie River at Arctic Red River* (10LC014). This station is just downstream of where the Arctic Red River flows into the Middle Channel at Tsiigehtchic. The next station downstream is at *km* 48.2, just downstream of Point Separation. This station, *Mackenzie River at Confluence East Channel* (10LC015), is actually located on the East Channel four kilometers downstream of where the East Channel leaves the Middle Channel. As the water surface slope is mild (less than 0.0001, as discussed later in Section 0), the water level reported at this gauge is a reasonably accurate approximation of the water level along the Middle Channel at *km* 48.2. The next gauging station is located on the Middle Channel just downstream of Horseshoe Bend at *km* 110.5. This station, which is named *Mackenzie River (Middle Channel) below Raymond Channel* (10MC008), is located on the Middle Channel 30.3 km upstream of the Napoiak Channel junction. *Mackenzie River (Outflow Middle Channel) below Langley Island* (10MC010) is located further downstream on the Middle Channel, past the Neklek Channel and Reindeer Channel junctions. As the name implies, this gauge is not directly on the Middle Channel, it is approximately 1 km from of the Middle Channel on the Arvoknar Channel, which flows from the Middle Channel. Figure 2.2 shows a map of this stations location. The water level collected at this station is a reasonably accurate approximately of the water level in the Middle Channel. The fifth gauge on the Middle Channel is *Mackenzie River (Kumak Channel) below Langley Island* (10LC019), located on the Kumak Channel, which has been included as the downstream portion of the Middle Channel in this study. This gauge is located at *km* 285; the Kumak Channel begins at *km* 281.

Four gauging stations operated by the WSC span the East Channel. The furthest upstream station, *Mackenzie River at Confluence East Channel* (10LC015), is located four kilometers downstream of where the East Channel leaves the Middle Channel. As discussed already, it is also considered representative of the water level on the Middle Channel at *km* 48.2. Another station along the East Channel is *Mackenzie River (East Channel) at Inuvik* (10LC002); located approximately 2.5 km downstream from the community of Inuvik, at *km* 144.2. The next station at *Mackenzie River (Middle Channel) at Tununuk Bay* (10LC012) is not actually located on the Middle Channel (or the East Channel). It is on an outflow channel that flows north from the Neklek Channel, about on kilometer upstream of where the Neklek Channel joins the East Channel, as shown in Figure 2.3. It provides a reasonably accurate approximation of the water level at *km* 232.2 along the East Channel, as it is two kilometers away. This water level is also representative of the water level at the downstream boundary of the Neklek Channel at *km* 232. is located further downstream on the East Channel at *km* 283.2.

The *Peel River above Fort McPherson* (10MC002) is the inflow boundary station for the West Channel. This station is located directly on the Peel River about 22 km upstream of the community of Fort McPherson. Another gauging station along the West Channel, named *Peel River at Frog Creek* (10MC022), is located downstream of Fort McPherson at *km* 53. It is 11.8 km upstream of where the West-Middle Connector Channel splits from the West Channel. The final West

Channel gauging station is *Mackenzie River (Peel Channel) above Aklavik* (10MC003). It is 6.5 kilometers upstream of the community of Aklavik, at *km* 173 along the West Channel. The West Channel outlet to Shallow Bay is 109 km downstream from this gauge.

One gauging station, *Mackenzie River (Napoiak Channel) above Shallow Bay* (10MC023), is located on Napoiak Channel *at km* 188.8, which is 48 km downstream of the Middle Channel. 15.5 km downstream of this gauge the Napoiak Channel terminates at the south tip of Shallow Bay. The single gauge on the Reindeer Channel is named *Mackenzie River (Reindeer Channel) at Ellice Island* (10MC011), located at *km* 276.5, which is 12.5 km upstream of Shallow Bay.

Water level was monitored at each of the WSC gauging stations in the Delta. Manual measurements of flow at the gauge locations were also conducted during the study period. For some of the gauging sites, the WSC developed a rating curve (a relationship between stage and discharge) to facilitate continuous flow reporting (based on the continuous water level measurement at these gauges). Water level measurements, manual flow measurements and rating curve formation are discussed in the following sections.

2.2 Water Level Measurements at WSC Gauging Stations

The Canadian Gravimetric Geoid (CGG05) was used as the vertical datum for all water level elevations and bed elevations that could be referenced to a known datum. As the water surface in the Delta is very flat, accurate conversions to

CGG05 Geoid are essential for determination of water level and bed slopes. For areas close to the Beaufort Sea, the CGG05 is considered the most accurate vertical geoid (Véronneau, 2006). CGG05 adjustments for the WSC gauging stations were calculated and provided by the WSC and are in shown in Table 2.3.

Table 2.3 List of CGG05 water level conversion for gauges operated by the WSC. (Data source: the WSC).

Station number	**WL conversion to CGG05 datum** (m)
10LC002	-10.856
10LC012	-9.822
10LC013	-9.731
10LC014	-0.024
10LC015	-0.824
10LC019	-9.637
10LC020	-8.634
10LC021	-9.065
10MC002	0.074
10MC003	-10.056
10MC008	-10.346
10MC010	-9.345
10MC011	-9.213
10MC022	2.336
10MC023	-10.603

The hydrograph availability at each of the gauging stations, as a result of the increased monitoring effort by WSC over the study period, is summarized in Table 2.4. ‘Open water’ refers to nearly continuous water level availability during the open water season, whereas ‘year-round’ refers to hydrograph availability over the entire year, including the ice covered season. ‘Intermittent’ refers to sparse water level availability over the entire year. For both the open water and year-round cases, there are periods of less than two weeks in length when water level may be unavailable at specific gauges.

Between 2007 and 2009, eight stations were upgraded to record and report water levels during the winter months as well as the open water season:

- *Big Lake at Taglu Island* (10LC020),
- *Mackenzie River at Kuluarpak Channel* (10LC021),
- *Mackenzie River (Peel Channel) above Aklavik* (10MC003),
- *Mackenzie River (Middle Channel) below Raymond Channel* (10MC008),
- *Mackenzie River (Outflow Middle Channel) below Langley Island* (10MC010),
- *Mackenzie River (Reindeer Channel) at Ellice Island* (10MC011),
- *Mackenzie River (Napoiak Channel) above Shallow Bay* (10MC023).

Table 2.4 Hydrograph availability at each gauging station operated by the WSC from 2006 to 2010. (Data source: the WSC).

Station	**2006**	**2007**	**2008**	**2009**	**2010**
10LC002	Year-round	Year-round	Year-round	Year-round	Year-round
10LC012	Open water	Open water	Open water	Open water	Open water
10LC013	Open water	Open water	Open water	Open water	Open water
10LC014	Year-round	Year-round	Year-round	Year-round	Year-round
10LC015	Open water	Open water	Open water	Open water	Open water
10LC019	Open water	Open water	Open water	Open water	Open water
10LC020	Open water	Open water	Open water	Year-round	Year-round
10LC021	Open water	Open water	Year-round	Year-round	Year-round
10MC002	Year-round	Year-round	Year-round	Year-round	Year-round
10MC003	Open water	Open water	Open water	Year-round	Year-round
10MC008	Open water	Open water	Open water	Open water	Year-round
10MC010	Open water	Open water	Intermittent	Open water	Year-round
10MC011	Open water	Open water	Open water	Year-round	Year-round
10MC022	Open water	Open water	Open water	Open water	Open water
10MC023	Open water	Open water	Open water	Year-round	Year-round

Each of the gauging stations were in operation before this study commenced with daily water levels published for each gauge. The WSC also provided unpublished hourly water levels at each station during the study period. Figures 2.4 and 2.5 are examples of the water level hydrographs over the study period from two different gauging stations. Figure 2.4 shows the hydrograph for *Mackenzie River at Arctic Red River* (10LC014), which is reported continuously. Figure 2.5 shows the water level hydrograph available during the open water season at *Mackenzie River at Confluence East Channel* (10LC015). Appendix B shows the hydrographs over the study period for each of the gauges in the Delta.

Each of the water level hydrographs follows the same general shape, with peak water levels evident in late May due to snowmelt runoff and breakup. Water levels are also tidally influenced, which contributes to twice diurnal fluctuations in the outer Delta gauges as was evident in the hourly Delta water level measurements. This effect is most pronounced at , which is located ~1 km from the outlet of the East Channel at Kittigazuit Bay. At this gauge, water levels fluctuate by up to 0.3 to 0.4 m every 6 hours during the summer months. This is similar to the tidal fluctuations noted in previous studies dating back to the 1960s (e.g. Mackay, 1963). Under an ice cover, the effects of tidal fluctuations on gauge levels are generally negligible. Water levels at *Mackenzie River at Kuluarpak Channel* (10LC021) are also tidally influenced, with water level fluctuations of up to 0.2 m during the open water season. Water level fluctuations due to tides are less evident at *Mackenzie River (Kumak Channel) below Langley Island* (10LC019) and at the *Mackenzie River (Reindeer Channel) at Ellice Island* (10MC011), but can still contribute to fluctuations of up to 0.05 m. Belanger

(2010) also noted this type of tidal variations along the Beaufort Sea and Kittigazuit Bay. Tidal effects are not distinguishable in the gauge records further upstream on the Middle Channel (e.g. *Mackenzie River (Outflow Middle Channel) below Langley Island* (10MC010)).

2.3 Manual Flow Measurements in the Mackenzie Delta

During the study period, the WSC conducted periodic manual flow measurements at each of the river stations. Appendix C presents these direct manual flow measurements between 2006 and 2010 at each of the WSC stations, with the exception of the *Peel River above Fort McPherson* (10MC002), for which manual measurement details were not available. While conducting manual flow measurements, manual water levels were also measured. These are shown on the water level hydrographs in Appendix B.

The frequency of manual flow measurements was increased as part of the IPY-SCARF collaboration. As a result, flow was manually measured at each gauge at least once during the 2007 open water season and once over the 2008 open water season. At numerous stations, additional flow measurements (beyond these two) were also conducted. Table 2.5 presents the location of manual flow measurements at gauges along each of the primary channels. With the exception of two gauges (10LC013 and 10MC010), each manual flow measurement was taken within two kilometers of the corresponding water level gauging and therefore the same location (station) was used. For the two remaining gauges, manual flow measurements were at a substantively different location:

- Manual flow measurements for the *Mackenzie River (East Channel) above Kittigazuit Bay* (10LC013) station were measured approximately 42.5 km upstream of the water level station at the outlet of the East Channel at *km* 240.7. The location is shown in Figure 2.6. This location was chosen by the WSC as the East Channel braches numerous times at the flow approaches Kittigazuit Bay, so this flow was more indicative of the total flow in the East Channel.

- At *Mackenzie River (Outflow Middle Channel) below Langley Island* (10MC010), the flow was measured manually on both the outflow channel (the Arvoknar Channel) and upstream of the Arvoknar Channel on the Middle Channel, as shown in Figure 2.7.

Table 2.5 Location of manual flow measurements at gauges along the primary channels of the Mackenzie Delta, 2006 to 2010.

Channel	**Station Number**	**Station at flow measurement** (km)
Middle Channel	10LC014	0.0
	10LC015	-
	10MC008	110.5
	10MC010	245.0
	10LC019	285.0
East Channel	10LC015	52.2
	10LC002	144.2
	10LC012	-
	10LC013	240.7
West Channel	10MC002	0.0
	10MC022	53.0
	10MC003	173.0
Napoiak Channel	10MC023	188.8
Reindeer Channel	10MC011	276.5

The location of the flow measurements at 10LC015 along the Middle Channel, and 10LC012 along the East Channel, are not listed in Table 2.5 as the flows reported at these gauging stations were not indicative of the flows in these channels. Manual flow measurements at *Mackenzie River at Confluence East Channel* (10LC015) were conducted only on the East Channel. Manual flow measurements at *Mackenzie River (Middle Channel) at Tununuk Point* (10LC012) were taken on the secondary outflow channel where the water level gauge station is located, as shown in Figure 2.3. This channel carries less than 100 m^3/s at all times of the year.

The WSC manual flow measurements were conducted using an Acoustic Doppler Current Profiler (ADCP), using their standard procedure for both ice-affected and open water cases (e.g. see Pelletier, 1990; Walker and Wang, 1997). Measurements during the open water season were completed by boat, whereas winter measurements were conducted using the standard practice of auguring holes in the ice cover. The expected accuracy of manual flow measurements based upon ideal measurement conditions, which may not always be possible in the Delta, is <±10% (Pelletier, 1988).

2.3.1 Gauge Stations with Established Rating Curves

Manual flow measurements are only available during specific timeframes and rating curve flows capture a more complete picture over time. Both during and before the study period, sufficient manual flow measurements were conducted by the WSC at five gauging stations so that continuous flows are reported (using a relationship between water surface elevation and discharge):

- *Mackenzie River at Arctic Red River* (10LC014)

- *Peel River above Fort McPherson* (10MC002)
- *Mackenzie River (Middle Channel) below Raymond Channel* (10MC008)
- *Mackenzie River (East Channel) at Inuvik* (10LC002)
- *Mackenzie River (Peel Channel) above Aklavik* (10MC003).

The WSC gauging stations that report flow include the two inflow gauge stations and one on each of the Middle, East and West Channels in the mid-Delta. Figures 2.8 to 2.12 present the flow hydrographs obtained during this study period at each of these five stations. Manual flow measurements are also shown on these plots.

The rating curves for the *Mackenzie River (Middle Channel) below Raymond Channel* (10MC008) and the *Mackenzie River (Peel Channel) above Aklavik* (10MC003) were only established in 2007. Flows at these two gauging stations are reported from 2007 to 2010, whereas flows are reported for 2006 to 2010 at the remaining three stations. Each of the flow hydrographs followed the same general shape each year. Flow gradually increased from January to May, when the spring snowmelt runoff wave was apparent. Peak flows were evident in May and June during spring breakup. However, the accuracy of flows reported during breakup is not known as it is logistically impractical to conduct manual measurements during this period. In addition, backwater effects from ice jams can be substantial, leading to an overestimate of flows during this period, as the stage-discharge relationship is not accurate during this time (Rouse *et al.*, 1997; Pelletier, 1990). Water levels and flows remained high in the summer months, in response to numerous rainfall events.

2.3.1.1 Rating Curve Accuracy

Tables 2.6 to 2.9 compare the manually measured flow (Q_m) to the hourly rating curve flows (Q_r) corresponding to measurements conducted for each of the four gauges, where available. The differences between the manually measured flows (Q_m) and flow based on the rating curves (Q_r) were less than 25% for all measurements; and were less than 10% for over 90% of the measurements. However, no manual measurements were completed during breakup and freeze-up, as conditions do not allow. Therefore, the accuracy of rating curve flow reported during this time is not known.

Table 2.6 Manually measured flow (Q_m) compared to hourly reported flows obtained from rating curve (Q_r) at *Mackenzie River at Arctic Red River* (10LC014). (Data source: the WSC).

Date	**Q_m** (m^3/s)	**Q_r closest hour** (m^3/s)	**Percent difference between Q_m and Q_r**	**Difference between Q_m and Q_r** (m^3/s)
23-Nov-06 20:54	2973	2973	0.0%	0
30-Jan-07 14:27	3778	3778	0.0%	0
12-Apr-07 14:19	3551	3535	0.5%	16
6-Dec-07 15:25	4072	4092	-0.5%	-20
7-Mar-08 14:40	4008	4257	-6.2%	-249
23-Apr-08 15:15	3869	3893	-0.6%	-24
8-Feb-09 15:00	4094	4095	0.0%	-1
5-May-09 12:53	6550	6550	0.0%	0
17-Dec-09 16:08	3854	3865	-0.3%	-11
4-Mar-10 14:05	4450	4452	-0.1%	-2

Table 2.7 Manually measured flow (Q_m) compared to hourly reported flows obtained from rating curve (Q_r) at *Mackenzie River (Middle Channel) below Raymond Channel* (10MC008). (Data source: The WSC)

Date	**Q_m** (m^3/s)	**Q_r closest hour** (m^3/s)	**Percent difference between Q_m and Q_r**	**Difference between Q_m and Q_r** (m^3/s)
14-Jun-07 13:09	16900	18175	-7.5%	-1275
5-Mar-08 13:25	3960	3960	0.0%	0
1-May-08 14:15	3876	3880	-0.1%	-4
25-Jun-08 15:00	16200	15445	4.7%	755
12-Aug-08 15:00	13000	11148	14.2%	1852
24-Sep-08 13:05	10200	10200*	0.0%	0
11-Feb-09 14:36	3990	3990	0.0%	0
11-May-09 14:30	8402	8400	0.0%	2
19-Jan-10 14:24	4434	4434	0.0%	0

*Q_r on day of manual measurement, as hourly was not reported

Table 2.8 Manually measured flow (Q_m) compared to hourly reported flows obtained from rating curve (Q_r) at *Mackenzie River (East Channel) at Inuvik* (10LC002). (Data source: the WSC).

Date	**Q_m** (m^3/s)	**Q_r closest hour** (m^3/s)	**Percent difference between Q_m and Q_r**	**Difference between Q_m and Q_r** (m^3/s)
3-Feb-07 14:40	30.8	31	0.6%	0
10-Apr-07 16:25	17.2	17	0.3%	0
21-Jun-07 17:07	409	381	-6.9%	-28
29-Nov-07 16:24	77.9	78	0.2%	0
29-Feb-08 14:39	47.9	37	-22.0%	-11
24-Apr-08 14:45	27.8	28	0.0%	0
11-Jun-08 15:37	431	431	0.1%	0
7-Aug-08 15:18	209	236	12.9%	27
28-Nov-08 15:39	48.4	48	0.1%	0
6-Mar-09 15:10	17.5	17	-0.5%	0
24-Apr-09 9:45	15	15	-0.4%	0
16-Dec-09 15:06	44.1	44	-0.2%	0
11-Mar-10 16:18	38.7	39	0.4%	0

Table 2.9 Manually measured flow (Q_m) compared to hourly reported flows obtained from rating curve (Q_r) at *Mackenzie River (Peel Channel) above Aklavik* (10MC003). (Data source: the WSC).

Date	**Q_m** (m^3/s)	**Q_r closest hour** (m^3/s)	**Percent difference between Q_m and Q_r**	**Difference between Q_m and Q_r** (m^3/s)
14-Jun-07 17:22	1190	1229	-3.3%	-39
26-Feb-08 14:15	218	218	0.0%	0
30-Apr-08 14:45	196	196	0.0%	0
25-Jun-08 19:30	860	991	-15.2%	-131
12-Aug-08 12:00	973	888	8.7%	85
24-Sep-08 16:08	846	812	4.0%	34
9-Feb-09 14:40	137	137	0.0%	0
16-Apr-09 14:10	189	190*	-0.4%	-1
10-Dec-09 13:50	139	139*	0.0%	0

*Q_r on day of manual measurement, as hourly was not reported

At the *Mackenzie River at Arctic Red River* (10LC014), all reported (rating curve) flows (Q_r) were less than 1% different from the manually measured flow with the exception of the measurement on 7-Mar-08, under ice covered conditions (when the difference was ~6%). On the Middle Channel at *Mackenzie River (Middle Channel) below Raymond Channel* (10MC008), the rating curve flows were less than 1% different from the manually measured flows, with the exception of three measurements: 14-Jun-07, 25-Jun-08 and 12-Aug-08, which were all during measured during the open water season. Thus, at this gauge, there is less confidence in the open water rating curve flows reported. Manually measured flows under ice-covered conditions all agreed within a 1% difference at this gauge.

Manually measured flows at the *Mackenzie River (East Channel) at Inuvik* (10LC002) were an order of magnitude smaller than the flows measured on the Middle Channel, ranging from 15 m^3/s under ice covered conditions to approximately 400 m^3/s in the summer. As a result, small magnitude differences (<30 m^3/s) between the measured and rating curve flow can result in large percentage differences. This was the case for 21-Jun-07, 29-Feb-08 and 7-Aug-09, when the percent difference in flow was up to 22%.

The gauging station *Mackenzie River (Peel Channel) above Aklavik* (10MC003) is located on the West Channel; flow at this gauge ranged from 150 m^3/s to 1,200 m^3/s. The majority of the recorded rating curve flows, including all winter measurements, were less than 10% different from the manually measured flow. However, flows greater than ~850 m^3/s resulted in the greatest difference between manually measured (Q_m) and recorded rating curve flows (Q_r) of up to ~14%.

Overall, the difference between the rating curve and the manually measured flows were within the expected error, as there are inherent error in both the manual measurements and rating curves. Although the manually measured flows do not always match the rating curve flow, time averaging of the rating curve flow allows them to be more indicative of the flow over a period. As a result, average recorded rating curve flow is used in further analysis, with the understanding that the reported flows may have an error of up to 25% during open water or simple ice-affected cases, but more likely less than 10% dependent on the gauge and time of year. During spring breakup and freeze-up the reliability of rating curve flows is unknown, but is expected to be poor.

2.3.1.2 Estimating Total Inflow to the Delta

The sum of the hourly flows reported on the *Mackenzie River at Arctic Red River* (10LC014) and the *Peel River above Fort McPherson* (10MC002) was assumed to comprise the entire inflow to the Delta. Both of these gauges continuously reported hourly flows over the study period. This approach was similar to that described by Anderson and Anderson (1974) and Fassnaucht (1993b). Fassnaucht (1993b) considered the inflow as the sum of the flow at the Mackenzie River at Arctic Red River, the Peel River above Fort McPherson and the Arctic Red near the mouth. However, *Mackenzie River at Arctic Red River* (10LC014) is located downstream of the confluence between the Mackenzie River and the Arctic Red River and, therefore, includes the flow from the Arctic Red River. Figure 2.13 shows this total inflow over the study period.

The water travel time from the inflow stations to specific locations in the Delta is not well understood, and the interactions between the Peel River and Mackenzie Delta systems are complex (Goulding *et al.*, 2009). There are numerous connections between the two inflow channels at different locations in the Delta downstream of the Turtle. For example, the West-Middle Connector Channel meets the Middle Channel 62.5 km from 10LC014 and 94.8 km from 10LC002. Even at this one connection only the travel distances are known and not the travel times. As a result, there are not enough data to assume an offset when summing the two gauges without introducing additional error. Therefore, the sum of flows reported at these stations at the same date and time is assumed as the inflow to the Delta.

As shown in the Figure 2.13, the peak inflow is observed annually in May during the spring melt runoff. This peak inflow ranged from 26,000 m^3/s in 2010 to 36,000 m^3/s in 2006. However, this peak inflow estimate is likely affected by ice breakup and thus possibly quite erroneous. Over the summer open water months of June, July, August, and September, flows increase and decrease due to rainfall events in the basin, but do not reach the peak magnitudes reported in May during snowmelt runoff. The lowest inflow, ranging from 2,370 m^3/s in 2010 to 3,610 m^3/s in 2008, was usually observed in late November or in early December following freeze-up. Inflow generally increased over December and January and then gradually fell until breakup occurred in May. At that time, inflow increased to peak inflow rapidly over the period of a few weeks.

A graph showing the percentage of inflow resulting from the flow at the two inflow gauges is shown in Figure 2.14. Overall, including both the open water and ice-affected seasons, the *Mackenzie River at Arctic Red River* (10LC014) typically accounted for ~95% of the inflow over the period, with *Peel River above Fort McPherson* (10MC002) accounting for the remaining ~5%. However, this varied depending upon the time of year. For example, during spring snowmelt runoff period, the flow from the *Peel River above Fort McPherson* (10MC002) was estimated to account for up to 25% of the total inflow to the Delta.

The importance of each of these inflows during each month of the year is shown in Figures 2.15 and 2.16, for 10LC014 and 10MC002, respectively. These figures show the daily percentages of inflow averaged over each month. The black bars show the range of percentages observed in each month over the period of this study (2006 to 2010). The greatest ranges (up to 20%) were evident in May, which was expected due to large fluctuations in inflow observed during spring snowmelt runoff and the potential for significant error due to ice effects.

Figure 2.17 also shows the percentage of inflow from the *Mackenzie River at Arctic Red River* (10LC014) averaged over the open water and ice-affected seasons. Figure 2.18 shows the same graph for the *Peel River above Fort McPherson* (10MC002). Summer was assumed as June to September. The ice-affected season was considered November to April. May and October were excluded due to variabilities in the timing of freeze-up and breakup. In 2006, only January to March were considered and in 2010 the average ice-affected season only considered to be only November and December, as these were the times when hourly data was provided. In general, the flow from the *Peel River above Fort McPherson* (10MC002) constituted a larger percentage of the inflow during the summer months compared to the ice-affected season. During the summer months, when the overall inflow was substantially higher, 7% of the flow came from the *Peel River above Fort McPherson* (10MC002). During the winter months the percentage of flow from each of the inflows was less variable and the *Peel River above Fort McPherson* (10MC002) averaged only ~3% of the inflow. This is similar to the flow splits measured by Anderson and Anderson (1974), who suggested the Mackenzie River provides 97% to ~98% of the inflow during the winter months. The flow proportions between the mid-Delta gauges with rating curves are examined in the following section.

2.3.1.3 Flow Comparison at Mid-Delta Gauges to Total Delta Inflow

The WSC gauges at *Mackenzie River (Middle Channel) below Raymond Channel* (10MC008), *Mackenzie River (East Channel) at Inuvik* (10LC002), and *Mackenzie River (Peel Channel) above Aklavik* (10MC003) report continuous flow, based upon the continuous water levels collected and rating curves. These gauges are located in the mid-Delta and roughly transect the Middle, East and West Channels. Figures 2.19 to 2.21 compare the inflow to the flow recorded at each of these gauges on a monthly basis over the study period. The black error bars were calculated in the same way as discussed for Figures 2.15 and 2.16.

Figures 2.22 to 2.24 show the flow at these gauges averaged over the open water and ice-affected seasons. The same assumptions as used to develop Figures 2.17 and 2.18 were used here. Overall, a greater percentage of the inflow (approximately 10% higher) was recorded at the *Mackenzie River (Middle Channel) below Raymond Channel* (10MC008) during the ice-affected season than during the summer months, as shown in Figure 2.10. Anderson and Anderson (1974) recorded a winter flow of 80% of the inflow on the Middle Channel close to this gauge, which is within the range recorded during this study period, but nearly 10% lower than the average found. Flows recorded at the *Mackenzie River (East Channel) at Inuvik* (10LC002) and the *Mackenzie River (Peel Channel) above Aklavik* (10MC003) were lower during the winter months than the summer months. Fassnacht (1993b) reported flow splits on the Middle, East and West Channels on three separate occasions with inflows ranging from 11,364 m^3/s to 24,619 m^3/s, to be 82 to ~86%, 4.2% to 6.4% and 1.4 to1.8%, respectively. These are all within the ranges found in the study period from 2006 to 2010, suggesting that flow split patterns could be similar to that recorded in 1984 and 1985.

The overall percentages of inflow at these gauges during the open water and ice-affected seasons are summarized in Table 2.10. The sum of the percentages is also shown as these gauges roughly transect the Middle, East and West Channels in the mid-Delta. The discrepancy between flows measured in the mid-Delta and the total inflow is likely due to flows in channels not measured and off-channel storage effects (Nafziger *et al.*, 2009). As nearly 5% more of the inflow is accounted for between these gauges during the winter months, it suggests that smaller (secondary or tertiary), channels were likely blocked or carried less of the flow during the ice covered season and, therefore, the Middle Channel carried a greater percentage of the total Delta inflow during the ice-affected season. Besides rating curve flows, periods of manual measurements are also indicative of flow split patterns and are discussed in the following section.

Table 2.10 Overall average percentages of inflow observed at the three mid-Delta gauges with rating curves. (Data source: the WSC).

Gauge	Open Water	Ice Affected
10MC008	78.80%	89.20%
10LC002	1.60%	0.80%
10MC003	5.10%	4.50%
SUM	85.5%	90.0%

2.3.2 Periods of Manual Flow Measurement at Gauges without Rating Curves

Altogether, there were 21 measurement campaigns during IPY-SCARF that represent the most comprehensive data on flow splits in the Delta ever to date. Table 2.11 shows the manual flow measurements (Q_m) available during each of these campaigns. The available reported (rating curve) flows (Q_r) are also presented in the table. In addition to manual flow measurements at gauges, both for those with and without rating curves, additional flow measurements at key locations were conducted during two of the periods: 2-Aug-08 to 12-Aug-08 and 4-Sep-09 to 17-Sep-09. Table 2.12 and Figure 2.25 show the locations and times of these additional flow measurements, as well as the measured flow.

The locations of the additional flow measurements were decided upon in collaboration with the WSC, so that important flow splits in the Delta were captured to aid in hydraulic understanding and modeling. Between 2-Aug-08 and 12-Aug-08 these additional measurements were taken downstream of Point Separation, and also spanned the West-Middle Connector Channel and the 10 kilometers upstream and downstream of the West-Middle Connector branch from the West Channel. Over 4-Sep-09 to 17-Sep-09, additional flow measurements were conducted both downstream of Point Separation and at the junctions of the Neklek and Reindeer Channels. The locations of those measurements that were taken on primary channels are noted in Table 2.13.

Table 2.11 Manual flow measurement campaigns at gauging stations operated by the WSC in the Mackenzie Delta.
Q_m - manual flow measurement(s) Q_r - average flow measurement from rating curve

Start date	End date	Flow condition	10LC002	10LC012	10LC013	10LC014	10LC015	10LC019	10LC021	10MC002	10MC003	10MC008	10MC010	10MC011	10MC022	10MC023	Additional	Number of days in period	Number of Q_m during period
23-Nov-06	23-Nov-06	Ice affected	Q_r			Q_mQ_r				Q_r								1	1
30-Jan-07	3-Feb-07	Ice affected	Q_mQ_r			Q_mQ_r				Q_r	Q_r	Q_r						5	2
10-Apr-07	12-Apr-07	Ice affected	Q_mQ_r			Q_mQ_r				Q_r	Q_r	Q_r						3	2
14-Jun-07	20-Jun-07	Open water	Q_mQ_r	Q_m		Q_r	Q_m	Q_m	Q_m	Q_r	Q_mQ_r	Q_mQ_r	Q_m	Q_m	Q_m	Q_m		7	12
2-Aug-07	2-Aug-07	Open water	Q_r		Q_m	Q_r				Q_r	Q_r	Q_r						1	1
29-Nov-07	6-Dec-07	Ice affected	Q_mQ_r			Q_mQ_r				Q_r	Q_r	Q_r						8	2
26-Feb-08	7-Mar-08	Ice affected	Q_mQ_r			Q_mQ_r				Q_r	Q_mQ_r	Q_mQ_r						11	4
23-Apr-08	2-May-08	Ice affected	Q_mQ_r			Q_mQ_r				Q_r	Q_mQ_r	Q_mQ_r						10	4
25-Jun-08	25-Jun-08	Open water	Q_r			Q_r				Q_r	Q_mQ_r	Q_mQ_r						1	2
11-Jun-08	11-Jun-08	Open water	Q_mQ_r			Q_r				Q_r	Q_r	Q_r						1	1
2-Aug-08	12-Aug-08	Open water	Q_mQ_r	Q_m	Q_m	Q_r	Q_m	Q_m	Q_m	Q_r	Q_mQ_r	Q_mQ_r	Q_m	Q_m	Q_m	Q_m	Q_m	11	20
24-Sep-08	24-Sep-08	Open water	Q_r			Q_r				Q_r	Q_mQ_r	Q_mQ_r						1	2
28-Nov-08	28-Nov-08	Ice affected	Q_mQ_r			Q_r				Q_r	Q_r	Q_r						1	1
8-Feb-09	11-Feb-09	Ice affected	Q_r			Q_mQ_r				Q_r	Q_mQ_r	Q_r						4	1
6-Mar-09	6-Mar-09	Ice affected	Q_mQ_r			Q_r				Q_r	Q_r	Q_r						1	1
13-Apr-09	24-Apr-09	Ice affected	Q_mQ_r			Q_r	Q_m			Q_r	Q_mQ_r	Q_mQ_r						12	3
5-May-09	11-May-09	Ice affected	Q_r			Q_mQ_r				Q_r	Q_r	Q_mQ_r						7	2
4-Sep-09	17-Sep-09	Open water	Q_r	Q_m		Q_r				Q_r	Q_r	Q_r					Q_m	14	8
10-Dec-09	17-Dec-09	Ice affected	Q_mQ_r			Q_mQ_r				Q_r	Q_mQ_r	Q_r						8	4
19-Jan-10	19-Jan-10	Ice affected	Q_r							Q_r	Q_r	Q_mQ_r						1	1
4-Mar-10	11-Mar-10	Ice affected	Q_mQ_r			Q_mQ_r				Q_r	Q_r	Q_r						8	2
Number of Q_m at each gauge			13	3	2	10	3	2	2	-	9	9	2	2	2	2			

Table 2.12 Additional discharge measurements (Q_m) taken by the WSC between 2-Aug-08 to 12-Aug-8 and 4-Sep-09 to 17-Sep-09.

Location	**Label in Figure 2.11**	**Date and Time**	**Discharge** (m^3/s)	**UTM Zone 8** (NAD83)
Peel River (West Channel) above Dry River	A	2-Aug-08 14:55	1415	516836 7503690
Peel River (West Channel) below Dry River	B	2-Aug-08 16:00	1384	517165 7504292
Peel Channel (West Channel) below Dry River	C	2-Aug-08 16:30	652	515857 7511051
Peel River (West-Middle Connector) at Mouth	D	2-Aug-08 17:05	707	520056 7508820
Mackenzie River above Peel River	E	2-Aug-08 19:30	1019	523950 7505651
Mackenzie River (Middle Channel) below East Channel	F	2-Aug-08 19:30	7961	533488 7521256
Little East Channel near Confluence	G	2-Aug-08 20:20	35.5	535125 7520585
East Channel at Confluence (adjacent 10LC015)	H	4-Sep-09 13:05	639	535748 7520215
Mackenzie River (Middle Channel) below East Channel	F	8-Sep-09 14:55	7390	532808 7521432
Mackenzie River above Peel River	I	9-Sep-09 13:45	1100	521932 7508396
Peel River (West-Middle Connector) at Mouth	D	9-Sep-09 14:47	433	520056 7508820
Mackenzie River (Middle Channel) above Neklek Channel	J	16-Sep-09 13:15	11300	513413 7641297
Mackenzie River - Neklek Channel	K	17-Sep-09 12:55	2250	506538 7651481
Mackenzie River - Reindeer Channel	L	17-Sep-09 13:51	4120	502885 7643610
Middle Channel below Reindeer Channel	M	17-Sep-09 15:08	4730	511486 7649871

Table 2.13 Location of additional flow measurements on primary channels taken by the WSC between 2-Aug-08 to 12-Aug-8 and 4-Sep-09 to 17-Sep-09.

Label in Figure 2.25	Channel	Station (km)
A	West Channel	58
B	West Channel	58.5
C	West Channel	68.5
D	West-Middle Connector Channel	66.8
F	Middle Channel	50.8
H	East Channel	51.5
J	Middle Channel	212.5
K	Middle Channel	225
L	Reindeerin Channel	230
M	Neklek Channel	225.5

Due to the large size of the Delta, it can take up to two weeks to conduct a full suite of flow measurements, and the highly variable backwater effects from tides, storm surges and ice ensure that no one set of data provides a perfect "snapshot" of the flows at a given point in time. However, these data still represent the most comprehensive flow distribution data ever collected in the Delta. Despite this, given the myriad of channels and highly variable flow conditions (both temporally and spatially), these data do have some limitations, which are expanded upon in the following sections.

Of the 21 flow measurement campaigns shown in Table 2.11, seven were conducted under open water conditions, while 14 took place during ice-affected conditions. Four of the open water campaigns and one of the ice-affected cases are of particular significance. During these five campaigns, manual measurements were conducted at locations without rating curves. These campaigns are highlighted in Table 2.11 and the flow measurements during each campaign period are shown in the following maps:

- Figure 2.26 – 14-Jun-07 to 20-Jun-07,
- Figure 2.27 – 2-Aug-07,
- Figure 2.28 – 2-Aug-08 to 12-Aug-08,
- Figure 2.29 – 4-Sep-09 to 17-Sep-09, and
- Figure 2.30 - 13-Apr-09 to 24-Apr-09 (ice-affected conditions).

Each map shows both the date and magnitude of measured flows (Q_m) and the range of flow over the period at each of the stations with rating curves ($\underline{Q_r}$).

The rating curve data did not agree with two of the manually measured flows (Q_m) during obtained 14-Jun-07 to 20-Jun-07, specifically those at the *Mackenzie River (Middle Channel) below Raymond Channel* (10MC008) and the *Mackenzie River (East Channel) at Inuvik* (10LC002). However, average rating curve values at these gauges were within 5% of the manual measurements, which is within the expected rating curve error. The remainder of the rating curve flows during each of the campaigns agreed with the manual flow measurements.

The intention was for measurement campaigns to be conducted during time periods when inflow was relatively unchanging (i.e. there was no runoff event), therefore, inflow changes during each period were considered. Flow hydrographs at each of the gauges for which there were rating curves, for a four week period centered on the middle of each measurement campaign, are shown in Figures 2.31 to Figure 2.35. These figures also illustrate the range of total inflow to the Delta (Figure a) during each measurement campaigns. Inflow data during each time period is also summarized in Table 2.14. The two open water campaigns in 2007 (14-Jun-07 to 20-Jun-07 and 2-Aug-07) had similar inflows (~10% difference in average). Those conducted from 2-Aug-08 to 12-Aug-08 and from 4-Sep-09 to 17-Sep-09 also had similar inflow to each other (<1 % difference in average), though they were not as large as the inflows recorded in 2007. The measurement campaign between 4-Sep-09 and 17-Sep-09 had the largest range of inflow over the period, but this was also the longest measurement campaign (14 days). Table 2.15 illustrates the percent changes in inflow over each period; that is, the ratio of the range of flows recorded over the period to the average flow during the period. Though the measurement campaign from 4-Sep-09 to 17-Sep-09 had the largest percent change during the period, the percent change per day was within the range found for the remaining periods.

Table 2.14 List of inflow to the Mackenzie Delta during the five periods with manual flow measurements at gauges without rating curves. (Data source: the WSC).

Start of Period	**End of Period**	**# of days**	**Averaged inflow over period** (m^3/s)	**Maximum inflow** (m^3/s)	**Minimum inflow** (m^3/s)	**Range over period** (m^3/s)
14-Jun-07	20-Jun-07	7	23512	24022	22107	1916
2-Aug-07	2-Aug-07	1	21316	21674	20970	704
2-Aug-08	12-Aug-08	11	14707	15710	14088	1622
4-Sep-09	17-Sep-09	14	14832	17277	13119	4158
13-Apr-09	24-Apr-09	12	3517	3621	3445	176

Table 2.15 List of inflow changes to the Mackenzie Delta during the five periods with manual flow measurements at gauges without rating curves. (Data source: the WSC).

Start of Period	**End of Period**	**Percent flow change over period**	**Average percent change in flow per day**
14-Jun-07	20-Jun-07	8.1%	1.2%
2-Aug-07	2-Aug-07	3.3%	3.3%
2-Aug-08	12-Aug-08	11.0%	1.0%
4-Sep-09	17-Sep-09	28.0%	2.0%
13-Apr-09	24-Apr-09	5.0%	0.4%

Table 2.16 also summarizes the flows shown in Figures 2.26 to 2.30, which were used for the modeling effort described in Chapter 4. The table shows the manually measured flow (Q_m), as well as the location of measurement along each of the primary channels for each measurement period. For locations with rating curves the average rating curve flow reported over the period is shown. The rating curve flow was chosen as it is more indicative of the flow over the entire campaign period and could, therefore, more meaningfully be compared to average inflow over the campaign period, as discussed in the following section.

Table 2.16 Manually measured flows along the primary channels during the five periods with manual flow measurements at gauges without rating curves. (Data source: the WSC).

Channel	**Gauge/Name**	**Station** (km)	**Q_m or Q_r** (m^3/s)				
			14-Jun-07 to 20-Jun-07	**02-Aug-07**	**2-Aug-08 to 12-Aug-08**	**4-Sep-09 to 17-Sep-09**	**13-Apr-09 to 24-Apr-09**
Middle	10LC014	0.0	22568	20578	13220	13665	3447
	F	50.8			7961	7390	
	10MC008	110.5	17903	17000	12003	12001	3217
	J	212.5				11300	
	K	225.0				2250	
	10MC010	245.0	6280		5020		
	10LC019	285.0	2830		2326		
East	H	51.2				639	
	10LC015	52.2	1110		577		639
	10LC002	144.2	397	358	241	240	15.3
	10LC013	283.2		4040	3718		
West	10MC002	0.0	944	738	1487	1167	70.1
	10MC022	53.0	725		1433		
	A	58.0			1384		
	B	58.5			1415		
	C	68.5			652		
	10MC003	173.0	1179	1015	908	703	196
West-Middle Connector	D	66.8			707	433	
Napoiak	10MC023	188.8	1010		632		
Reindeer	L	230.0				4120	
	10MC011	276.5	4630		2945		
Neklek	M	225.5				4730	

2.3.3 Flow Comparison to Total Delta Inflow over Measurement Campaigns

A map showing the rating curve and manually measured flows as percentages of the average total inflow to the Delta over each measurement campaign is presented for each period in Figures 2.36 to 2.40. These maps show that the percentages of flow at the measurement sites were very similar between the two 2007 open water measurement periods. This was expected as the inflow during these two periods was only ~10% different and changes in channel morphology would not be expected in the two months between the measurement campaigns. For the 2008 and 2009 campaigns, the manual flow measurement percentages (in terms of total Delta inflow) were also very similar.

Figure 2.41 shows a map compiling the ranges in percentages of total Delta inflow at each location for the four open water campaigns. The range in manual flow measurement (in terms of total Delta inflow) are shown for all but the five gauges with rating curves, where the range in flow (in terms of the total Delta inflow) over the entire open water period is shown. The black symbols show the number of flow measurements that the average and range of percentages were based upon and are, therefore, indicative of the confidence in the percent range shown. A comparison of the flow splits measured in the Turtle area (Table 2.17) shows that measurements in this area were relatively consistent when compared to the total Delta inflow. Of the flow percentages manually measured in the upper delta, the *Peel River at Frog Creek* (10MC022) had a largest range (3.1% to 9.8%

in terms of total Delta inflow), though the flow recorded upstream at the *Peel River above Fort McPherson* (10MC002) also had a large range in flow between these two periods (2.8 to 15% in terms of total Delta inflow).

Table 2.17 Open water flow splits measured in the Turtle area as percentage of total inflow to the Delta. (Data source: the WSC).

Measurement Campaign	**Secondary Channel B**	**East Channel** (just d/s of Middle Channel)	**Middle Channel** (just d/s of East Channel)	**West-Middle Connector Channel** (between *km* 64.8 and 68.8)
14-Jun-07 to 20-Jun-07		4.7% at *km* 52.2		
2-Aug-08 to 12-Aug-08	6.9%	3.9% at *km* 52.2	54.1% at *km* 50.8	4.8% at *km* 66.8
4-Sep-09 to 17-Sep-09	7.4%	4.3% at *km* 51.5	49.8% at *km* 50.8	2.9% at *km* 66.8

Flow distributions through the Quadrapus were not consistent during open water measurements. In particular, this inconsistency was observed in 2009 when flow measurements were conducted very close to the Middle Channel on each leg of the Quadrapus, as shown in Figure 2.42 (later referred to as Quadrapus Flow Scenario B in Chapter 4). The percentage of total Delta inflow measured through the Quadrapus is also summarized in Table 2.18, including the flow split measured by Fassnaught (1993b). In 2009, a significantly (~10-20%) lower flow percentage (in terms of total Delta inflow) was measured on the Middle Channel downstream of the Quadrapus when compared to the other periods. Flow splits on both the Neklek and Reindeer Channels were also different, though the Neklek Channel was only measured once during the study period. It is not known whether these measurement differences are due to a natural (and significant) variability in the flow distribution through the Quadrapus or whether they are simply related to conducting measurements at different location (ie: because of losses (gains) to (from) other intermediate channels). Additional flow distribution measurements, both at the Quadrapus and at the downstream gauges during the same time frame are suggested to clarify this issue.

Table 2.18 Open water flow splits measured through the Quadrapus as percentage of total inflow to the Delta. (Data source: the WSC and Fassnaught (1993b)).

Measurement Campaign	**Middle Channel** (u/s of the Quadrapus)	**Neklek Channel**	**Reindeer Channel**	**Middle Channel** (d/s of the Quadrapus)
14-Jun-07 to 20-Jun-07	-	-	19.7% at *km* 276.5	26.7% at *km* 245
2-Aug-08 to 12-Aug-08	-	-	20.0% at *km* 276.5	34.1% at *km* 245
4-Sep-09 to 17-Sep-09	76.2% at *km* 212.5	31.9% at *km* 225.5	27.8% at *km* 230	15.2% at *km* 225
Fassnaught (1993b)	80%	20% (locations not specified)	30%	30%

A map showing the range of inflow percentages measured for the ice-affected season (from November to April) is shown in Figure 2.43. This figure illustrates the lack of manual flow measurements during the winter season, as the split of the East Channel was the only manual flow measurement under ice at a site without a rating curve. Though this manual flow measurement (shown in Figures 2.30 and 2.40) was of similar magnitude to that recorded during the summer months, it accounted for nearly four times the relative inflow (in terms of the total Delta inflow reported during the period). Additional winter measurements at this location are needed to confirm whether this is the typical flow split during winter at this junction. In addition, Anderson and Anderson (1974) documented reversing flow on the West-Middle Connector Channel (from *km* 64.8 to *km* 68.8) during two of three measurements conducted during winter. Reversing flows at this location were also recorded by Mackay (1963). Additional flow measurements during the winter months are suggested at the junction of the West and West-Middle Connector Channel junction (~*km* 64 to 68), as this channel junction was not measured during the ice-affected season in this study.

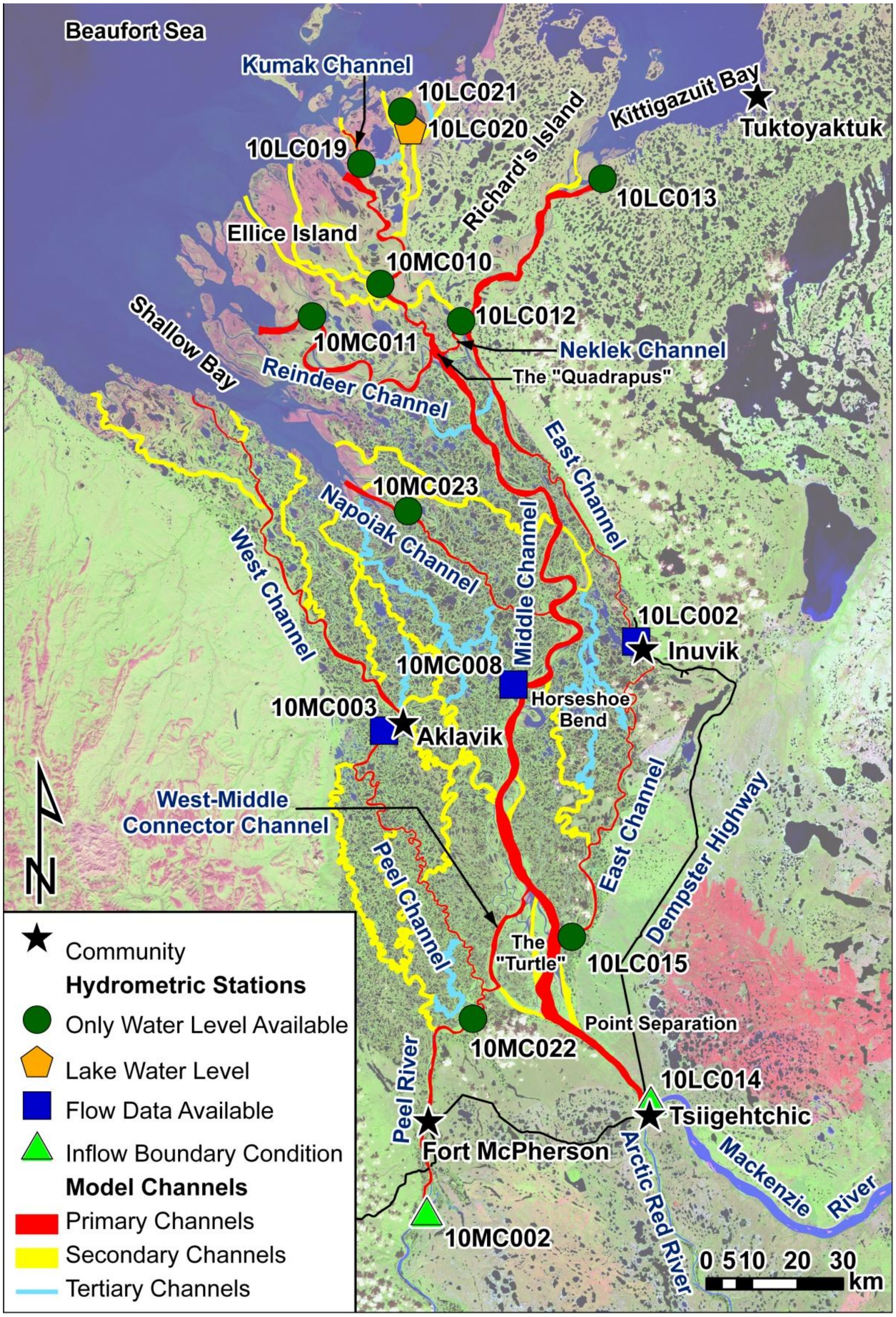

Figure 2.1 Location map of the Mackenzie Delta, including hydrometric monitoring stations operated by the WSC, and primary channel names (adapted from Nafziger *et al*., 2009).
(Base image source: Industry Tourism and Investment, NWT).

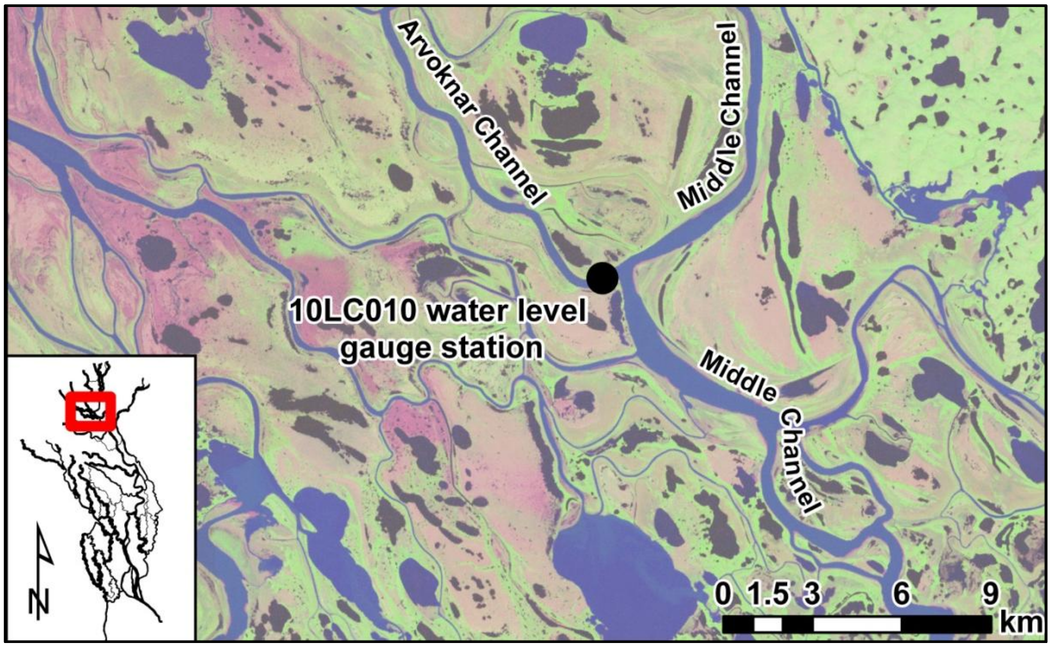

Figure 2.2 Location of water level measurement at the WSC station *Mackenzie River (Outflow Middle Channel) below Langley Island* (10MC010).
(Data source: the WSC).
(Base image source: Industry Tourism and Investment, NWT).

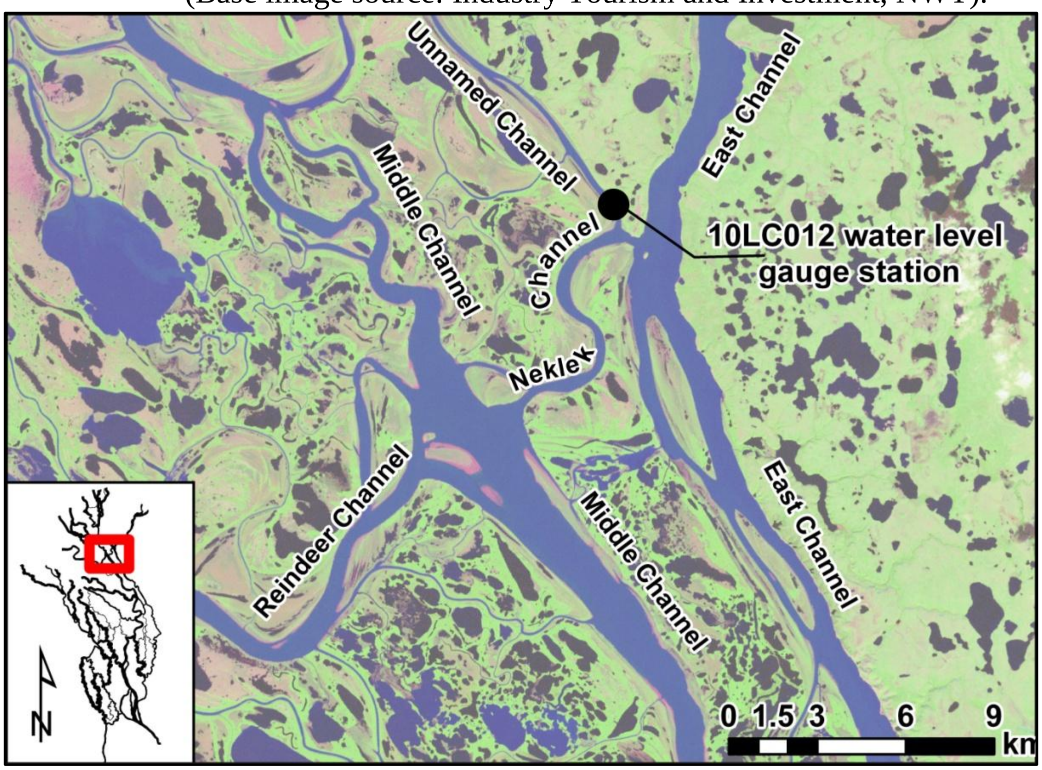

Figure 2.3 Location of water level measurement at the WSC station *Mackenzie River (Middle Channel) at Tununuk Bay* (10LC012).
(Data source: the WSC).
(Base image source: Industry Tourism and Investment, NWT).

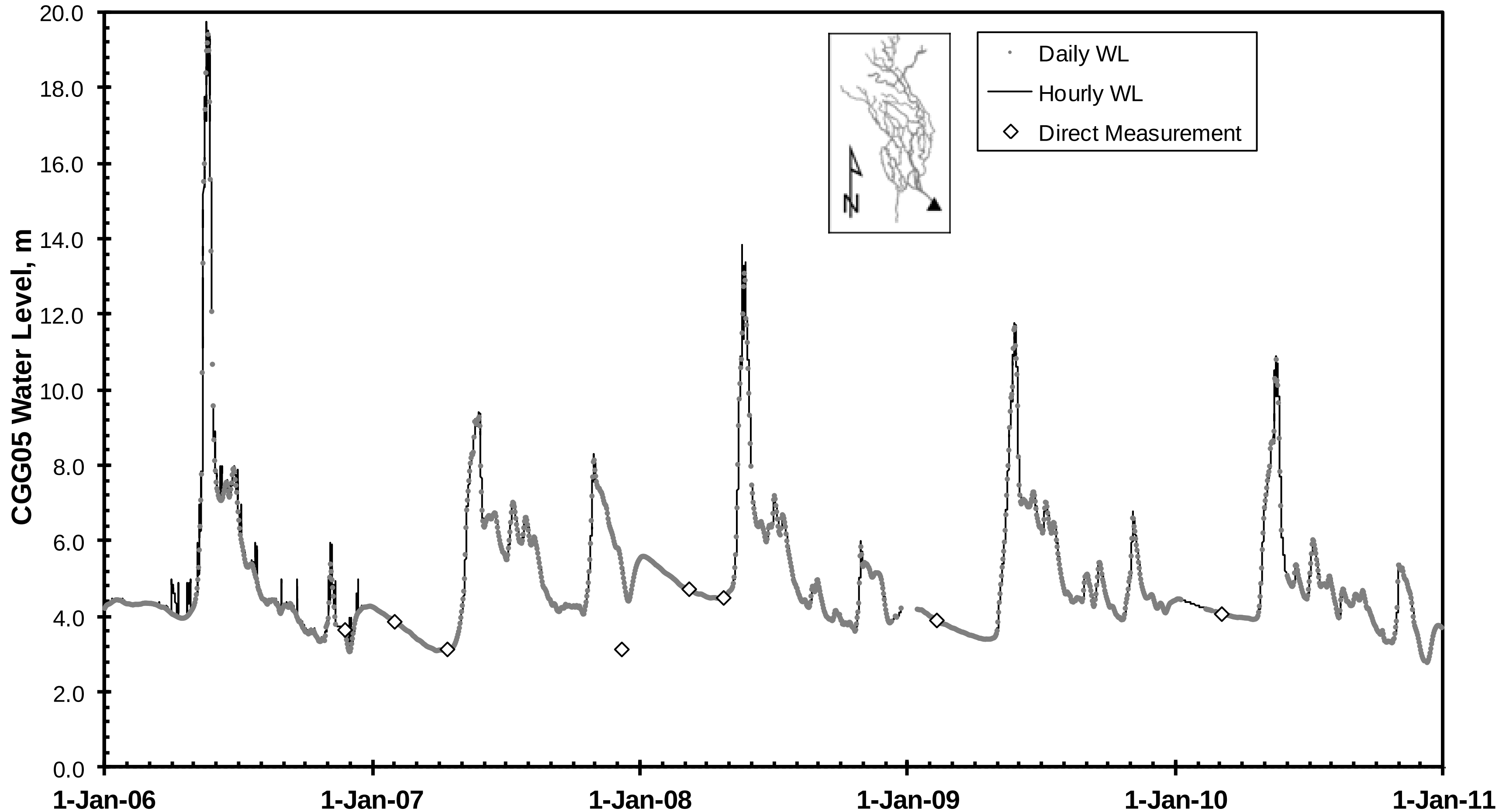

Figure 2.4 Example of continuous water level available at Water Survey of Canada gauge *Mackenzie River at Arctic Red River* (10LC014) from 2006 to 2010. (Data source: the WSC).

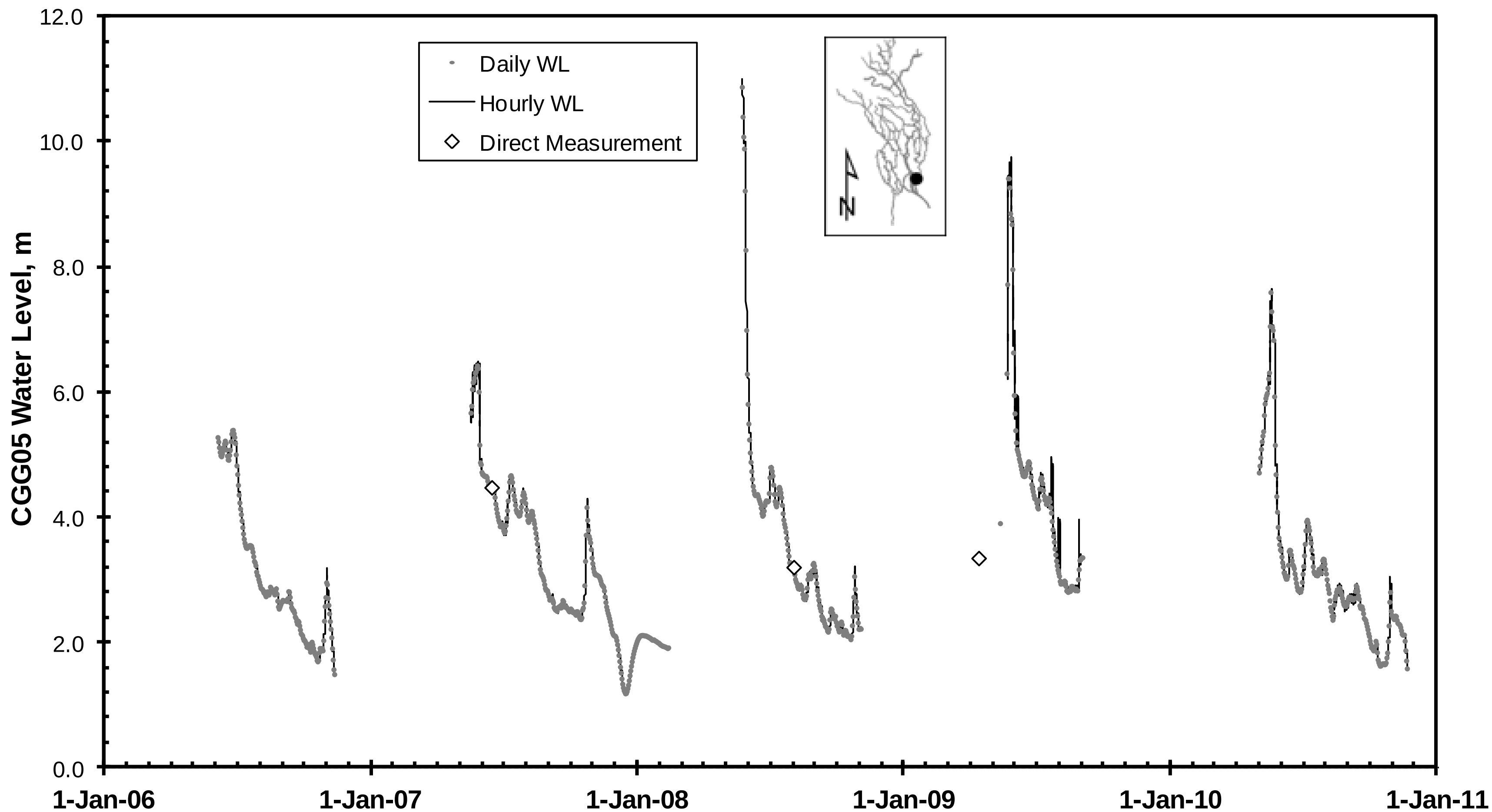

Figure 2.5 Example of intermittent water levels available at Water Survey of Canada gauge at *Mackenzie River at Confluence East Channel* (10LC015) from 2006 to 2010. (Data source: the WSC).

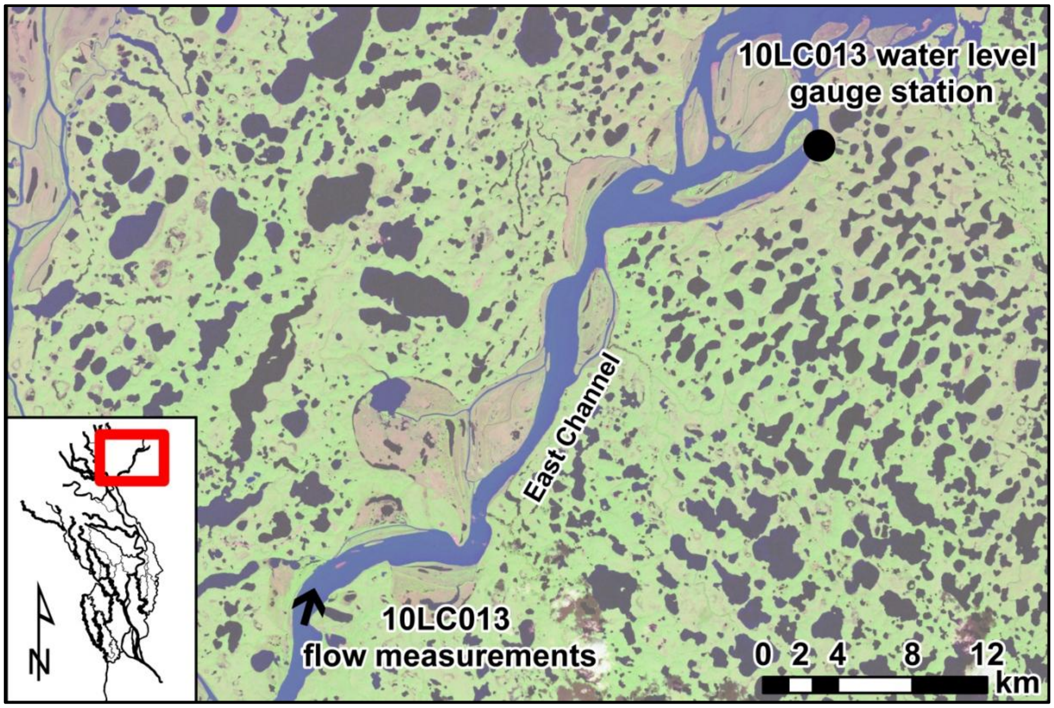

Figure 2.6. Location of flow measurements at the WSC station the .
(Data source: the WSC).
(base image source: Industry Tourism and Investment, NWT)

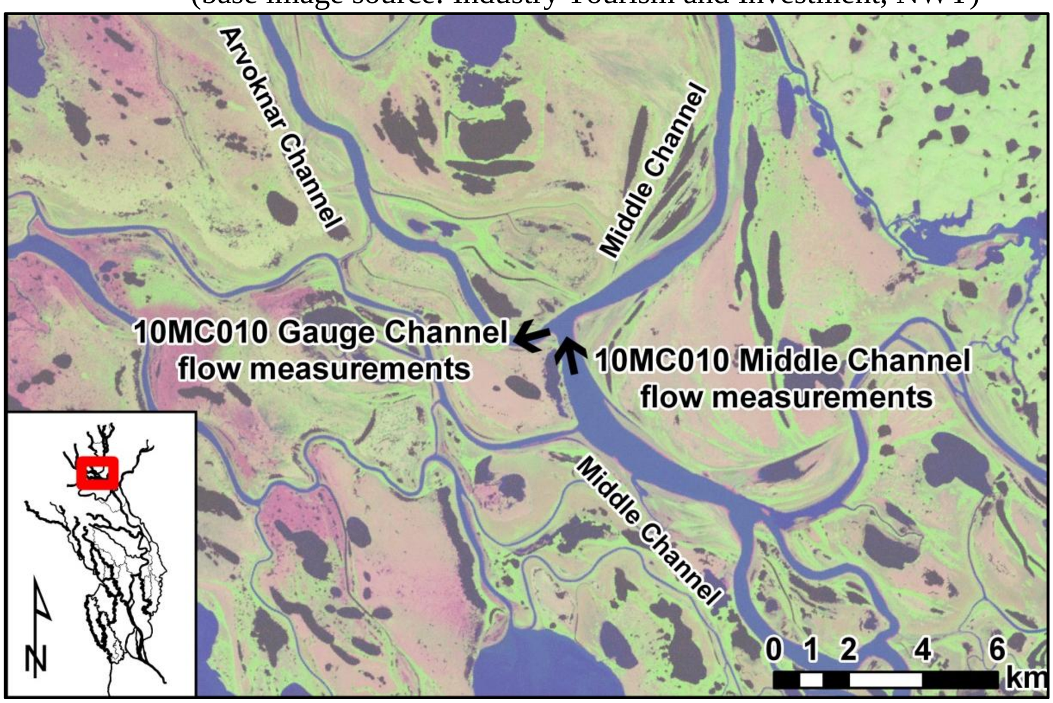

Figure 2.7 Location of flow measurements at the WSC station the *Mackenzie River (Outflow Middle Channel) below Langley Island* (10MC010).
(Data source: the WSC).
(base image source: Industry Tourism and Investment, NWT)

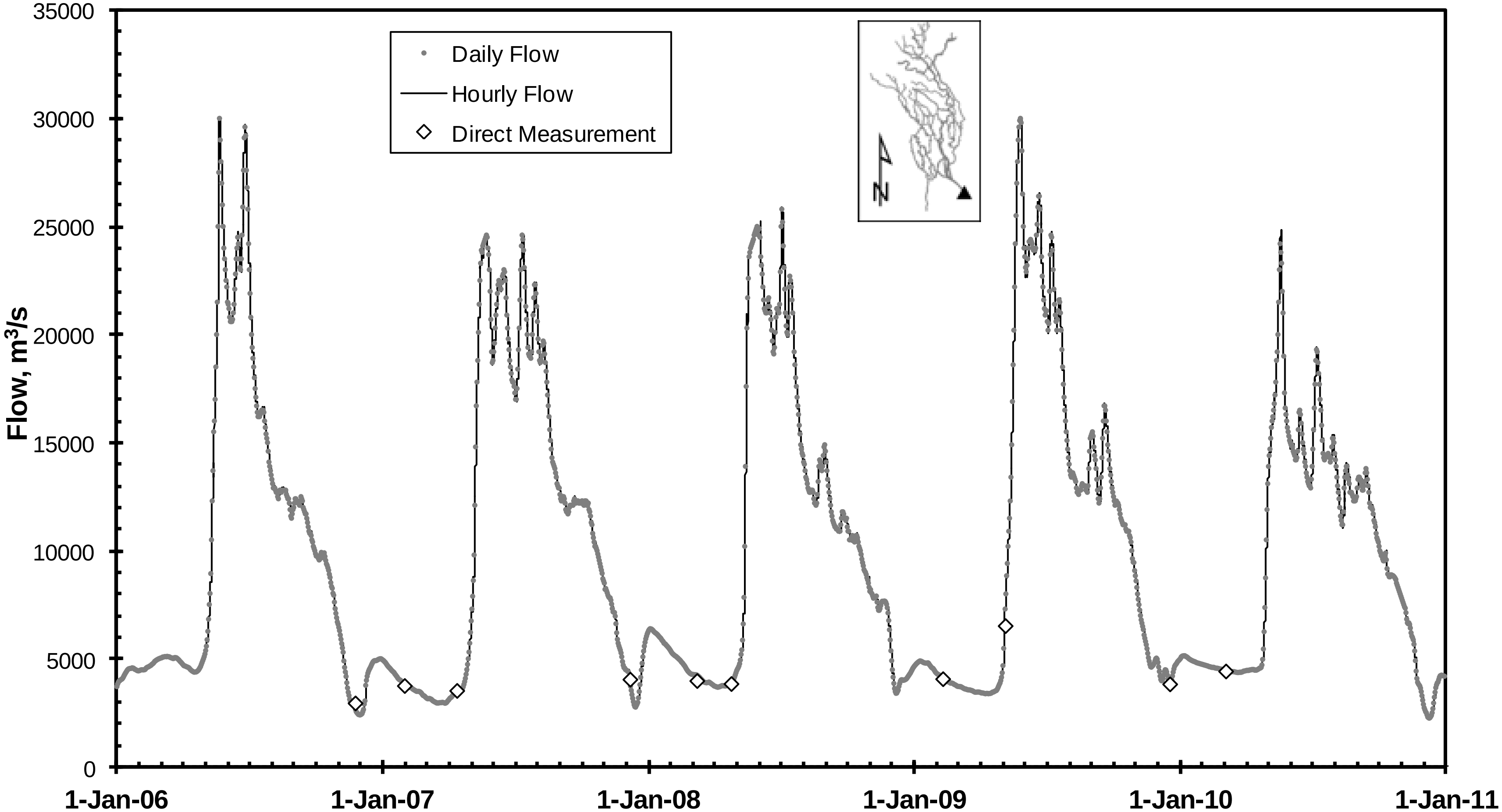

Figure 2.8 Discharge hydrograph from 2006 to 2010 at the WSC gauge *Mackenzie River at Arctic Red River* (10LC014). (Data source: the WSC).

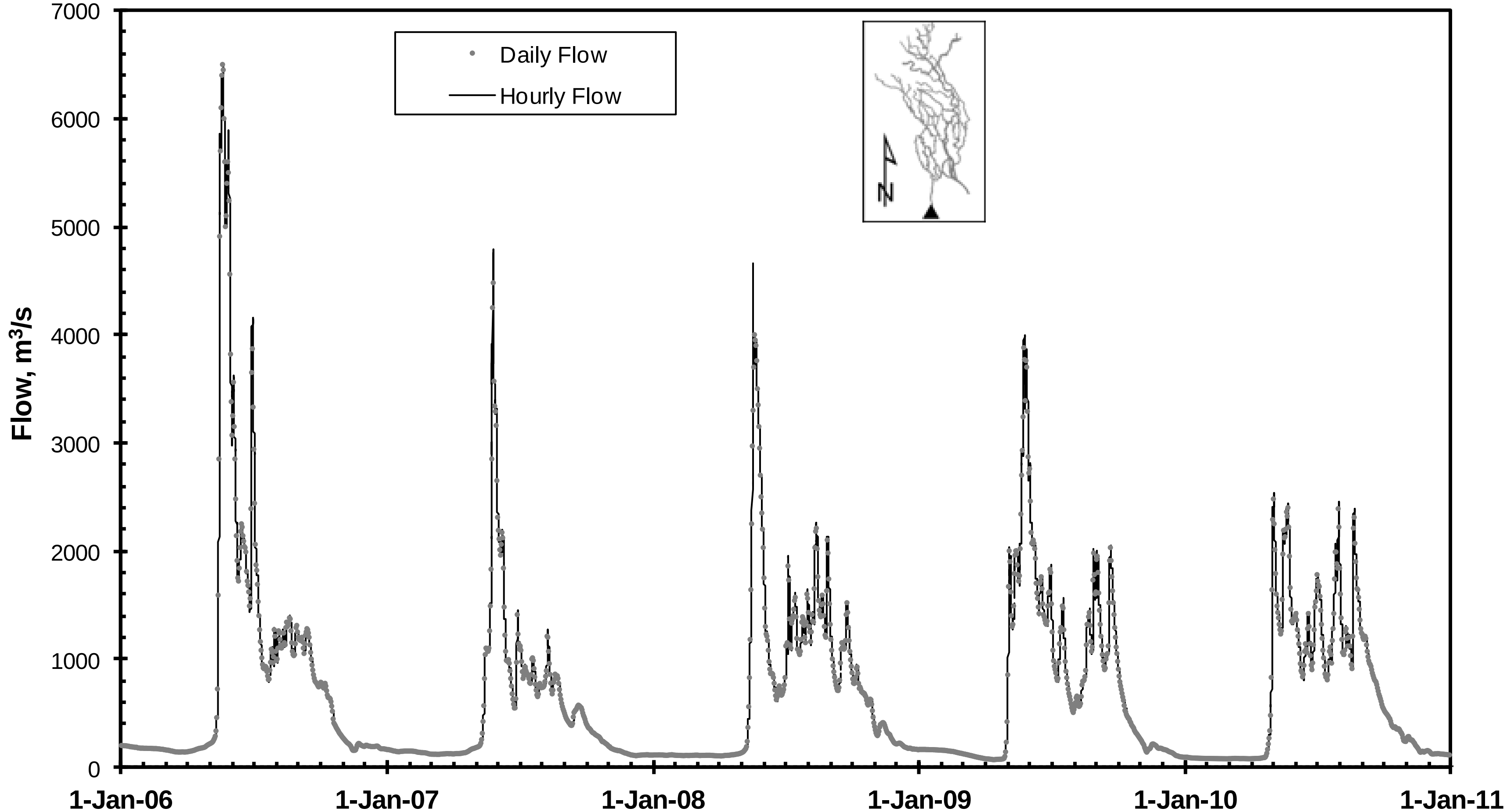

Figure 2.9 Discharge hydrograph from 2006 to 2010 at WSC gauge at *Peel River above Fort McPherson* (10MC002). (Data source: the WSC).

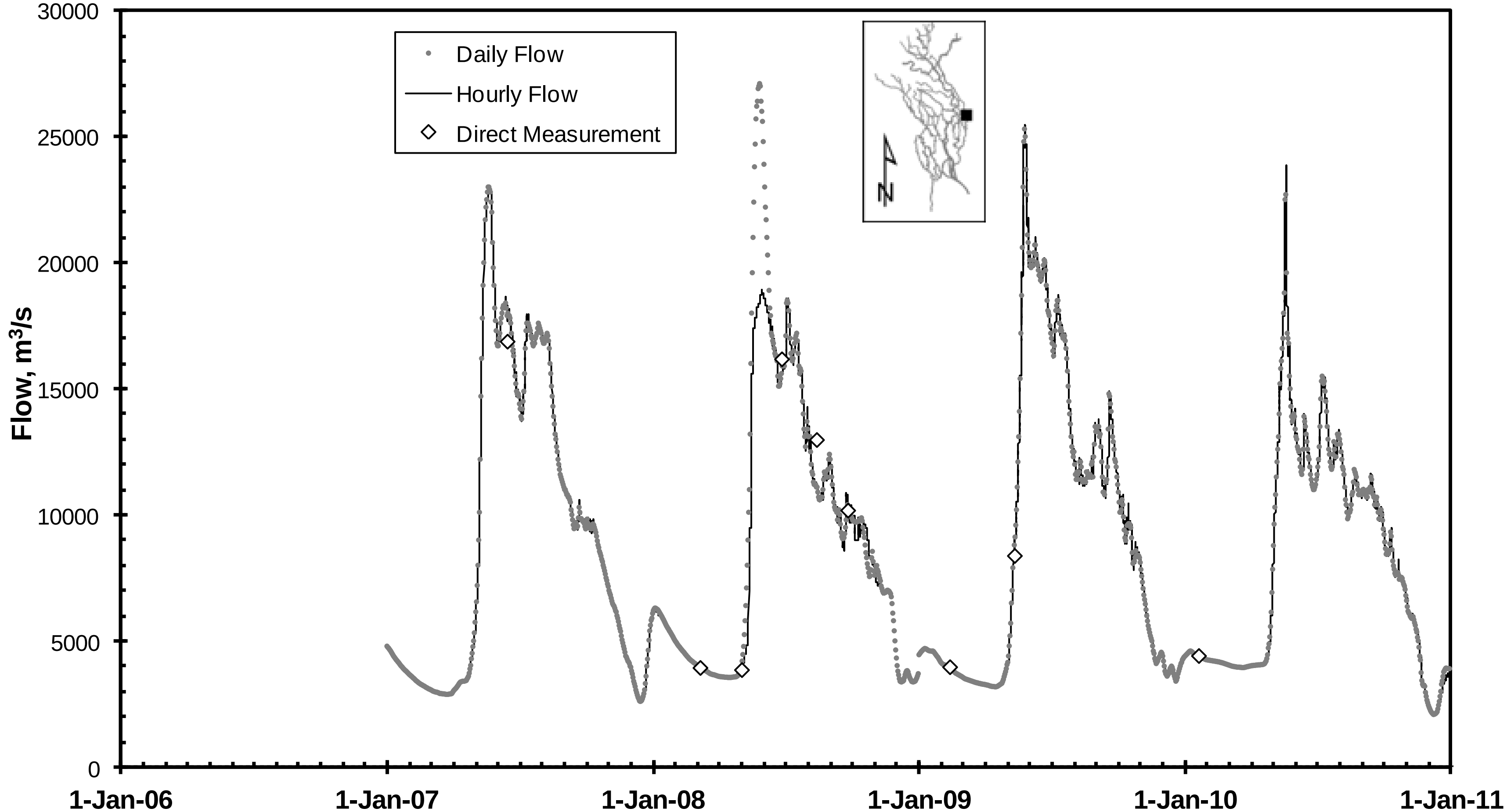

Figure 2.10 Discharge hydrograph from 2006 to 2010 at the WSC gauge *Mackenzie River (Middle Channel) below Raymond Channel* (10MC008). (Data source: the WSC).

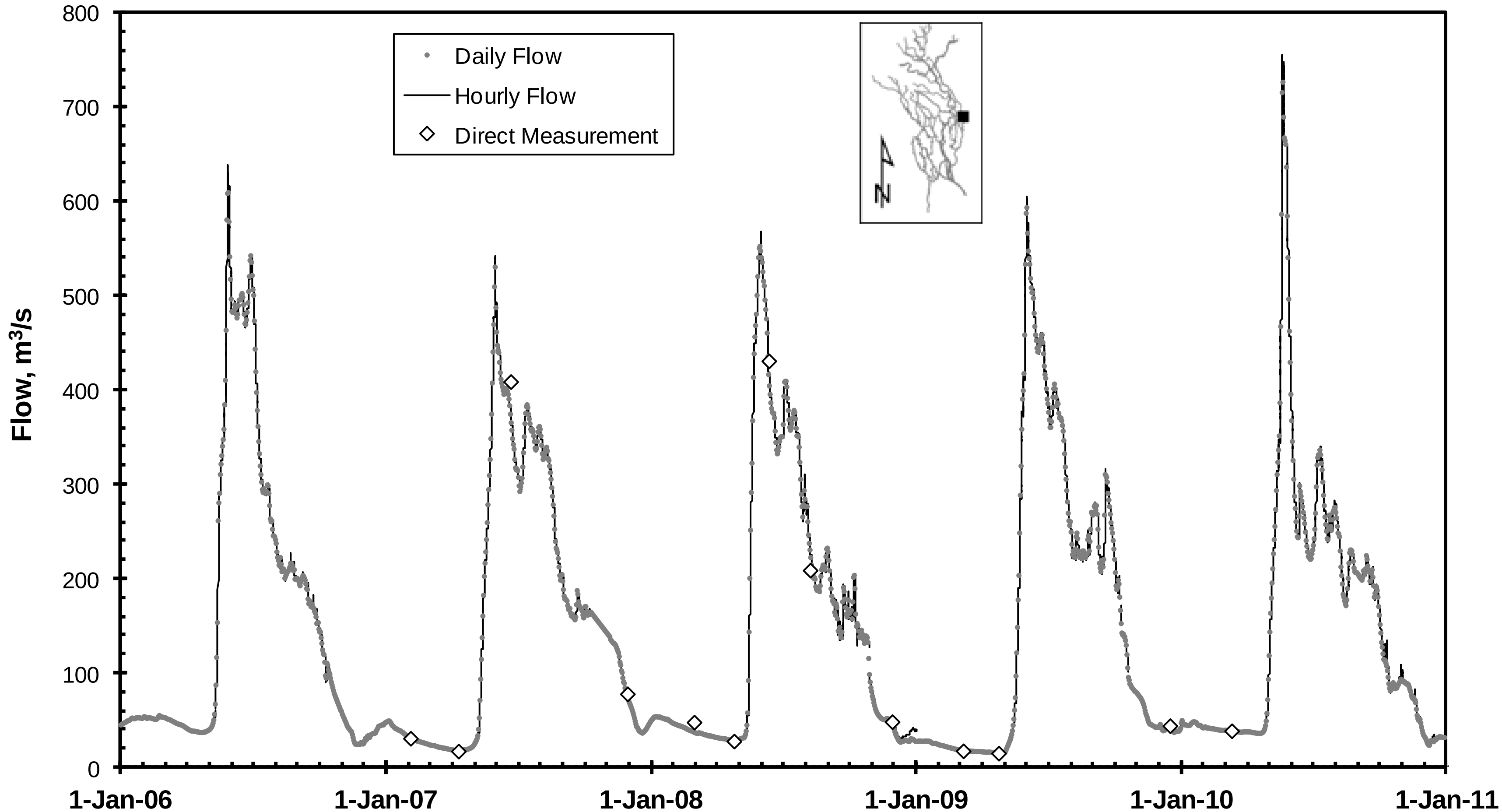

Figure 2.11 Discharge hydrograph from 2006 to 2010 at the WSC gauge *Mackenzie River (East Channel) at Inuvik* (10LC002). (Data source: the WSC).

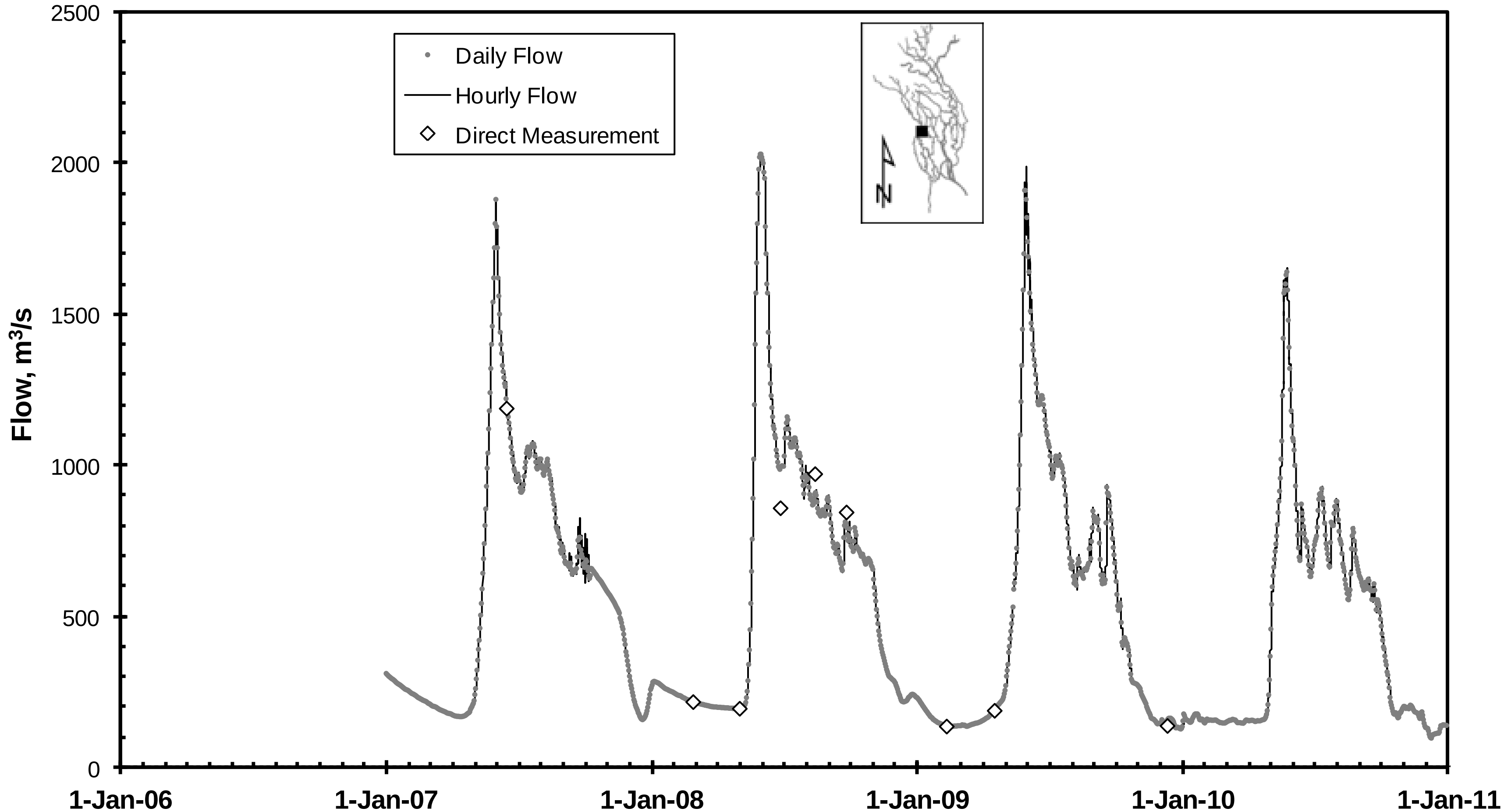

Figure 2.12 Discharge hydrograph from 2006 to 2010 at the WSC gauge *Mackenzie River (Peel Channel) above Aklavik* (10MC003). (Data source: the WSC).

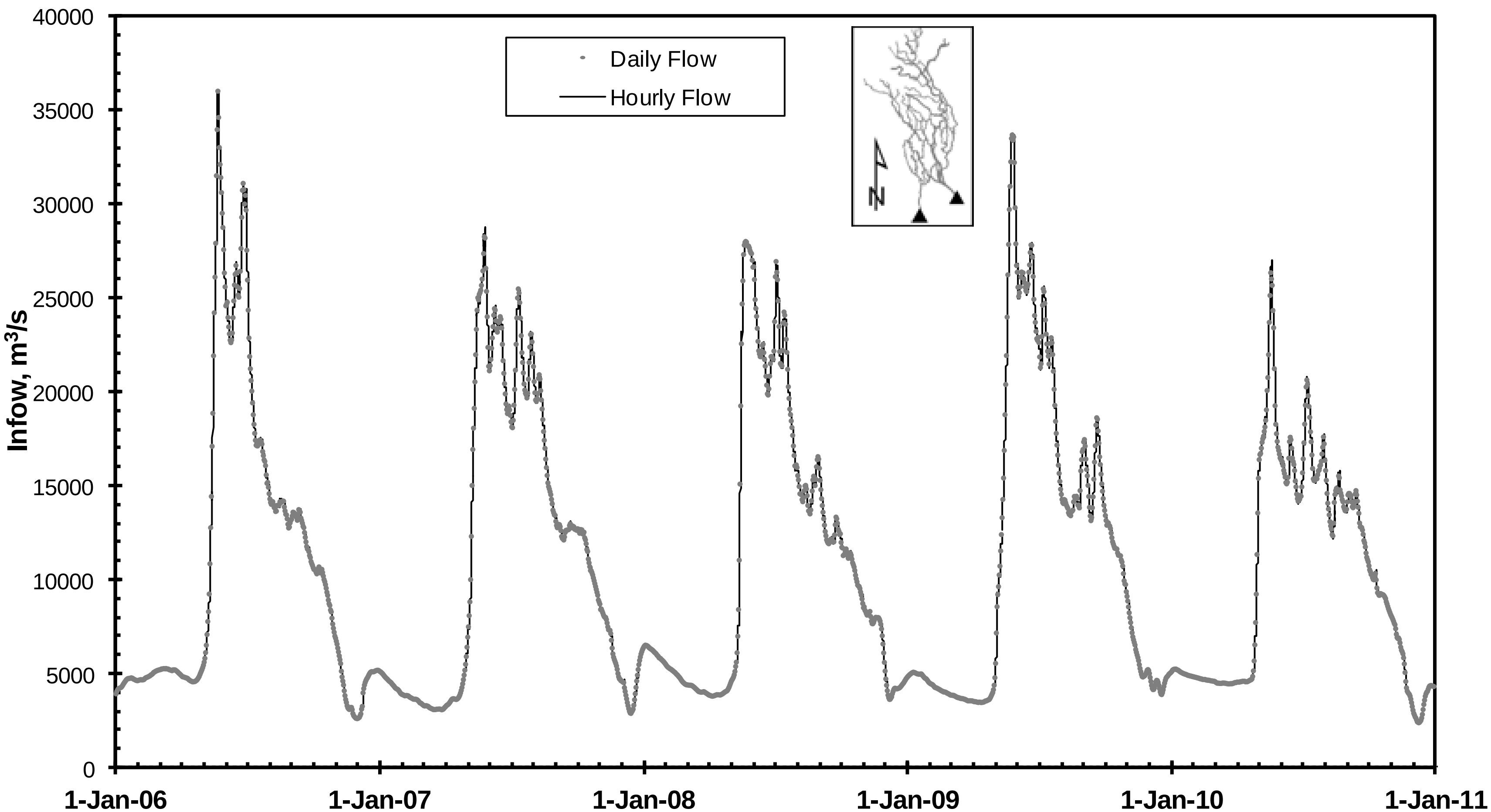

Figure 2.13 Inflow to the Mackenzie Delta from 2006 to 2010 (sum of flow at the WSC stations *Mackenzie River at Arctic Red River* (10LC014) and *Peel River above Fort McPherson* (10MC002)). (Data source: the WSC).

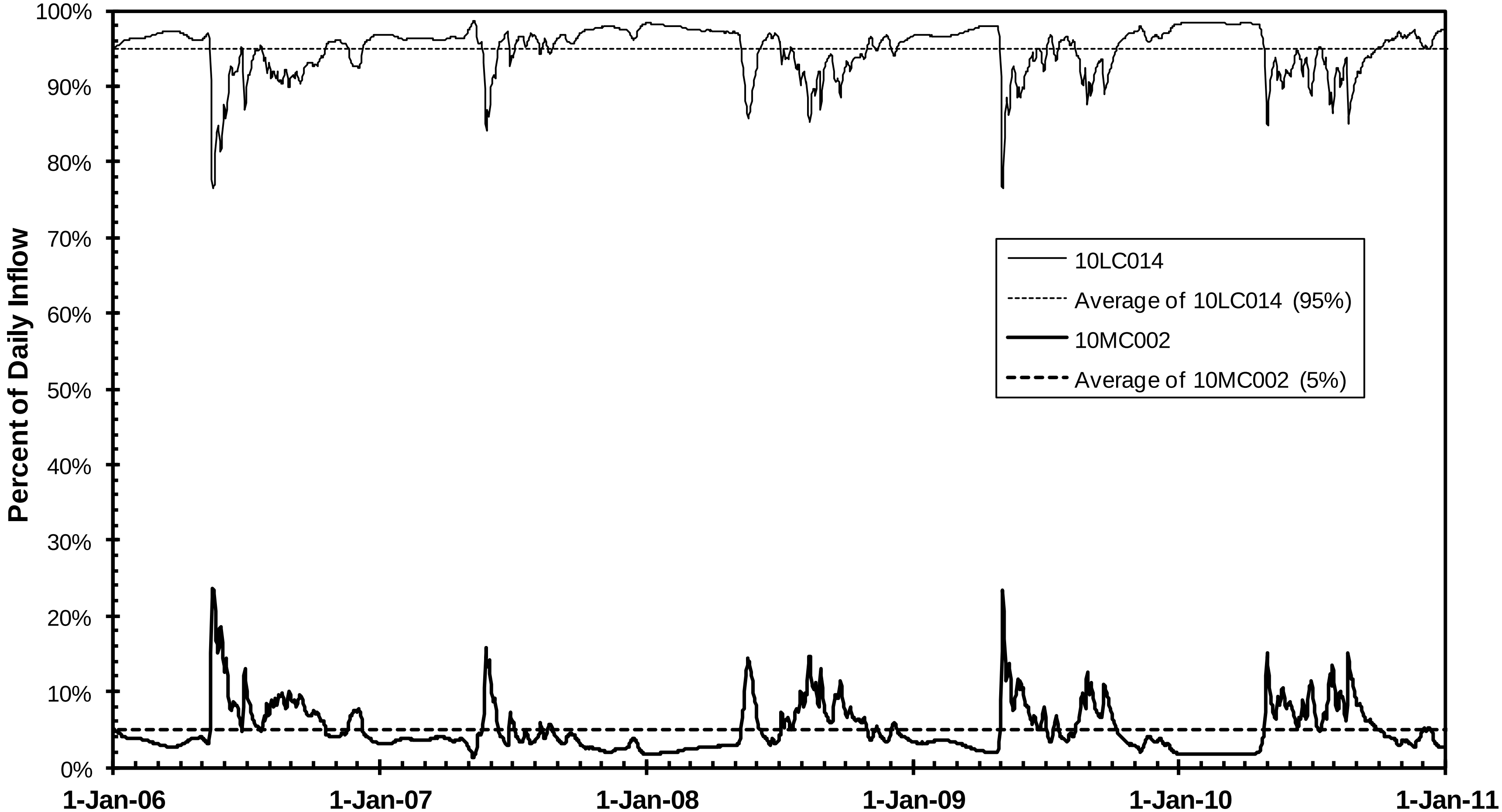

Figure 2.14 Daily percentage of inflow from *Mackenzie River at Arctic Red River* (10LC014) and *Peel River above Fort McPherson* (10MC002) over study period from 2006 to 2010. (Data source: the WSC).

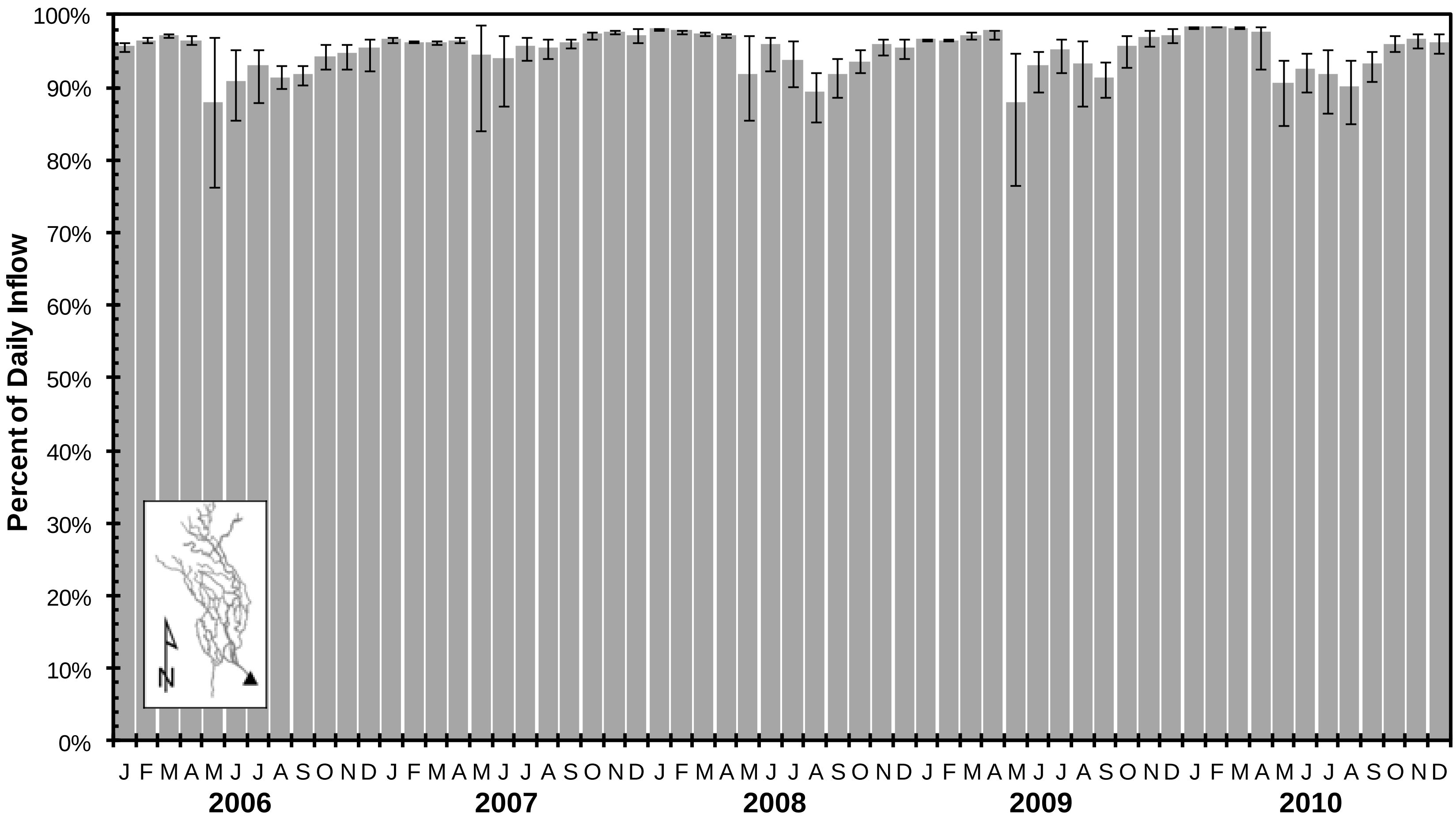

Figure 2.15 Daily percentage of inflow at *Mackenzie River at Arctic Red River* (10LC014) averaged over each month of the study period. Error bars show the range of percent over each month. (Data source: the WSC).

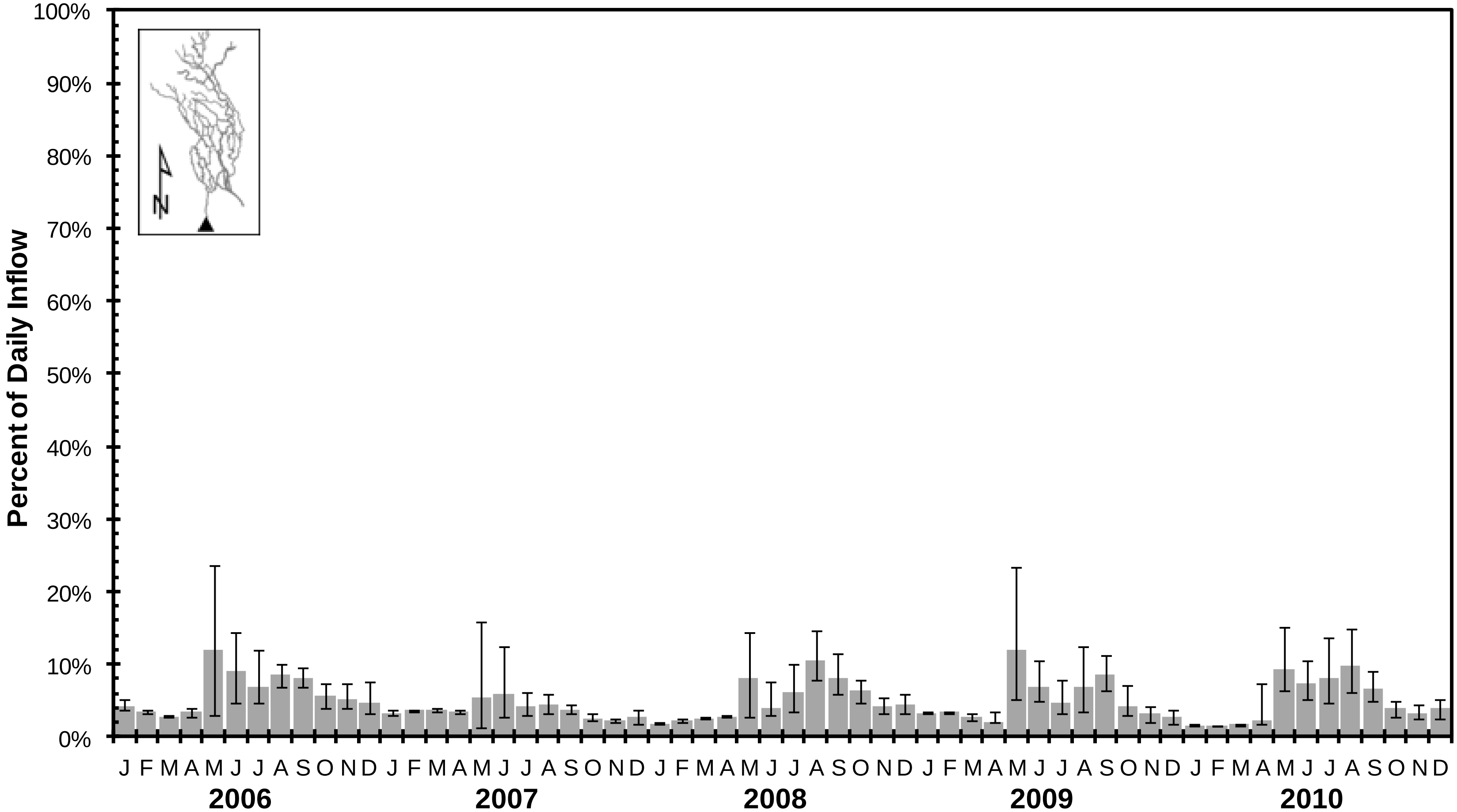

Figure 2.16 Daily percentage of inflow at *Peel River above Fort McPherson* (10MC002) averaged over each month of the study period. Error bars show the range of percent over each month. (Data source: the WSC).

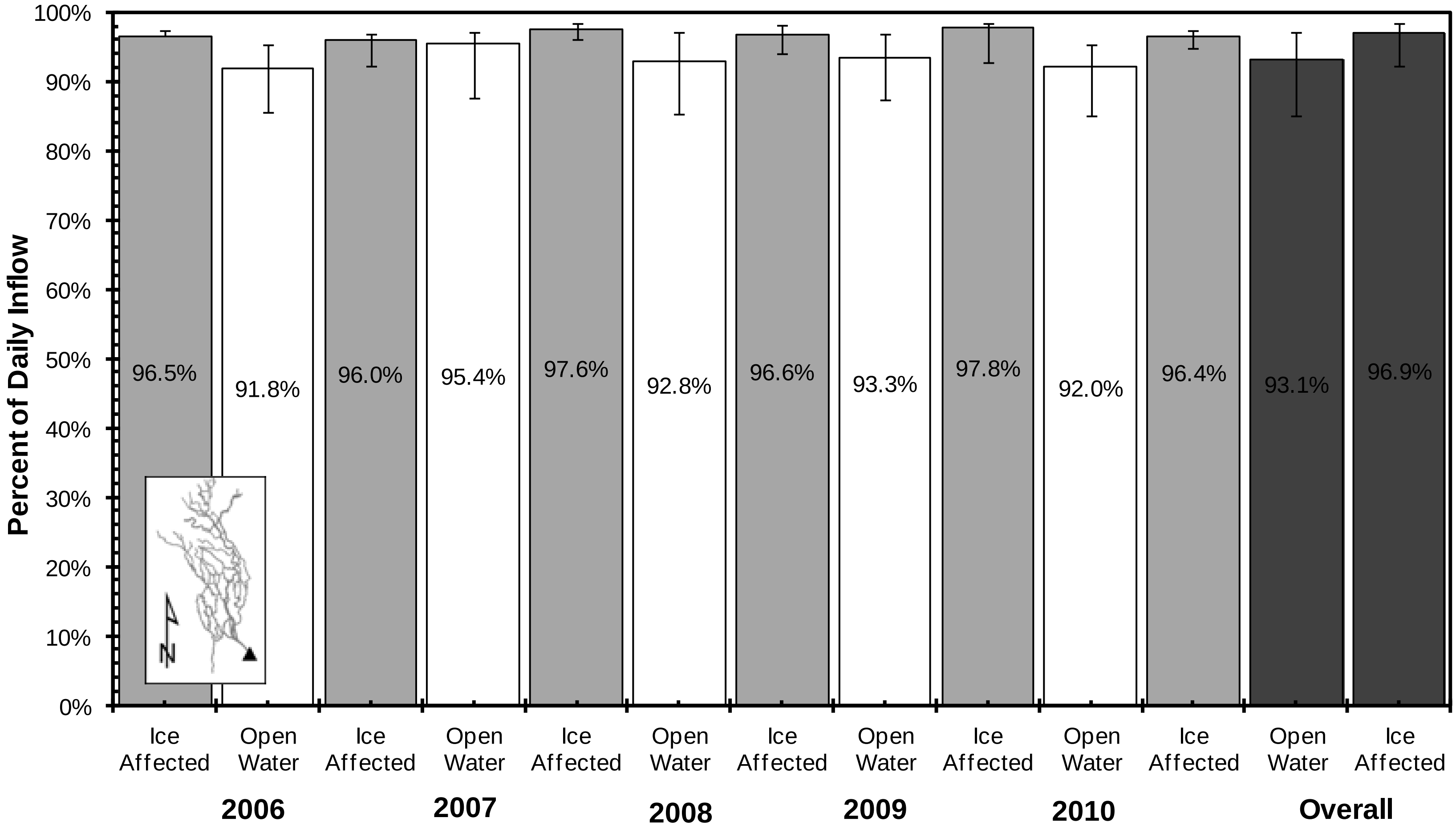

Figure 2.17 Daily percentage of inflow at *Mackenzie River at Arctic Red River* (10LC014) averaged over the open water season (assumed June to September) and ice affected season (assumed November to April). Error bars show the range of percent over each season. (Data source: the WSC).

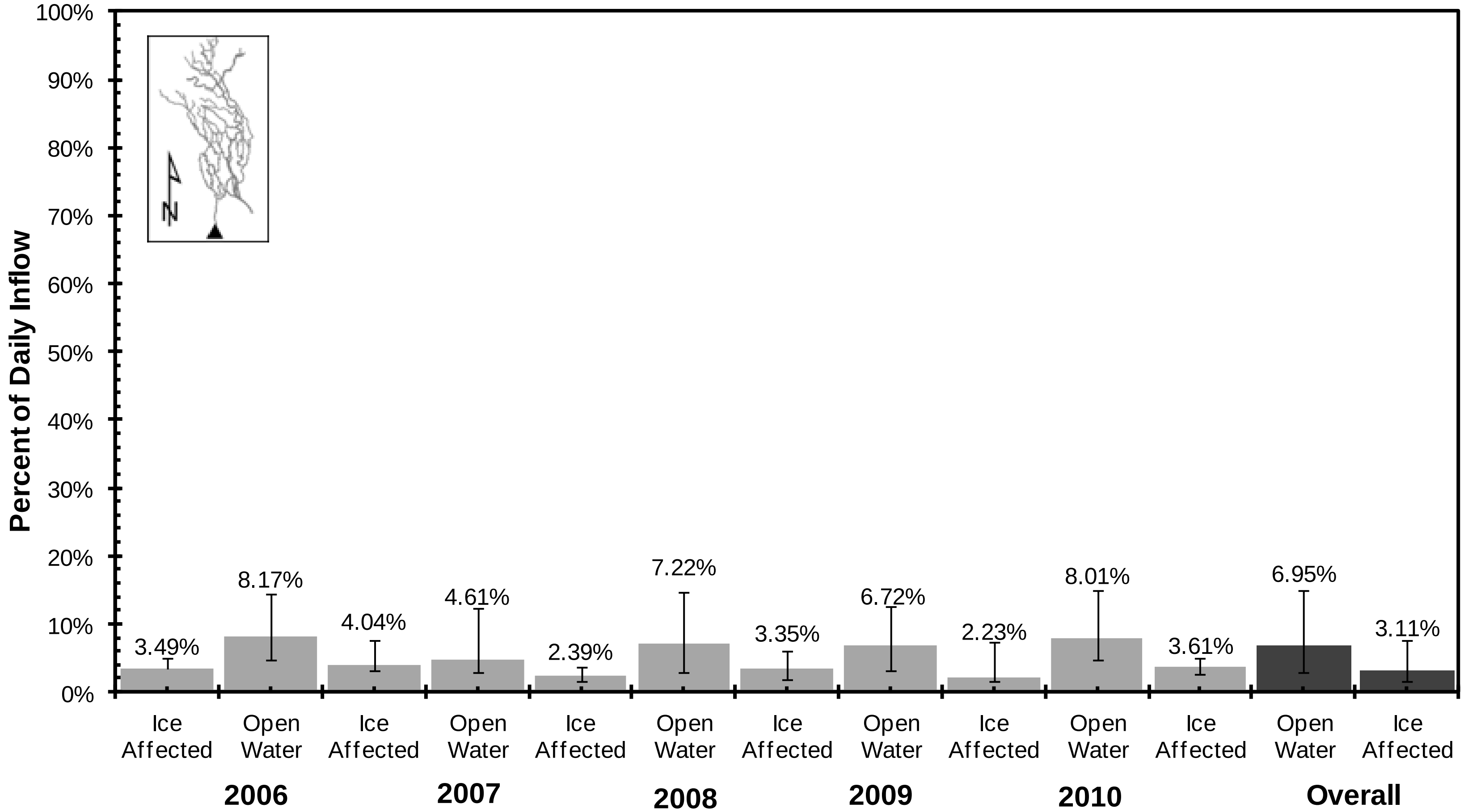

Figure 2.18 Daily percentage of inflow at *Peel River above Fort McPherson* (10MC002) averaged over the open water season (assumed June to September) and ice affected season (assumed November to April). Error bars show the range of percent over each season. (Data source: the WSC).

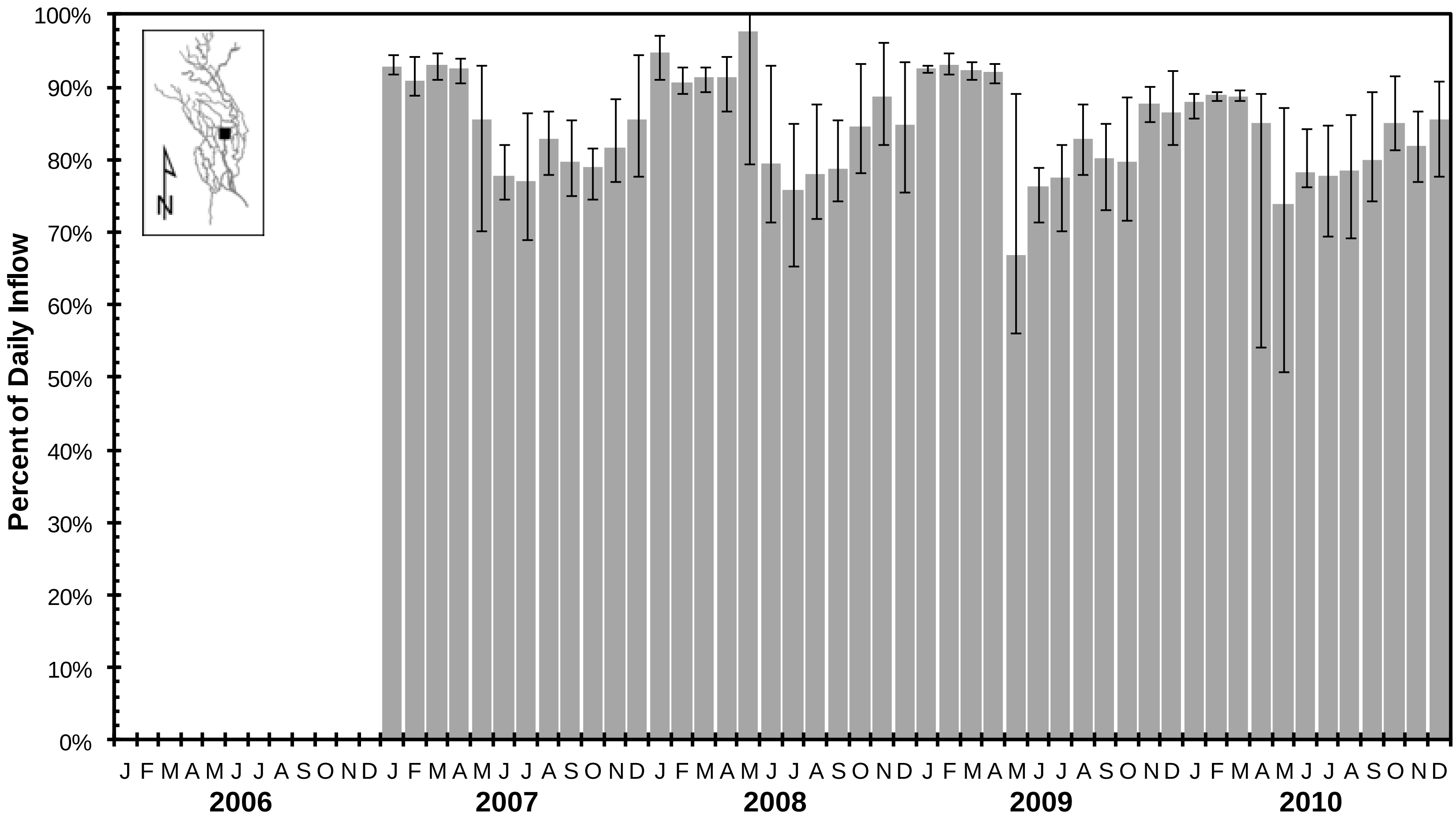

Figure 2.19 Daily percentage of inflow averaged over each month of the study period at *Mackenzie River (Middle Channel) below Raymond Channel* (10MC008). Error bars show the range of percent over each month. (Data source: the WSC).

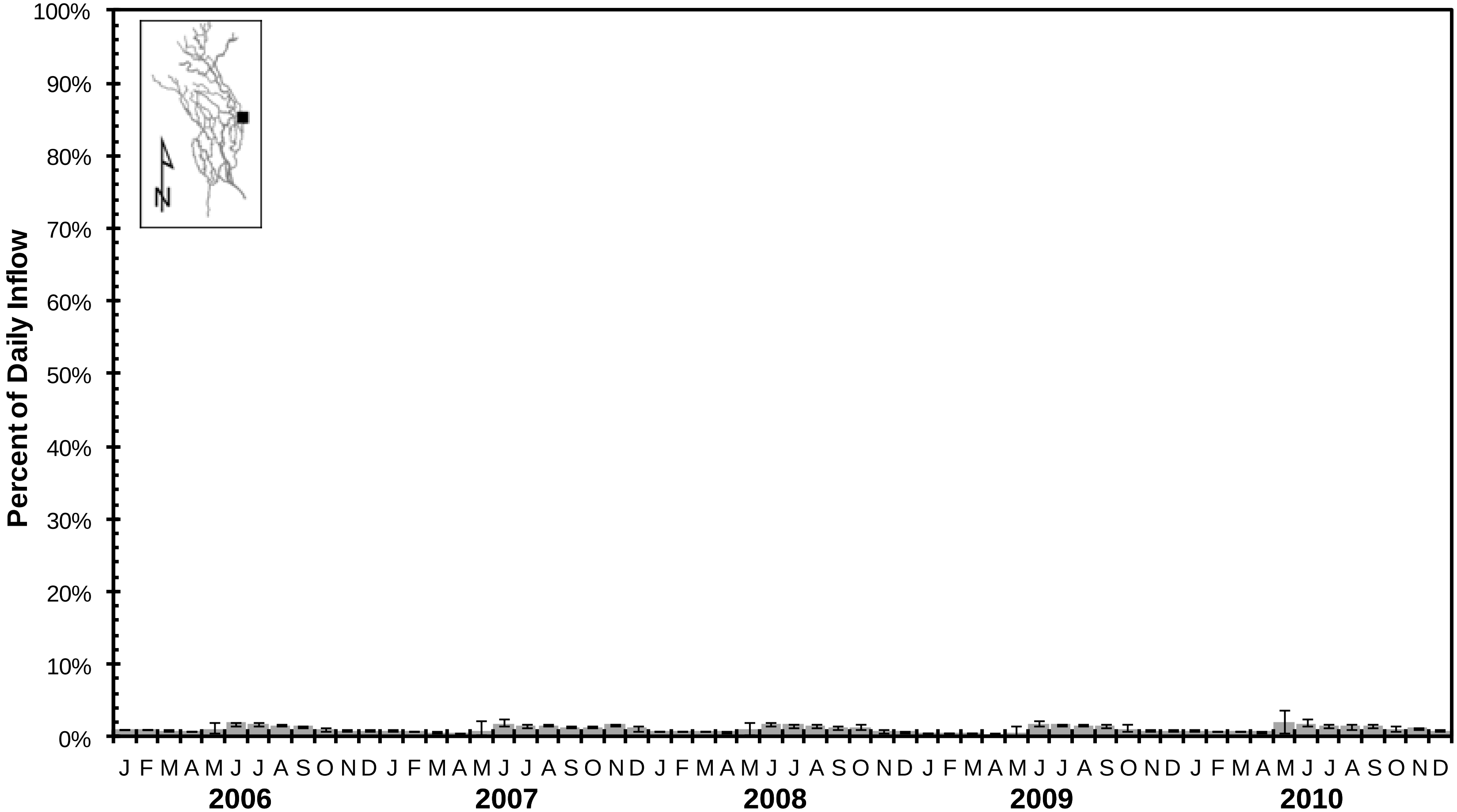

Figure 2.20 Daily percentage of inflow at *Mackenzie River (East Channel) at Inuvik* (10LC002) averaged over each month of the study period. Error bars show the range of percent over each month. (Data source: the WSC).

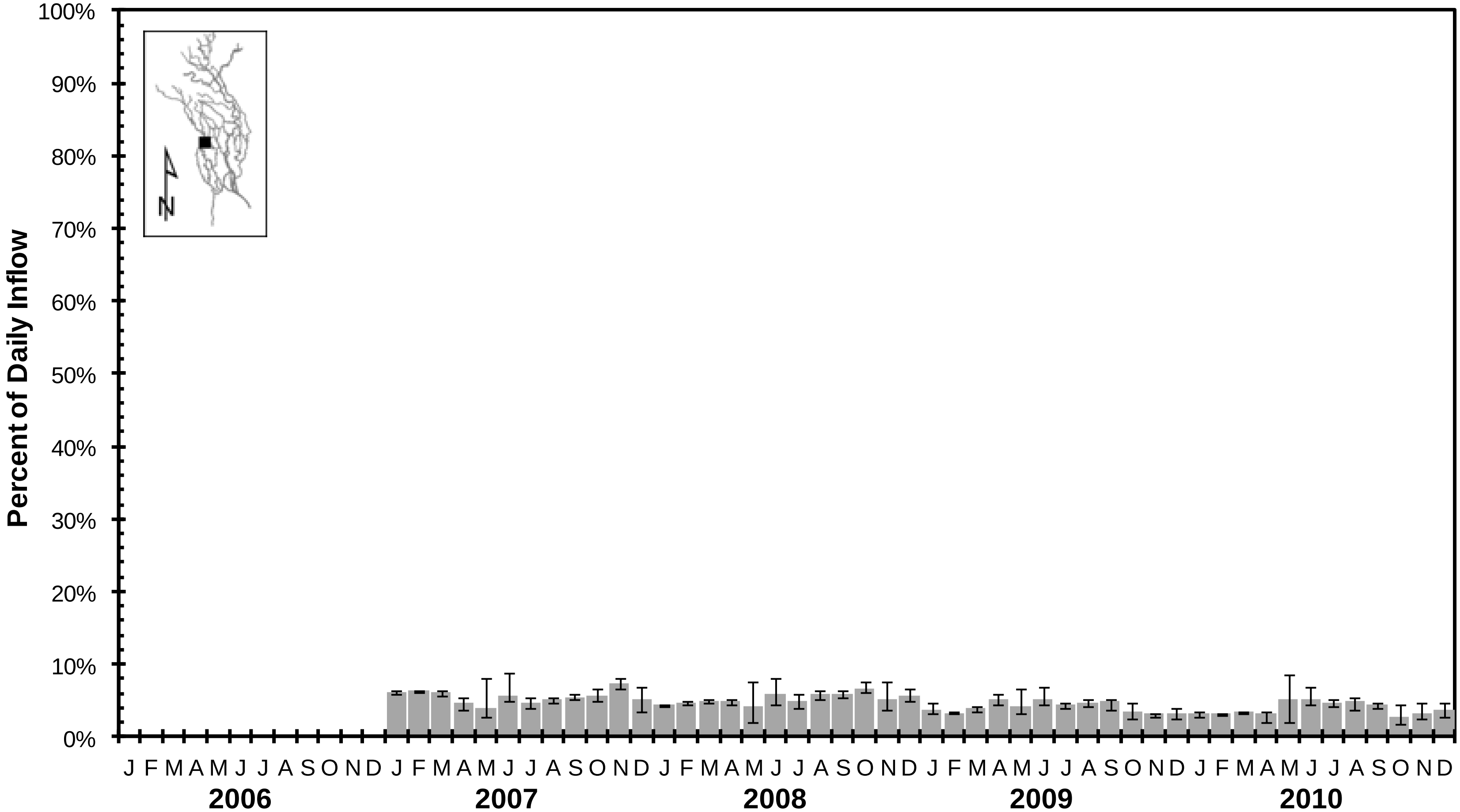

Figure 2.21 Daily percentage of inflow at *Mackenzie River (Peel Channel) above Aklavik* (10MC003) averaged over each month of the study period. Error bars show the range of percent over each month. (Data source: the WSC).

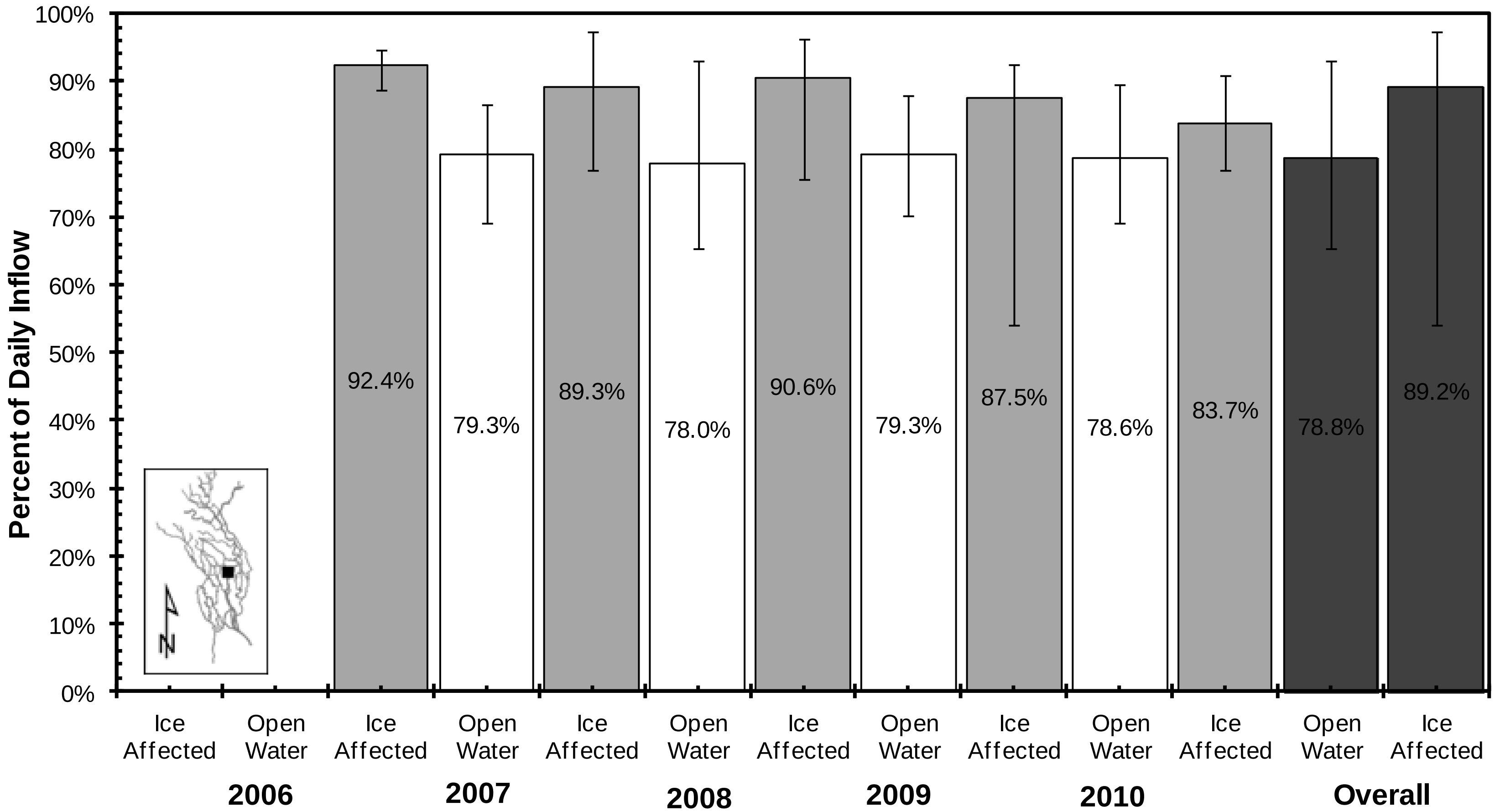

Figure 2.22 Daily percentage of inflow at *Mackenzie River (Middle Channel) below Raymond Channel* (10MC008) averaged over the open water season (assumed June to September) and ice affected season (assumed November to April). Error bars show the range of percent over each season. (Data source: the WSC).

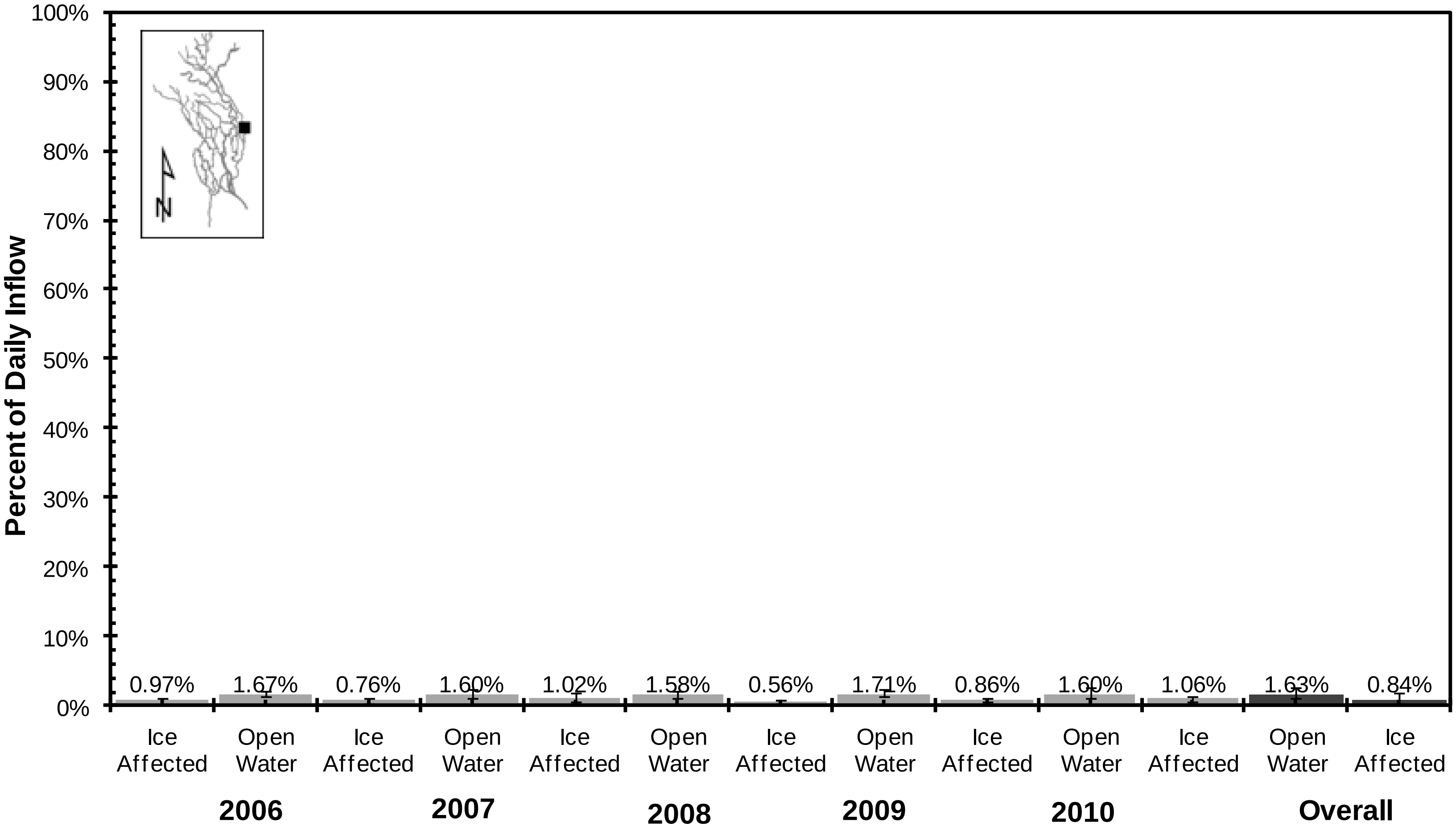

Figure 2.23 Daily percentage of inflow at *Mackenzie River (East Channel) at Inuvik* (10LC002) averaged over the open water season (assumed June to September) and ice affected season (assumed November to April). Error bars show the range of percent over each season. (Data source: the WSC).

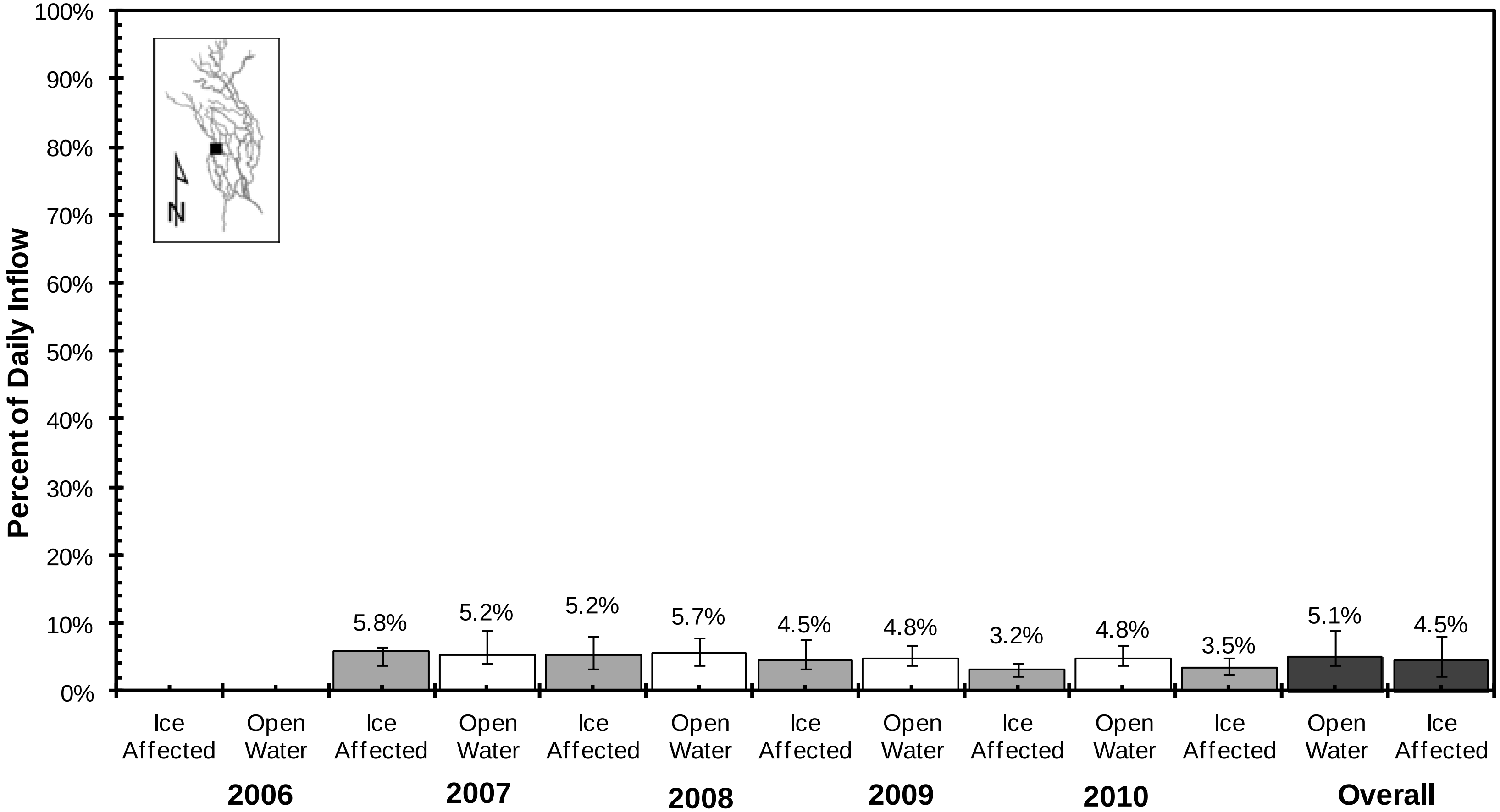

Figure 2.24 Daily percentage of inflow at *Mackenzie River (Peel Channel) above Aklavik* (10MC003) averaged over the open water season (assumed June to September) and ice affected season (assumed November to April). Error bars show the range of percent over each season. (Data source: the WSC).

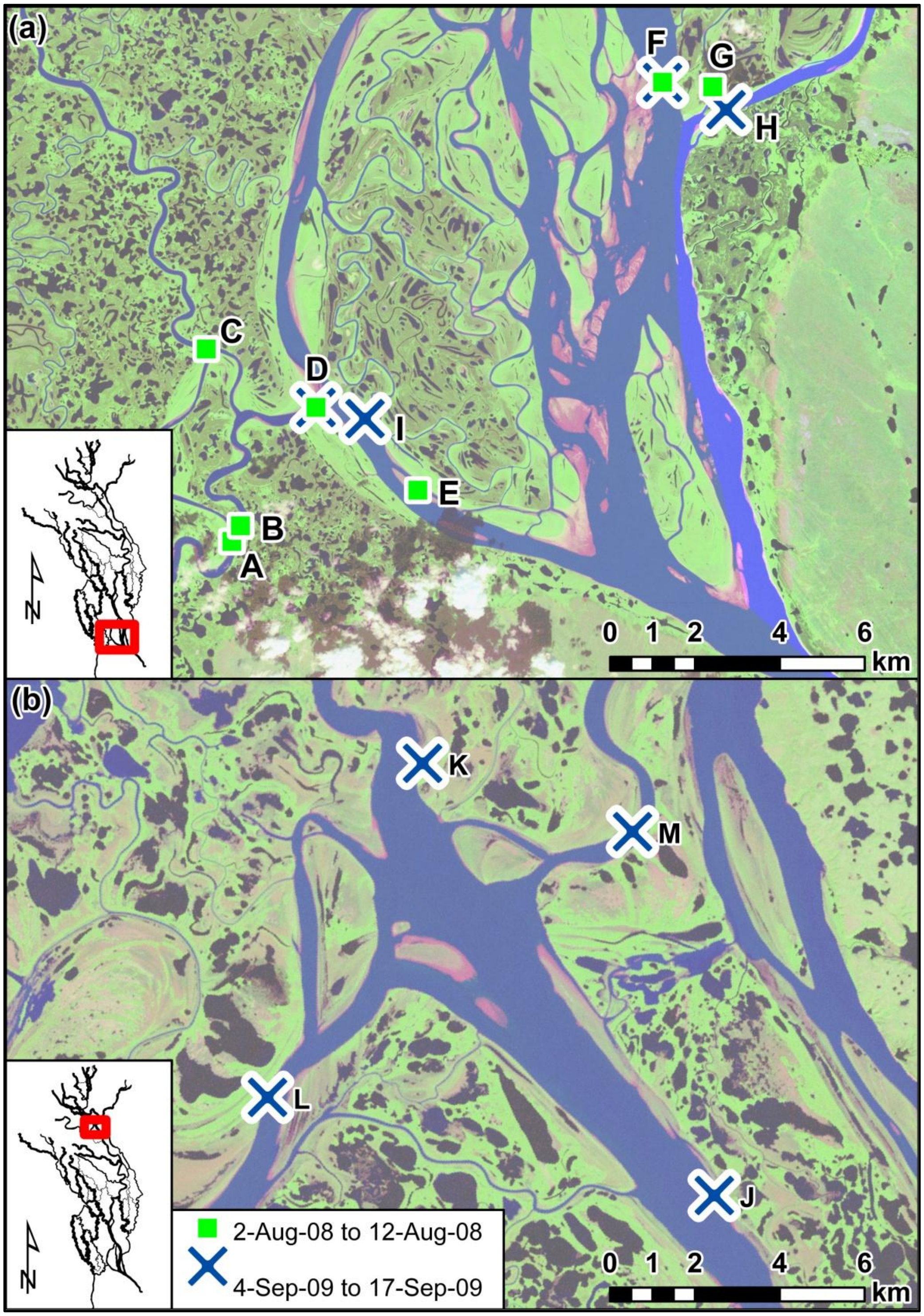

Figure 2.25 Location map of additional flow measurements between 2-Aug-08 to 12-Aug-8 and 4-Sep-09 to 17-Sep-09 by (a) the East and West Channel junctions and (b) the Neklek and Reindeer Channel junctions.
(Base image source: Industry Tourism and Investment, NWT).
(Data source: the WSC).

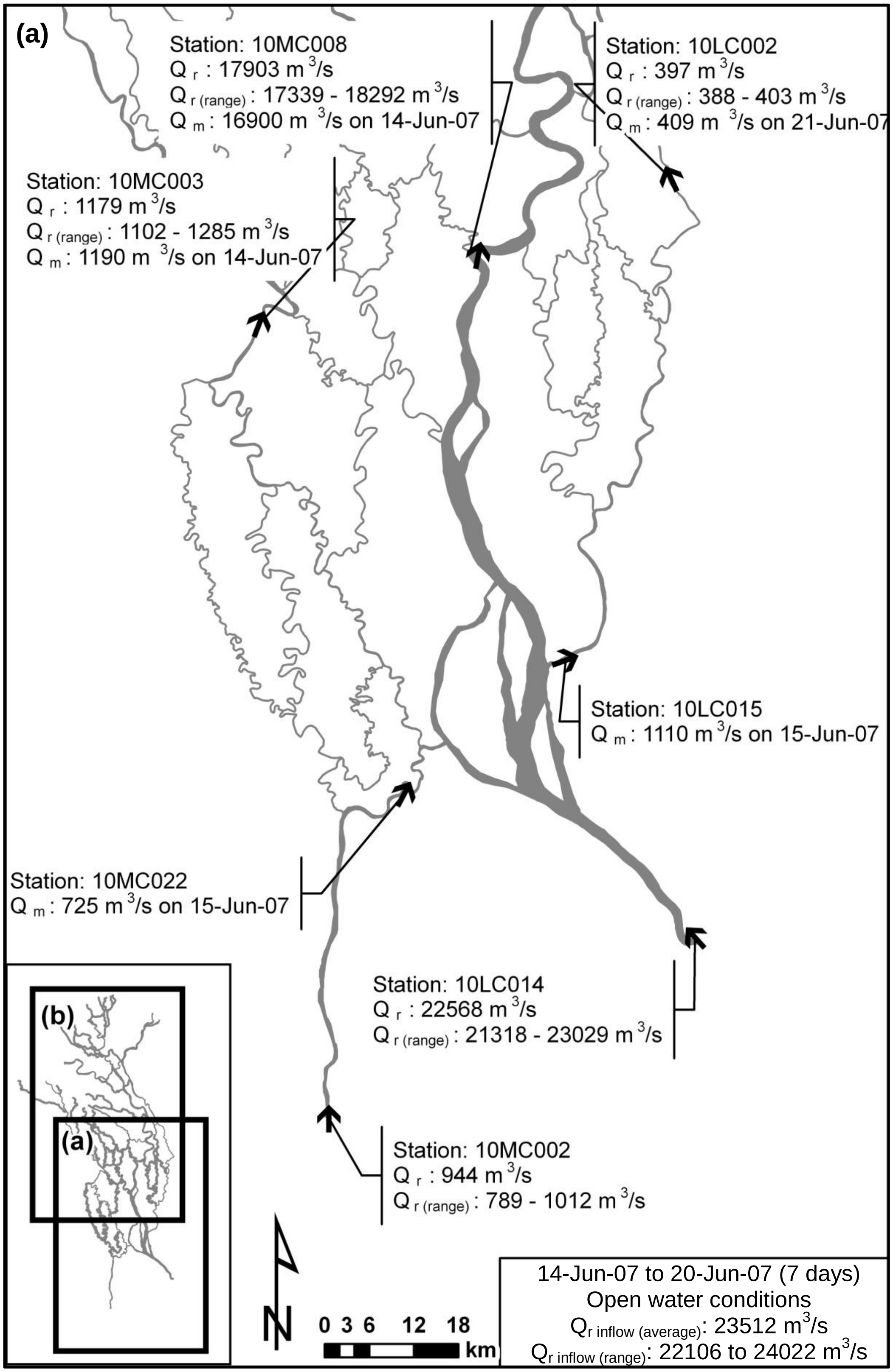

Figure 2.26 Manually measured and rating curve flows between 14-Jun-07 and 20-Jun-07 in the (a) upper Delta and (b) lower Delta. (Data source: the WSC).

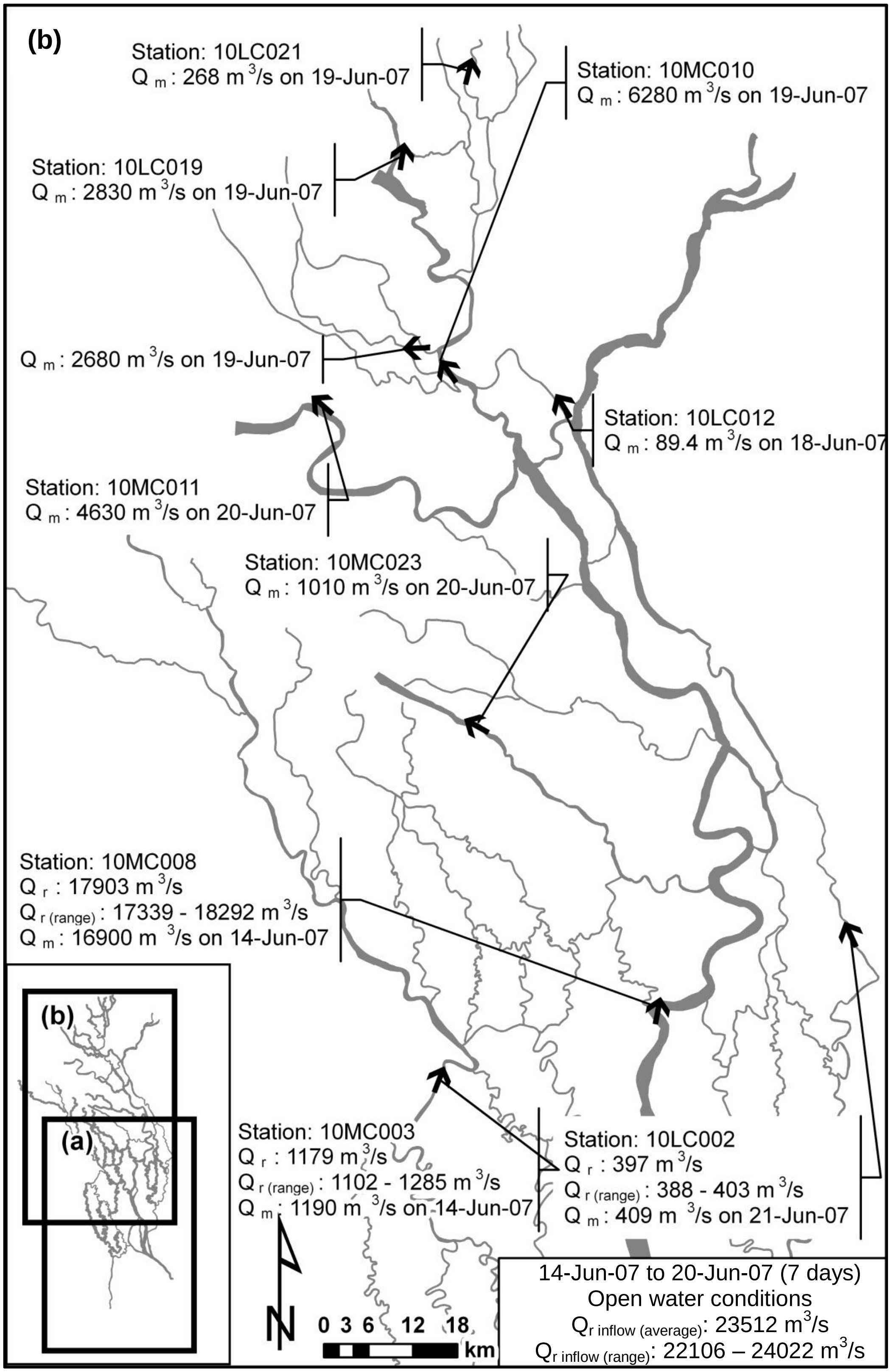

Figure 2.26 continued Manually measured and rating curve flows between 14-Jun-07 and 20-Jun-07 in the (a) upper Delta and (b) lower Delta. (Data source: the WSC).

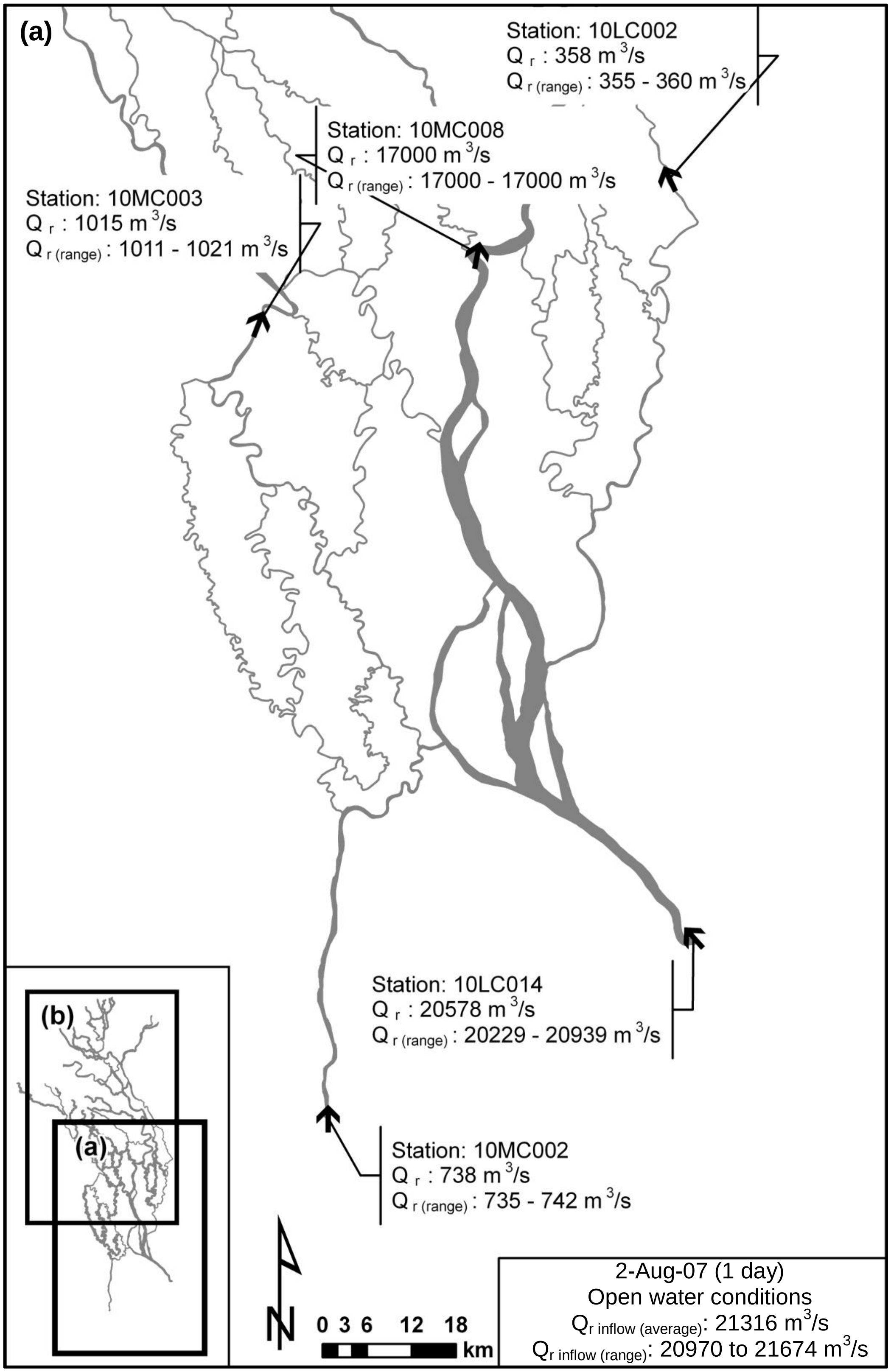

Figure 2.27 Manually measured and rating curve flows on 2-Aug-07 in the (a) upper Delta and (b) lower Delta.
(Data source: the WSC).

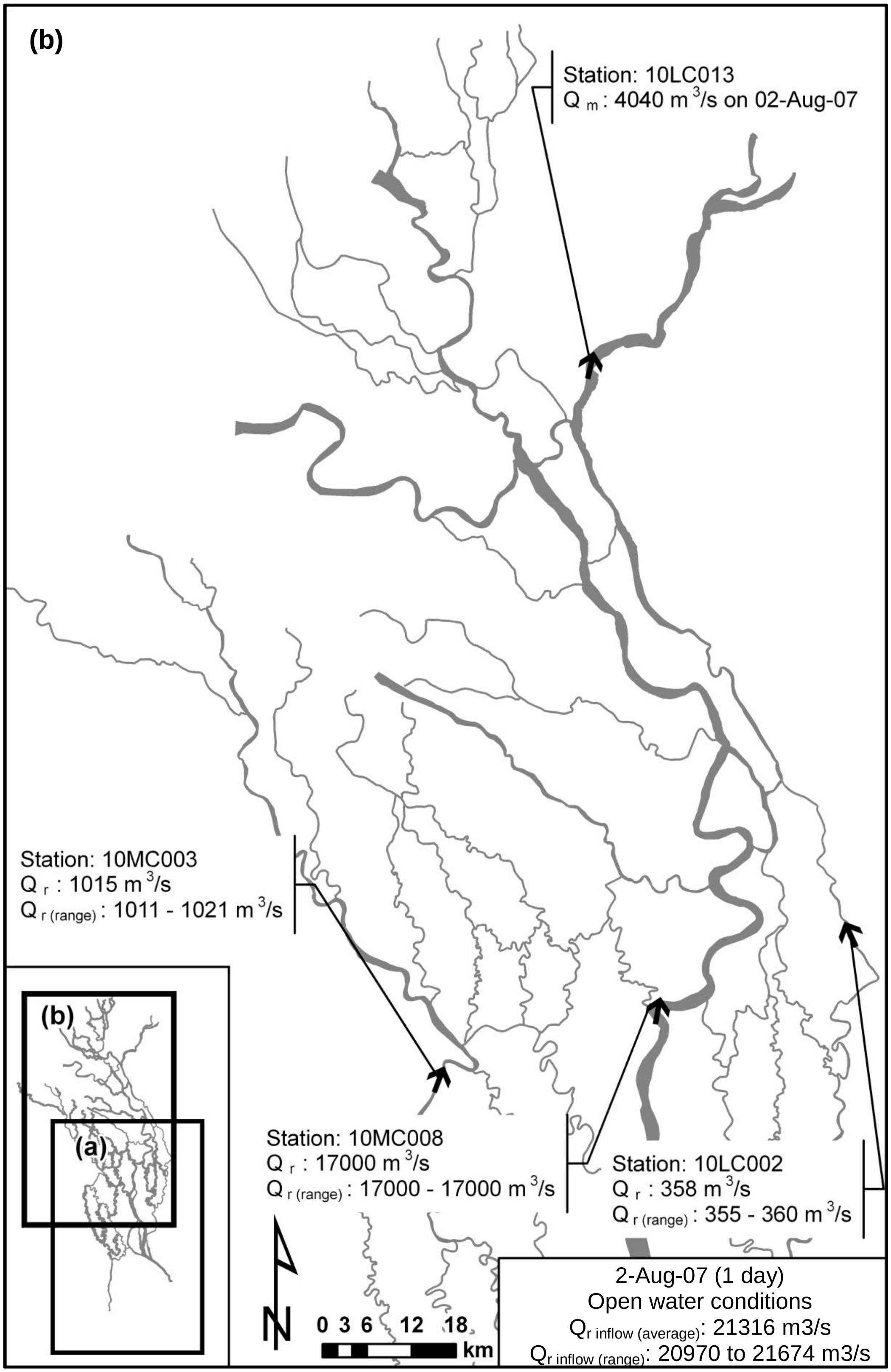

Figure 2.27 continued Manually measured and rating curve flows on 2-Aug-07 in the (a) upper Delta and (b) lower Delta.
(Data source: the WSC).

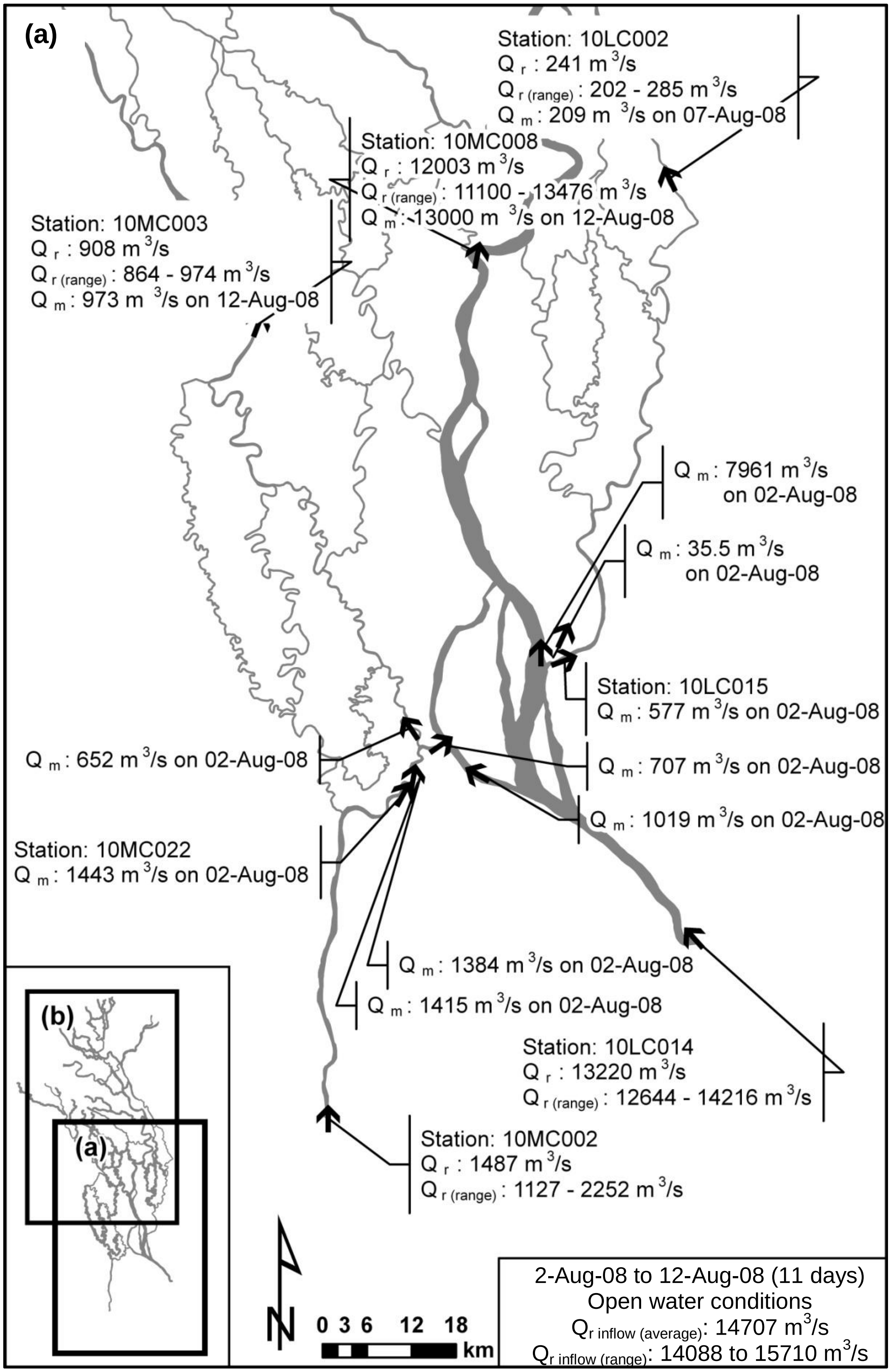

Figure 2.28 Manually measured and rating curve flows between 2-Aug-08 and 12-Aug-08 in the (a) upper Delta and (b) lower Delta. (Data source: the WSC).

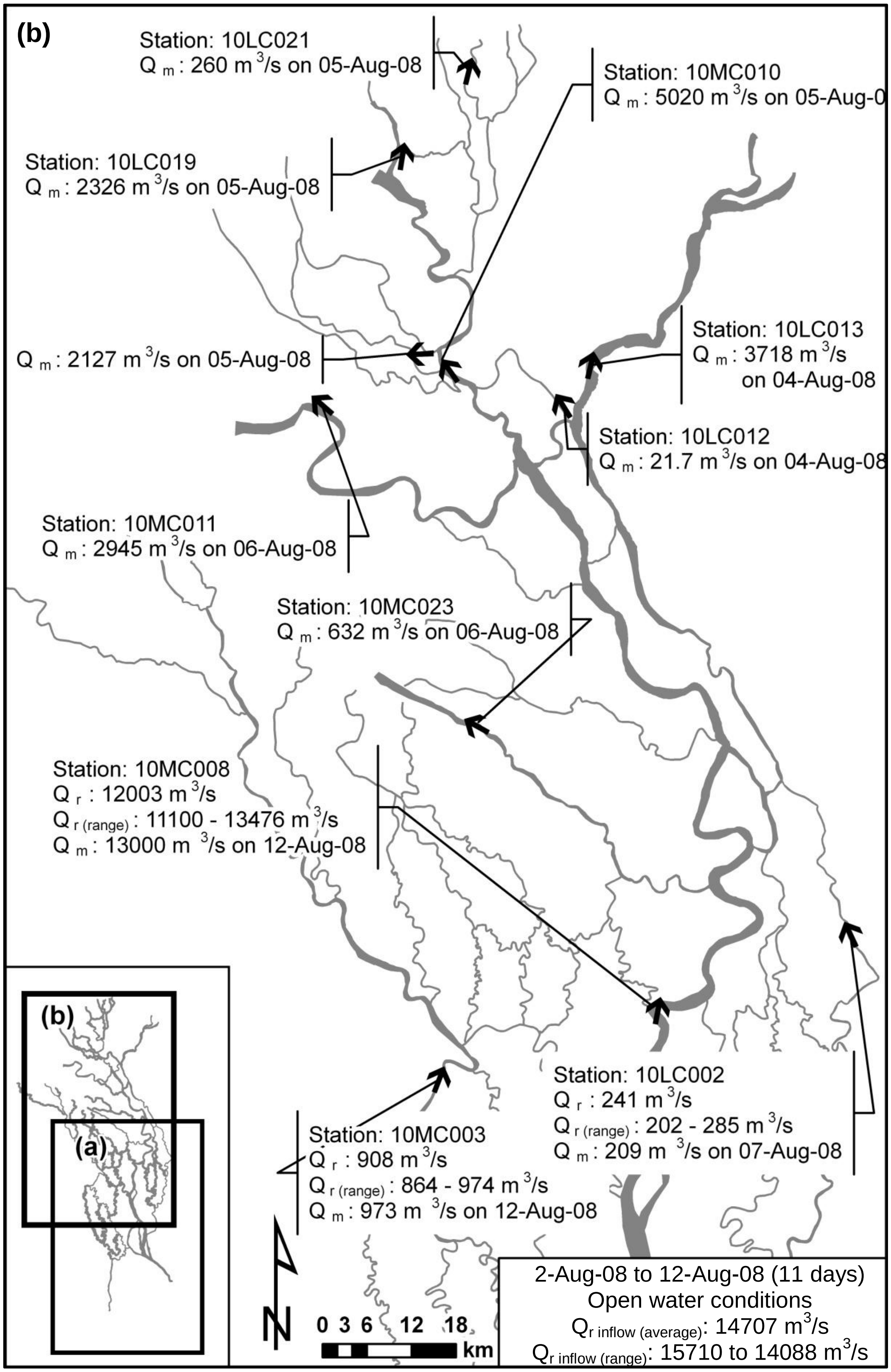

Figure 2.28 continued Manually measured and rating curve flows between 2-Aug-08 and 12-Aug-08 in the (a) upper Delta and (b) lower Delta. (Data source: the WSC).

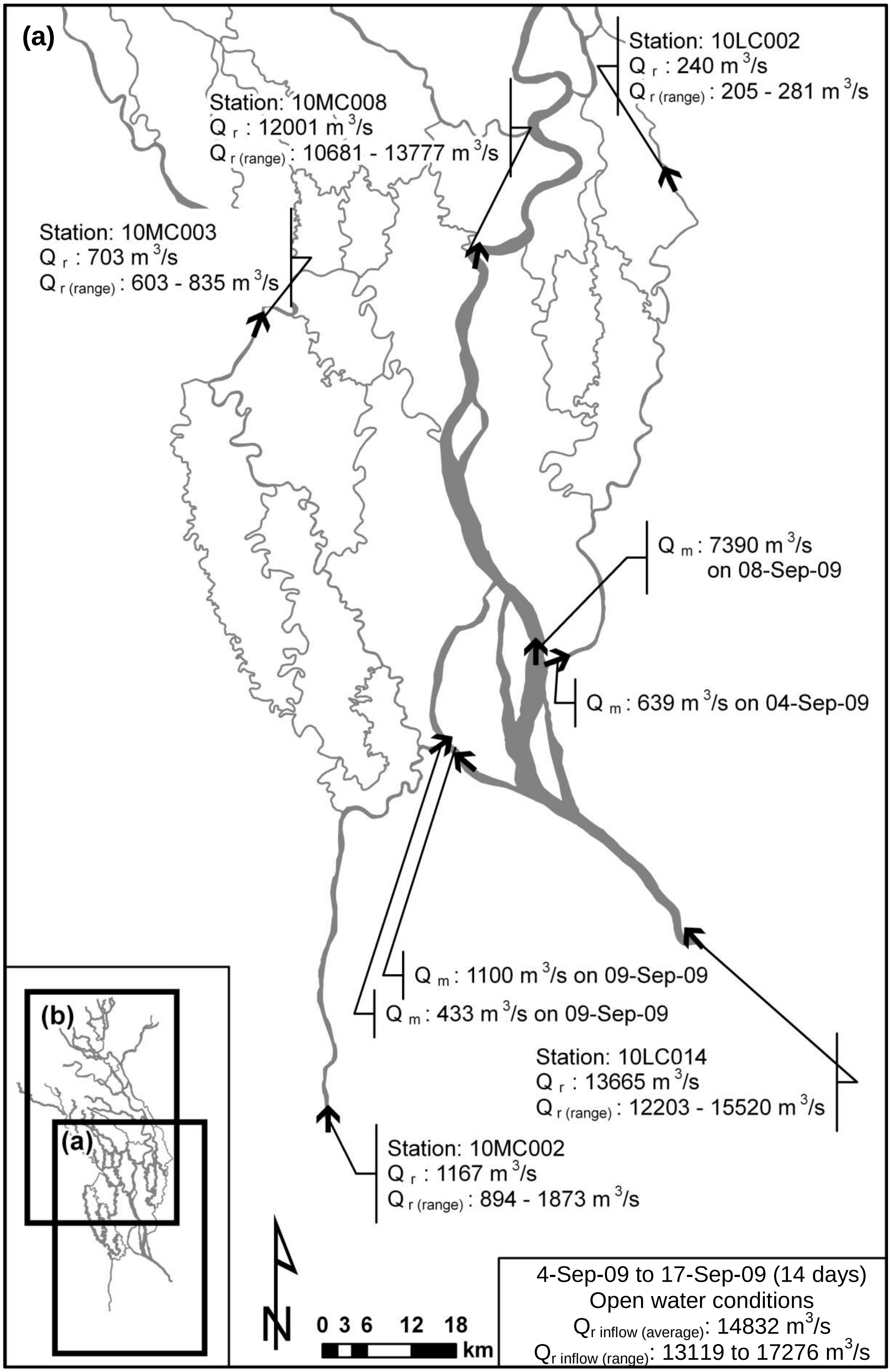

Figure 2.29 Manually measured and rating curve flows between 4-Sep-09 and 17-Sep-09 in the (a) upper Delta and (b) lower Delta. (Data source: the WSC).

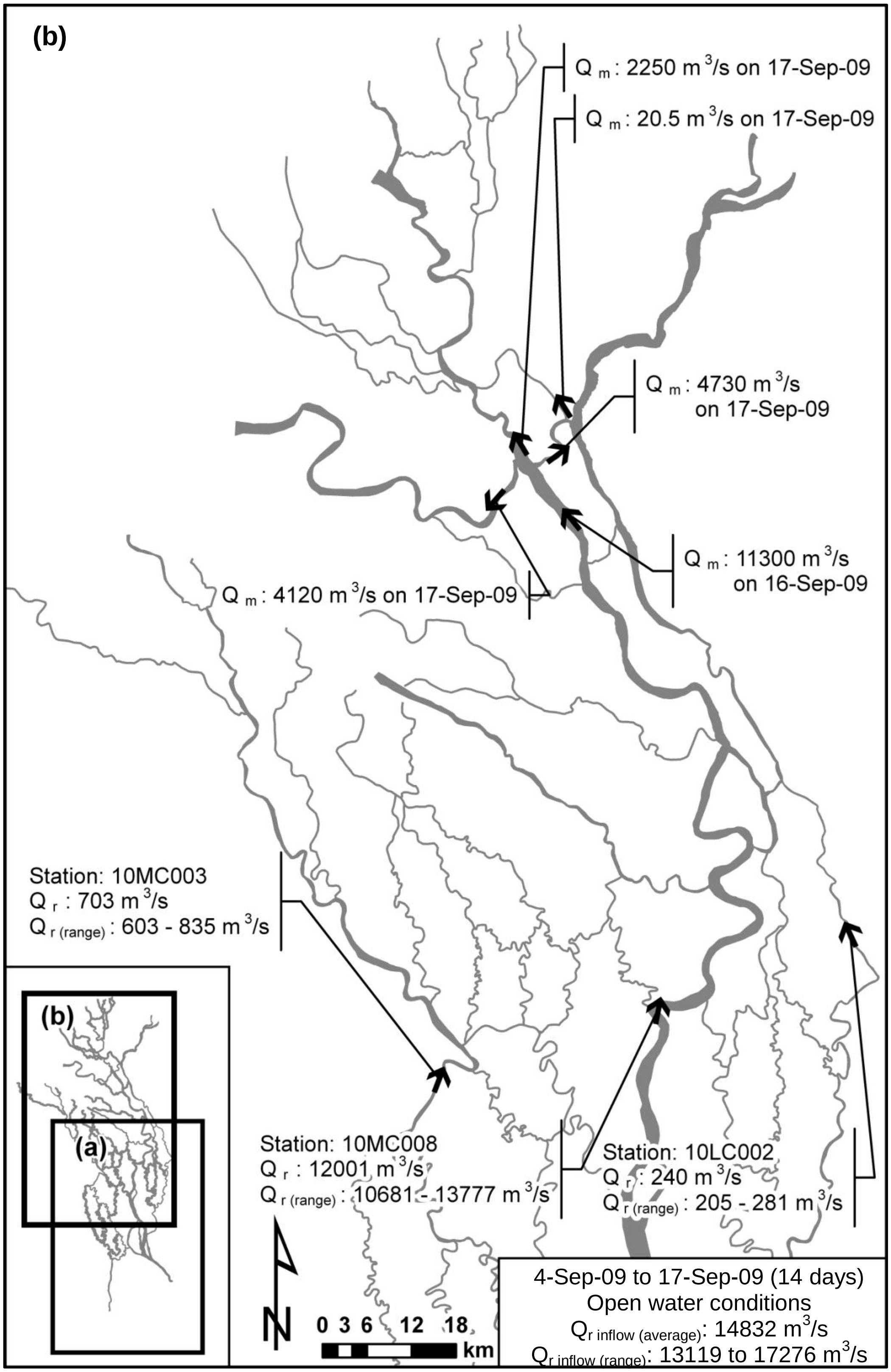

Figure 2.29 continued Manually measured and rating curve flows between 4-Sep-09 and 17-Sep-09 in the (a) upper Delta and (b) lower Delta. (Data source: the WSC).

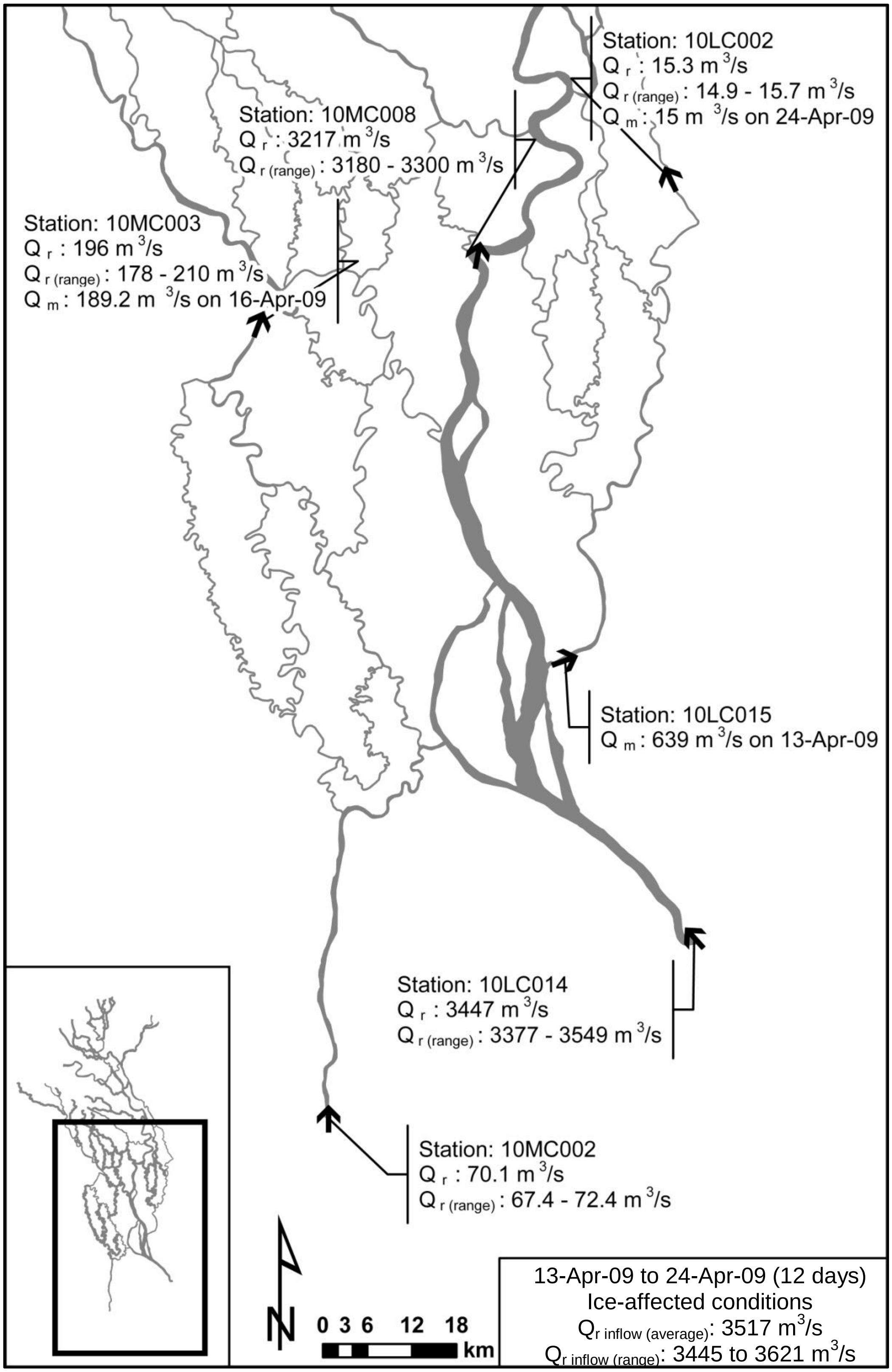

Figure 2.30 Manually measured and rating curve flows between 13-Apr-09 and 16-Apr-09.
(Data source: the WSC).

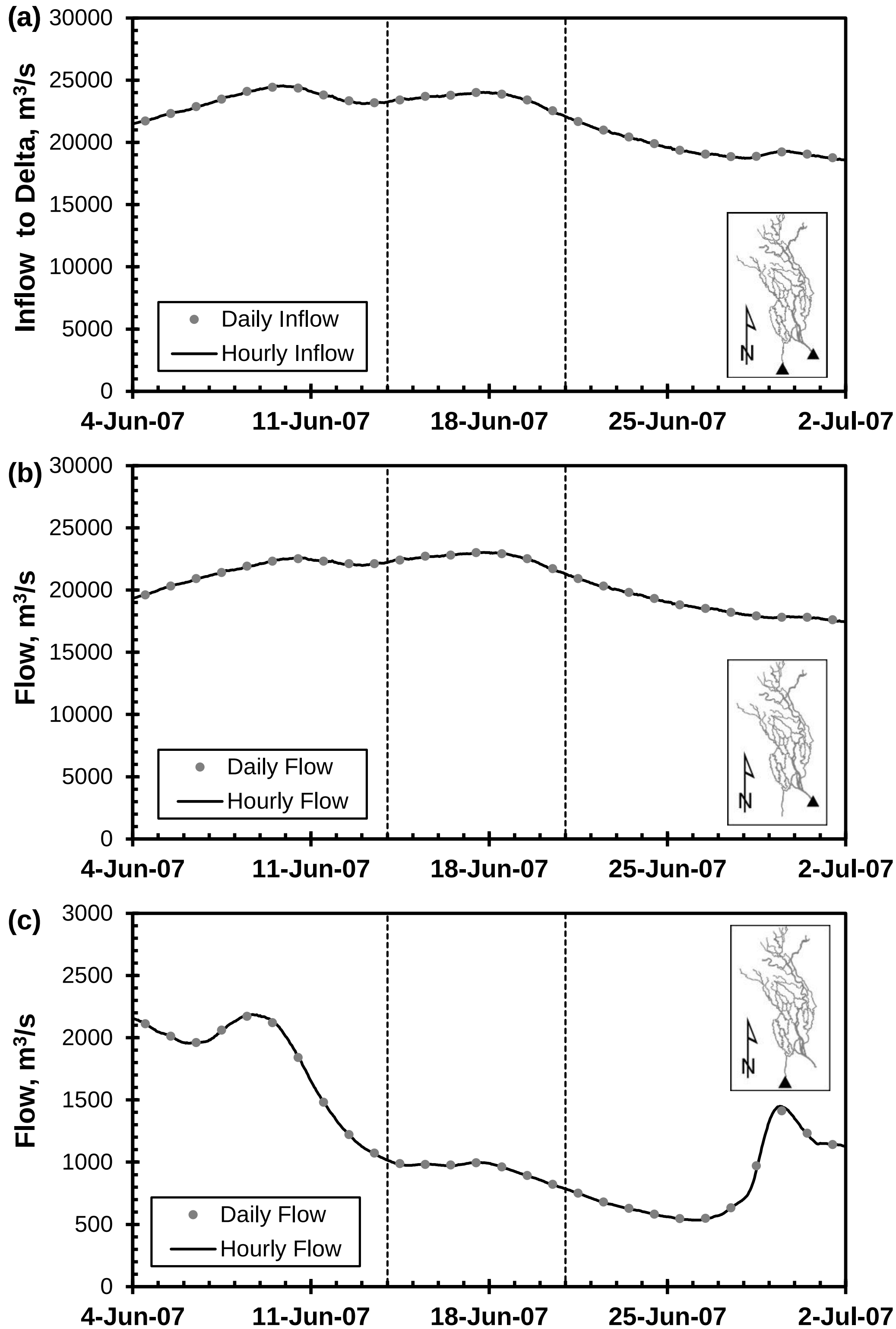

Figure 2.31 Inflow and flow at gauges with rating curves for the manual flow measurement period from 14-Jun-07 to 20-Jun-07 for (a) Inflows (b) 10LC014 (c) 10MC002. (Data source: the WSC).

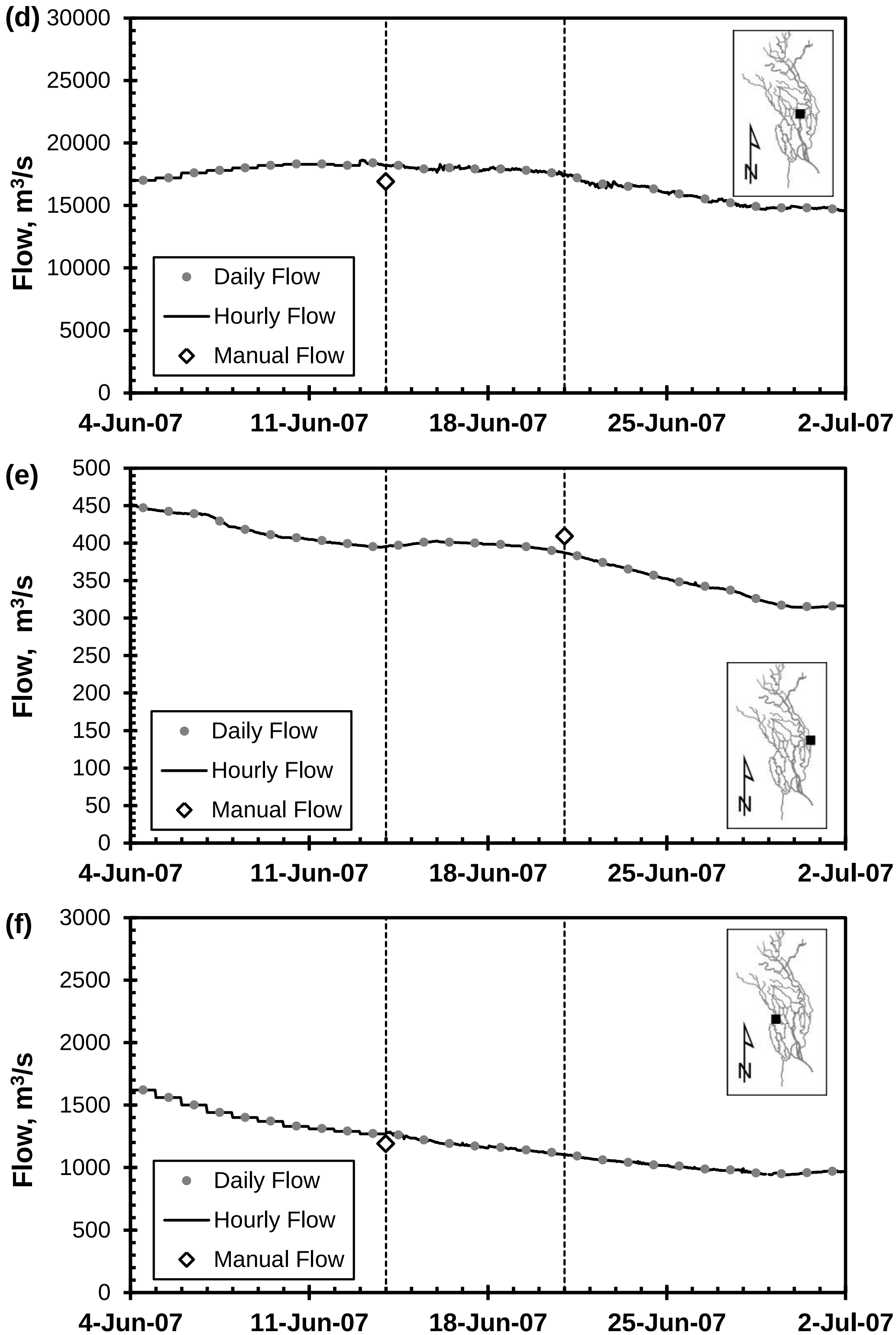

Figure 2.31 continued Inflow and flow at gauges with rating curves for the manual flow measurement period from 14-Jun-07 to 20-Jun-07 for (d) 10MC008 (e) 10LC012 and (f) 10MC003 (Data source: the WSC).

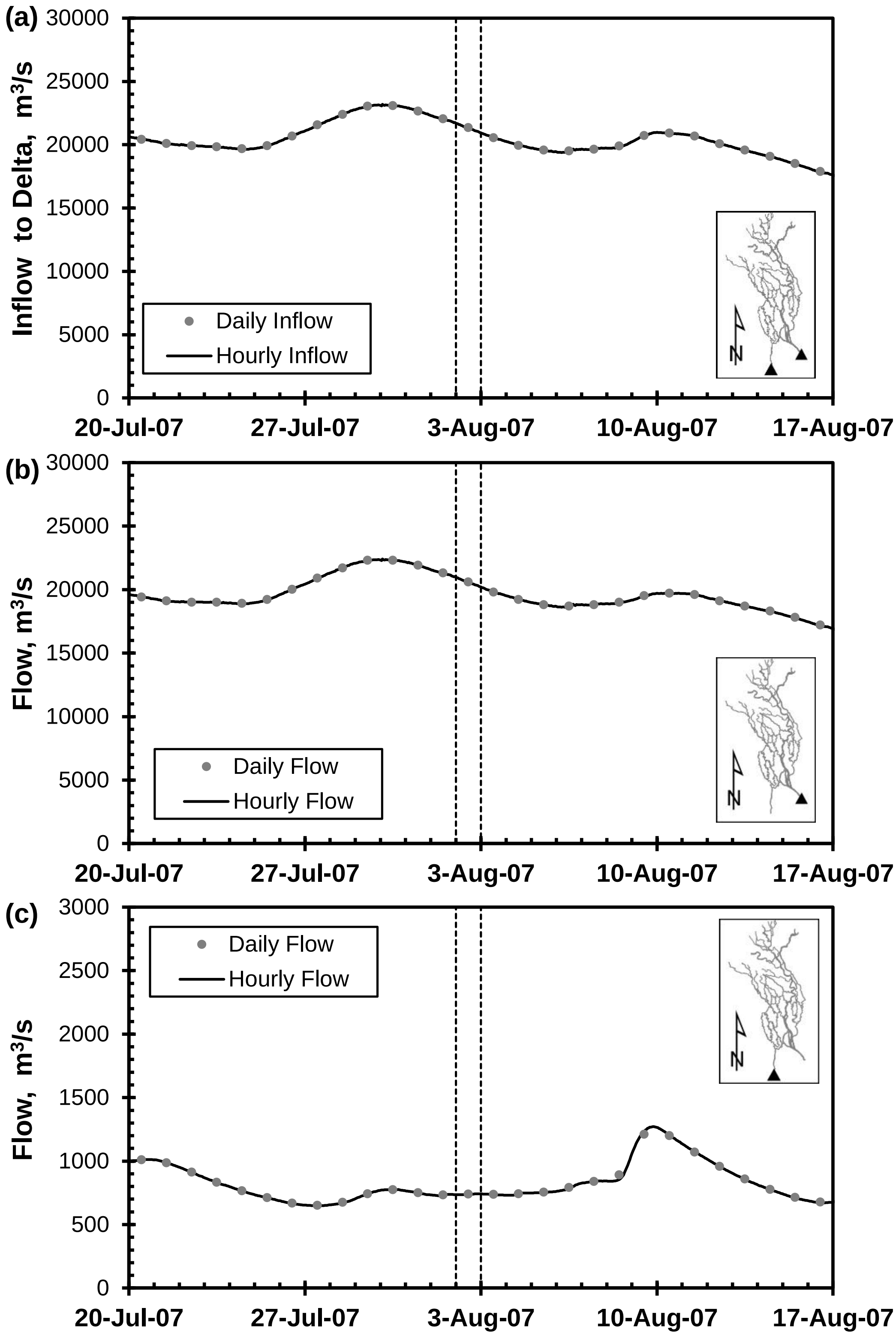

Figure 2.32 Inflow and flow at gauges with rating curves for the flow measurement period on 2-Aug-07 for (a) Inflow (b) 10LC014 (c) 10MC002. (Data source: the WSC).

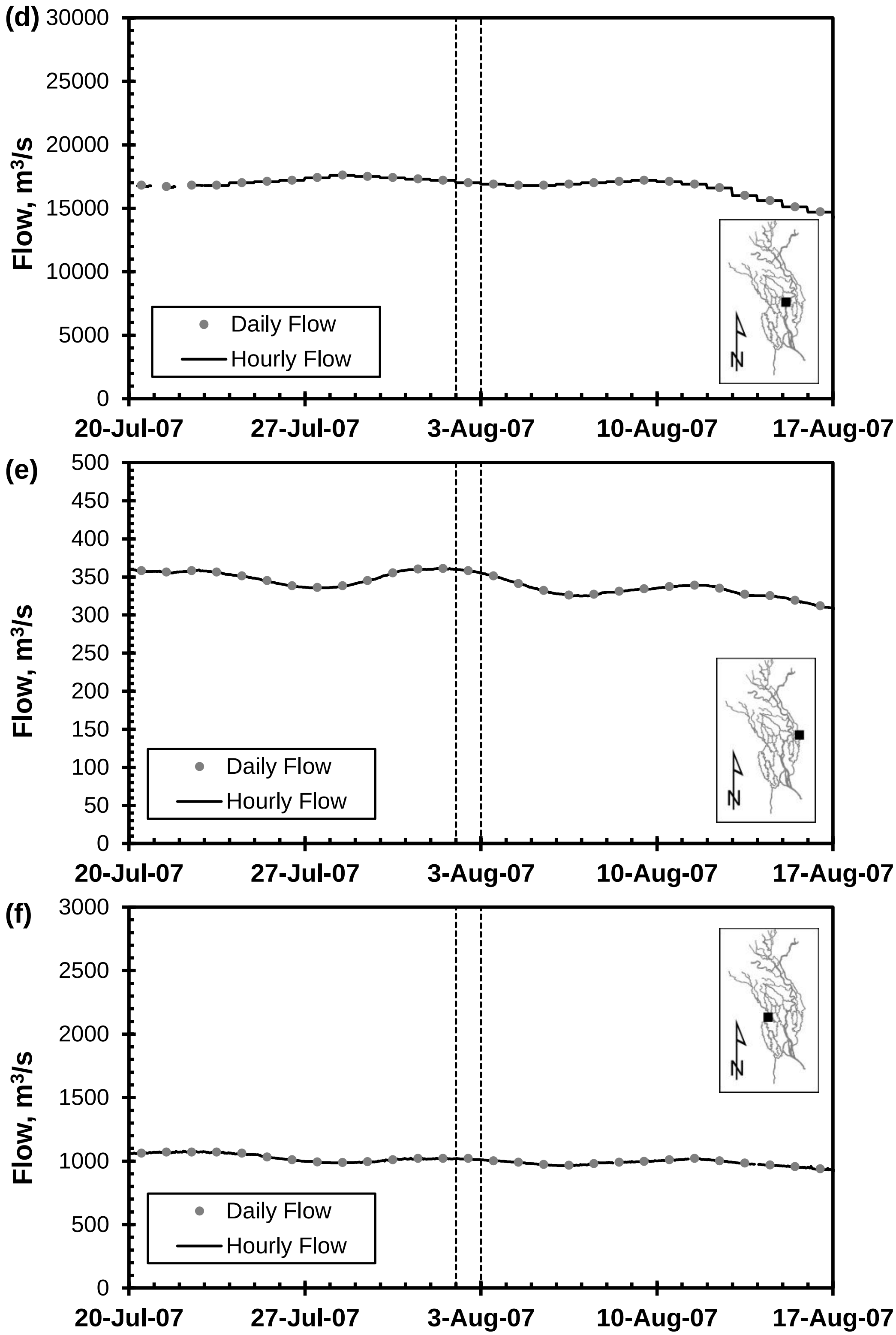

Figure 2.32 continued Inflow and flow at gauges with rating curves for the flow measurement period on 2-Aug-07 for (d) 10MC008 (e) 10LC012 and (f) 10MC003. (Data source: the WSC).

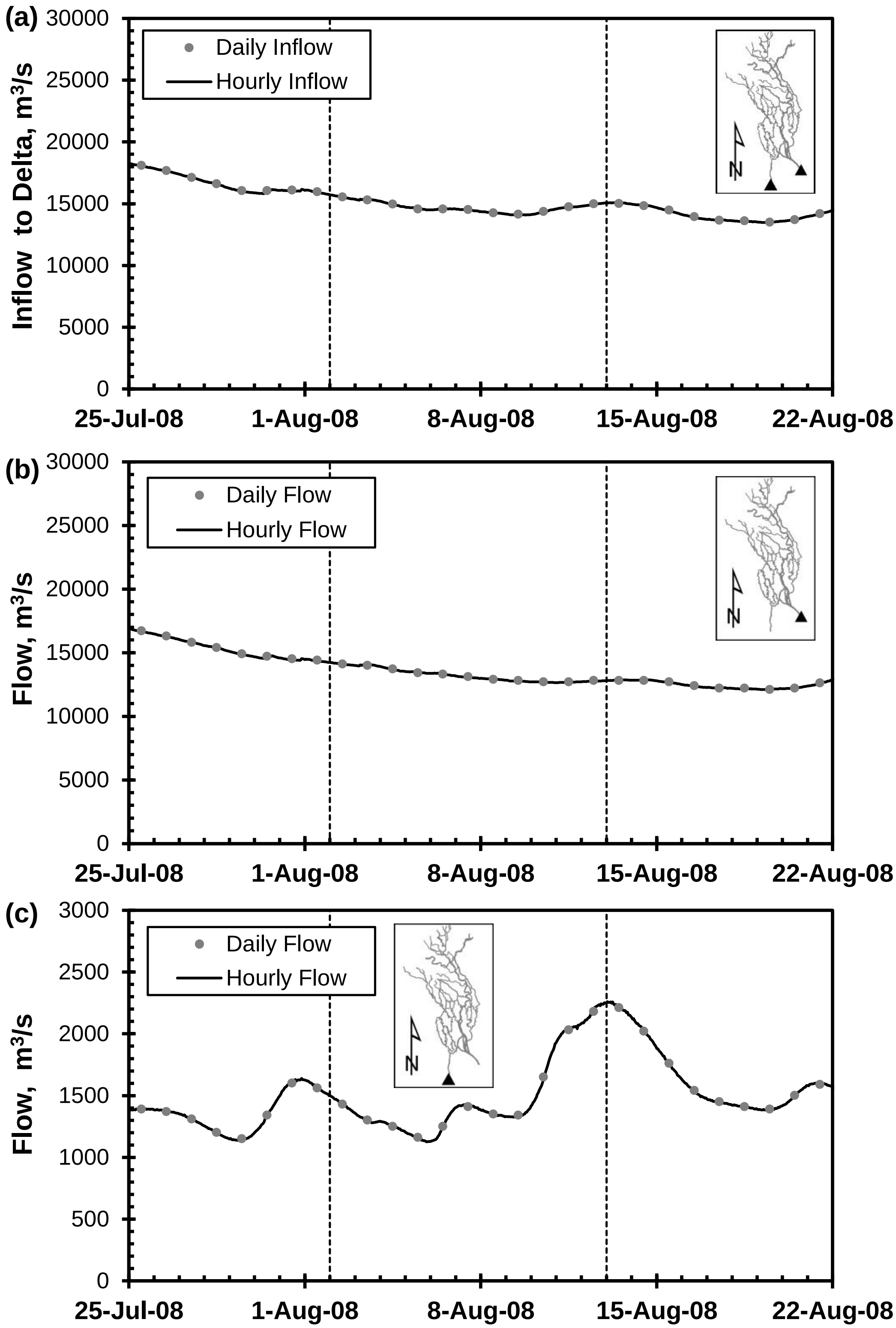

Figure 2.33 Inflow and flow at gauges with rating curves for the flow measurement period from 2-Aug-08 to 12-Aug-08 for (a) Inflow (b) 10LC014 (c) 10MC002. (Data source: the WSC).

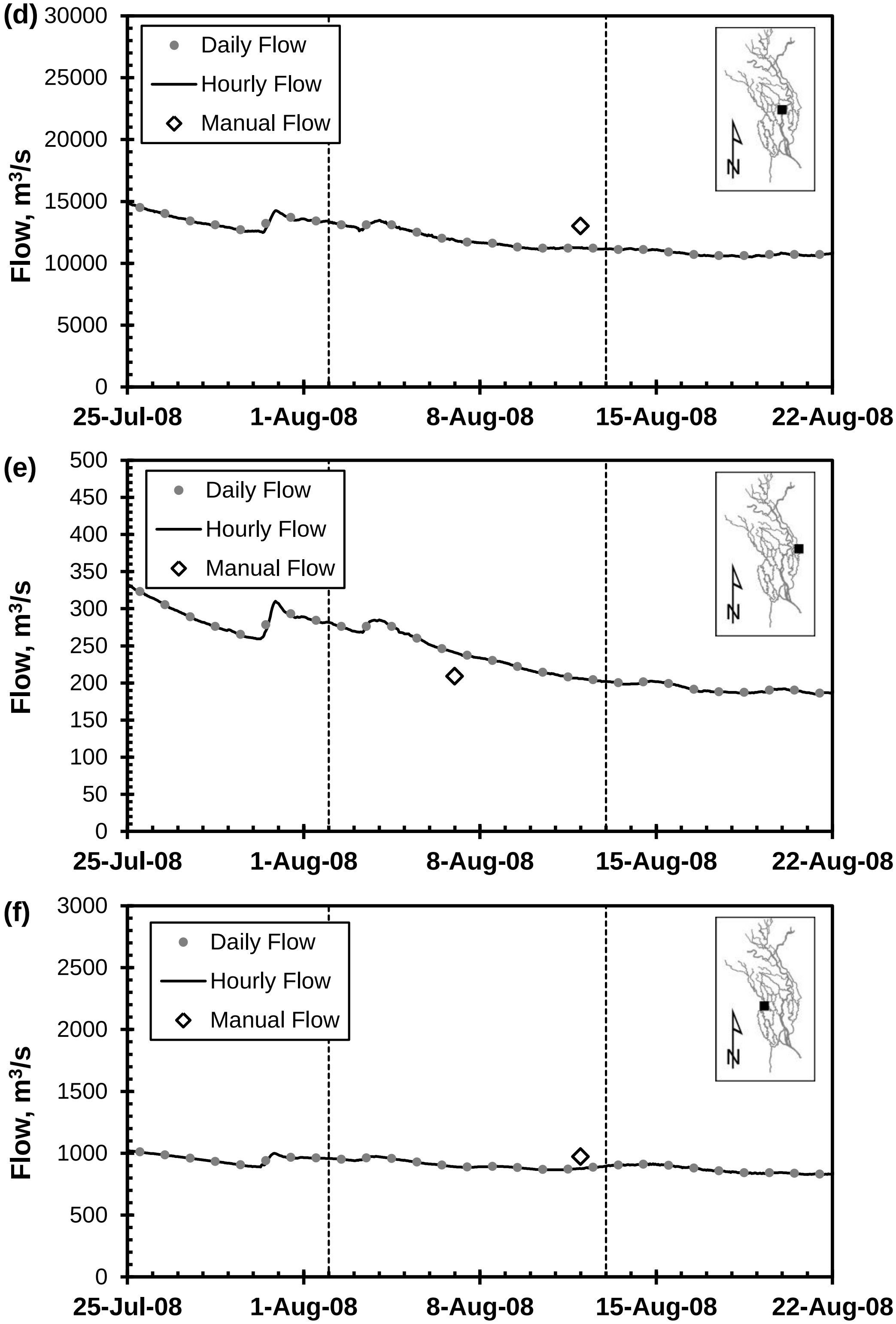

Figure 2.33 continued Inflow and flow at gauges with rating curves for the flow measurement period from 2-Aug-08 to 12-Aug-08 for (d) 10MC008 (e) 10LC012 and (f) 10MC003. (Data source: the WSC).

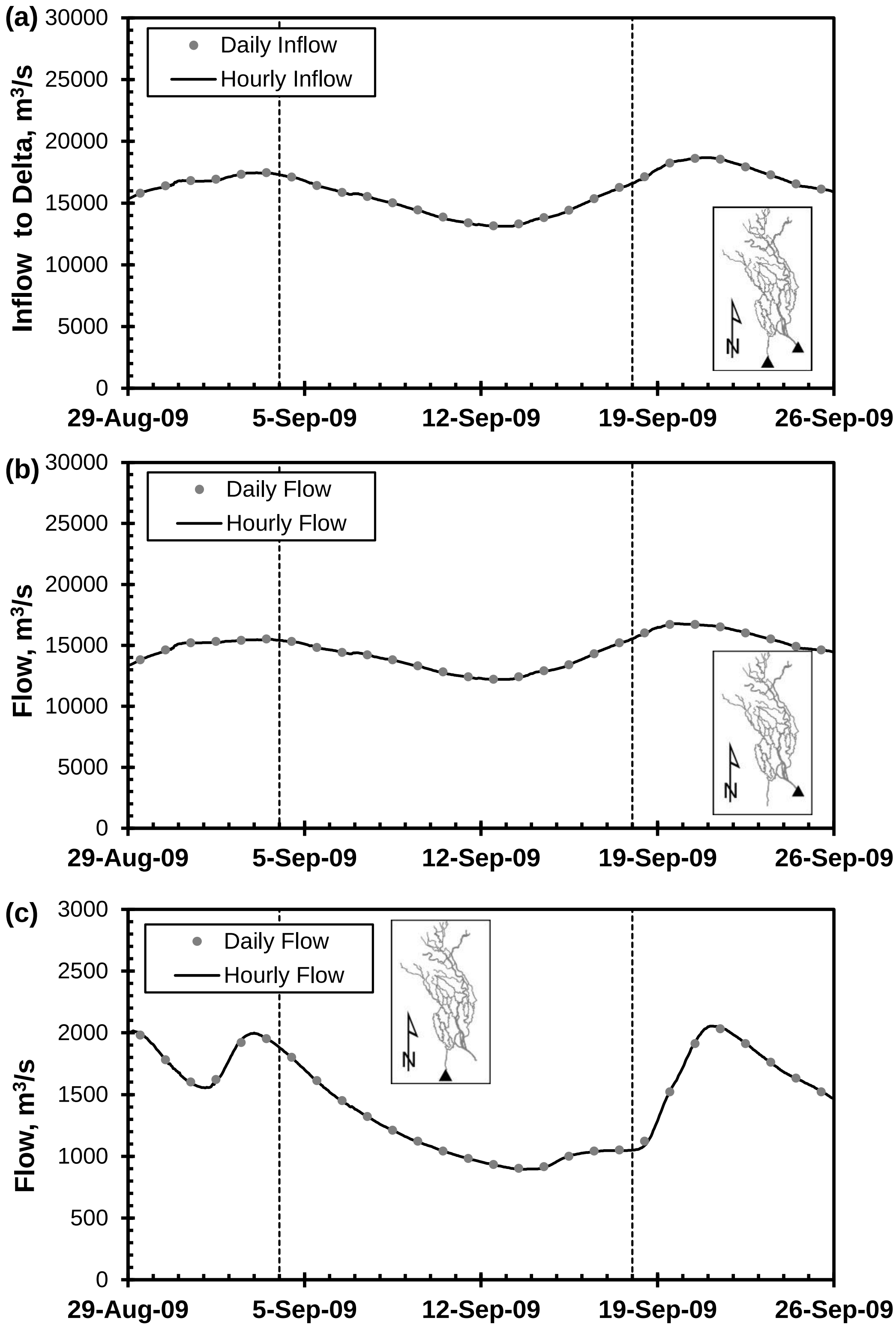

Figure 2.34 Inflow and flow at gauges with rating curves for the flow measurement period from 4-Sep-09 to 17-Sep-09 for (a) Inflow (b) 10LC014 (c) 10MC002. (Data source: the WSC).

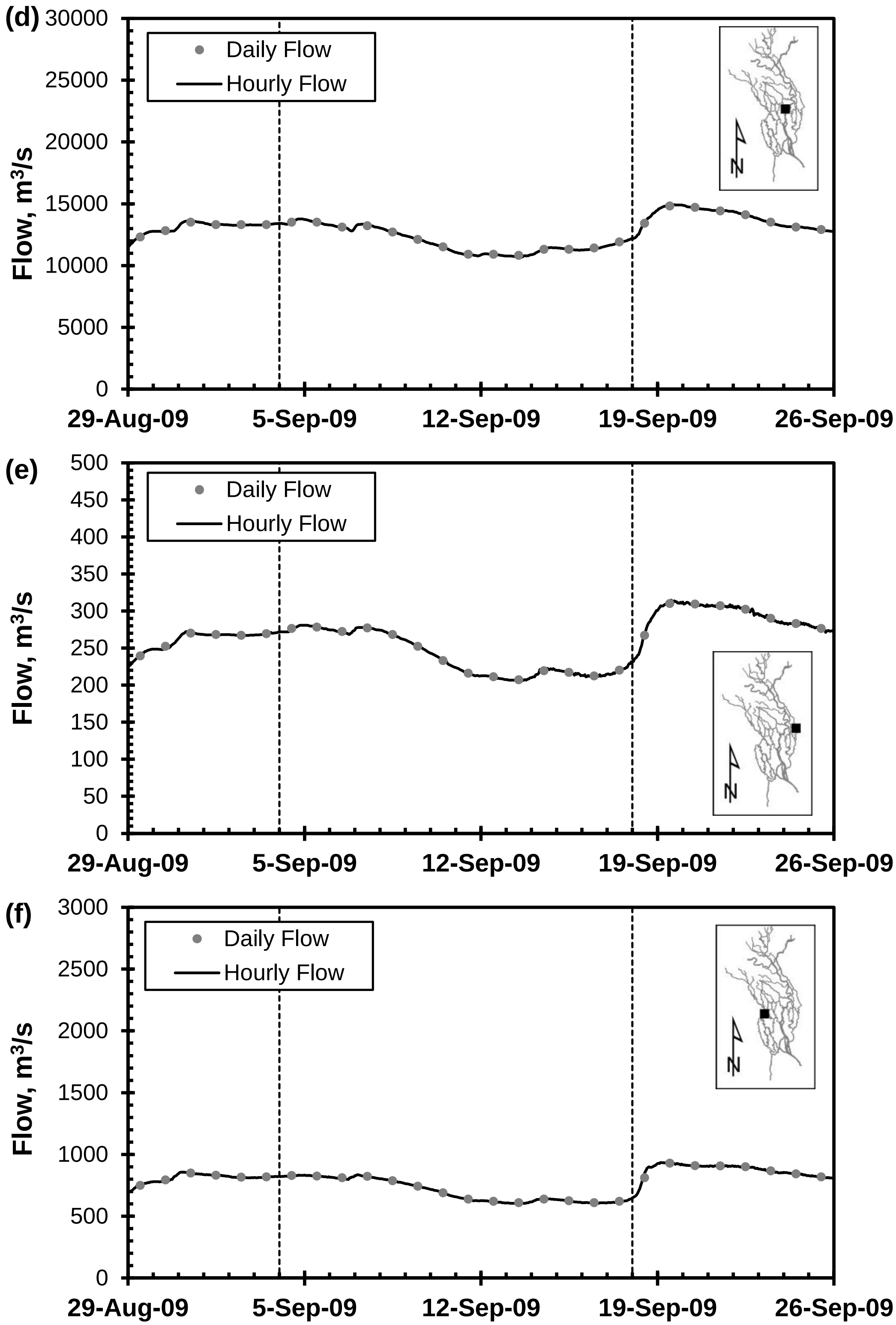

Figure 2.34 continued Inflow and flow at gauges with rating curves for the flow measurement period from 4-Sep-09 to 17-Sep-09 for (d) 10MC008 (e) 10LC012 and (f) 10MC003. (Data source: the WSC).

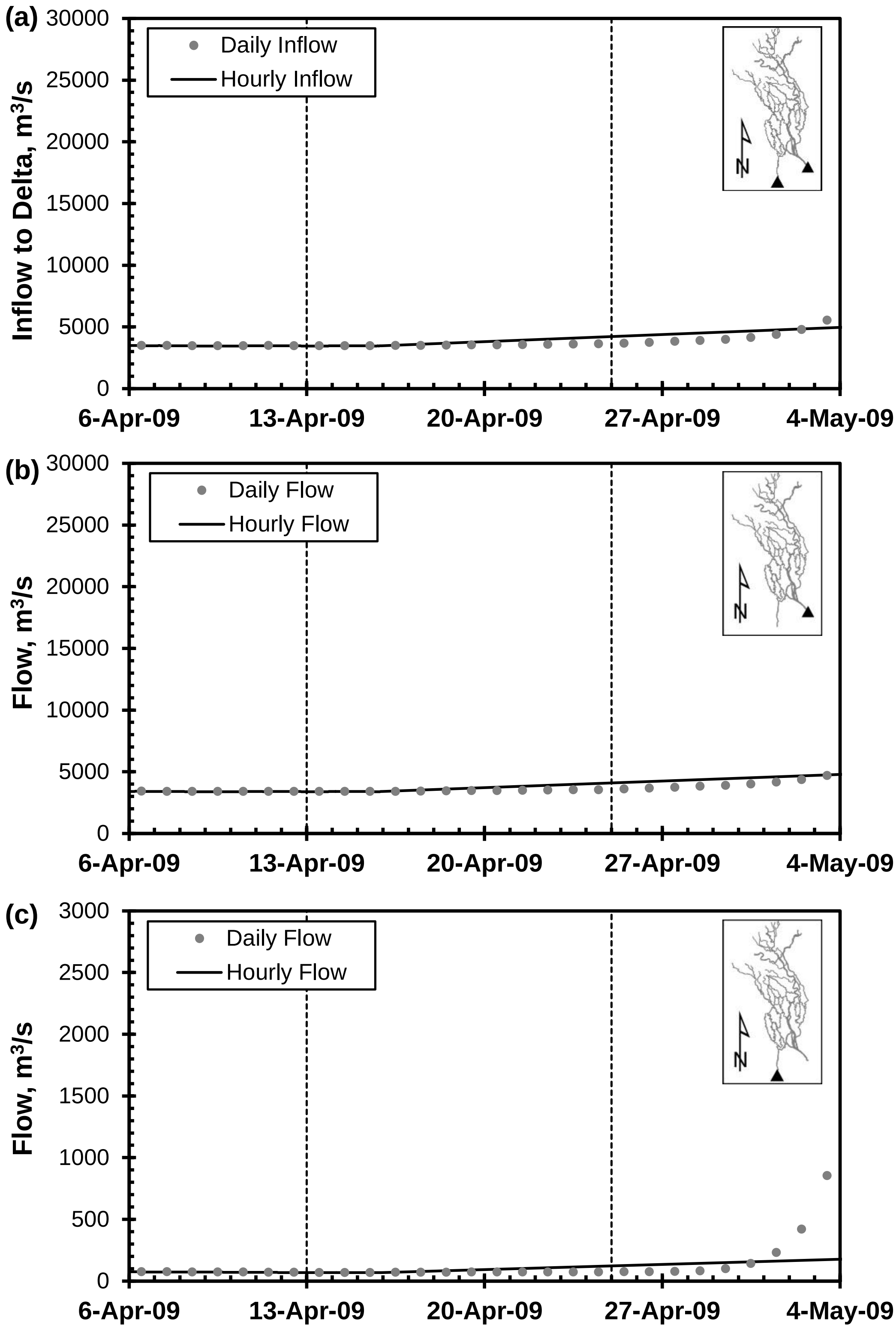

Figure 2.35 Inflow and flow at gauges with rating curves for the flow measurement period from 13-Apr-09 to 24-Apr-09 for (a) Inflow (b) 10LC014 (c) 10MC002 (Data source: the WSC).

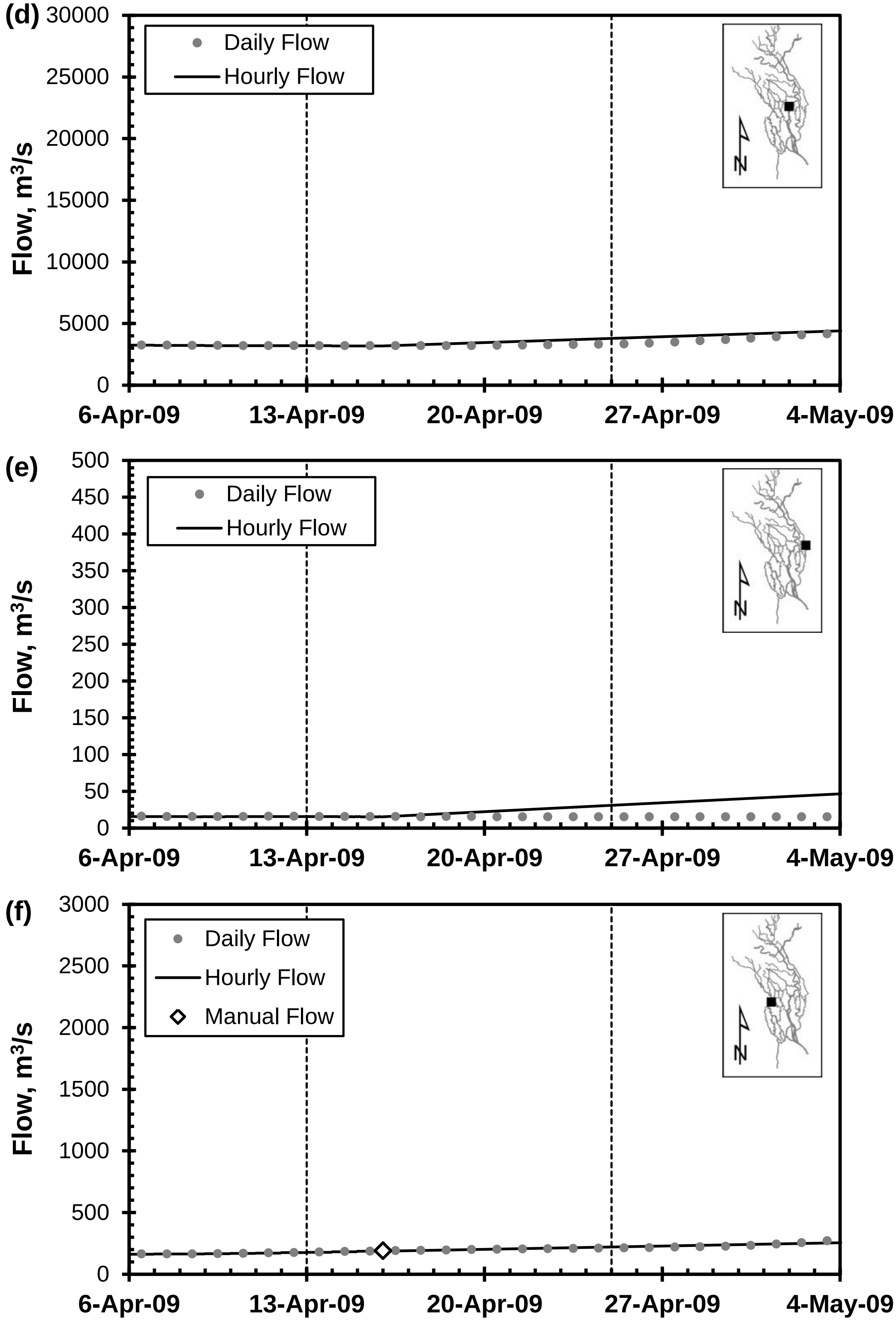

Figure 2.35 continued Inflow and flow at gauges with rating curves for the flow measurement period from 13-Apr-09 to 24-Apr-09 for (d) 10MC008 (e) 10LC012 and (f) 10MC003. (Data source: the WSC).

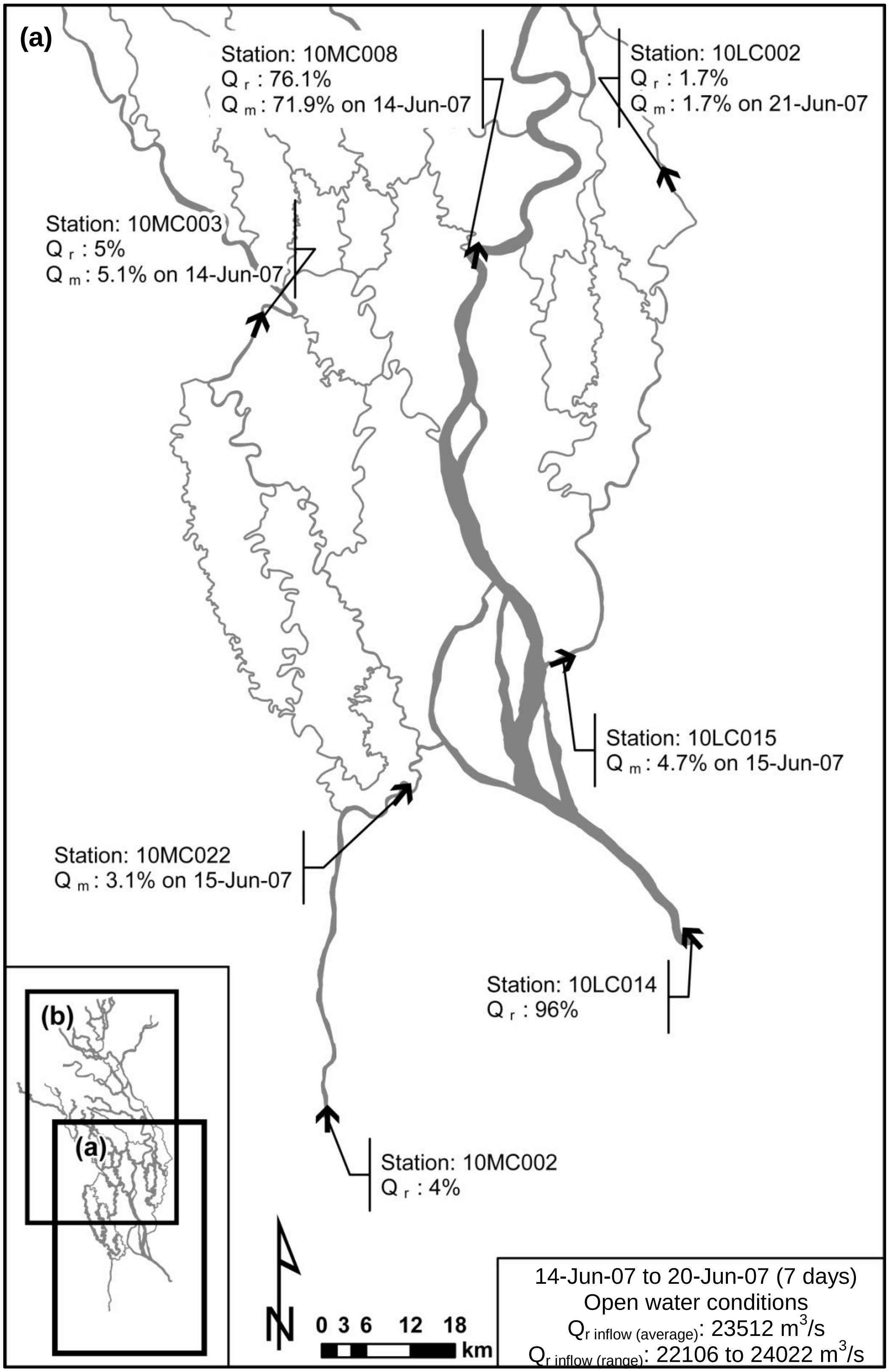

Figure 2.36 Flow as percentage of average inflow between 14-Jun-07 and 20-Jun-07 in the (a) upper Delta and (b) lower Delta. (Data source: the WSC).

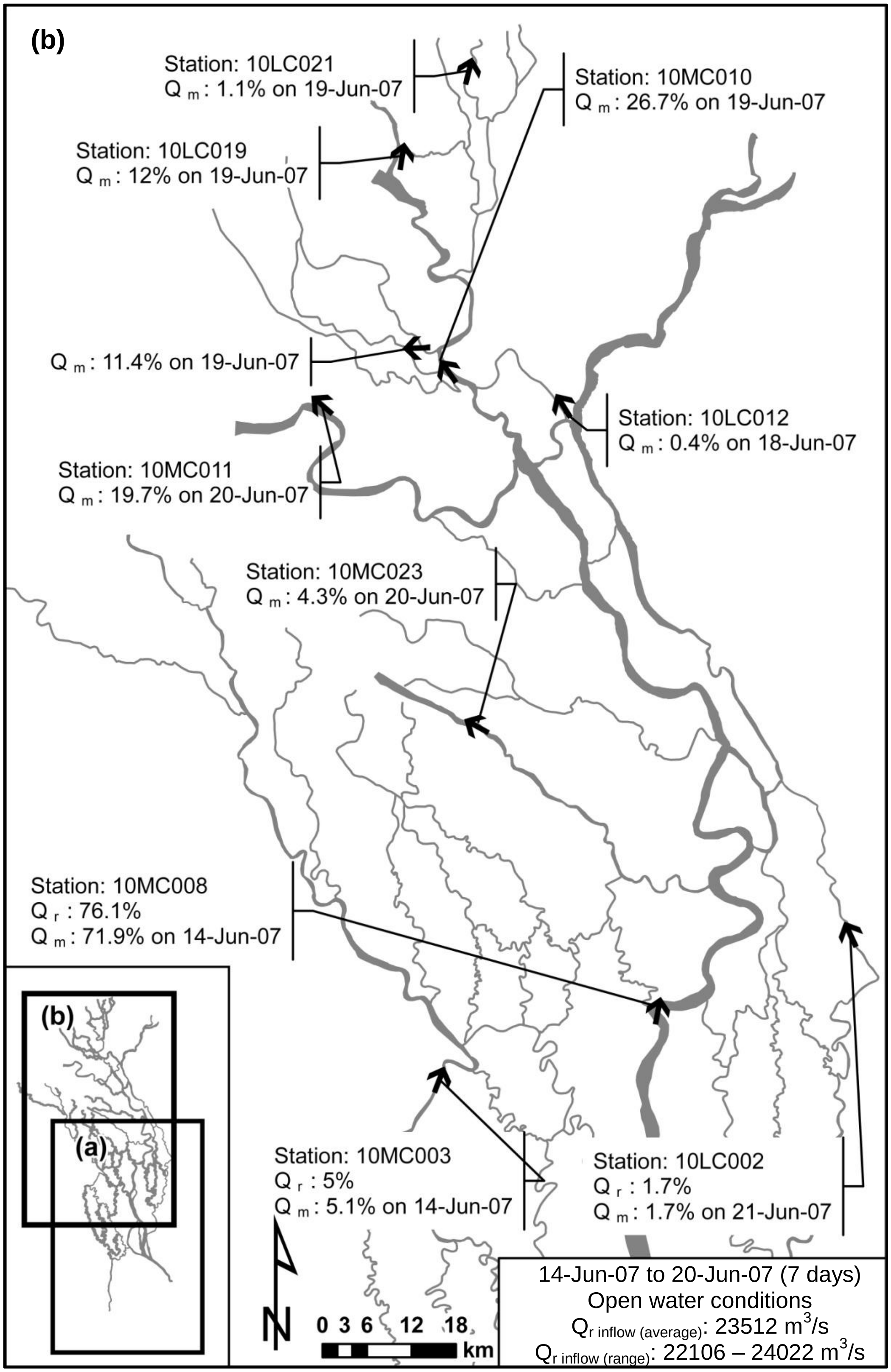

Figure 2.36 continued — Flow as percentage of average inflow between 14-Jun-07 and 20-Jun-07 in the (a) upper Delta and (b) lower Delta. (Data source: the WSC).

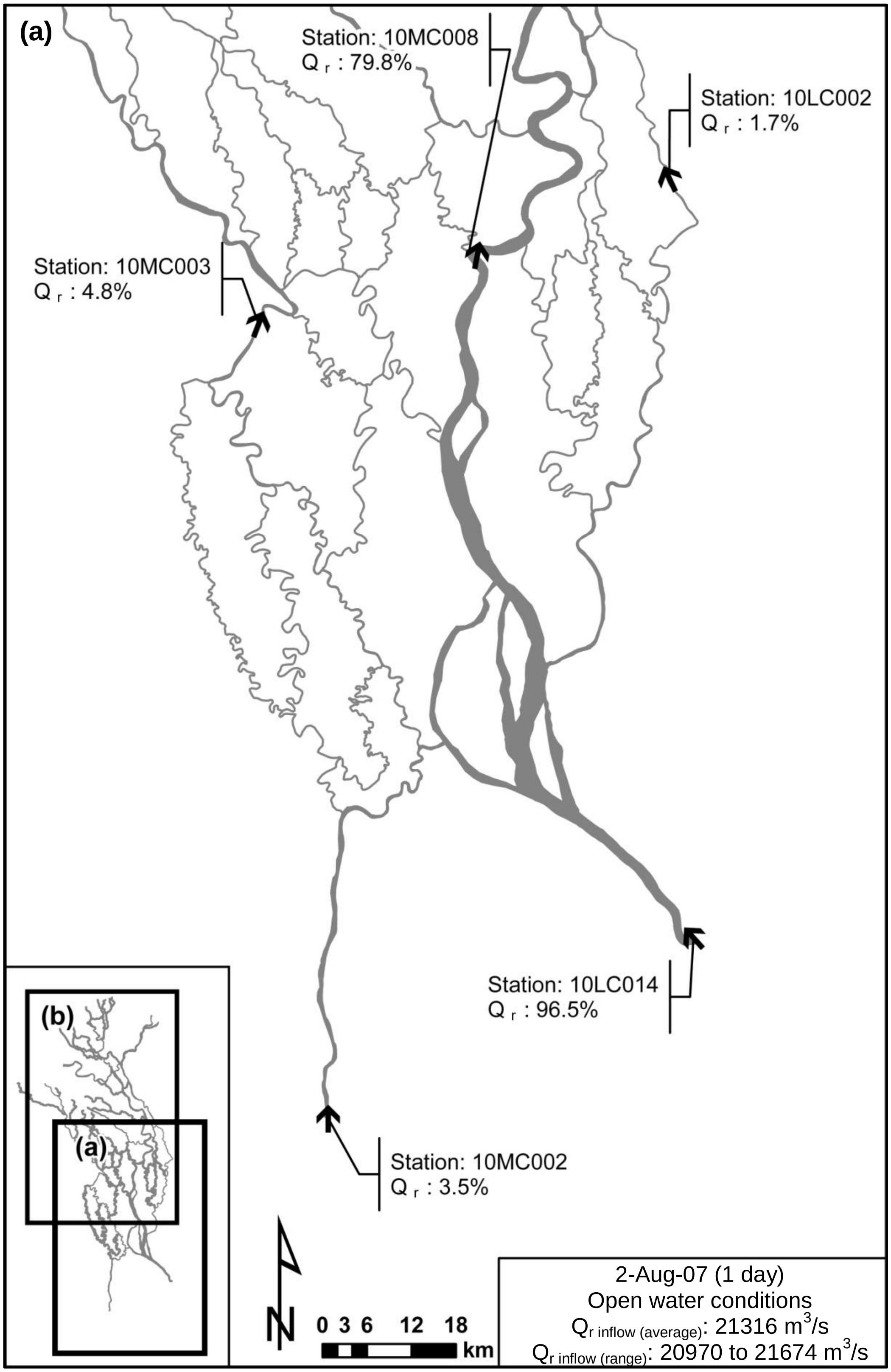

Figure 2.37 Flow as percentage of average inflow on 2-Aug-07 in the (a) upper Delta and (b) lower Delta.
(Data source: the WSC).

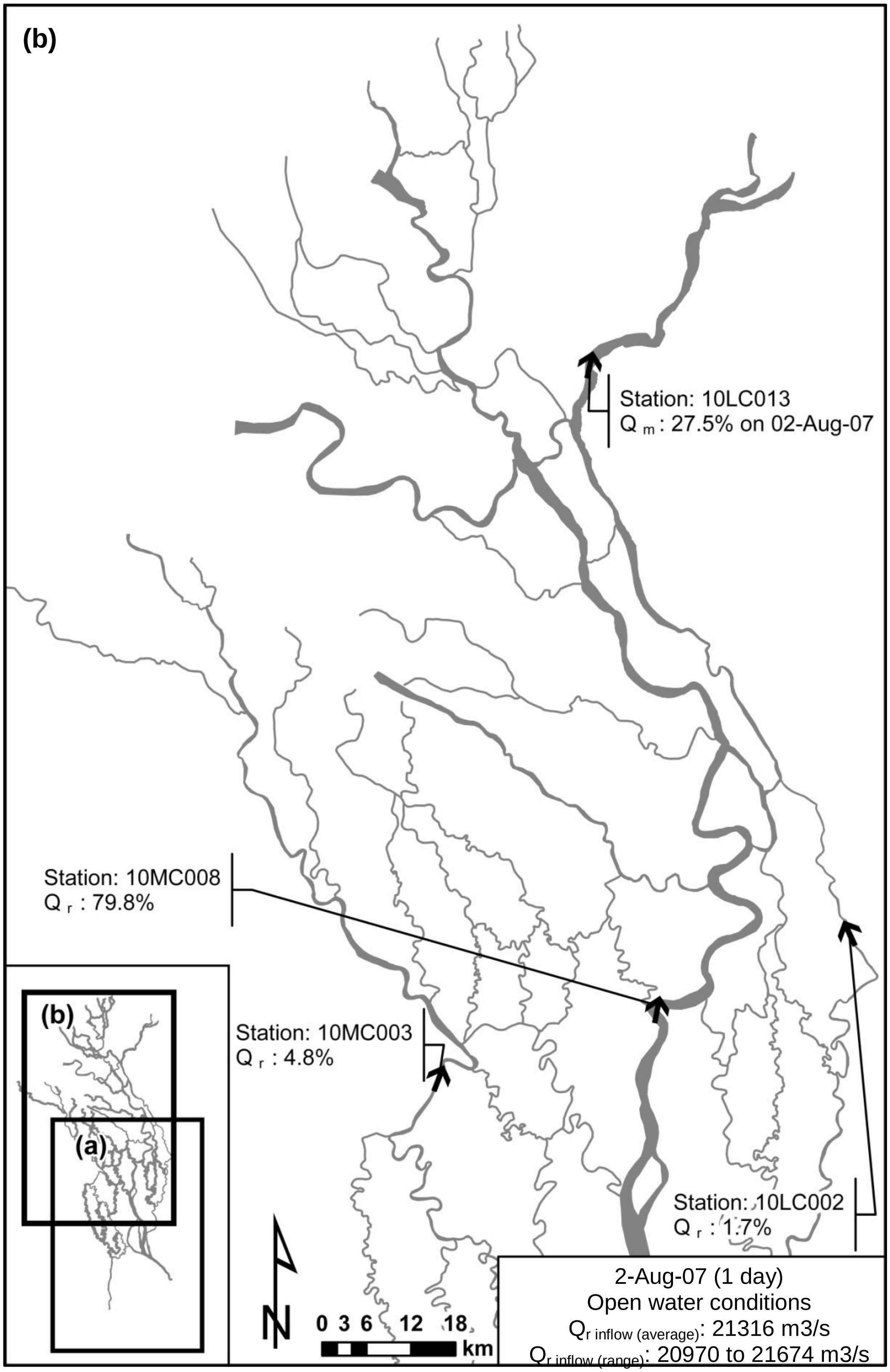

Figure 2.37 continued — Flow as percentage of average inflow on 2-Aug-07 in the (a) upper Delta and (b) lower Delta.
(Data source: the WSC).

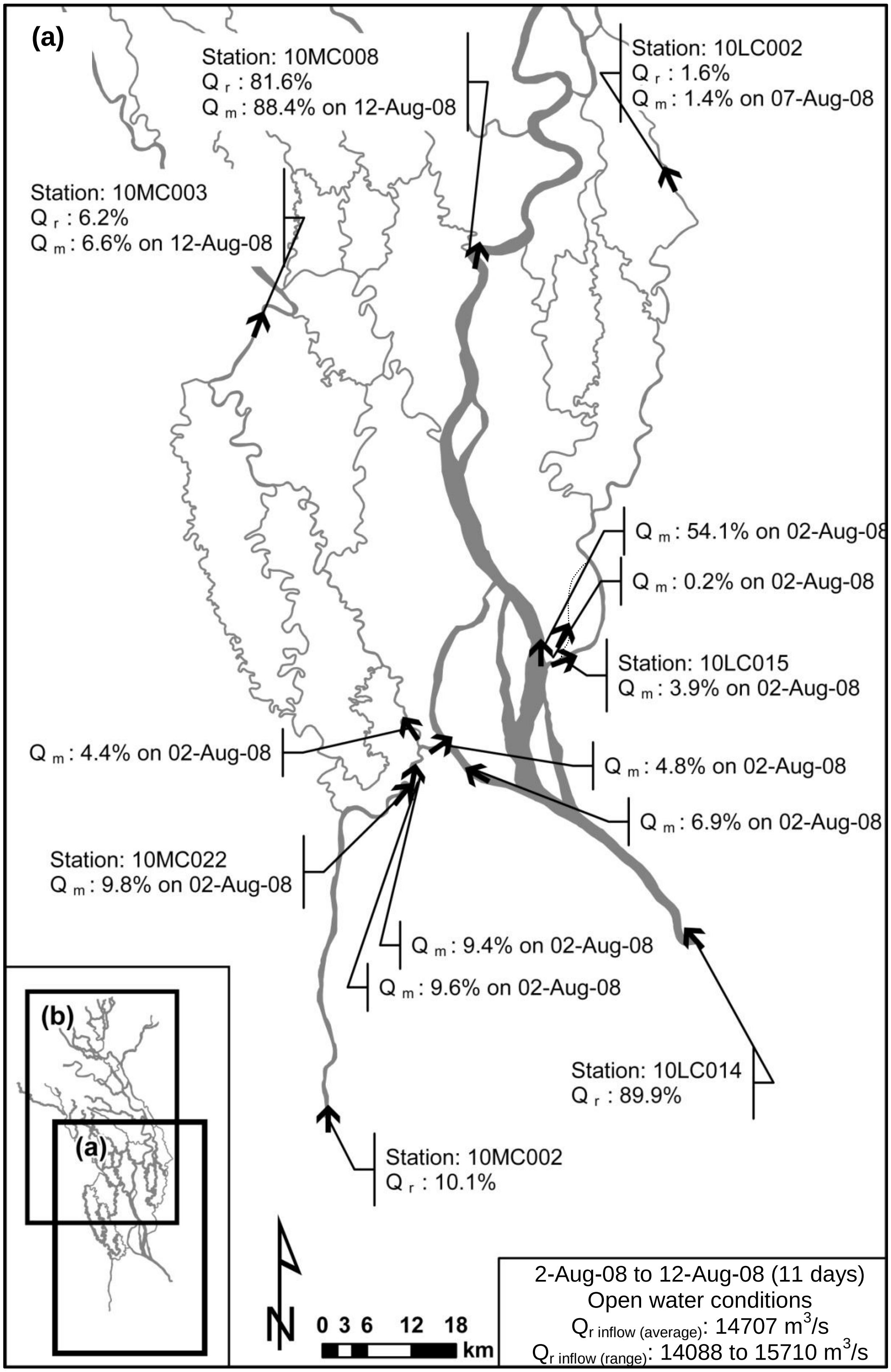

Figure 2.38 Flow as percentage of average inflow between 2-Aug-08 and 12-Aug-08 in the (a) upper Delta and (b) lower Delta. (Data source: the WSC).

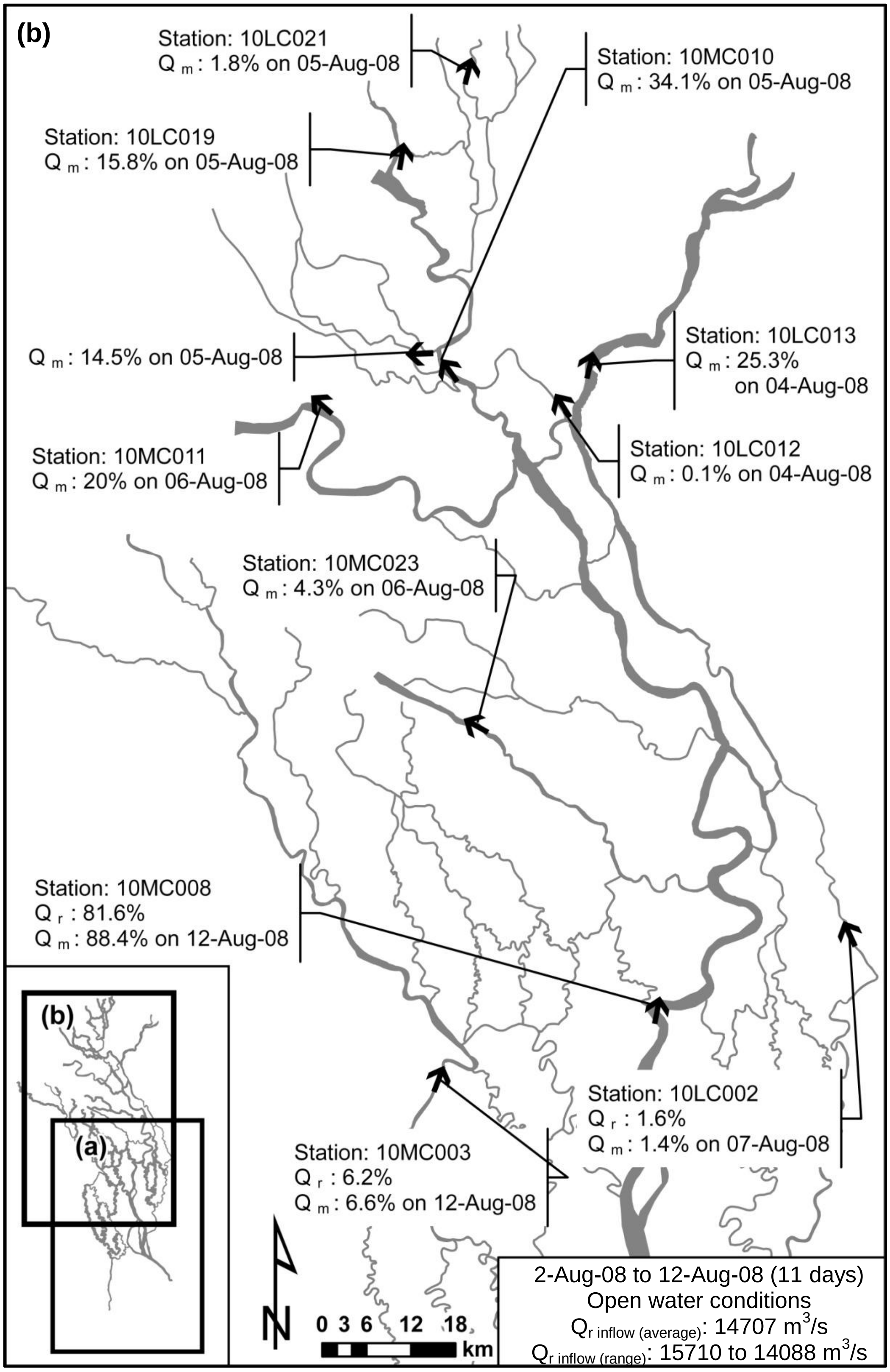

Figure 2.38 continued Flow as percentage of average inflow between 2-Aug-08 and 12-Aug-08 in the (a) upper Delta and (b) lower Delta. (Data source: the WSC).

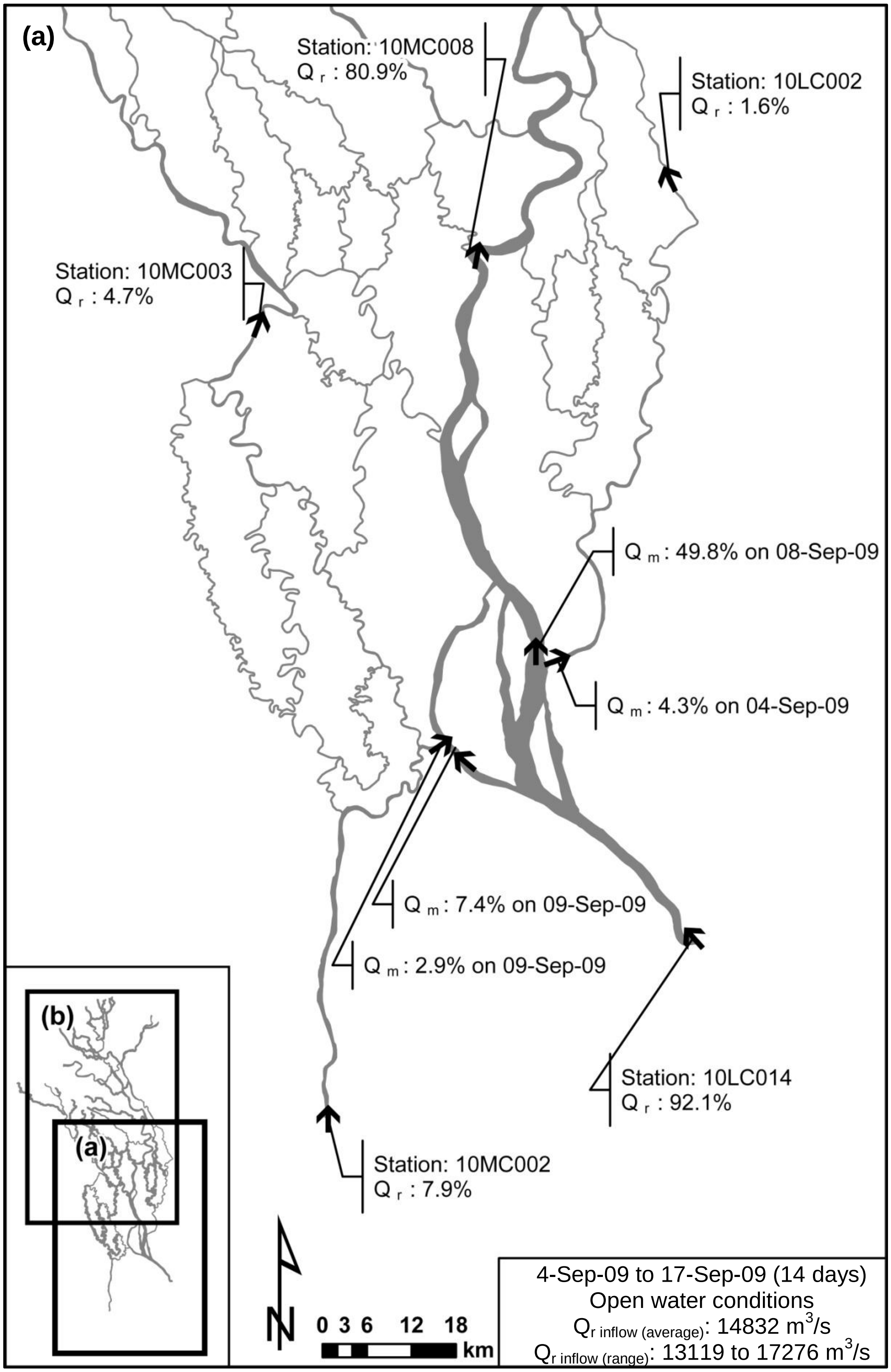

Figure 2.39 Flow as percentage of average inflow between 4-Sep-09 and 17-Sep-09 in the (a) upper Delta and (b) lower Delta. (Data source: the WSC).

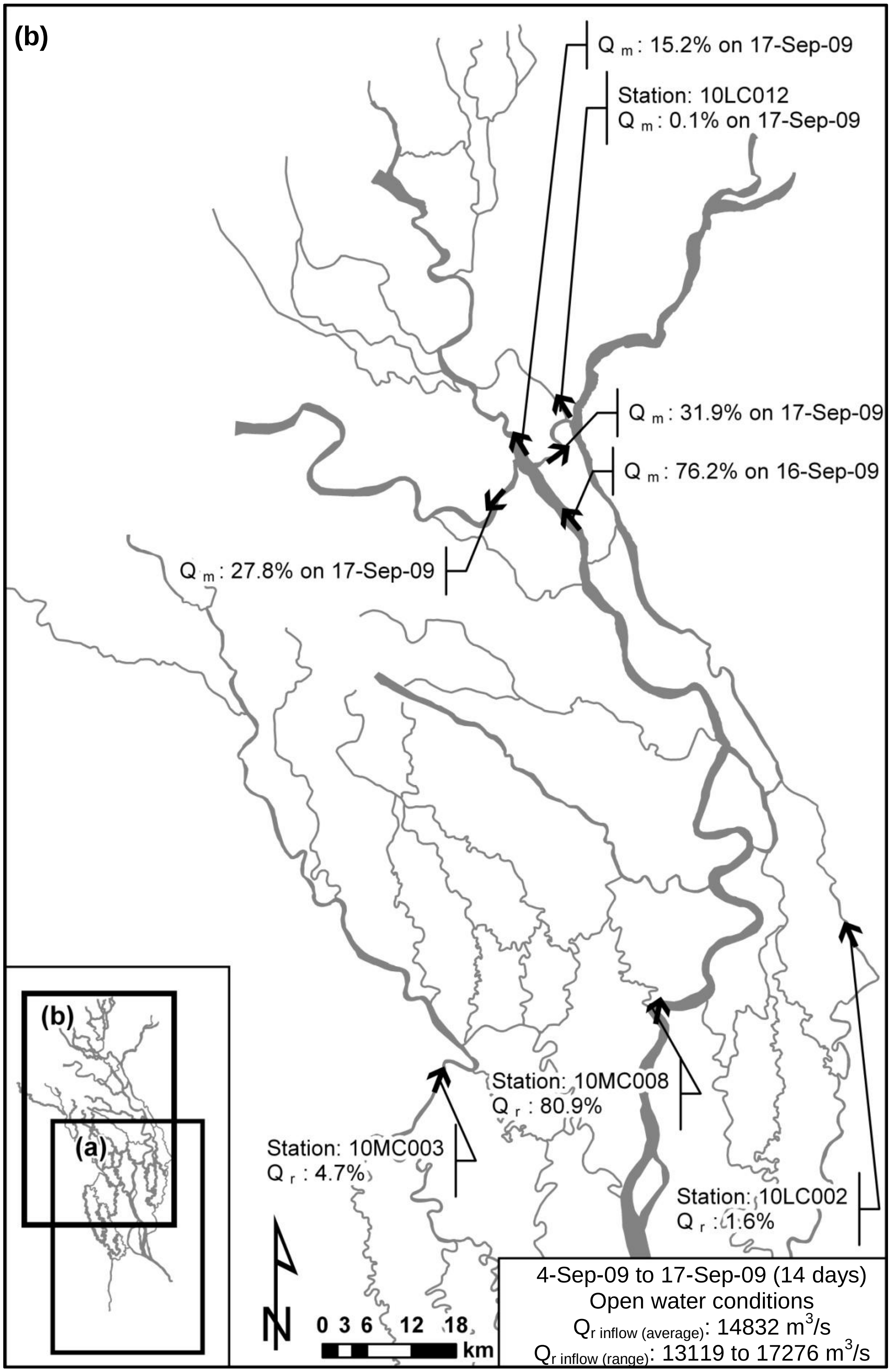

Figure 2.39 continued Flow as percentage of average inflow between 4-Sep-09 and 17-Sep-09 in the (a) upper Delta and (b) lower Delta. (Data source: the WSC).

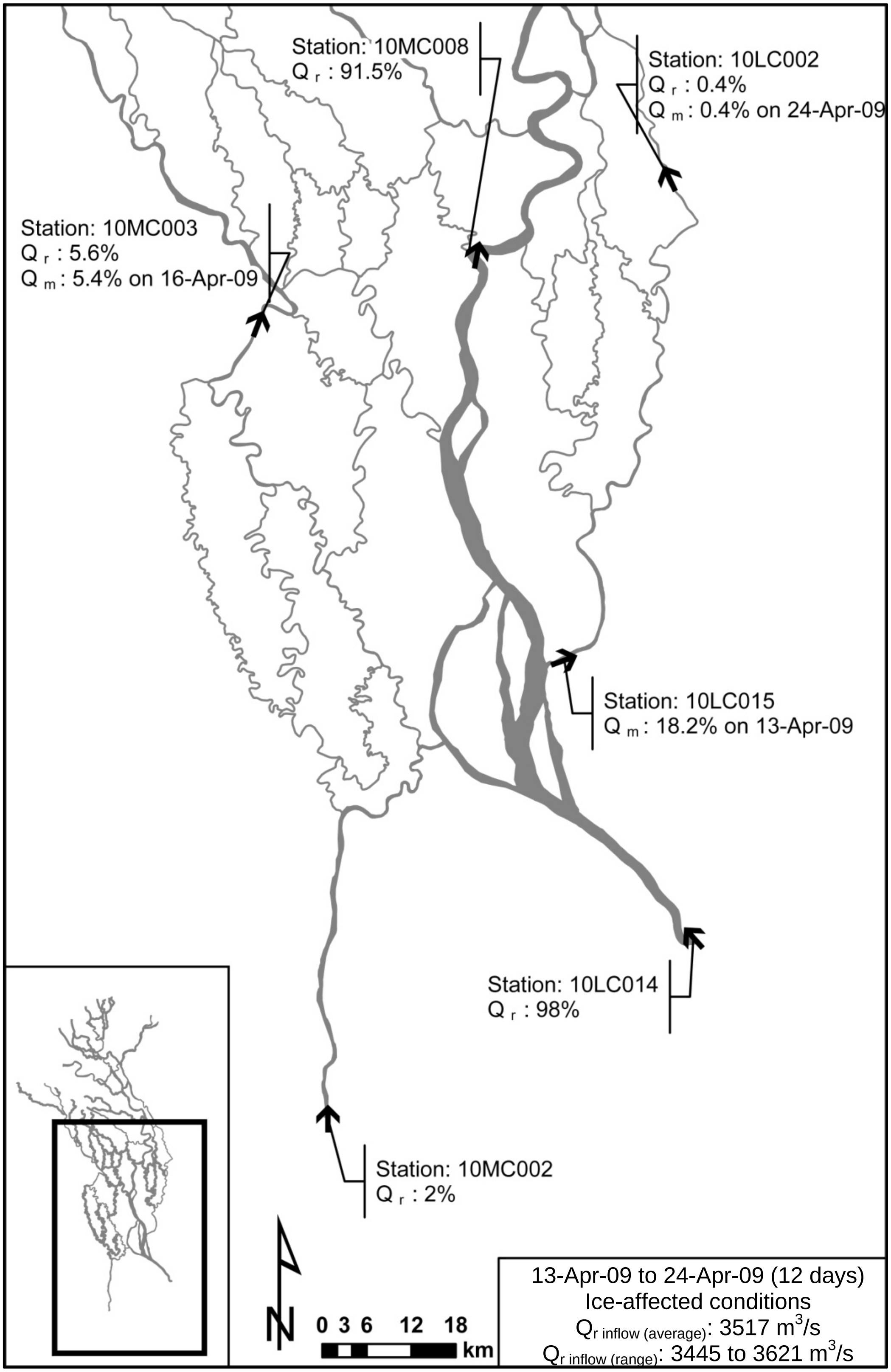

Figure 2.40 Flow as percentage of average inflow between 13-Apr-09 and 16-Apr-09. (Data source: the WSC).

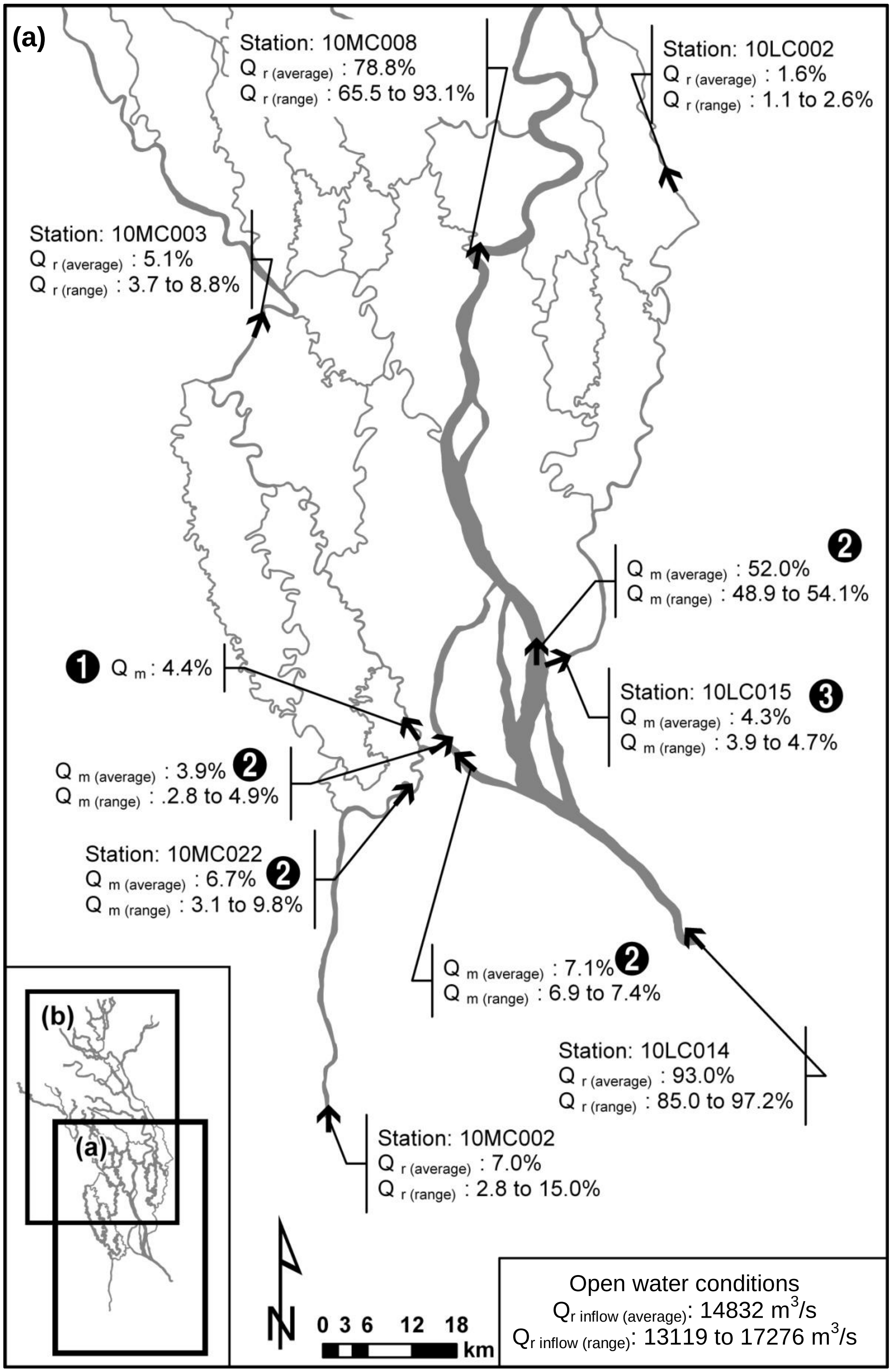

Figure 2.41 Average and ranges in the percent of flow during summer open water conditions in (a) upper Delta and (b) lower Delta. Symbol shows the number of measurements the range is based upon. (Data source: the WSC).

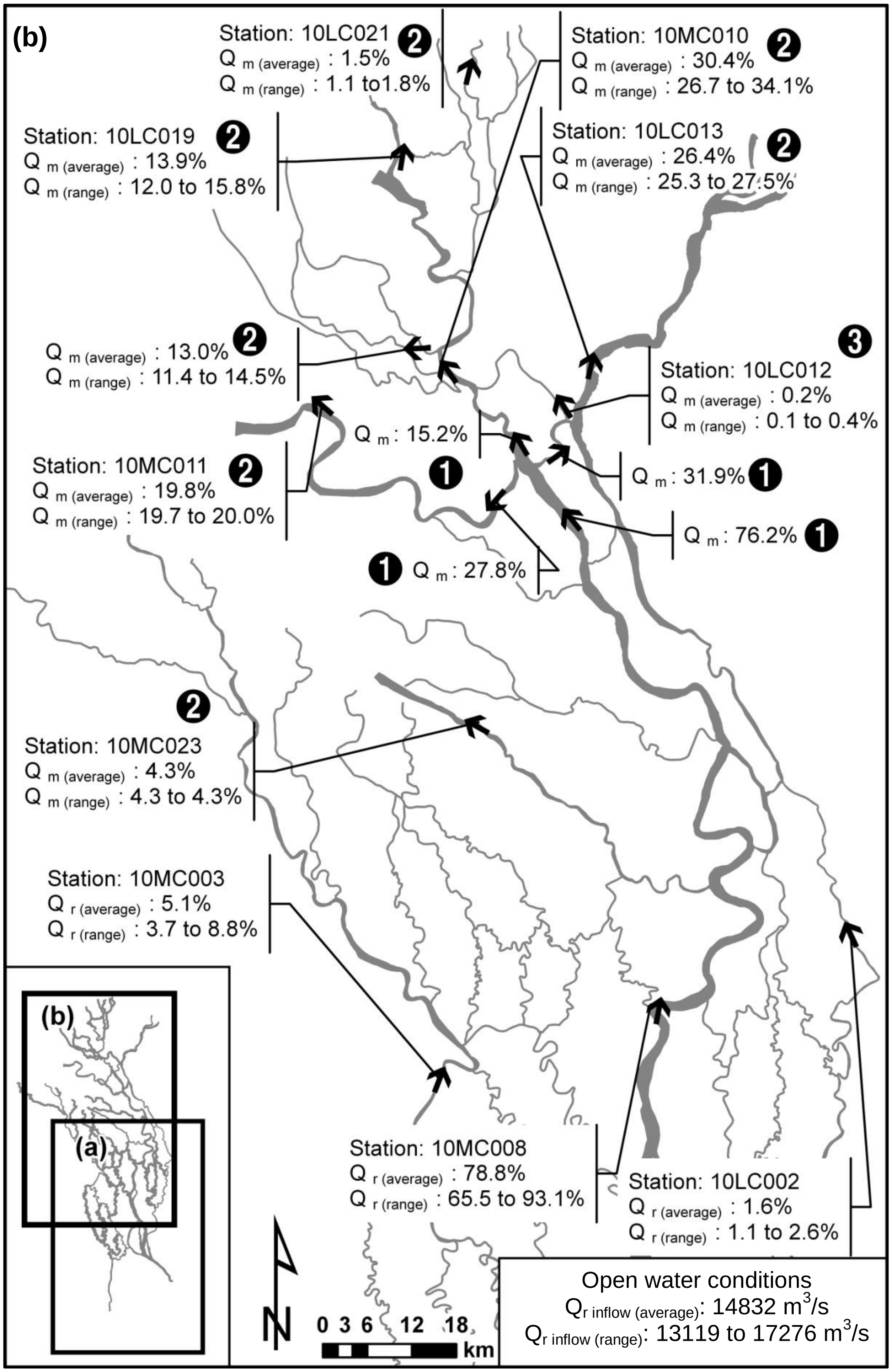

Figure 2.41 continued Average and ranges in the percent of flow during summer open water conditions in (a) upper Delta and (b) lower Delta. Symbol shows the number of measurements the range is based upon. (Data source: the WSC).

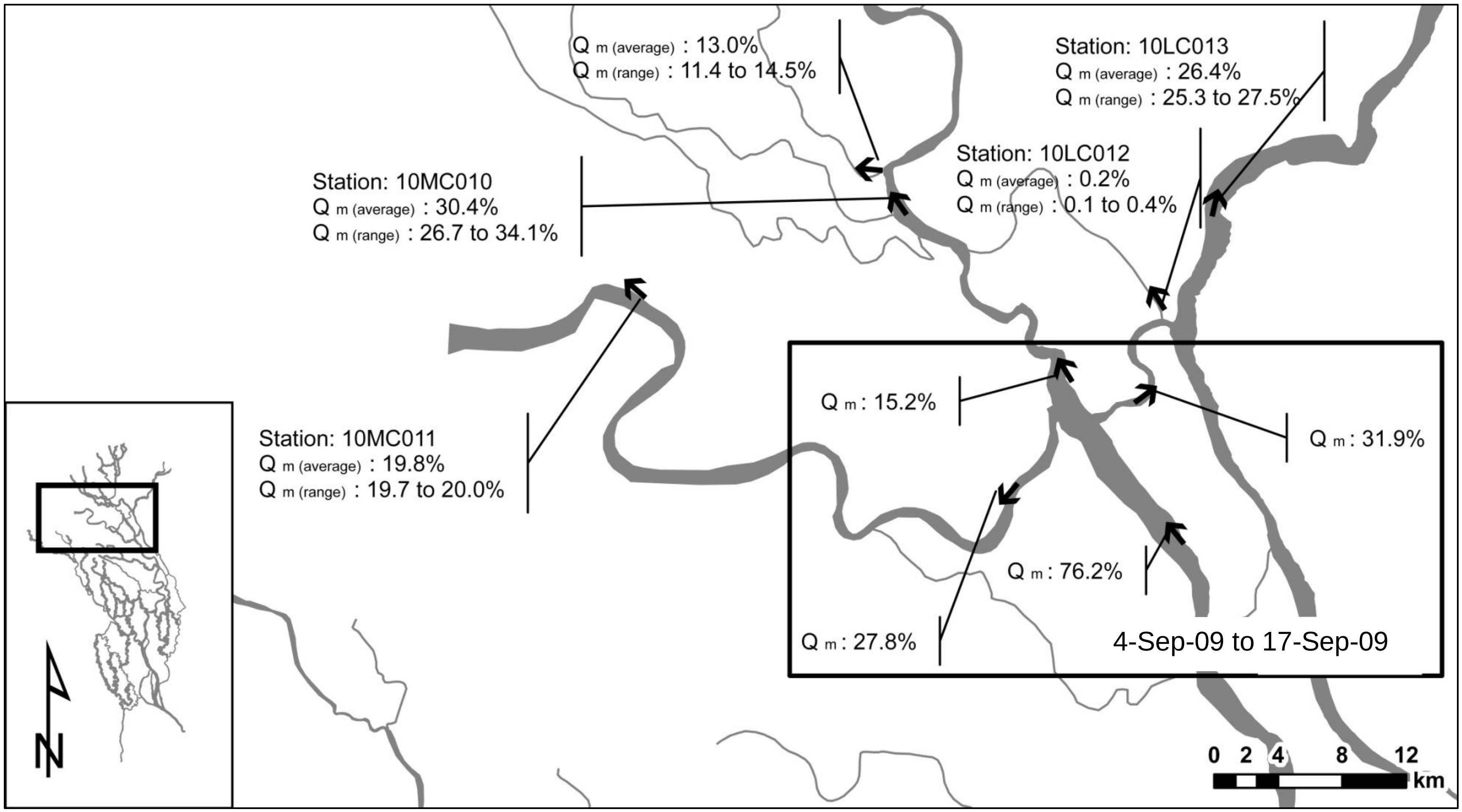

Figure 2.42 Flows measured during 4-Sep-09 to 17-Sep-09 in the "Quadrapus" compared to ranges of other flows measured during other periods. (Data source: the WSC).

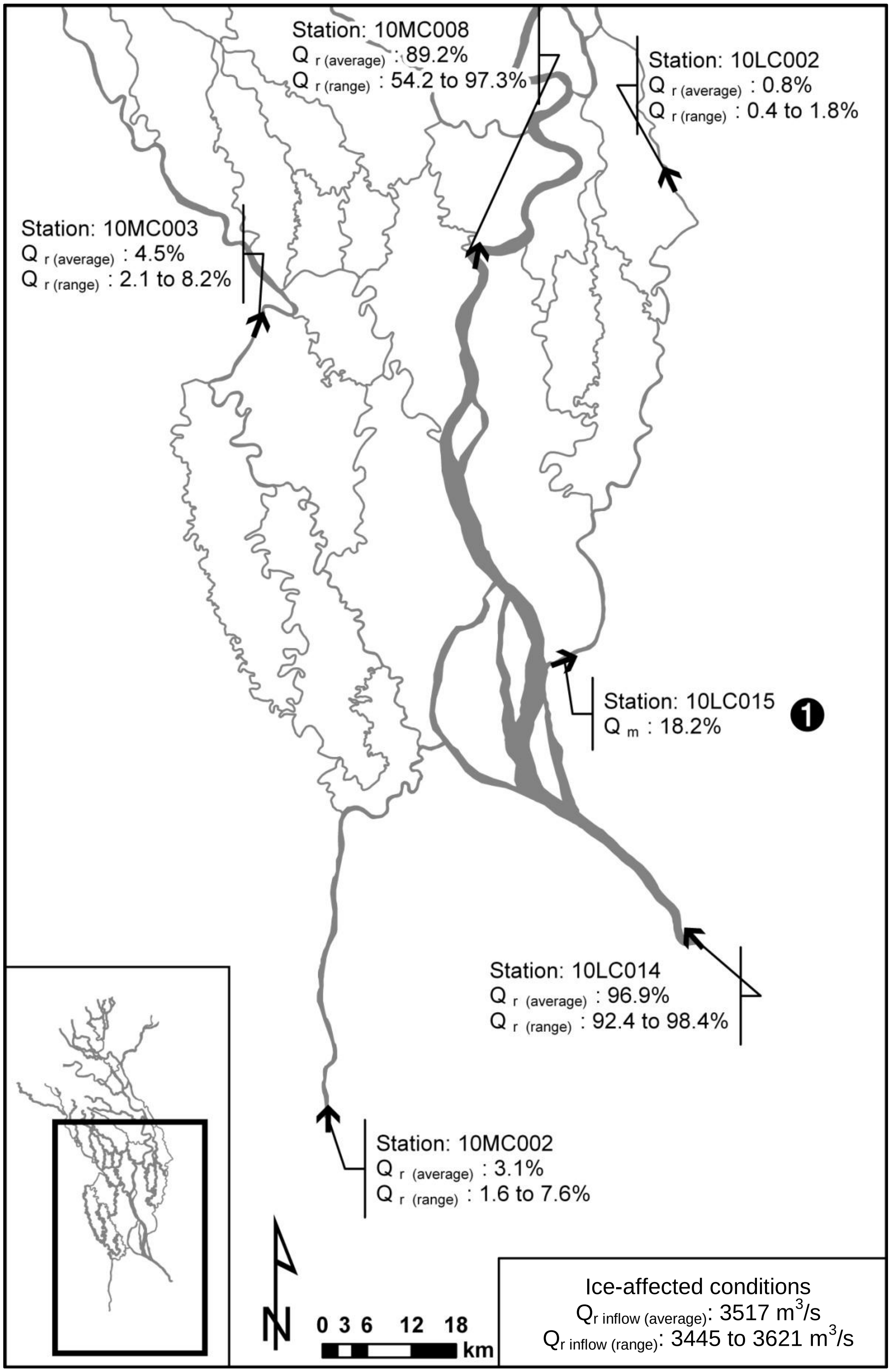

Figure 2.43 Average and ranges in the percent of flow during ice-covered winter conditions. Symbol shows the number of measurements the range is based upon. (Data source: the WSC).

3.0 Ice Processes in the Mackenzie Delta

Determining flow distributions in the Delta, is an essential component of understanding the nutrient loading to the Beaufort Sea, which is a primary goal of IPY-SCARF. However, the effect of ice on flow distributions is not well understood. Flow splits cannot be directly measured during ice jam events and very few have even been measured for simple ice covered flow conditions. In this chapter, the available data on ice processes in the Mackenzie Delta that was collected as part of this study are compiled. The contributions of IPY-SCARF partners are noted and synopsis of breakup during each of the study years is provided.

3.1 Ice-Affected Winter Conditions

The Mackenzie Delta is ice covered for up to eight months of the year (Bigras, 1990), with a full ice cover usually forming by late October (Bélanger, 2010). In most years, freeze-up begins on the lakes and then smaller channels, before a full ice cover is formed on the larger channels (Terroux *et al.*, 1981). This section reports on data measured during the winter months. Ice thickness measurements and groundfast ice mapping are presented.

3.1.1 Ice Thickness Data

Previous studies dating back to 1974 have documented ice thicknesses on the channels of the Mackenzie Delta. Anderson and Anderson (1974) documented ice thicknesses ranging from 0.7 m to 1.6 m, with a mean of 1.0 m to 1.2 m and found that ice thickness generally increased with increasing latitude. Terroux *et al.* (1981) documented ice thicknesses between 0.77 m and 1.75 m.

During the IPY-SCARF study period, winter ice thickness measurements were manually collected by both NRCan and the WSC by drilling cores in the ice cover. The WSC collected ice thicknesses at gauging sites during manual flow measurements and these data are shown in Table 3.1. NRCan collected manual ice thickness measurements during two timeframes: February to March 2009 and April 2010. The locations of these ice thickness measurements are shown in Figure 3.1. In addition to documenting ice thickness, NRCan also determined ice type in a lab, by analyzing thin sections of each core under polarized light. All ice thicknesses sampled along the Middle and East Channel are shown in Figures 3.2 and 3.3, respectively. The filled in symbols indicate groundfast ice, which is discussed further in the following section. On the Middle Channel, the average ice thickness for February to March 2009 was ~1 m, while in April 2010 this average was ~1.4 m. Additional ice thickness measurements may be needed to determine whether this is the result of ice thickness variations between years or due to increasing average thickness over the winter months. Though average ice thickness measurements were similar to the range measured by Anderson and Anderson (1974), a trend towards increased ice thicknesses in the north was not evident along the Middle or East Channel in this study. Including both the WSC and NRCan ice cores, the average ice thickness measured on the primary channels was ~1.0 m.

Table 3.1 Ice thicknesses recorded by the WSC over the study period. (Data source: the WSC).

Gauge	Date	Ice Thickness (m)
10LC002	29-Jan-08 14:39	0.75
	29-Feb-08 12:00	0.67
	24-Apr-08 14:43	1.11
	28-Nov-08 14:39	0.35
10MC003	26-Feb-08 16:15	0.61
	30-Apr-08 14:10	0.79
10MC008	11-Feb-09 14:10	0.68

Ice transects were also measured during the study period from 2006 to 2010 using a Ground Penetrating Radar (GPR). Stevens *et al.* (2009) used GPR transects to successfully characterize permafrost depths and groundfast versus floating ice cover, in the near-shore zone of the Mackenzie Delta. Figure 3.4 shows the location, and date of GPR surveys conducted by the University of Calgary in addition to those described in Stevens *et al.* (2009). NRCan also measured GPR transects on some of the primary channels in April of 2010 as part of the IPY-SCARF effort. Future work, as part of IPY-SCARF, will involve processing these transect data to yield ice thicknesses and comparing to manually measured ice thicknesses.

3.1.2 Groundfast Ice Mapping

In 2011, NRCan produced a groundfast ice information product, mapping the extent of groundfast ice in the Delta during the winter of 2009/2010 (Drouin and van der Sanden, 2011). A prototype example of the groundfast ice information product is shown in Figure 3.5. It was produced using RADARSAT-2 images

(Drouin and van der Sanden, 2011) and overlaying a land mask, so that channels areas could be identified. Image sites in the Delta were chosen based on the primary, secondary and tertiary channels considered for the MDHM. Locations of groundfast ice were compared with available manual ice measurements taken in April 2010 (Drouin and van der Sanden, 2011). Figure 3.5 shows groundfast ice in the outer Delta, particularly at the outlets of the Reindeer and East Channels. Past *km* 281 on the Middle Channel, nearly completely groundfast ice is shown, further substantiating that during winter flow likely routes through the Kumak Channel from *km* 281 to 293.5, as discussed in Section 1.1.1. Groundfast ice was also shown at the outlet of the Middle Channel (Kumak Channel) at *km* 293.5 and at the outlet of the Kuluarpak/Harry Channel.

3.2 Breakup Observations between 2006 and 2010

Breakup observations on the Mackenzie Delta are extremely time consuming, labour intensive and expensive due to the remote nature and large size of the Delta. Still, observations of river ice breakup have been documented in the Mackenzie Delta since the 1900s (Mackay, 1963), though most observations of ice breakup have been qualitative (e.g. Terroux *et al.*, 1981). One of the objectives of IPY-SCARF was to implement an intensive field program, including reconnaissance flights to document the evolution of breakup during each year of the study period and to provide data on ice cover conditions, to be used in the MDHM. The following sections report these observations.

3.2.1 Oblique Angle Flight Photos during the Study Period

A total of 23,714 oblique angle photos were taken by IPY-SCARF partners from fixed wing aircraft and helicopters during spring breakup over the five years of this study. In addition to those photos taken by persons from the University of Alberta (UofA), the photo contributions from each of the IPY-SCARF partners are shown in Appendix A. These photos were collected in a repository so that ice conditions on specific dates could be mapped with the intention of deducing the sequence of events during breakup in each year. However, not all photos were taken by river ice specialists and not all photos could be used to characterize ice conditions. In addition, not all of the photos could be geo-referenced and, therefore, it was not always possible to identify the location at which the photos were taken. Oblique photos were also supplemented with satellite imagery to provide a more complete picture of breakup sequencing.

3.2.2 Satellite Images obtained during Breakup

Satellite images that document the extent and condition of ice cover can be extremely valuable for documenting an ice breakup event. As part of this study, synthetic aperature radar (SAR) satellite images were acquired during the breakup period for each of the years of study at one to five day increments. Although large ice jams and flooding are sometimes visible in the pre-processed images, they are difficult to interpret without processing. For the 2008 breakup, NRCan produced post-processed satellite ice cover maps (van der Sanden and Drouin, 2011b) and flood condition maps (van der Sanden and Drouin, 2011a) that provide a snapshot view of the entire Delta over the breakup period. An example of the 26-May-08 ice cover product, showing the ice roughness is presented in Figure 3.6. Ice conditions were deduced from these, with smooth ice cover implying intact ice and rough ice being interpreted as ice jams. These conditions were compared with observations from available oblique flight photos (example shown in Figure 3.7) and were found to be in reasonable agreement. As a mask was used on the ice cover product so that the ice roughness is only shown within the summer channel boundaries, the land cover map was produced to supplement and show the extent of inundation above the summer water distribution. An example of this flood conditions product, showing the extent of flooding on 26-May-08, is shown in Figure 3.8. Because the processed satellite images provide exact geo-referenced maps of different ice conditions and the boundaries of ice jam activity when flights are not possible, they catalogue the formation and release of major ice jams over the entire breakup period and are very valuable for documentation of ice processes during breakup. To date, NRCan has processed a total of 11 ice cover maps from satellite images between 16-May-08 and 22-Jun-08 (van der Sanden and Drouin, 2011b), as well as a prototype of the land cover map for 26-May-08 (van der Sanden and Drouin, 2011a). Though extent of coverage area varies for each map, the processed images agree very well with localized fixed-wing and helicopter observations of ice conditions, particularly in cases where ice jams are known to have occurred and roughness contrasts in ice cover are more pronounced.

Distinguishing between intact ice and deteriorated ice when interpreting the satellite images can be difficult, especially in cases where there is melt water on the ice surface. Therefore, changing ice conditions leading up to breakup were not always correctly documented in the images. For example, some images seemed to overestimate the amount of open water, when comparing to oblique photographs (i.e. thermally deteriorating ice was reported as open water). The implications for this misclassification to modeling can be large due to the significantly different hydraulics between ice covered and open water conditions. However, overcoming such misclassifications may be not possible, as SAR cannot penetrate water. In addition, the roughness scale used for both the ice cover and land cover maps was difficult to verify. Still, the images provided a consistent view of the ice conditions over the entire breakup period and often over the entire Delta area. Most important, they gave a good view of how conditions were changing as breakup evolved in 2008.

3.2.3 Breakup Progression between 2006 and 2010

The following section discusses the sequence of breakup for each of the study years. The sequencing was deduced using geo-referenced oblique photos, satellite imagery, water levels at gauging stations monitored by the WSC, and reports (including Mackenzie Basin High Water Reports provided by the WSC (Environment Canada) and Mackenzie Delta Breakup Flooding Reports provided by the Bedford Institute of Oceanography (NRCan)) detailing conditions in the Delta. When possible, breakup progression maps were created showing the ice conditions on the primary, secondary and tertiary channels that were observed during flights. Hydrographs showing the water levels reported at each of the gauges on the (a) Middle, (b) East, (c) West, (d) Napoiak and (e) Reindeer Channel over the breakup period are shown for each year of 2006 to 2010 in Figure 3.9 to 3.13. The peak water level is also indicated, and the vertical lines show the timing of the ice progression maps produced in each year. For 2006, it was not possible to develop breakup progression maps, as photos were not geo-referenced. The most detailed photographs were available for 2008, as was the processed satellite imagery described in the previous section. As a result, a nearly complete sequence of breakup was deduced for 2008. For 2007, 2009 and 2010, breakup progression maps were completed for the days where data were available and an incomplete sequence of events was deduced. However, spatial coverage varied and was incomplete for each of the days when conditions were mapped. The ice classification scheme is defined in the following section.

3.2.3.1 Classification of Ice Conditions

Ice conditions were mapped using oblique photos for channels that were part of the primary, secondary and tertiary network using summer channel widths, with areas outside of these banks masked. Although these masked areas (particularly in the Turtle and outer delta) are inundated with water and ice during breakup this was not shown in the ice condition maps. For the purposes of developing the breakup progression maps, ice covers were classified as one of seven types:

- Intact,
- Deteriorated,

- Broken,
- Accumulation,
- Ice Jam,
- Ice Run or
- Open Water.

The distinction between intact and deteriorated ice was determined considering the degree of border ice inundation and channel widening due to stage increase, as well as albedo increase due to rotting of ice. If more than half the channel ice was either inundated or open water, then the ice was classified as deteriorated, otherwise the ice was classified as intact. Ice with hinge cracks, which run parallel to channel banks, was also considered deteriorated. Broken ice was identified by the presence of transverse cracks, which run perpendicular to the channel banks. Transverse cracking is often followed by ice movement, termed an ice run, which can involve conditions ranging from very low surface concentrations to one hundred percent concentrations of ice. Accumulations occur when large pieces of ice stop at a bend or constriction, but do not consolidate such that pieces remain horizontal and not pushed up on edge. Ice jams were identified as large accumulations in which ice pieces are collapsed upon each other and, therefore, are likely obstructing flow.

3.2.3.2 2006 Breakup Progression

In 2006, ice jams resulted in peak water levels that caused significant flooding across much of the Delta, including at the communities of Inuvik and Aklavik; as a result, 2006 was classified as an extreme ice-driven event by Goulding *et al.* (2009). In 2006, 2,563 oblique photos were taken between 20-May-06 and 30-May-06. Though large ice jams could be identified in these photos, the exact locations of the toe and head of jams could not be determined.

In 2006, water levels started to rise at the *Mackenzie River at Arctic Red River* (10LC014) on 05-May-06 (Figure 3.9a) and a week later also rose at the *Peel River above Fort McPherson* (10MC002) (Figure 3.9c). On 19-May-06, a large ice jam was reported on the Middle Channel from Tsiigehtchic at *km* 0 to Rosses Island (at ~ *km 79)* with broken ice downstream of the jam to Horseshoe Bend at ~ *km* 105, and intact ice downstream of *km* 105.[2] The following day, the water level at *Mackenzie River at Arctic Red River* (10LC014) peaked at 19.76 m (Figure 3.9a), but reports did not indicate when the jam released. Water levels at the *Peel River above Fort McPherson* (10MC002) remained at a peak of ~ 13.3 m until 22-May-06. On 26-May-06, an ice jam was reported 5 to 10 km below Alkavik[3] and over the subsequent days water levels rose at *Mackenzie River (Peel Channel) above Aklavik* (10MC003), peaking at 6.18 m on 28-May-08 (Figure 3.9c) before the ice jam released. An ice jam at Inuvik (~*km* 144) was reported to release between 29-May-06 and 30-May-06[4], but that peak water level at *Mackenzie River (East Channel) at Inuvik* (10LC002) (Figure 3.9b) was not recorded as there is a gap in the gauge history. On 31-May-06, it was estimated

[2] High Water Report for May 19, 2006, Rich Klakowich, Water Survey of Canada, Yellowknife, NWT.

[3] High Water Report for May 26, 2006, Murray Jones, Water Survey of Canada, Yellowknife, NWT.

[4] Special High Water Report for May 30, 2006, Angus Pippy, Water Survey of Canada, Yellowknife, NWT.

that 95% of the Delta was covered in water and numerous ice jams were reported in the area of the Quadrapus[5]. Extensive flooding and overflow were also observed in the outer Delta between 30-May-06 and 2-June-06,[6] and peak water levels at the downstream gauges of the Middle and East Channel were recorded on 31-May-06 and 1-Jun-06, respectively. Overall, as shown in Figure 3.9, peak water levels occurred successively and decreased in magnitude in the downstream direction along each channel (Goulding *et al.*, 2009).

3.2.3.3 2007 Breakup Progression

In 2007, breakup progressed successively from upstream to downstream and was mostly thermal in nature. In early May of 2007, major ice jams were observed on the Mackenzie River ~550 and ~370 km upstream of *Mackenzie River at Arctic Red River* (10LC014) (Beltaos and Carter, 2009), but no ice jams were reported in the Delta. Between 14-May-07 and 26-May-07, 2,194 oblique flight photos were taken with extensive areas photographed on 23-May-07 and 25-May-07. Figure 3.14 and 3.15 show the largely deteriorated ice cover in the upper Delta on 23-May-07 and 25-May-07, respectively. Only small accumulations were observed on the East and West Channels, and on Secondary Channel B. On the *Mackenzie River at Arctic Red River* (10LC014), the water level stayed at a peak of ~9.3 m between 22-May-07 and 28-May-07 (Figure 3.10a) and a higher peak water level of 11.71 m was observed at *Peel River above Fort McPherson* (10MC002) on 26-

---

[5] High Water Report for May 31, 2006, Angus Pippy, Water Survey of Canada, Yellowknife, NWT.

[6] Mackenzie Delta Breakup Flooding 2005-2006, Steve Solomon, Bedford Institute of Oceanography, Natural Resource Canada, Dartmouth, NS.

May-07 (Figure 3.10c). Ice moved past the Turtle between 29-May-07 and 31-May-07[7] after the peak water levels had passed. These peak water levels progressed to the downstream gauges over the next week, with a peak water level of 4.23 m observed at *Mackenzie River (East Channel) at Inuvik* (10LC002) on 1-Jun-07 (Figure 3.10b). As no significant ice jamming occurred in the Delta, water levels were much lower than typical and flooding in the upper Delta was limited. The peak extent of river outflow onto sea was ice observed between the 18-May-07 and 20-May-07[8].

3.2.3.4 2008 Breakup Progression

In 2008, large ice jams formed in both the Middle and East Channels and resulted in extensive flooding. Between 21-May-08 and 04-Jun-08, 9,906 oblique photos were captured, with extensive coverage available in the upper and mid-Delta between 23-May-08 and 30-May-08. Processed satellite imagery (van der Sanden and Drouin, 2011b, described in Section 3.2.2), was used to supplement the oblique photos and extend the limits of ice conditions presented on the breakup progression maps for this year. On 16-May-08, an ice jam at Arctic Red River was reported[9]. Three days later on 19-May-08, the water level at the *Peel River above Fort McPherson* (10MC002) gauge peaked at 11.31 m (Figure 3.11a) while water levels at the *Mackenzie River at Arctic Red River* (10LC014) continued to

---

7 Mackenzie Basin High Water Report for May 30, 2007, Angus Pippy, Water Survey of Canada, Yellowknife, NWT.

8 Outer Delta Flooding and Breakup, May 21, 2007, Report #13, Steve Solomon, Bedford Institute of Natural Resource Canada, Dartmouth, NS.

9 High Water Report for May 16, 2008, Angus Pippy, Water Survey of Canada, Yellowknife, NWT.

rise (Figure 3.11c). On 21-May-08, an ice run was reported at Fort McPherson[10] and water levels peaked and continued to rise at *Mackenzie River at Arctic Red River* (10LC014) as the upstream ice jam at reported on 16-May-08 released. On 22-May-08 intact conditions on the Middle Channel downstream of *km* 124 and deteriorated conditions on distributary channels were observed (Figure 3.16). Later on this day an 8 km jam with a toe at ~ *km* 69 along the Middle Channel was also reported (Beltaos and Carter, 2009). On 23-May-08 this jam was between 36 and 40 km long with the toe at ~ *km* 74 (Figure 3.17). In addition, a 12 km long ice jam in the East Channel toed at *km* 70 was also observed. On this day, water levels began to decline at *Mackenzie River at Arctic Red River* (10LC014) (Figure 3.11a). On 25-May-08, the toe of the jam in the Middle Channel at *km* 74 was observed to be relatively unchanged and an ice run upstream of the jam was seen (Figure 3.18). The East Channel ice jam was 15 km long with the toe located at *km* 71.

Figure 3.19 shows the East Channel junction on 25-May-08, with the ice run on the Middle Channel in the foreground and the ice jam in the Middle Channel in the background. Small sections with ice of accumulations followed by open water sections were also observed on both the East and West Channels upstream of Inuvik and Aklavik, respectively. The Middle Channel ice jam was observed to be 44 km long, with the toe located at the island at *km* 80, as shown in the photo in Figure 3.20. Figure 3.21 also shows the condition the East Channel jam which

[10] High Water Report for May 21, 2008, Angus Pippy, Water Survey of Canada, Yellowknife, NWT.

also increased to a length to 18.5 km, with the toe located at *km 72*.

On 27-May-09 (Figure 3.22) the toe locations of the Middle and East Channel jams were unchanged and the jams appeared to be melting. Peak water levels at the mid-Delta gauges were recorded between 26-May-08 and 30-May-08 and were very similar in magnitude, ranging from ~ 4.9 to ~ 5.6 m. The jam in the Middle Channel was observed to be in the process of clearing on 30-May-08 (Figure 3.23) (Beltaos and Carter, 2009). Overall, peak water levels occurred successively and decreased in magnitude in a downstream direction along each channel in a similar pattern as observed in 2006, although peak water levels were lower in 2008.

3.2.3.5 2009 Breakup Progression

During breakup in 2009, 5,755 oblique angle flight photos were taken between 06-May-09 and 08-Jun-09, including extensive coverage of ice jammed areas between 21-May-09 and 30-May-09. The first ice movement at Tsiigehtchic was reported on 4-May-09[11] as water levels at *Mackenzie River at Arctic Red River* (10LC014) began to rise (Figure 3.12a). On 21-May-09 (Figure 3.24) a mostly intact and deteriorated ice cover was observed north of the Turtle, while open water and small ice accumulations were observed along the West and West-Middle Connector Channels. Conditions evolved over the following days, and a building ice jam with the toe between *km* 76 and *km* 80 on the Middle Channel was observed on 24-May-09 (Figure 3.25), with sections of broken ice

[11] High Water Report for May 6, 2009, Angus Pippy, Water Survey of Canada, Yellowknife, NWT.

downstream of the toe. Water levels at *Mackenzie River at Arctic Red River* (10LC014) continued to rise until 26-May-09 when they peaked at 11.78 m (Figure 3.12a). The following day (27-May-09) a 36 km long jam was observed on the Middle Channel with the toe at ~ *km* 71 (Figure 3.26). A 21 km jam on the East Channel, with the toe at *km* 73, just downstream of where the East Channel leave the Middle Channel, as well as a small jam at Inuvik. The jam at Inuvik released before 30-May-09.

On 30-May-09, the ice jams on the Middle and East Channels (just downstream of where it begins), were observed (Figure 3.27), but the toe in the Middle Channel had shifted down to ~ *km* 77 and the toe in the East Channel had receded to ~ *km* 69. Two days later, a peak water level of 5.24 m at *Mackenzie River (Middle Channel) below Raymond Channel* (10MC008) was recorded likely indicating that the ice jam in the Middle Channel had released (Figure 3.12a).

Overall, ice jam activity in the upper/mid-Delta resulted in significant water levels at the upstream gauges. Peak water levels were not successive along each of the channel as observed in 2006 and 2008, as water levels peaked at *Mackenzie River at Confluence East Channel* (10LC015) and *Peel River at Frog Creek* (10MC022) two days earlier than their respective upstream gauges.

3.2.3.6 2010 Breakup Progression

The field program in 2010 included 3,296 oblique photos captured between 11-May-10 and 21-May-10. Ice cover conditions were mapped between 19-May-10 and 21-May-10. A peak water level at *Peel River above Fort McPherson*

(10MC002) was recorded very early in the season on 5-May-10, but also peaked again on 19-May-10 (Figure 3.13c). Ice movement at Tssigehtchic was reported between 09-May-10 and 10-May-10[12] and water levels peaked at 10.89 m at *Mackenzie River at Arctic Red River* (10LC014) (Figure 3.13a) on 19-May-10. On the same day, a 30 km long ice jam with the toe at ~ *km* 61 (Figure 3.28) was seen. Though the toe of the jam was observed to be stopped, the jam was consolidating upstream of the toe and an incoming ice run was observed up to *km* 0 on the Middle Channel. Downstream of the ice jam toe, conditions were deteriorated, while small accumulations and open water segments were seen on the East Channel.

By 21-May-10, the ice jam in the Middle Channel was 34 km long and the toe had pushed down to *km* 66 (Figure 3.29). Downstream of the ice jam, deteriorated ice was observed down to the Quadropus at ~ *km* 221. Open water along the West Channel upstream of Aklavik was also observed. On the same day, the water level at *Peel River at Frog Creek* (10MC022) (Figure 3.13a) peaked at 11.45 m, which was more than 1.5 m higher than the peak at the *Peel River above Fort McPherson* (10MC002) (Figure 3.13c). Ice conditions remained unchanged overnight, with some melt apparent.

---

[12] High Water Report for April 22, 2010, Angus Pippy, Water Survey of Canada, Yellowknife, NWT.

3.2.4 Channel-Lake Connections During Breakup

Channel lake connections are very important for the replenishment of nutrients to the delta's lakes (Lesack and Marsh, 2007; Emmerton *et al.*, 2007; Marsh, 1986). During breakup these connections are most evident, as peak water levels result in the flooding of lakes that are normally cut off from the channel network (Bigras, 1990). Numerous channel-lake connections were observed in the oblique photos. Examples of channel-lake connections during spring breakup are shown in Figure 3.30(a) and (b). Figure 3.30(a) shows an ice run on the East Channel, with ice running through a side channel into a lake on 23-May-08. A lake channel connection, in which the bank between the East Channel had eroded, causing ice to flow into a lake adjacent to the channel, is shown in Figure 3.30(b).

3.2.5 Overall Progression of Breakup Observed Between 2006 and 2010

Some consistent patterns in the formation and release of ice jams were evident over the five years of study from 2006 to 2010. In four of the five years, a long ice jam formed along the Middle Channel with the toe being between *km* 60 and 80. The exception was 2007, for which breakup was mostly thermal and no ice jams were documented anywhere in the Delta. This Middle Channel ice jam stayed in place for greater than three days in each of the four years, with the toe often pushing downstream over that period. In at least two of the five years, an ice jam occurred on the East Channel, with a toe being located between *km* 60 and 71, was observed. Although small ice jams and accumulations were common in both the East and West Channels, no other consistencies were documented.

Overall, ice deteriorated first in the smaller channels and peak water levels tended to occur first in the upper Delta and progressed downstream, though gauges at *Peel River at Frog Creek* (10MC022) and *Mackenzie River at Confluence East Channel* (10LC015) did not always follow this trend. In addition, the downstream gauges on the Middle and East Channel (*Mackenzie River (Kumak Channel) below Langley Island* (10LC019) and , respectively) could have peaked earlier than those water levels upstream as continuous measurement were only available in one year. Water level peaks along the Middle and East Channels were always highest at the upstream gauges and lower at each successive gauge downstream. On the West Channel, peak water levels at *Peel River at Frog Creek* (10MC022) were higher than water levels observed upstream at *Peel River above Fort McPherson* (10MC002) in two of the three years where data were available for both gauging stations.

Overall, there was a broad range of peak water levels observed at each of the stations, particularly at the upstream gauging stations. For example at the *Mackenzie River (East Channel) at Inuvik* (10LC002), peak water levels ranged from 9.4 m in 2007 (when no ice jams were observed) to 19.7 m in 2006 (when large ice jams were observed). This illustrated shows how ice jams dramatically affect water levels during the breakup period.

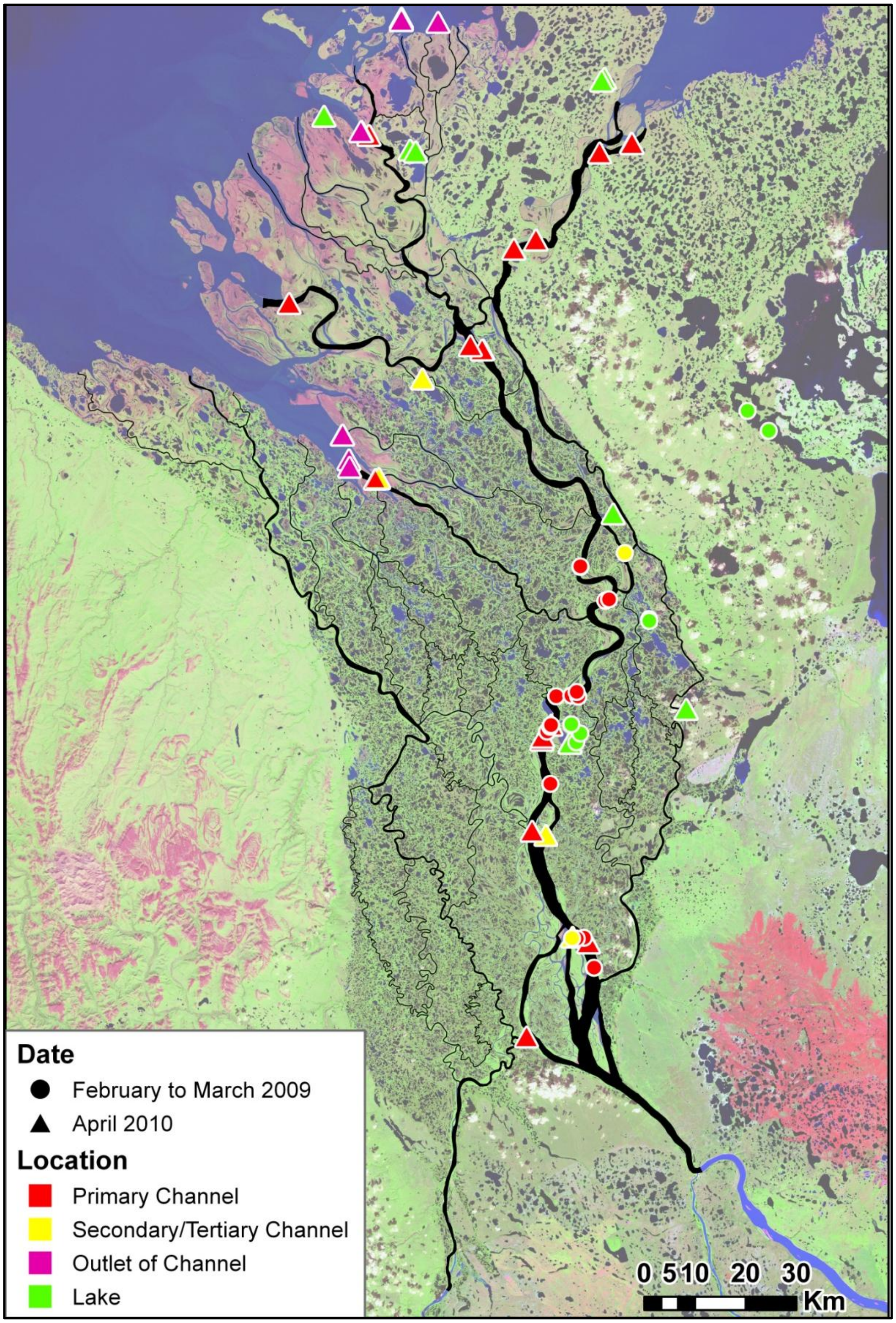

Figure 3.1 Location of ice thickness measurements in 2009 and 2010 in the Mackenzie Delta
(Data source: NRCan).
(Base image source: Industry Tourism and Investment, NWT).

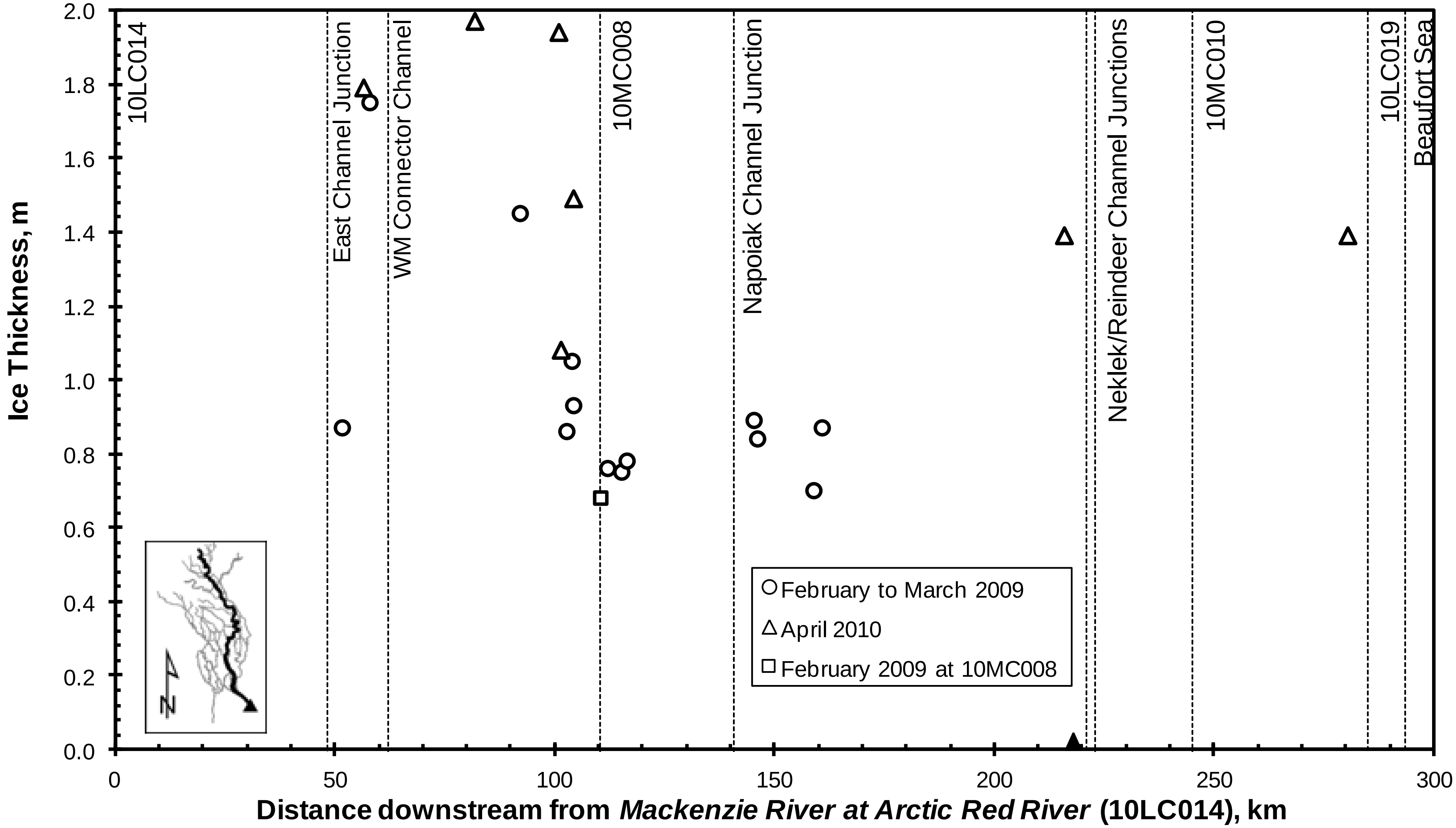

Figure 3.2 Ice thickness measurements along the Middle Channel of the Mackenzie Delta. Filled in symbols indicate groundfast ice. (Data source: NRCan and the WSC).

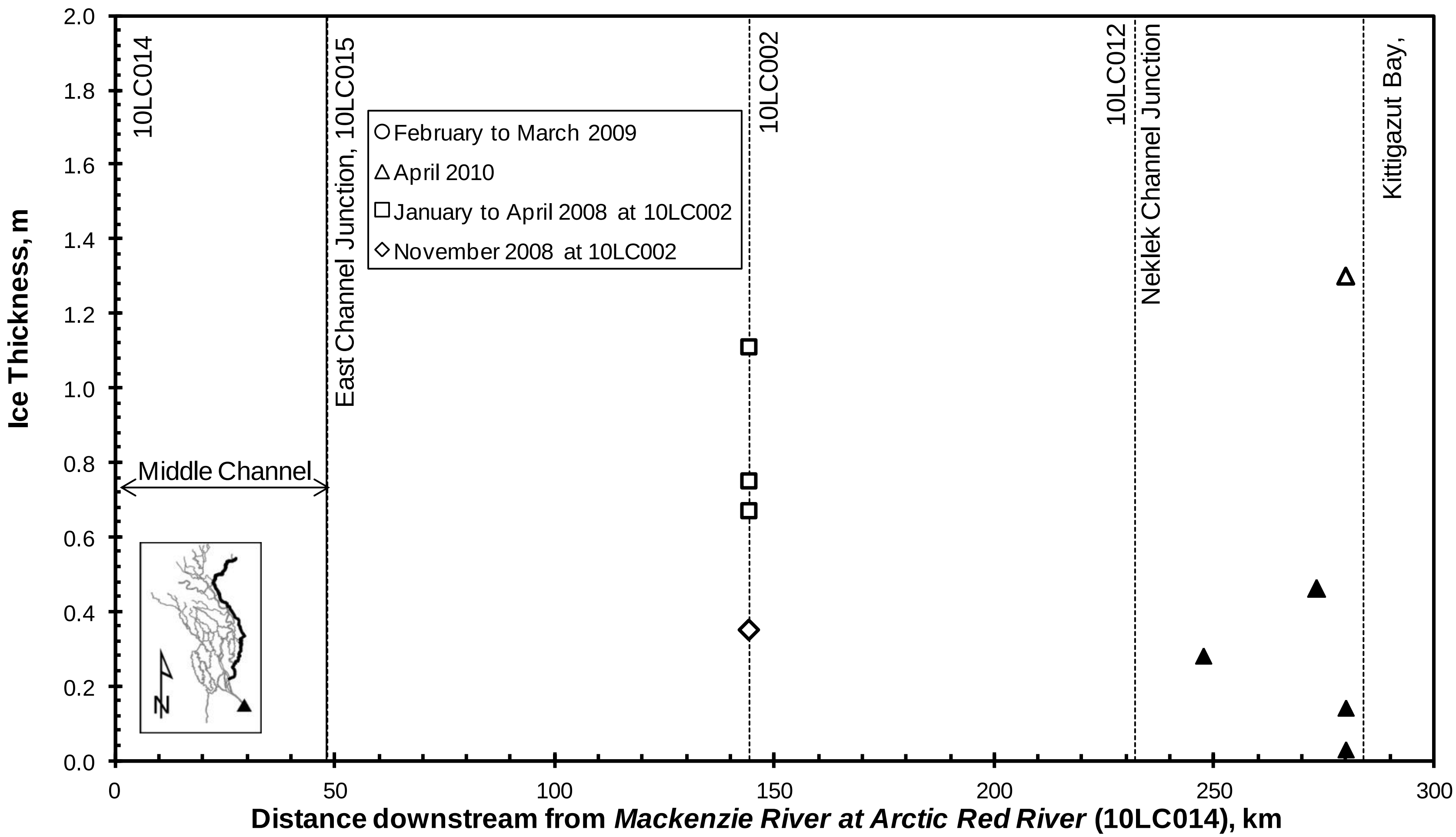

Figure 3.3 Ice thickness measurements along the East Channel of the Mackenzie Delta. Filled in symbols indicate groundfast ice. (Data source: NRCan and the WSC).

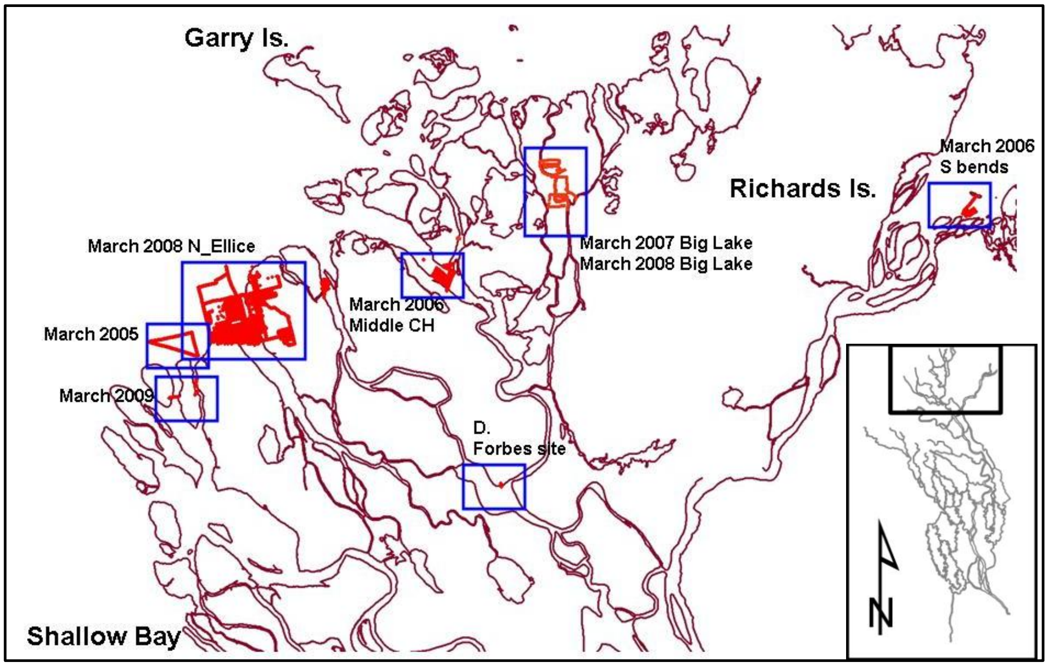

Figure 3.4 GPR transects surveyed by the University of Calgary. (source: Personal communication, C. Stevens, Department of Geoscience, University of Calgary, Calgary, AB, Canada).

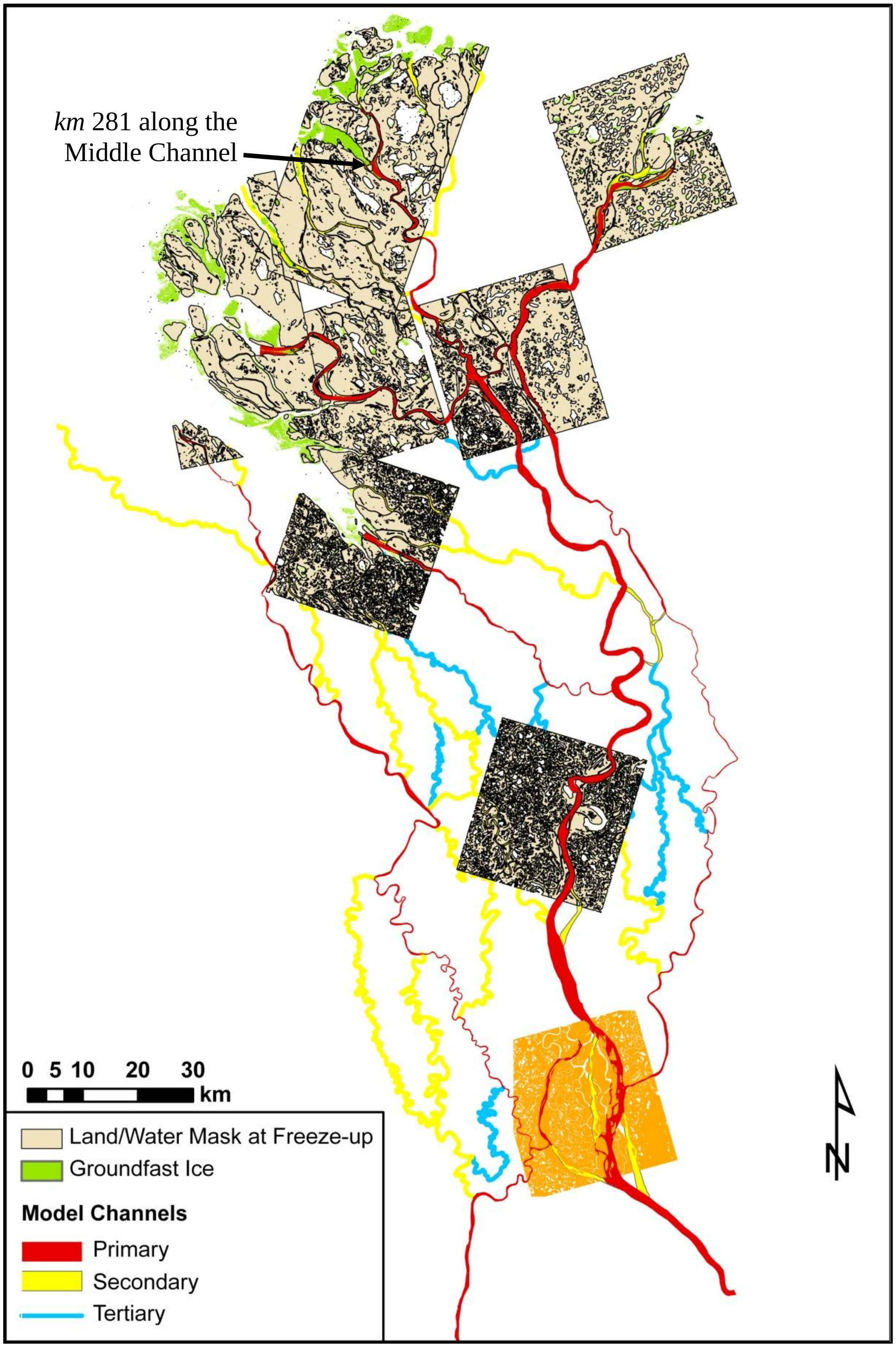

Figure 3.5 Screenshot of prototype groundfast ice information product for Mackenzie River Delta, winter 2009/2010. (adapted from Drouin and van der Sanden, 2011).

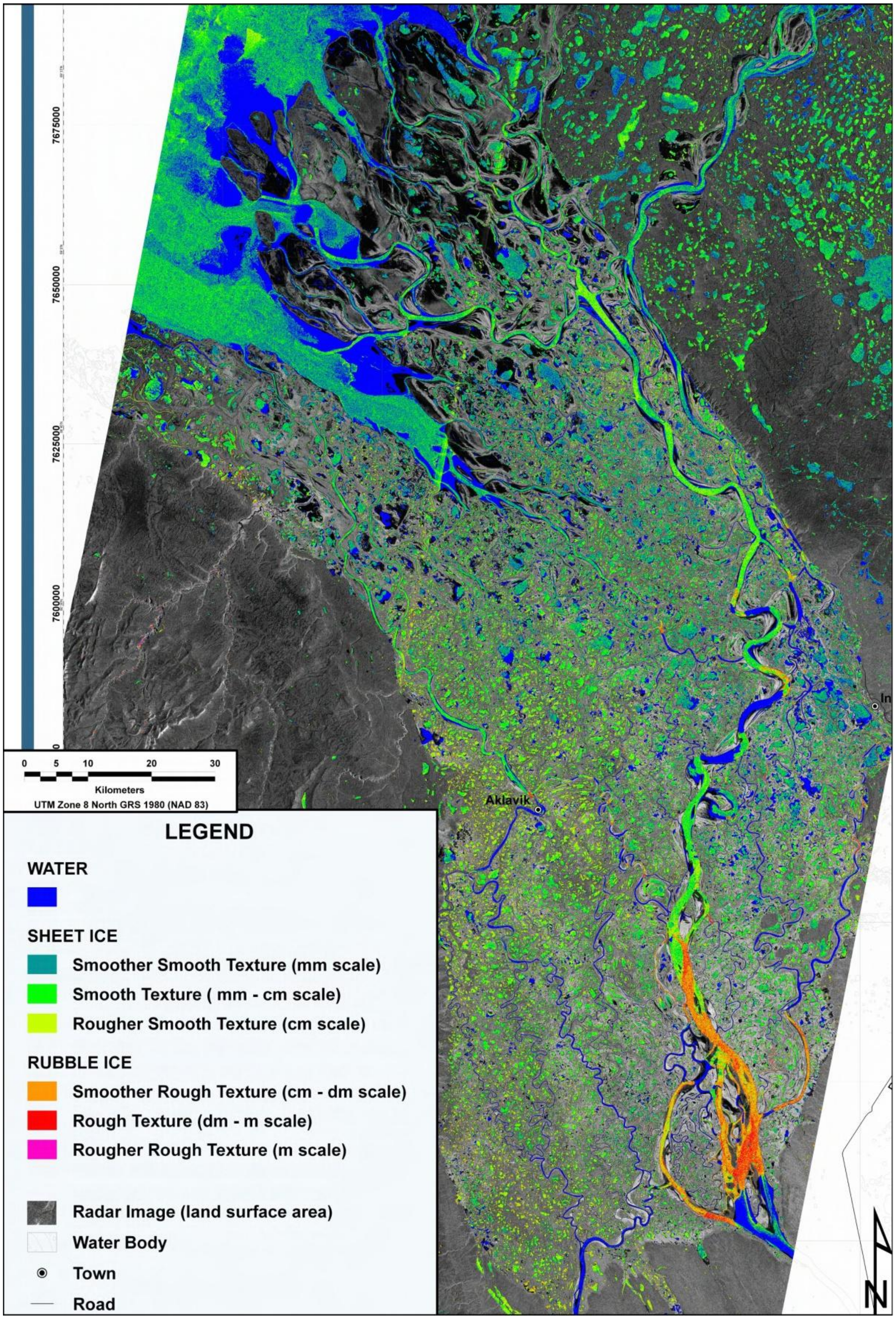

Figure 3.6 Example of Spring 2008 Ice Cover Product for 26-May-08 produced by NRCan using satellite imagery (adapted from van der Sanden and Drouin (2011b)).

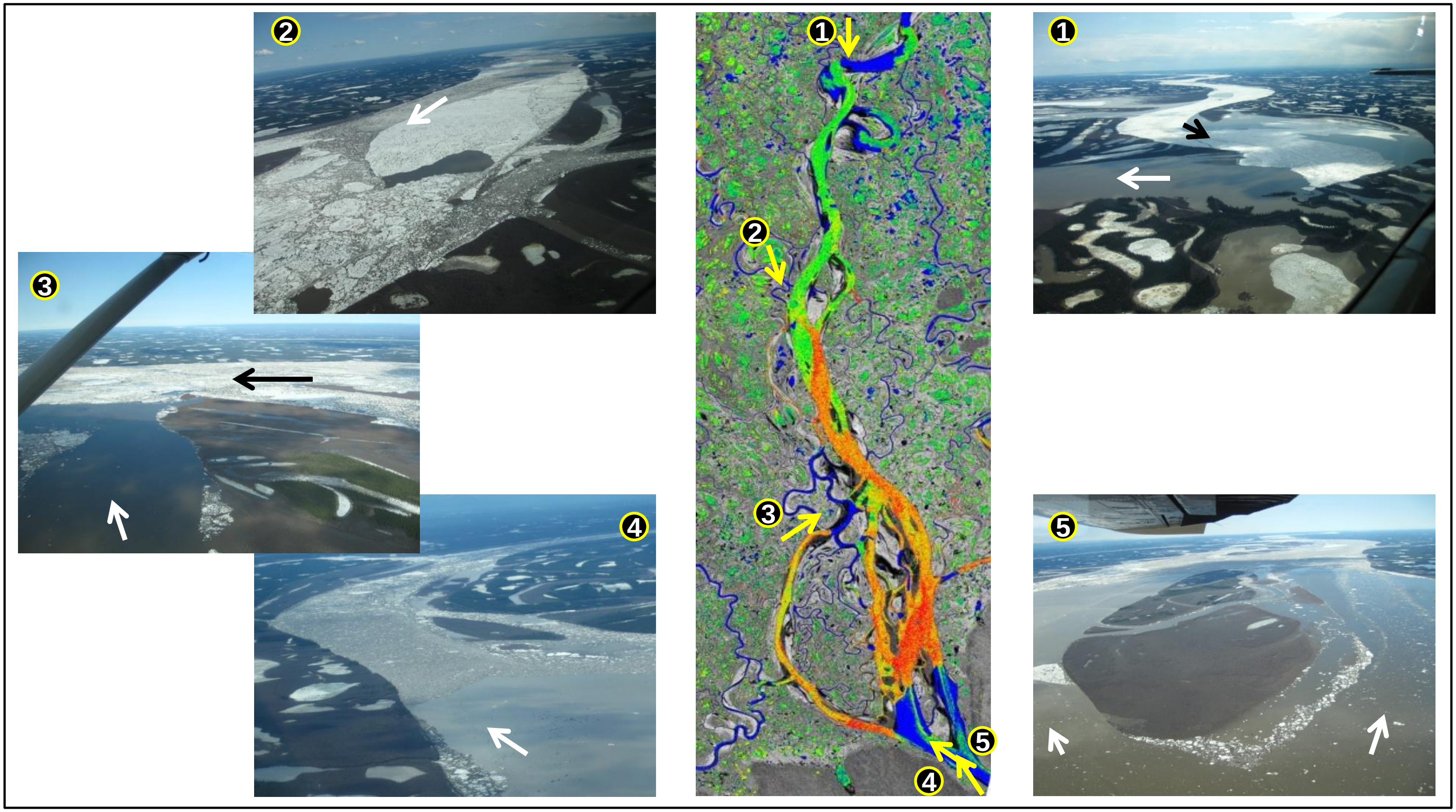

Figure 3.7 Oblique photo comparison (UofA photos) to example of Spring 2008 Ice Cover Product for 26-May-08 produced by NRCan using satellite imagery (adapted from van der Sanden and Drouin (2011b)).

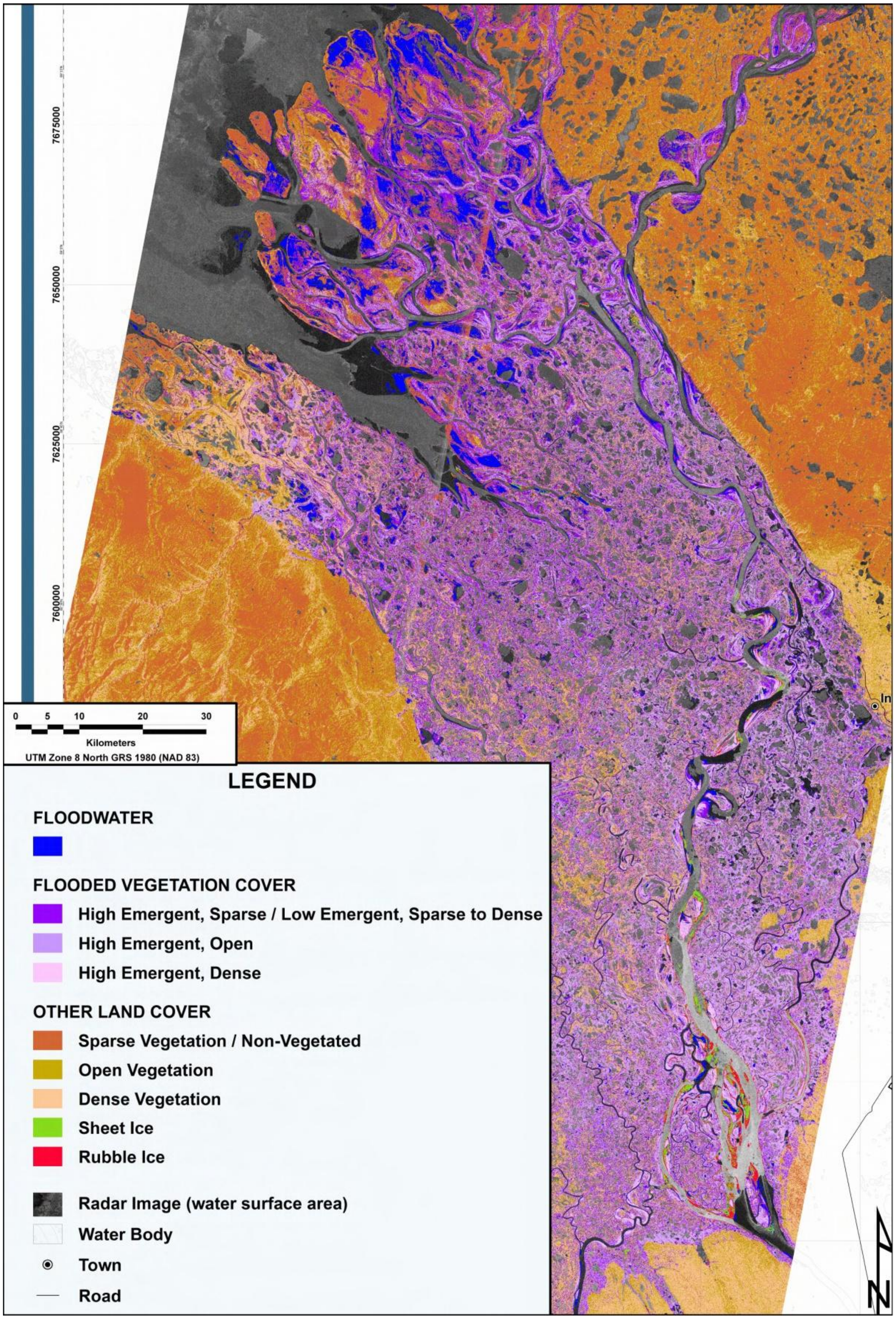

Figure 3.8 Example of Spring 2008 Flood Condition Product for 26-May-08 produced by NRCan using satellite imagery (adapted from van der Sanden and Drouin (2011a)).

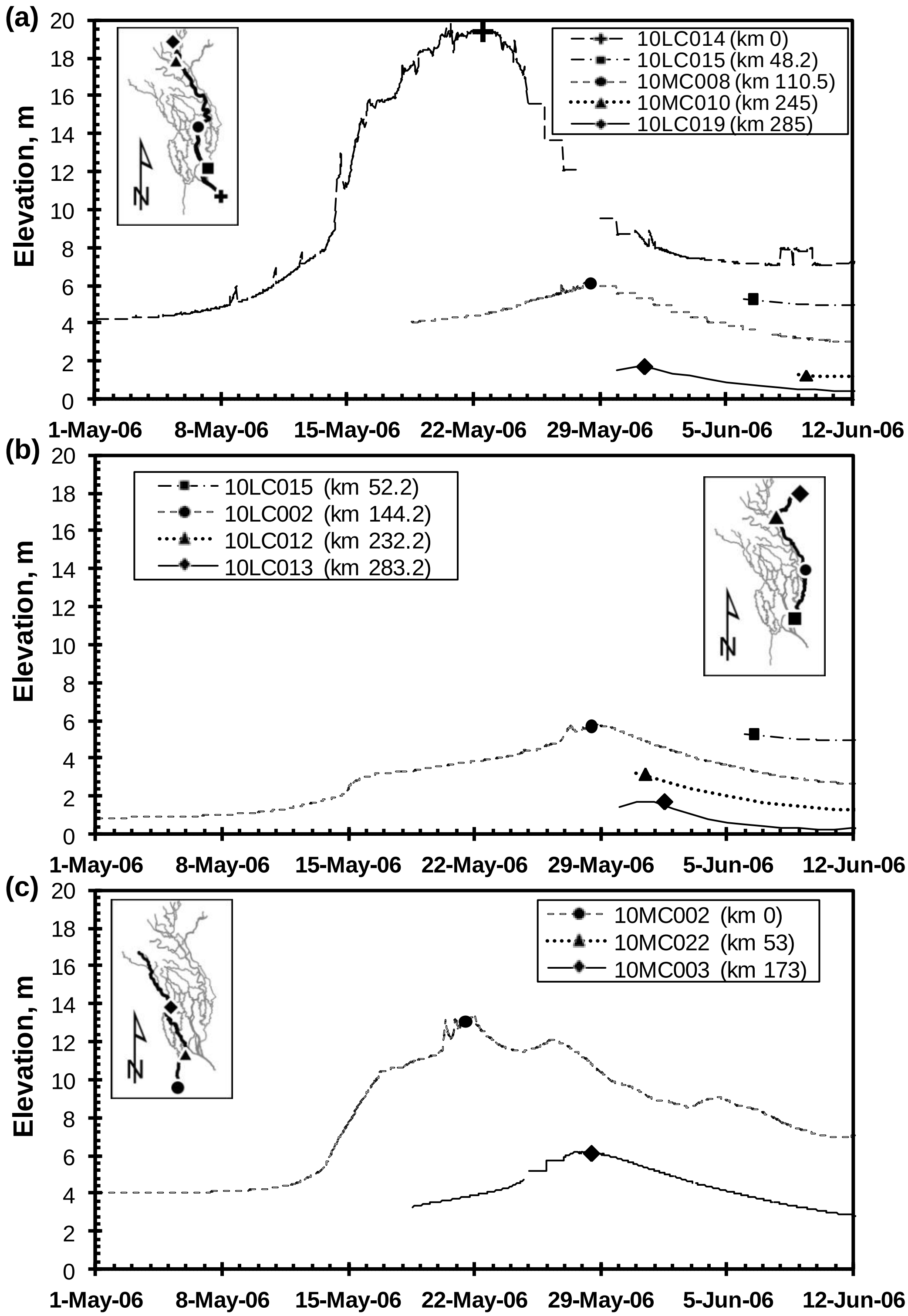

Figure 3.9 Water levels at stations along the (a) Middle Channel (b) East Channel (c) West Channel (d) Napoiak Channel and (f) Reindeer Channel during breakup in 2006. Symbols show peak water level. (Data source: the WSC)

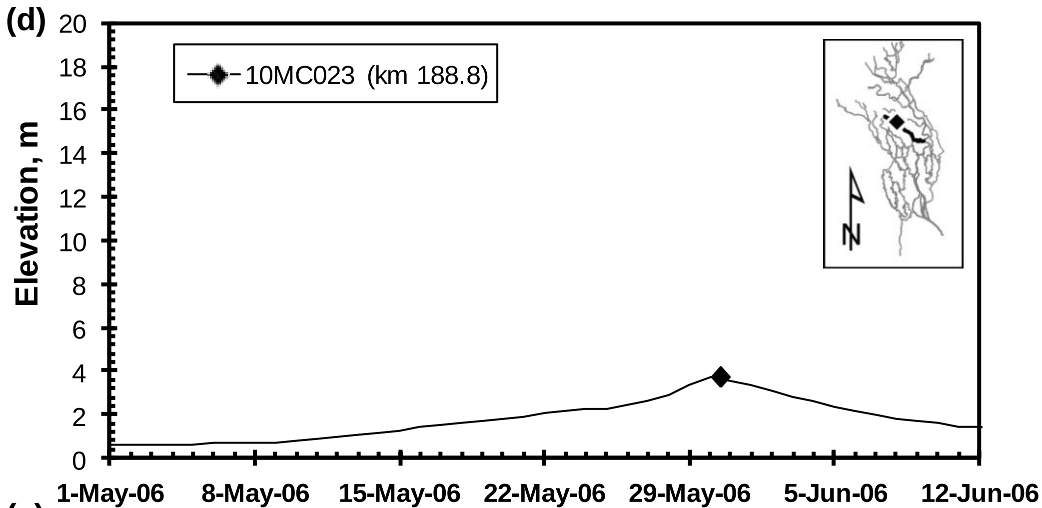

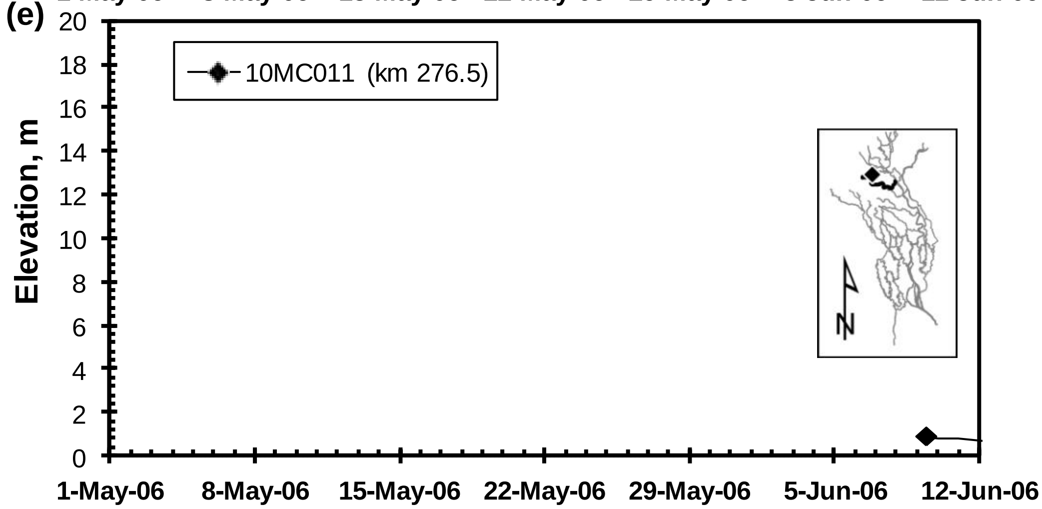

Figure 3.9 continued — Water levels at stations along the (a) Middle Channel (b) East Channel (c) West Channel (d) Napoiak Channel and (f) Reindeer Channel during breakup in 2006. Symbols show peak water level. (Data source: the WSC).

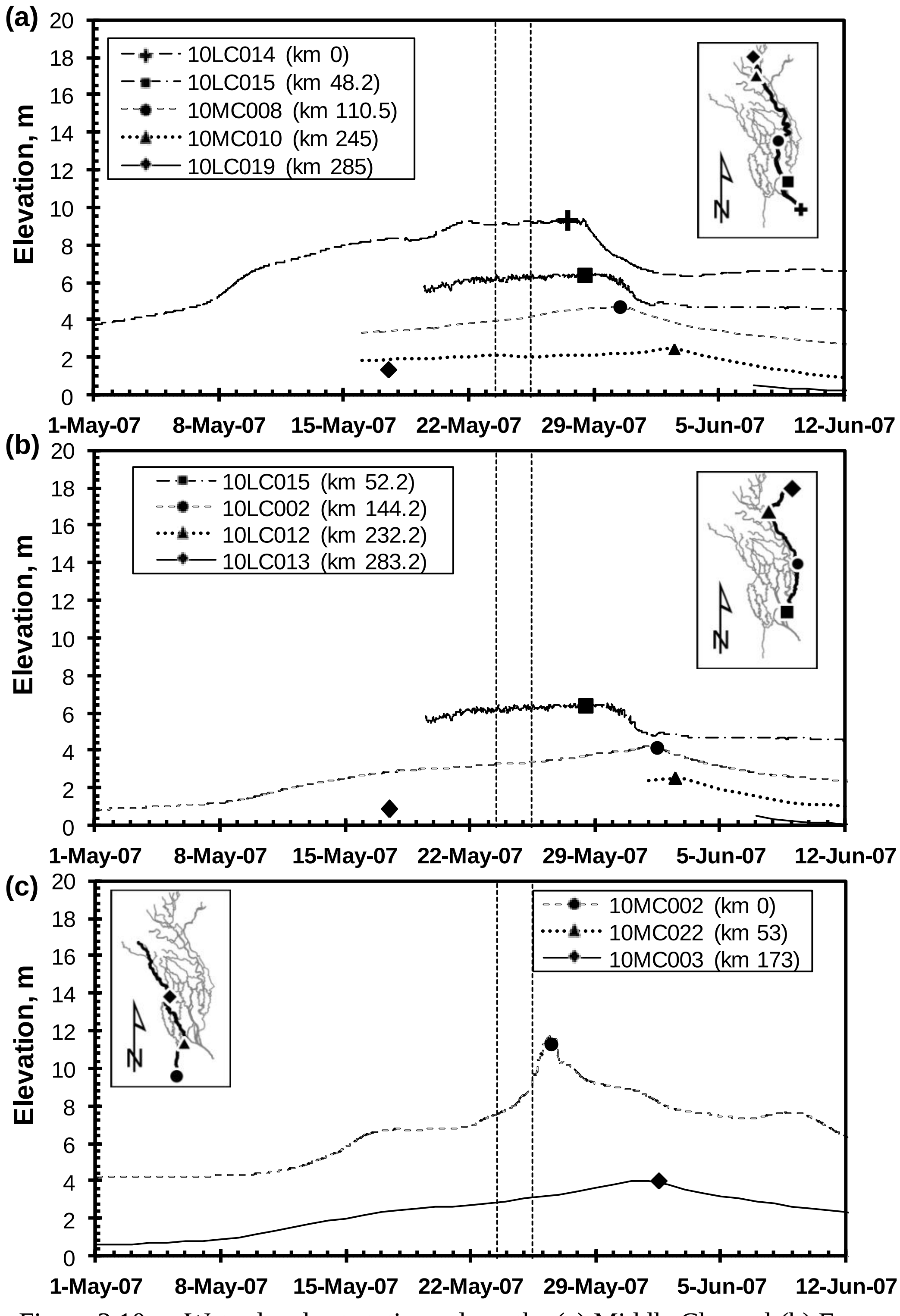

Figure 3.10 Water levels at stations along the (a) Middle Channel (b) East Channel (c) West Channel (d) Napoiak Channel and (f) Reindeer Channel during breakup in 2007. Symbols show peak water level. Vertical lines show timing of ice condition maps. (Data source: the WSC)

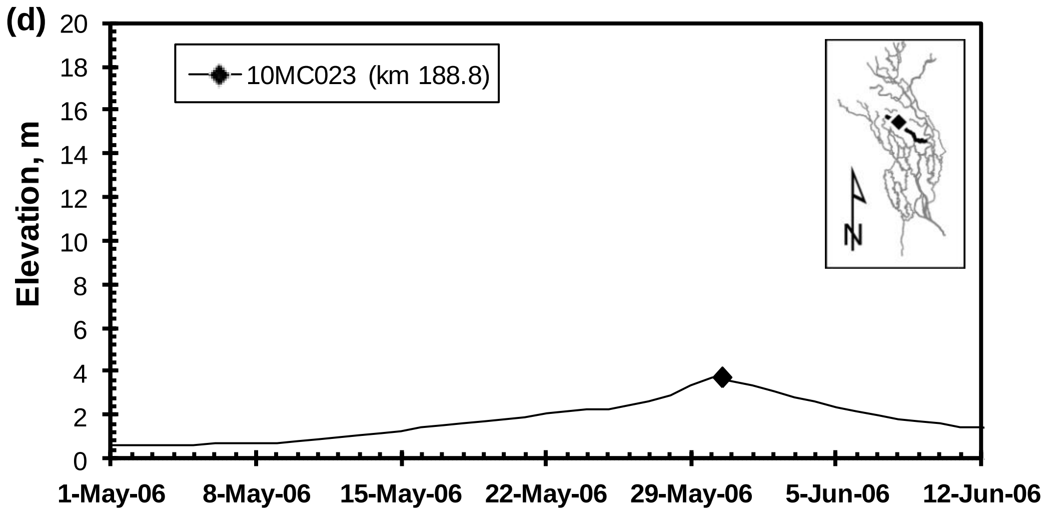

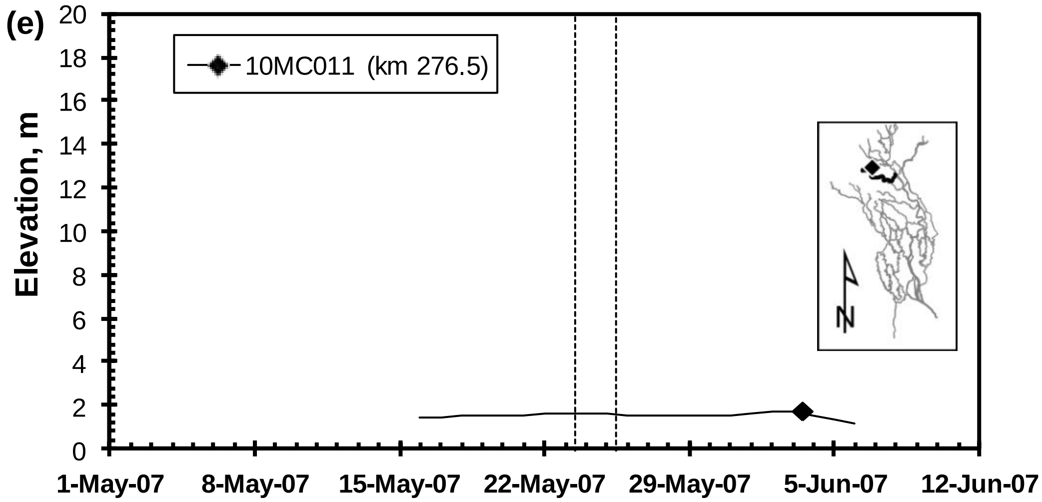

Figure 3.10 continued — Water levels at stations along the (a) Middle Channel (b) East Channel (c) West Channel (d) Napoiak Channel and (f) Reindeer Channel during breakup in 2007. Symbols show peak water level. Vertical lines show timing of ice condition maps. (Data source: the WSC).

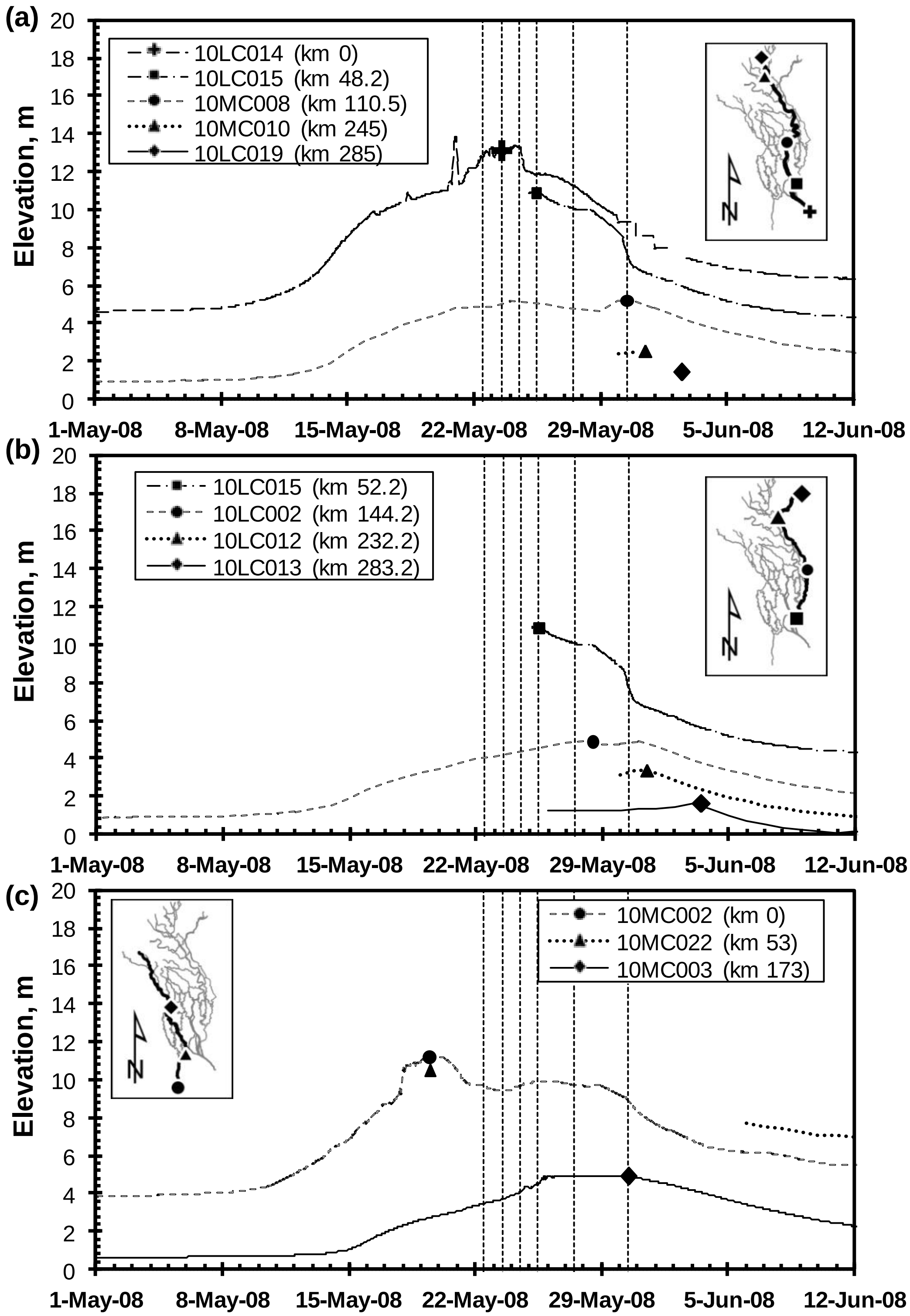

Figure 3.11 Water levels at stations along the (a) Middle Channel (b) East Channel (c) West Channel (d) Napoiak Channel and (f) Reindeer Channel during breakup in 2008. Symbols show peak water level. Vertical lines show timing of ice condition maps. (Data source: the WSC)

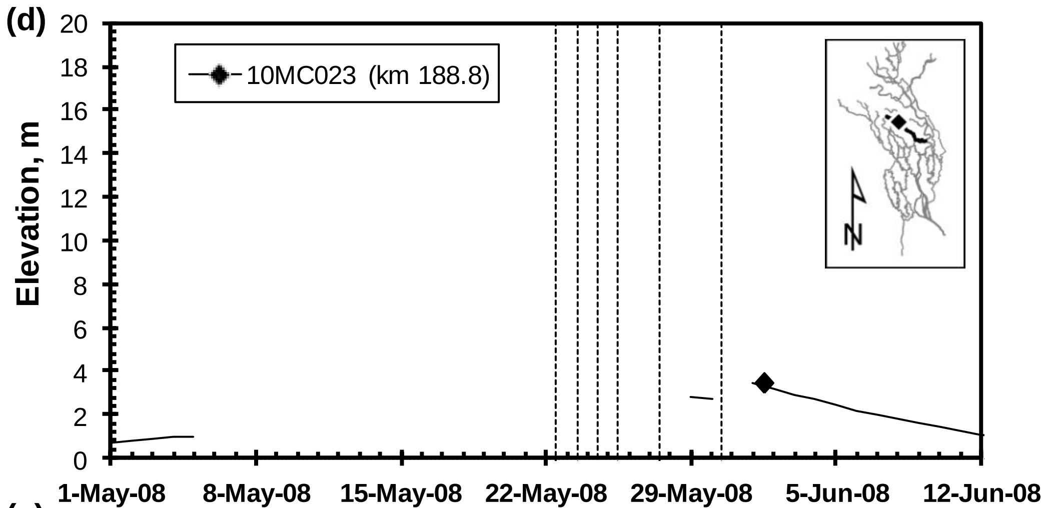

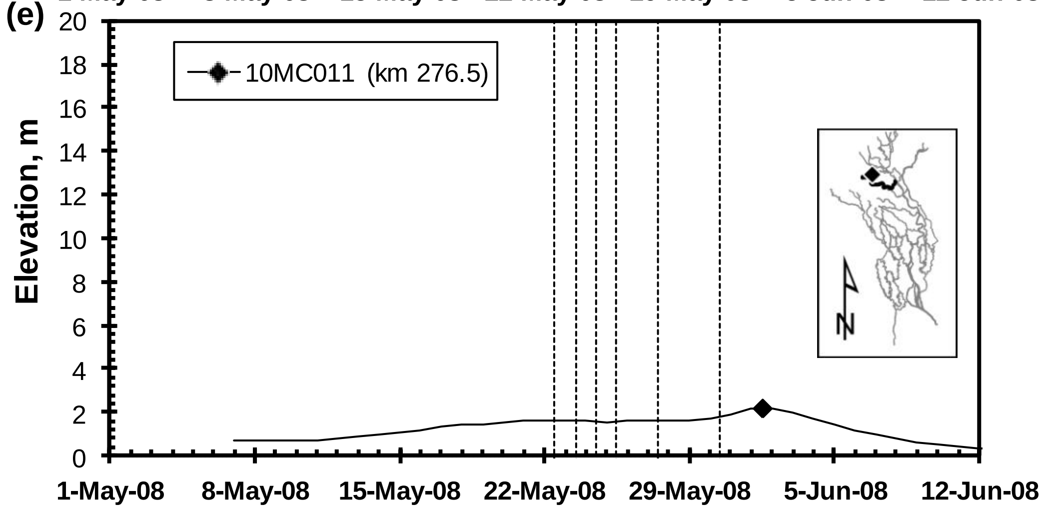

Figure 3.11 continued Water levels at stations along the (a) Middle Channel (b) East Channel (c) West Channel (d) Napoiak Channel and (f) Reindeer Channel during breakup in 2008. Symbols show peak water level. Vertical lines show timing of ice condition maps. (Data source: the WSC).

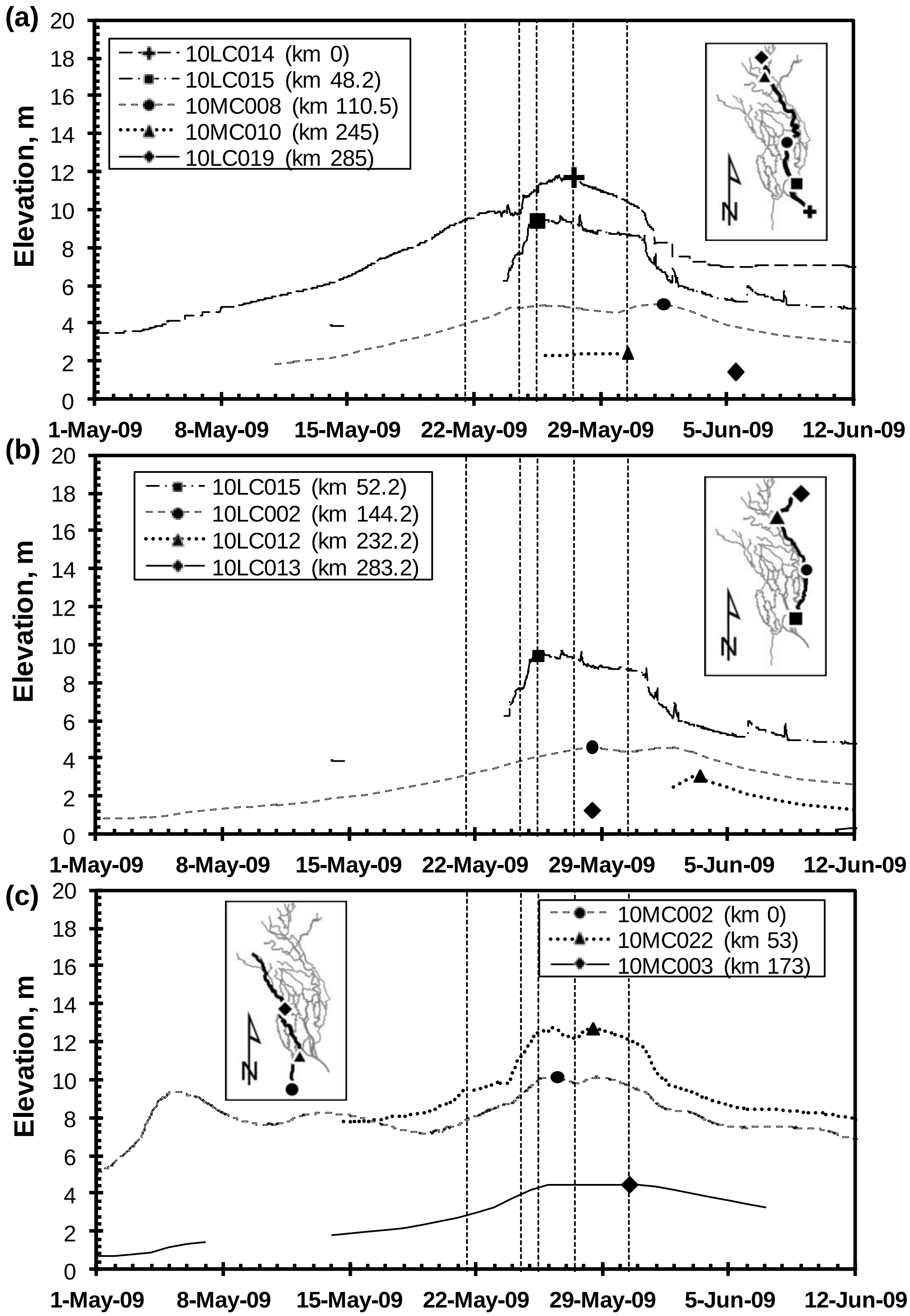

Figure 3.12 Water levels at stations along the (a) Middle Channel (b) East Channel (c) West Channel (d) Napoiak Channel and (f) Reindeer Channel during breakup in 2009. Symbols show peak water level. Vertical lines show timing of ice condition maps. (Data source: the WSC)

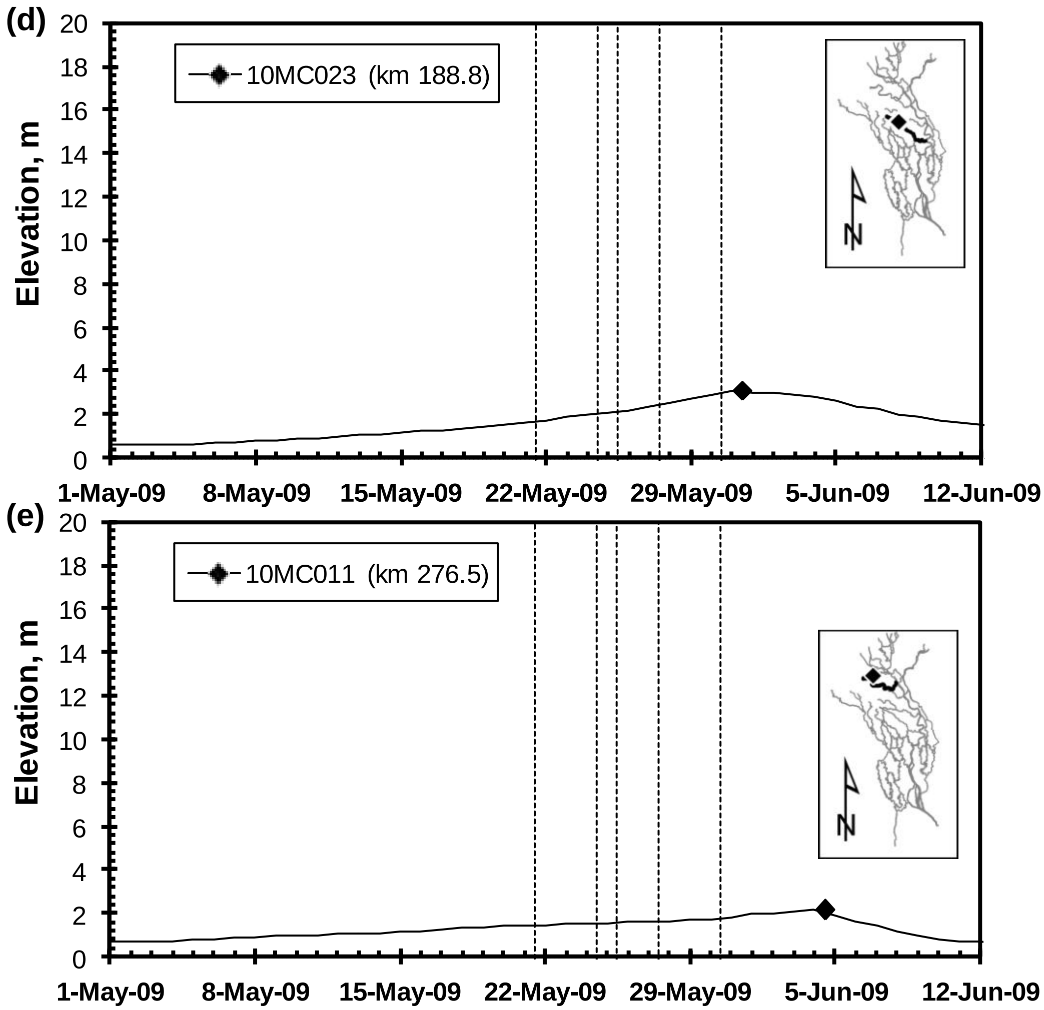

Figure 3.12 continued

Water levels at stations along the (a) Middle Channel (b) East Channel (c) West Channel (d) Napoiak Channel and (f) Reindeer Channel during breakup in 2009. Symbols show peak water level. Vertical lines show timing of ice condition maps. (Data source: the WSC).

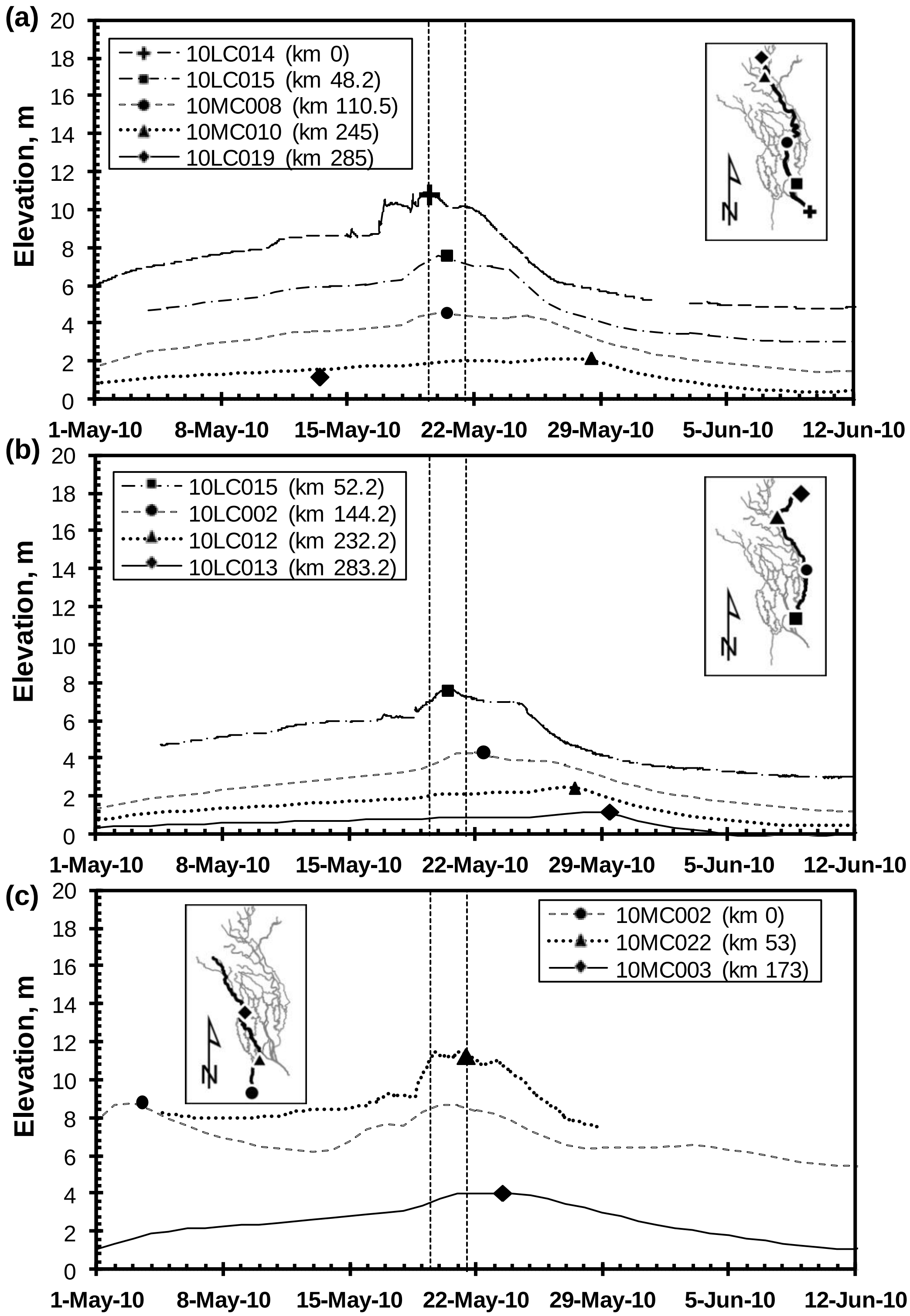

Figure 3.13 Water levels at stations along the (a) Middle Channel (b) East Channel (c) West Channel (d) Napoiak Channel and (f) Reindeer Channel during breakup in 2010. Symbols show peak water level. Vertical lines show timing of ice condition maps. (Data source: the WSC)

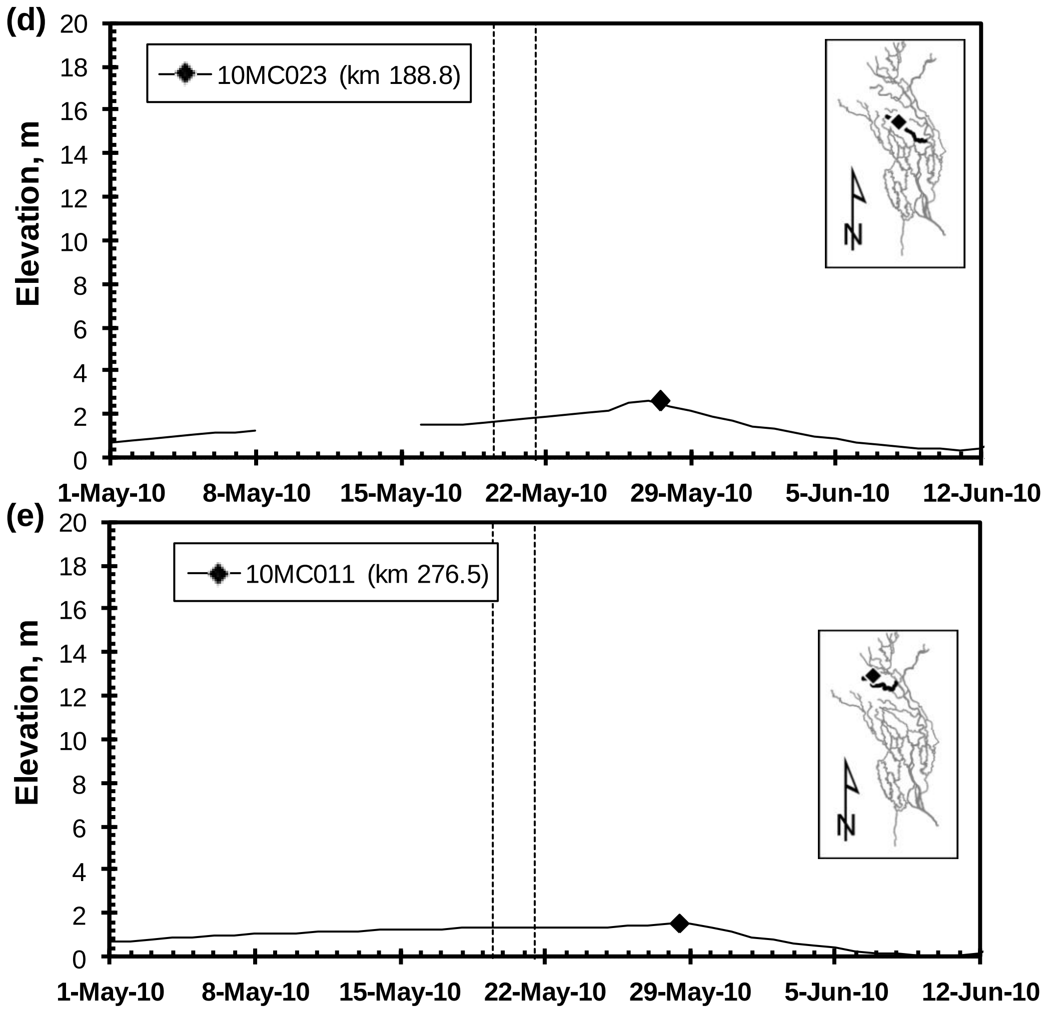

Figure 3.13 continued Water levels at stations along the (a) Middle Channel (b) East Channel (c) West Channel (d) Napoiak Channel and (f) Reindeer Channel during breakup in 2010. Symbols show peak water level. Vertical lines show timing of ice condition maps. (Data source: the WSC).

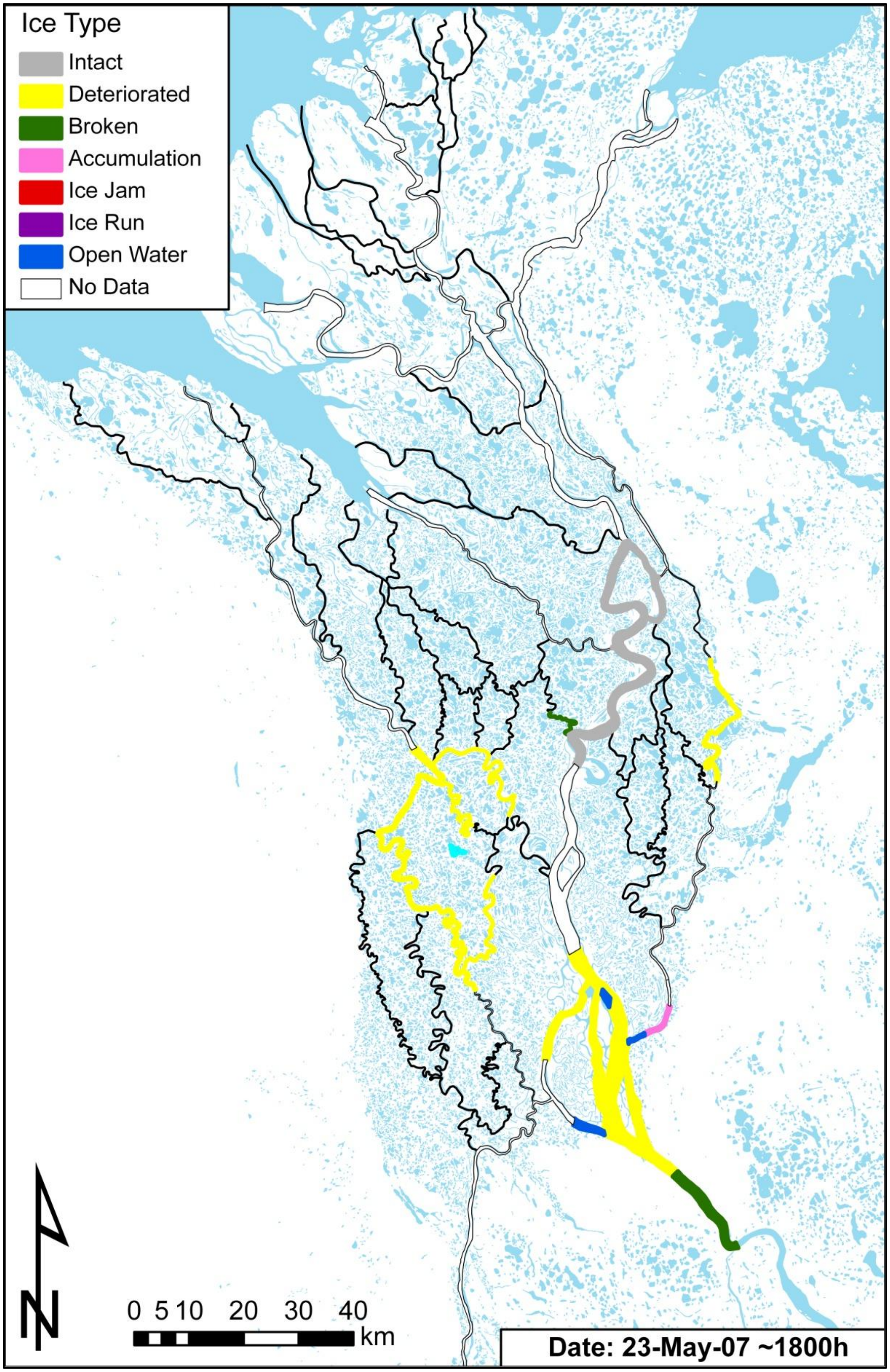

Figure 3.14 Map of 2007 breakup progression on 23-May-07. (data source: oblique photos).

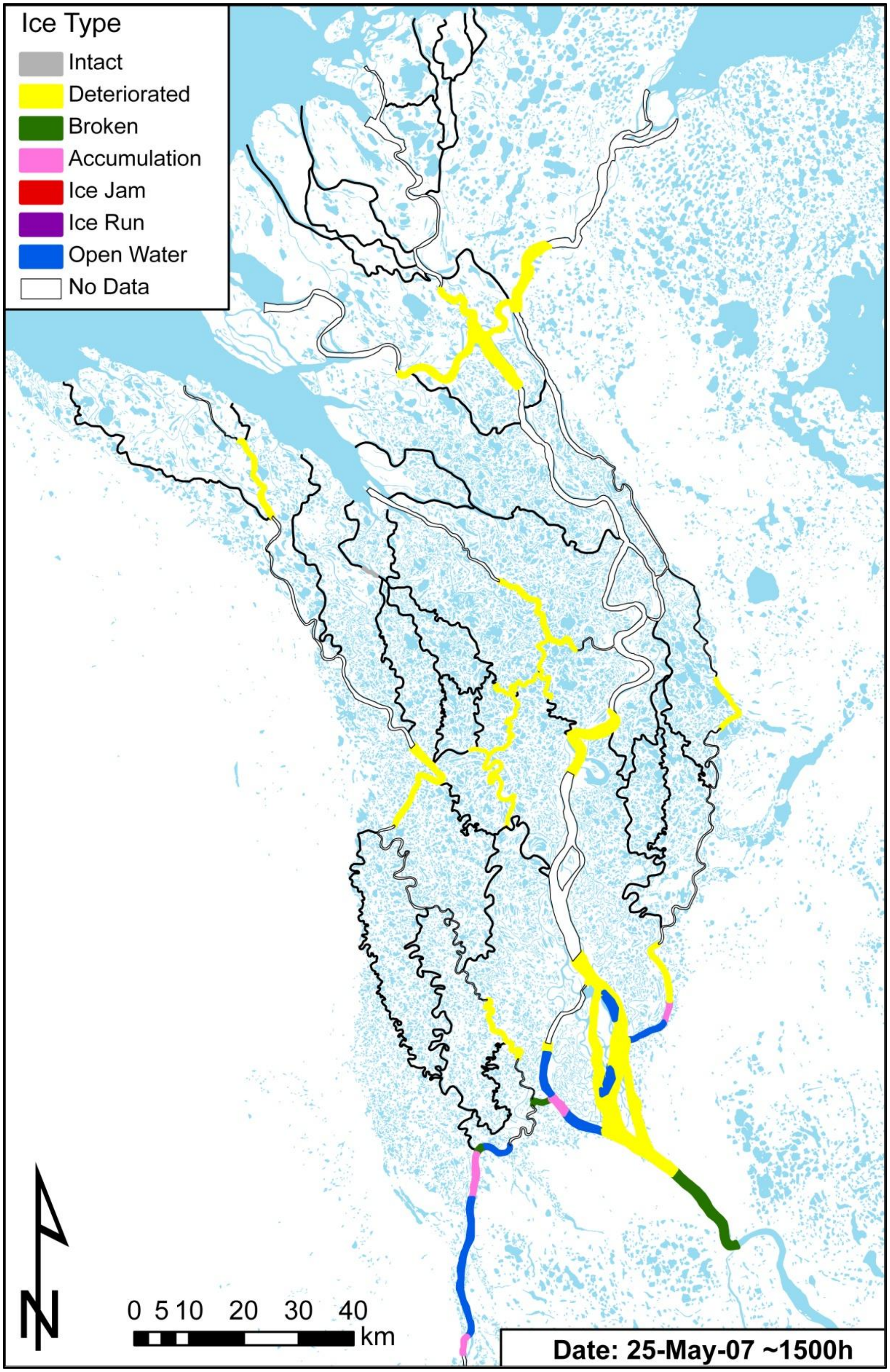

Figure 3.15 Map of 2007 breakup progression for 25-May-07. (data source: oblique photos).

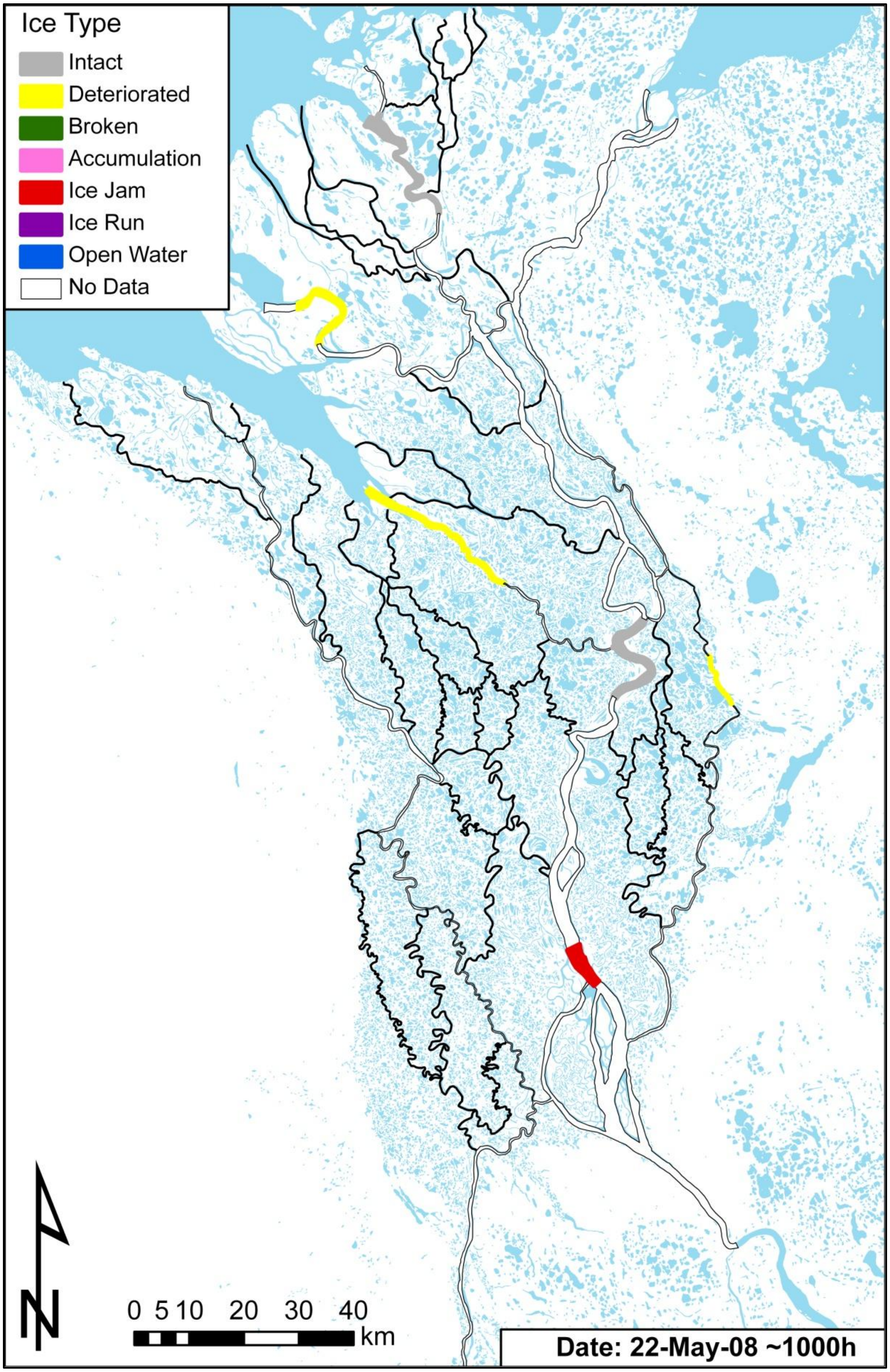

Figure 3.16 Map of 2008 breakup progression on 22-May-08. (data source: oblique photos).

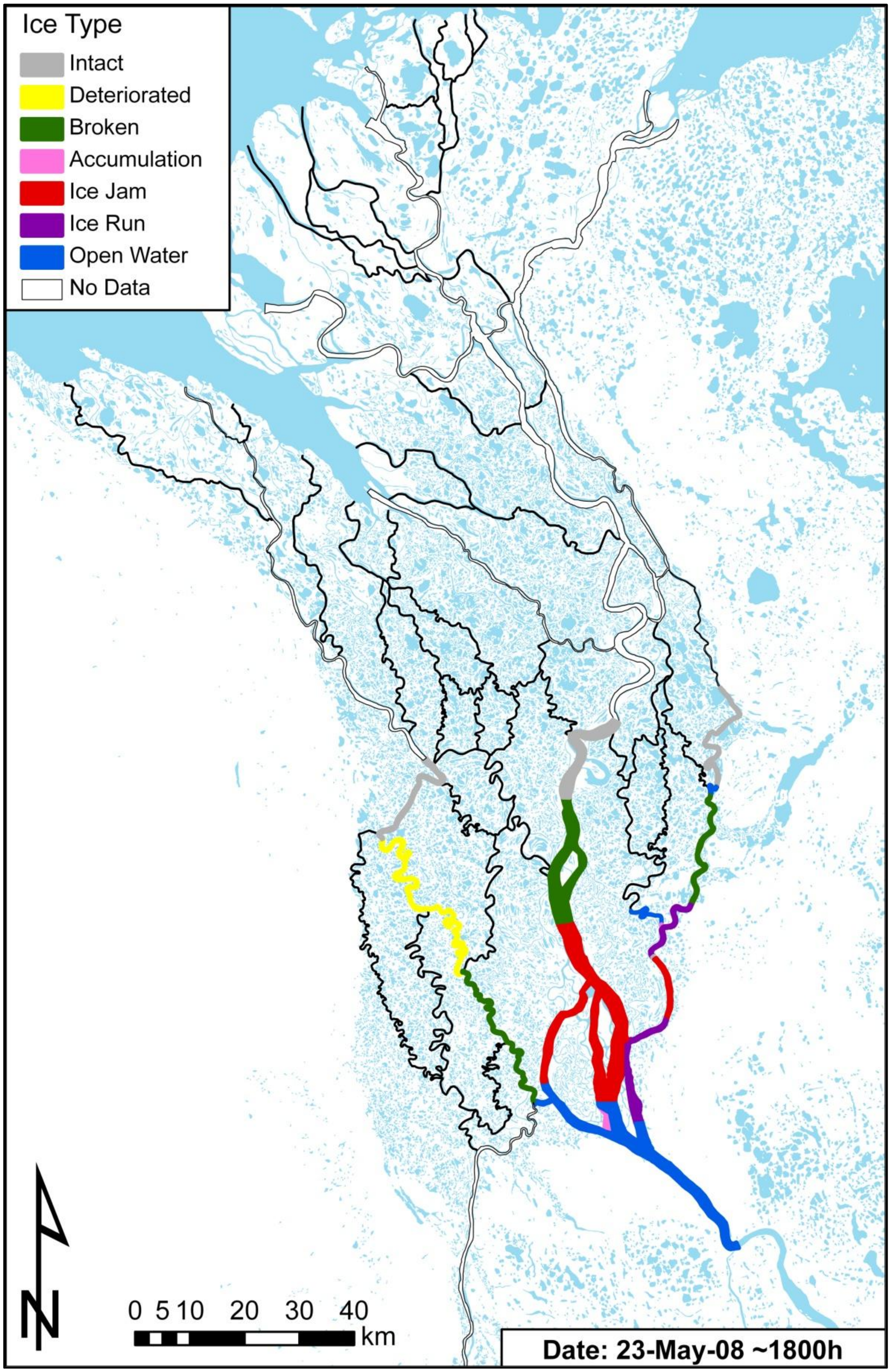

Figure 3.17 Map of 2008 breakup progression for 23-May-08. (data source: oblique photos and van der Sanden and Drouin (2011b)).

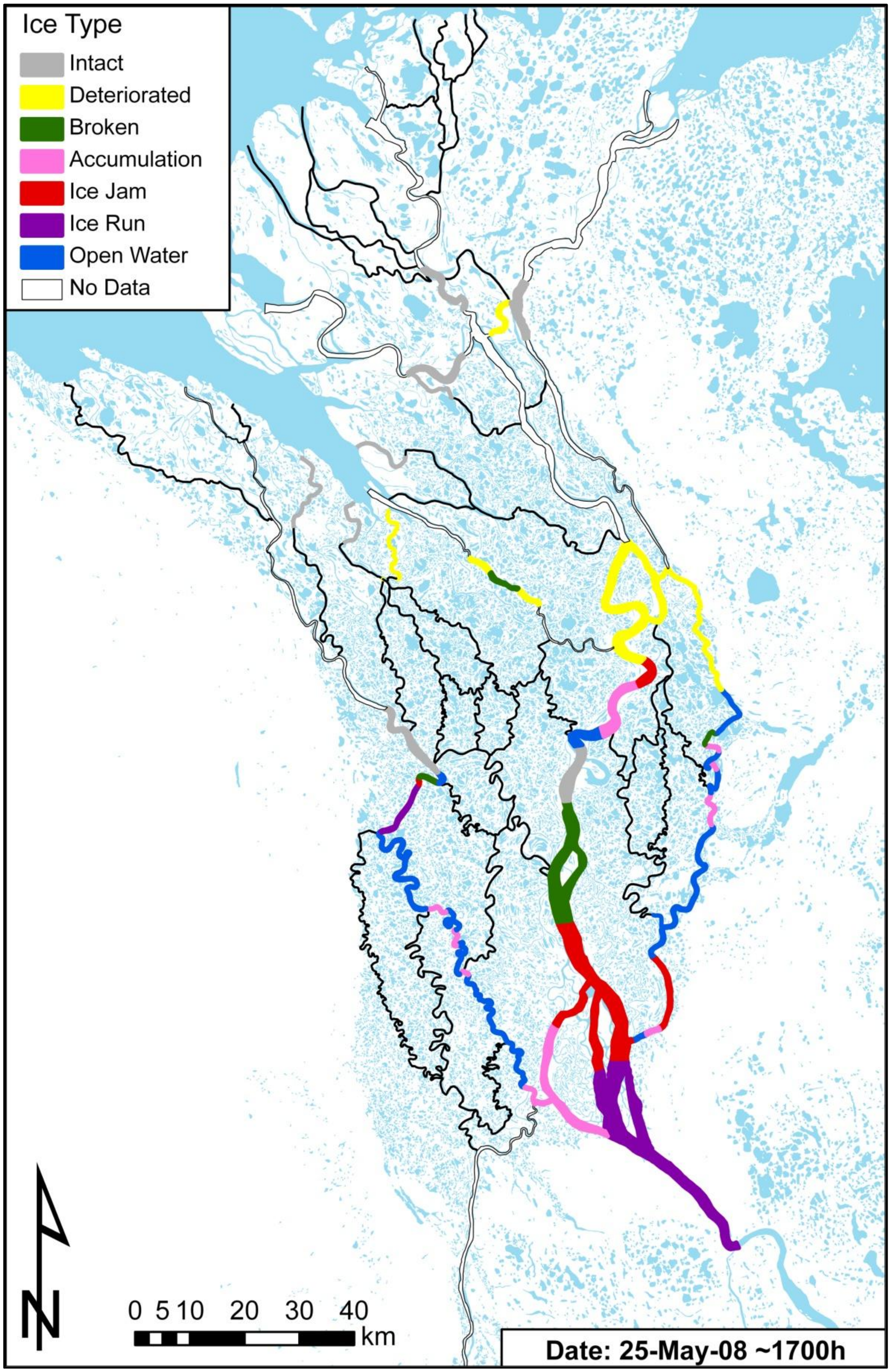

Figure 3.18 Map of 2008 breakup progression on 25-May-08. (data source: oblique photos and van der Sanden and Drouin (2011b)).

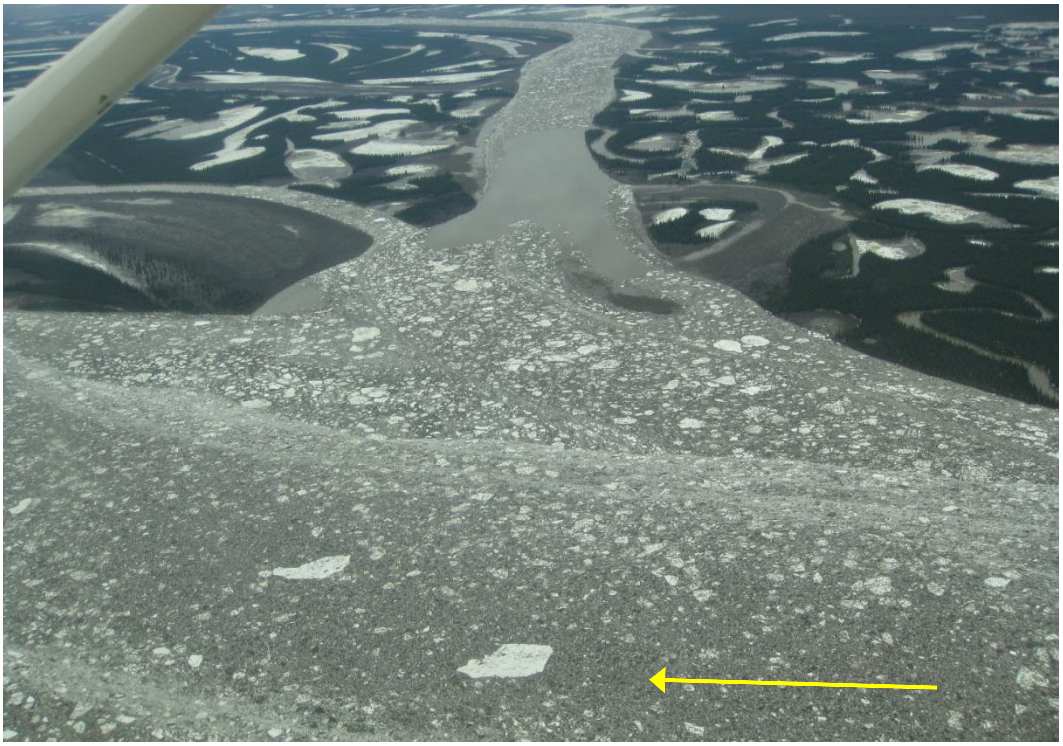

Figure 3.19 Oblique angle flight photo looking west at East/Middle Channel junction showing ice run in foreground and ice jam on East Channel in background on 25-May-08 ~1700h (UofA Photo).

Figure 3.20 Oblique angle flight photo looking upstream to toe of Middle Channel ice jam on 26-May-08 1800h (UofA Photo).

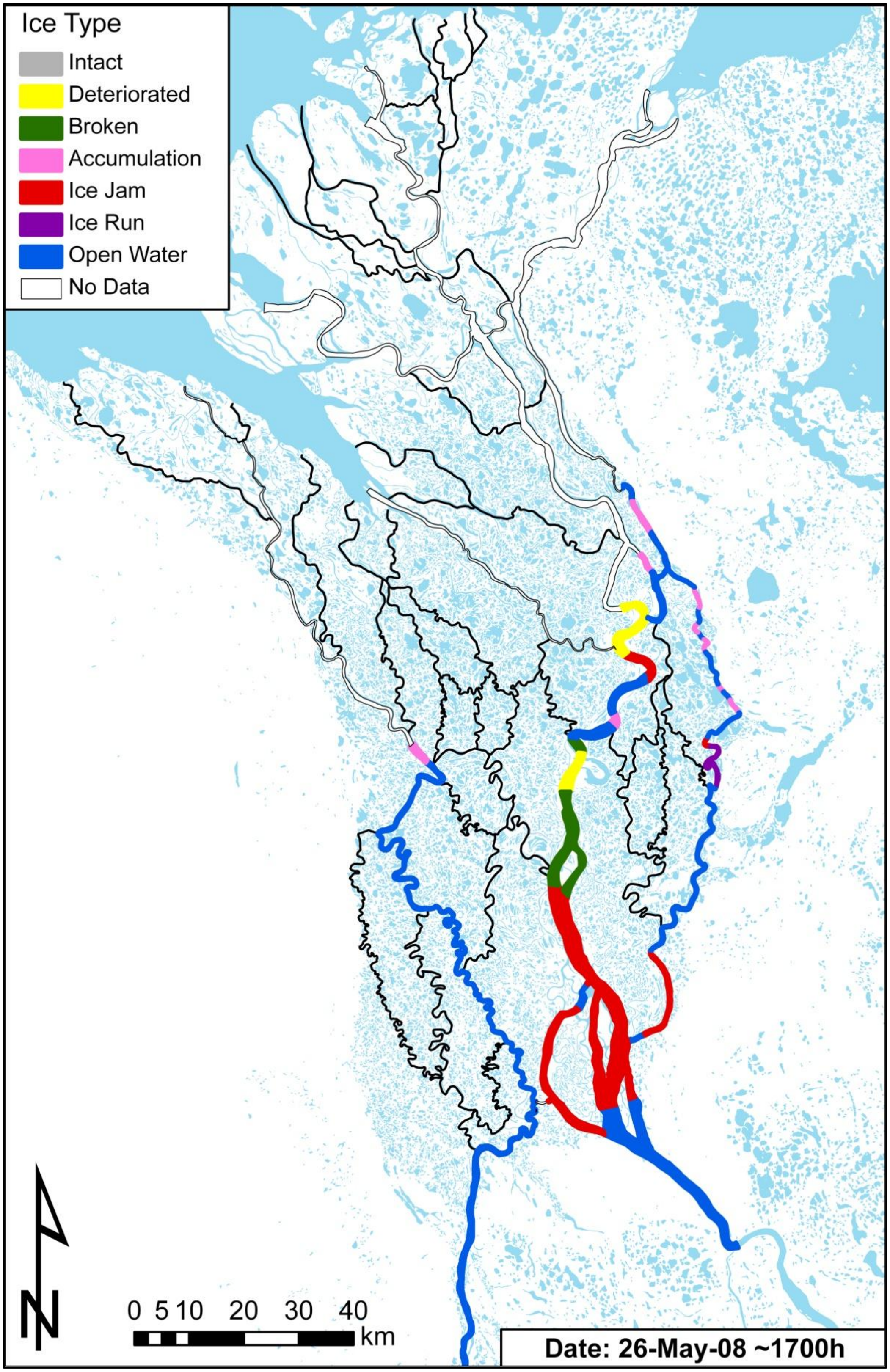

Figure 3.21 Map of 2008 breakup progression for 26-May-08. (data source: oblique photos and van der Sanden and Drouin (2011b)).

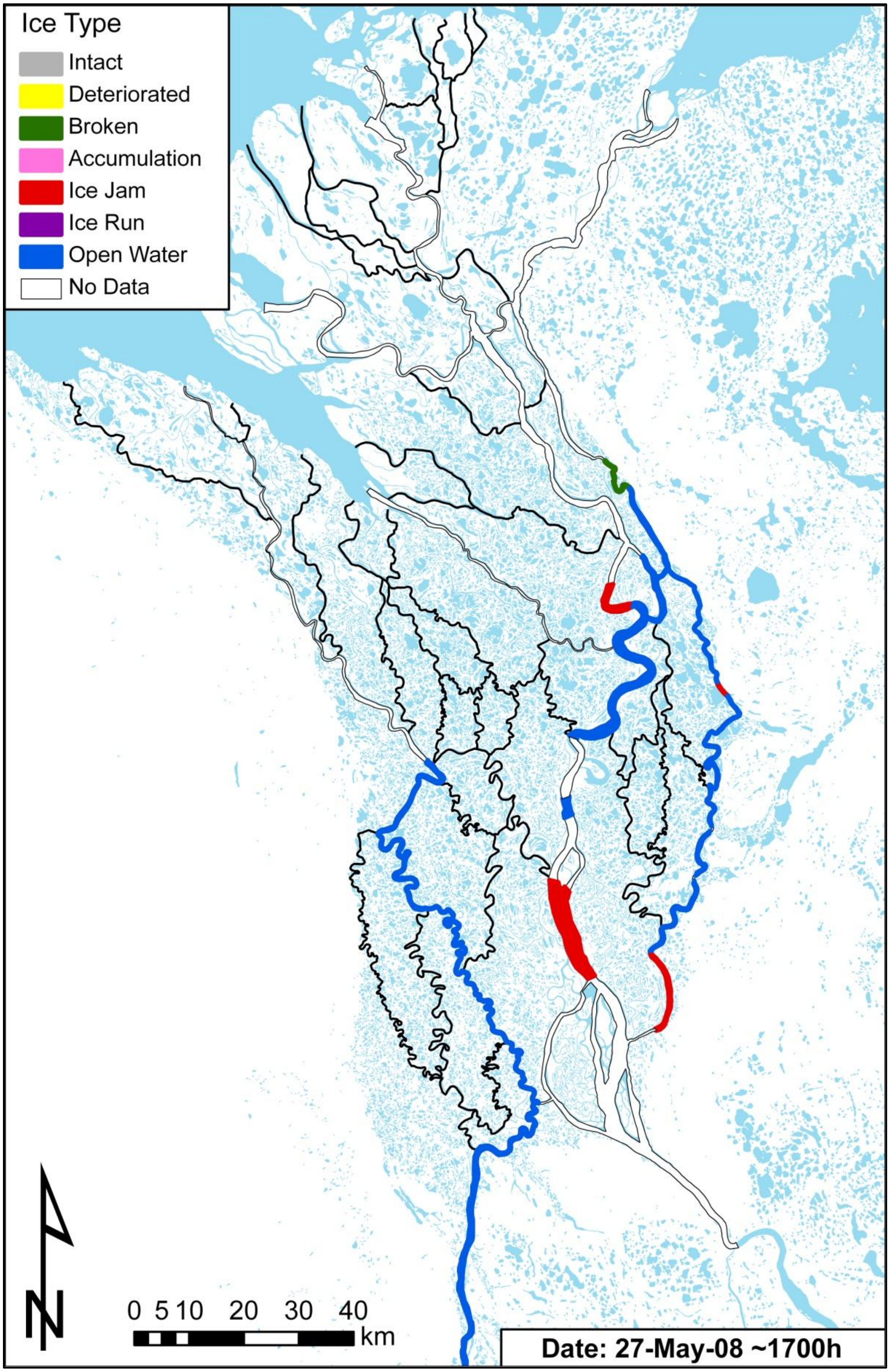

Figure 3.22 Map of 2008 breakup progression on 27-May-08. (data source: oblique photos and van der Sanden and Drouin (2011b)).

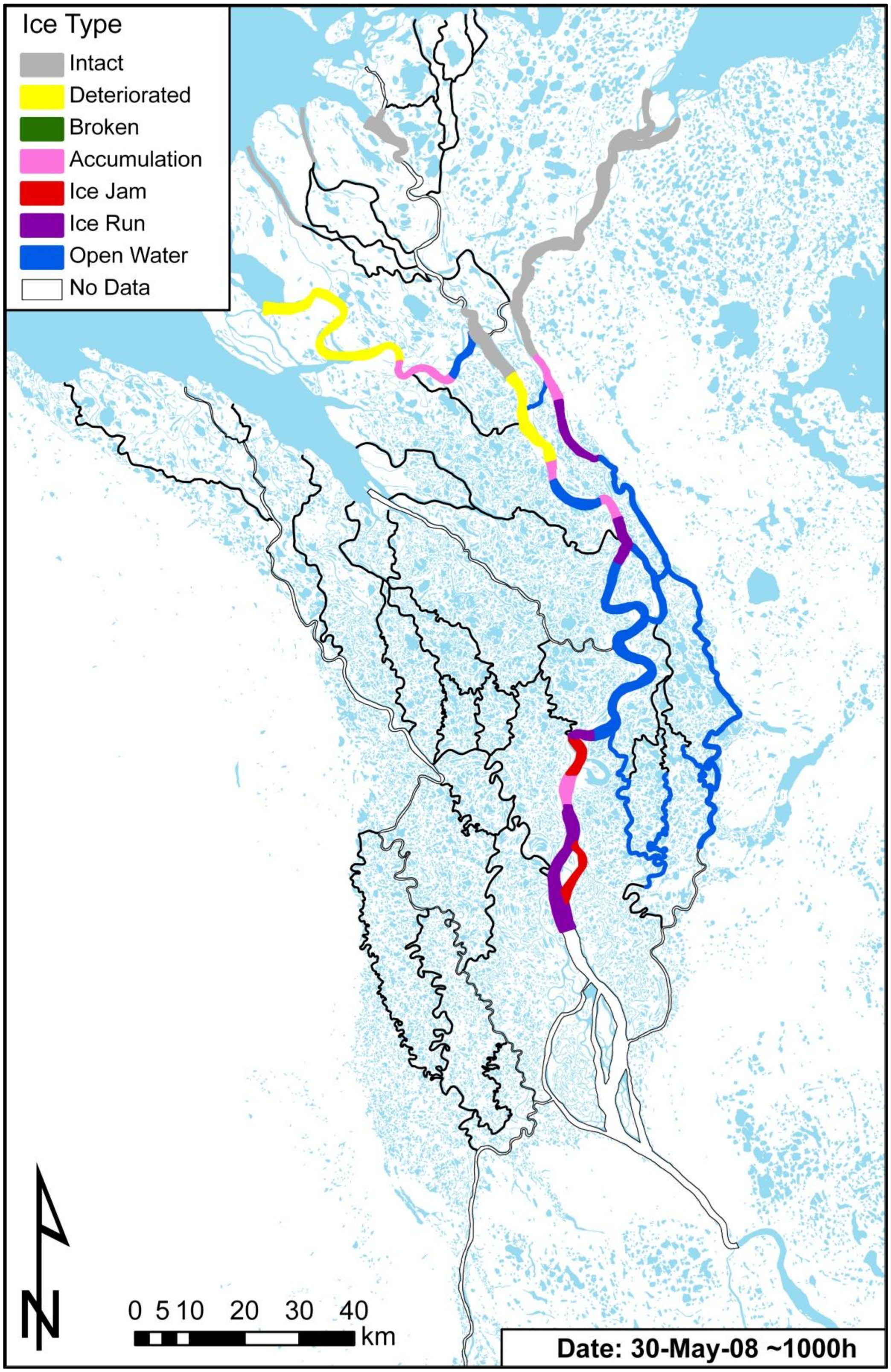

Figure 3.23 Map of 2008 breakup progression for 30-May-08. (data source: oblique angle flight photos).

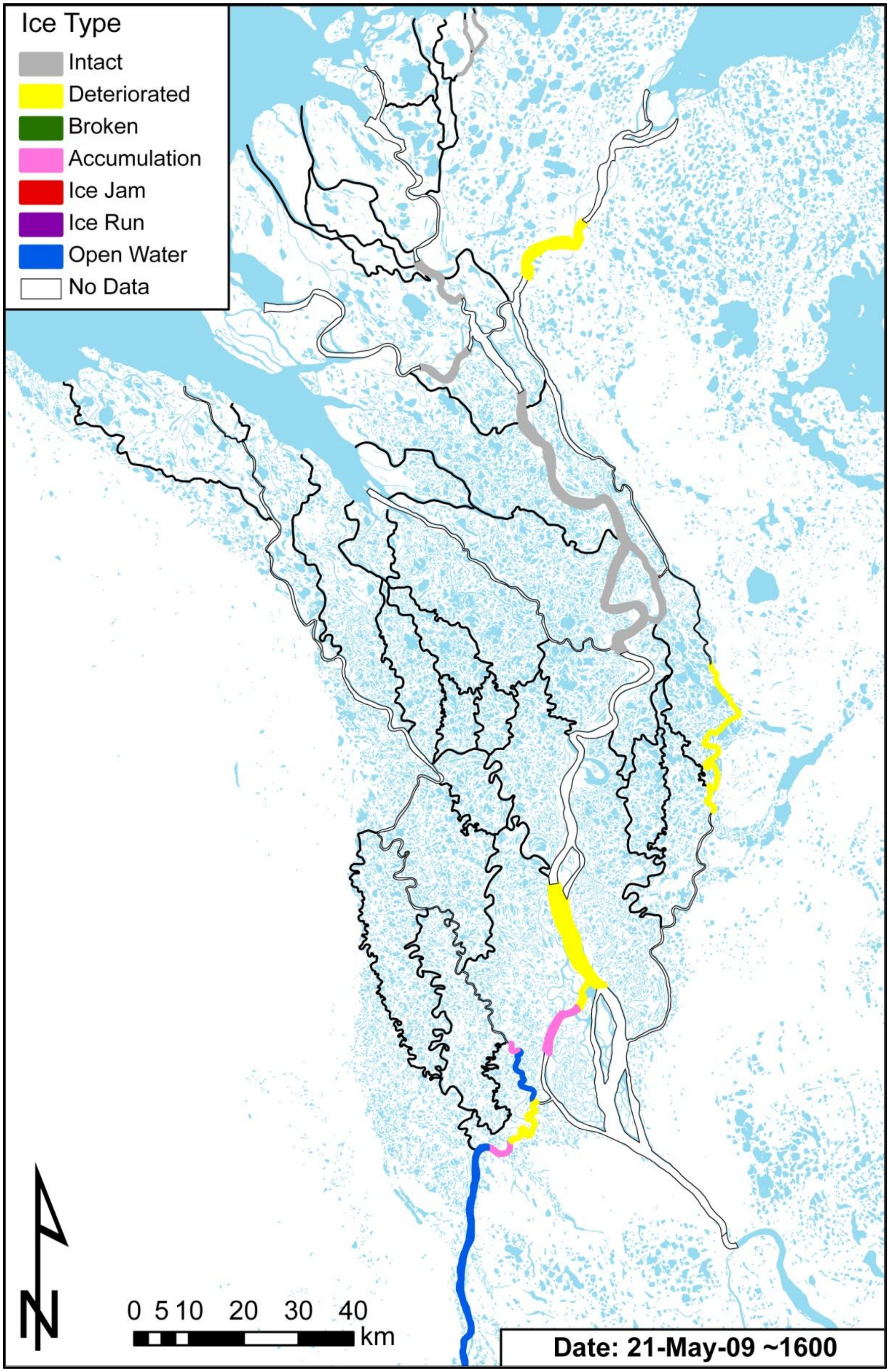

Figure 3.24 Map of 2009 breakup progression on 21-May-09. (data source: oblique photos).

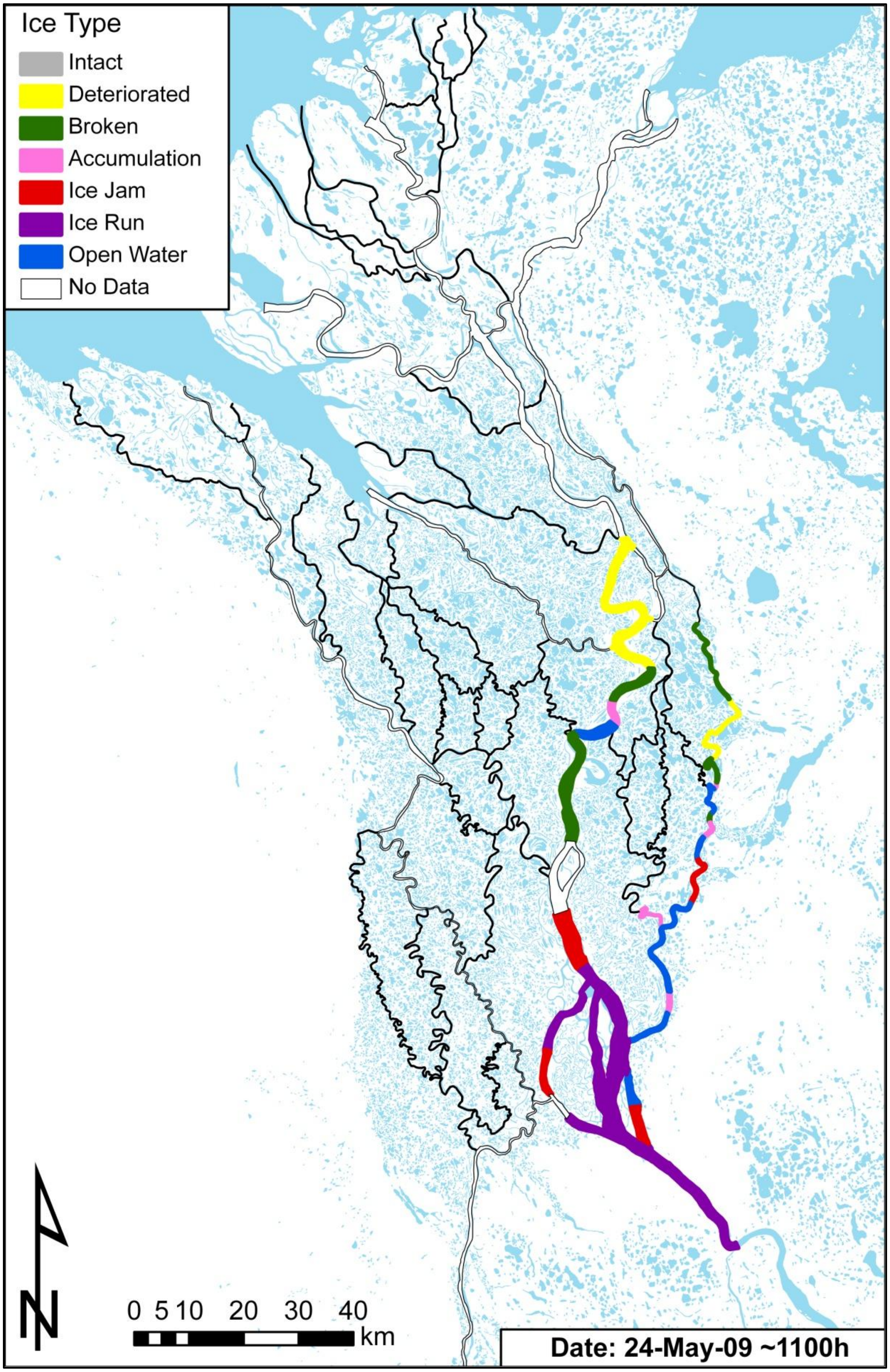

Figure 3.25 Map of 2009 breakup progression for 24-May-09. (data source: oblique photos).

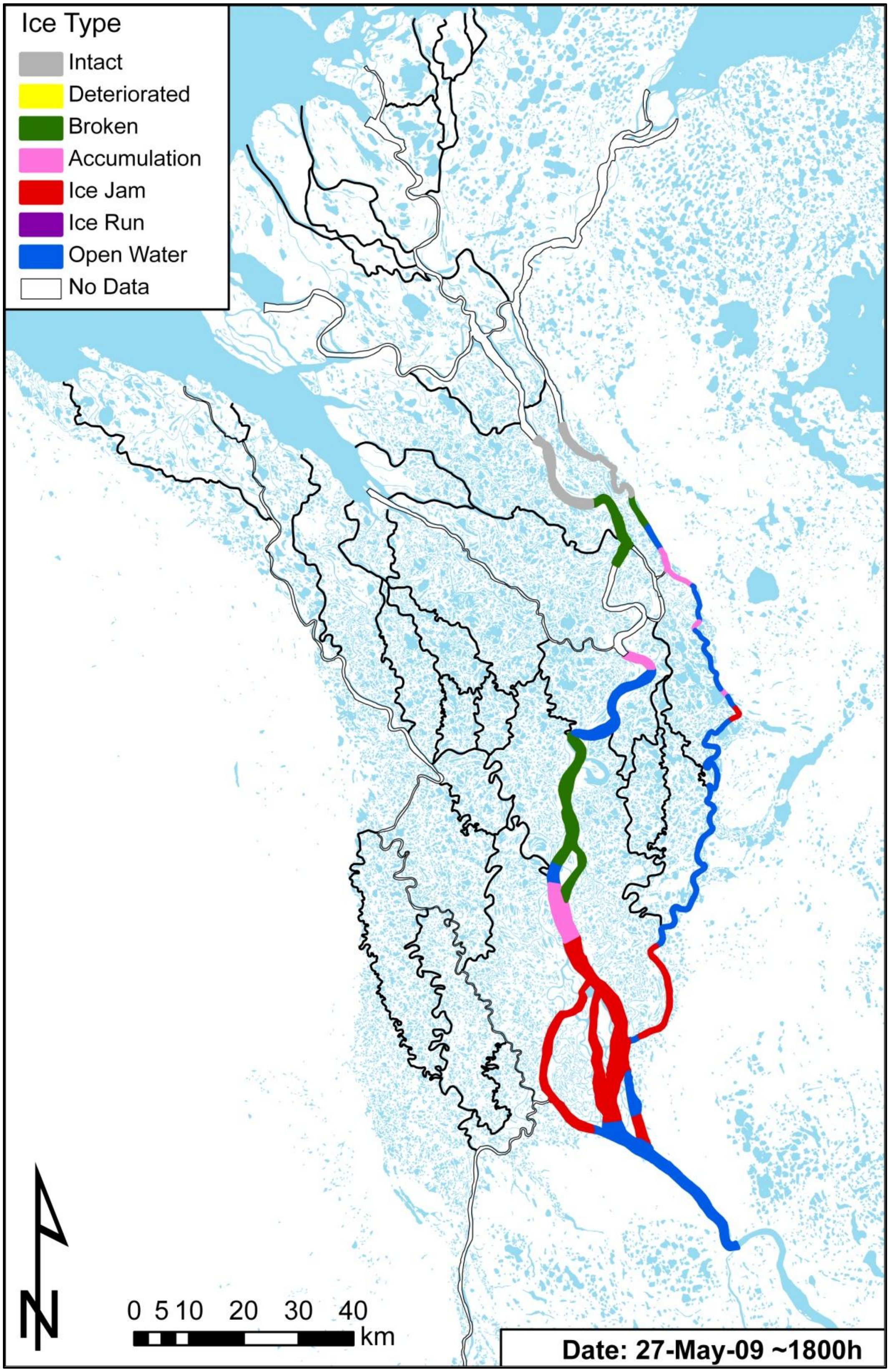

Figure 3.26 Map of 2009 breakup progression on 27-May-09. (data source: oblique photos).

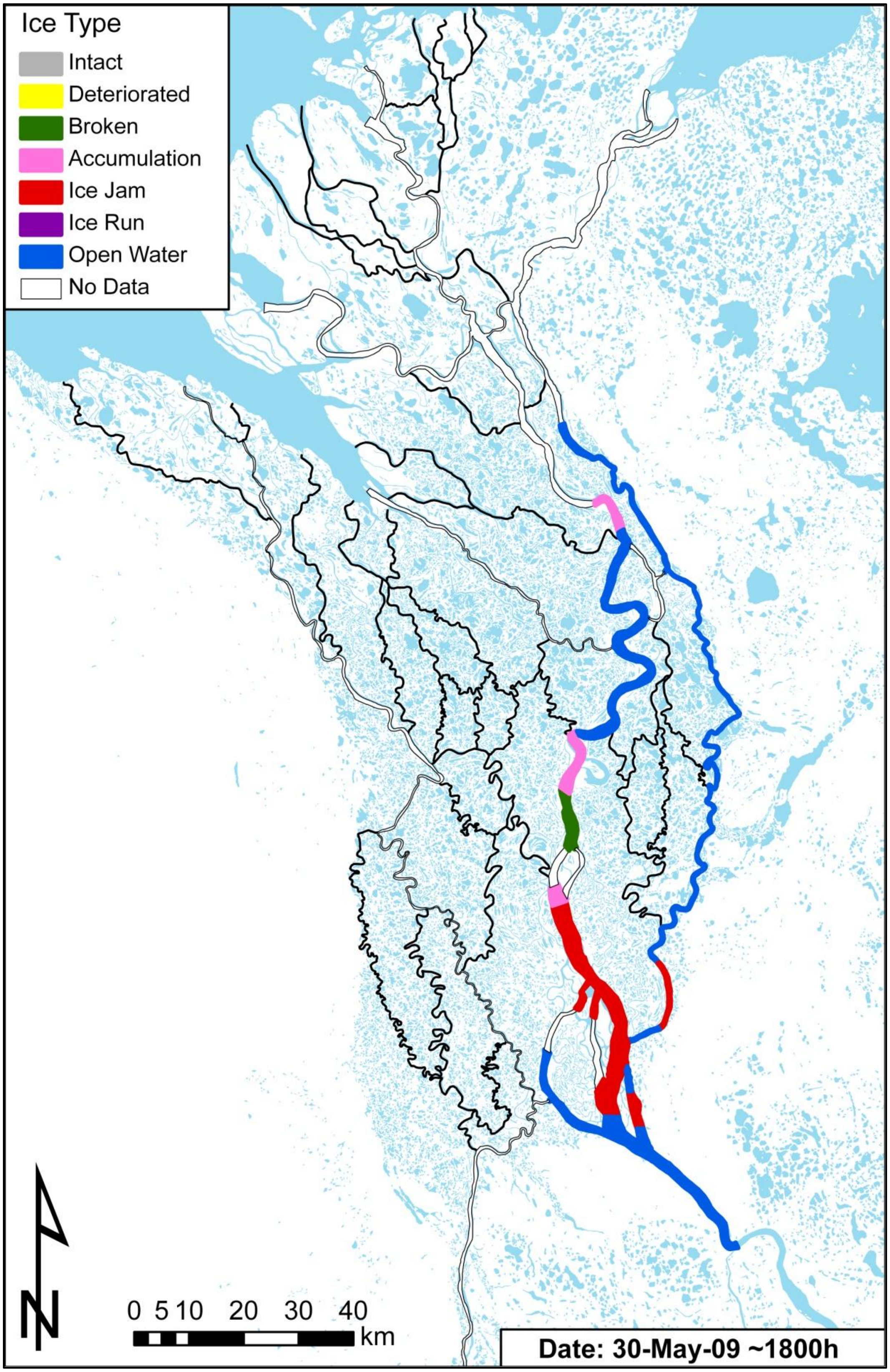

Figure 3.27 Map of 2009 breakup progression on 30-May-09. (data source: oblique photos).

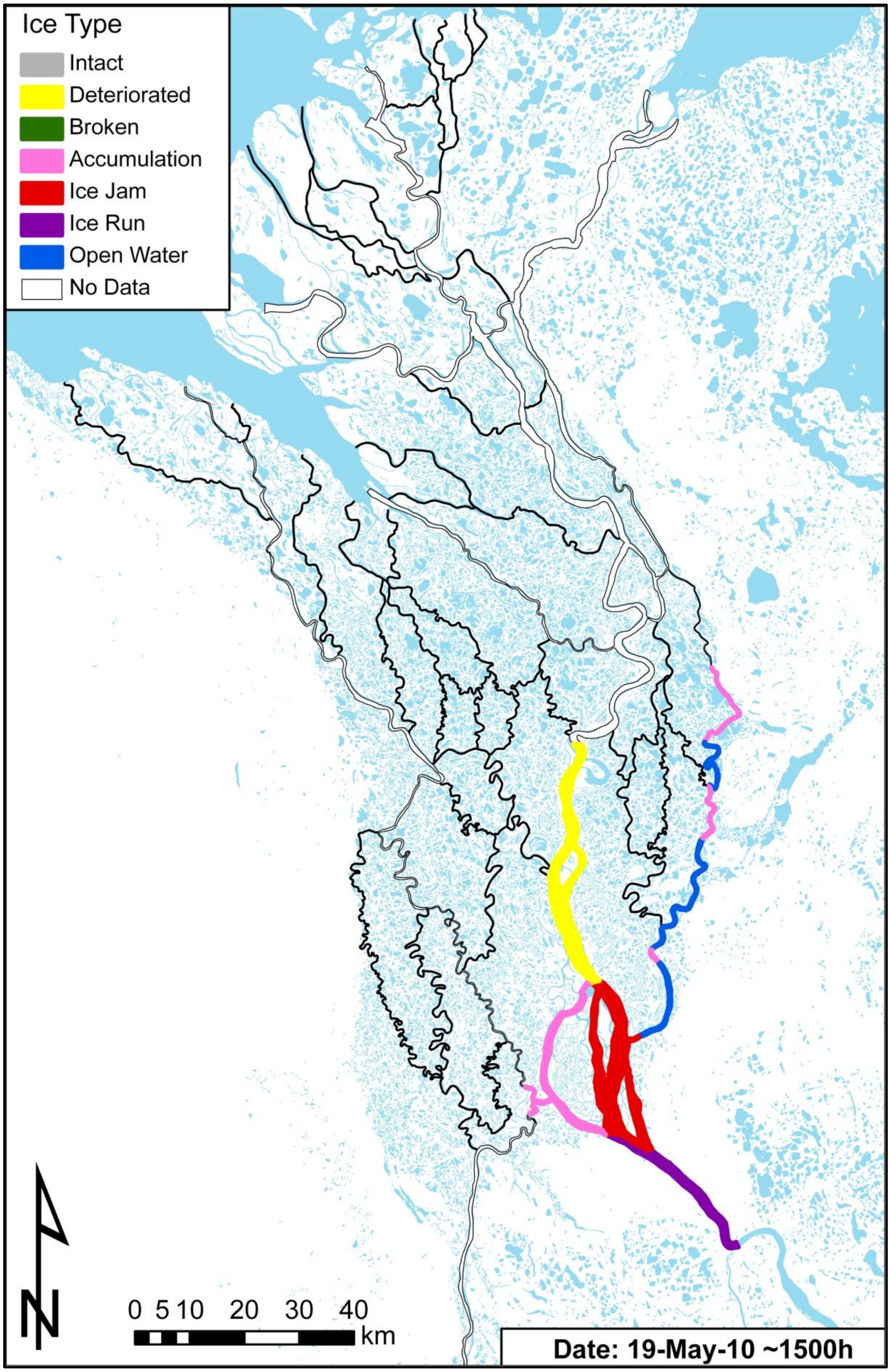

Figure 3.28 Map of 2010 breakup progression on 19-May-10. (data source: oblique photos)

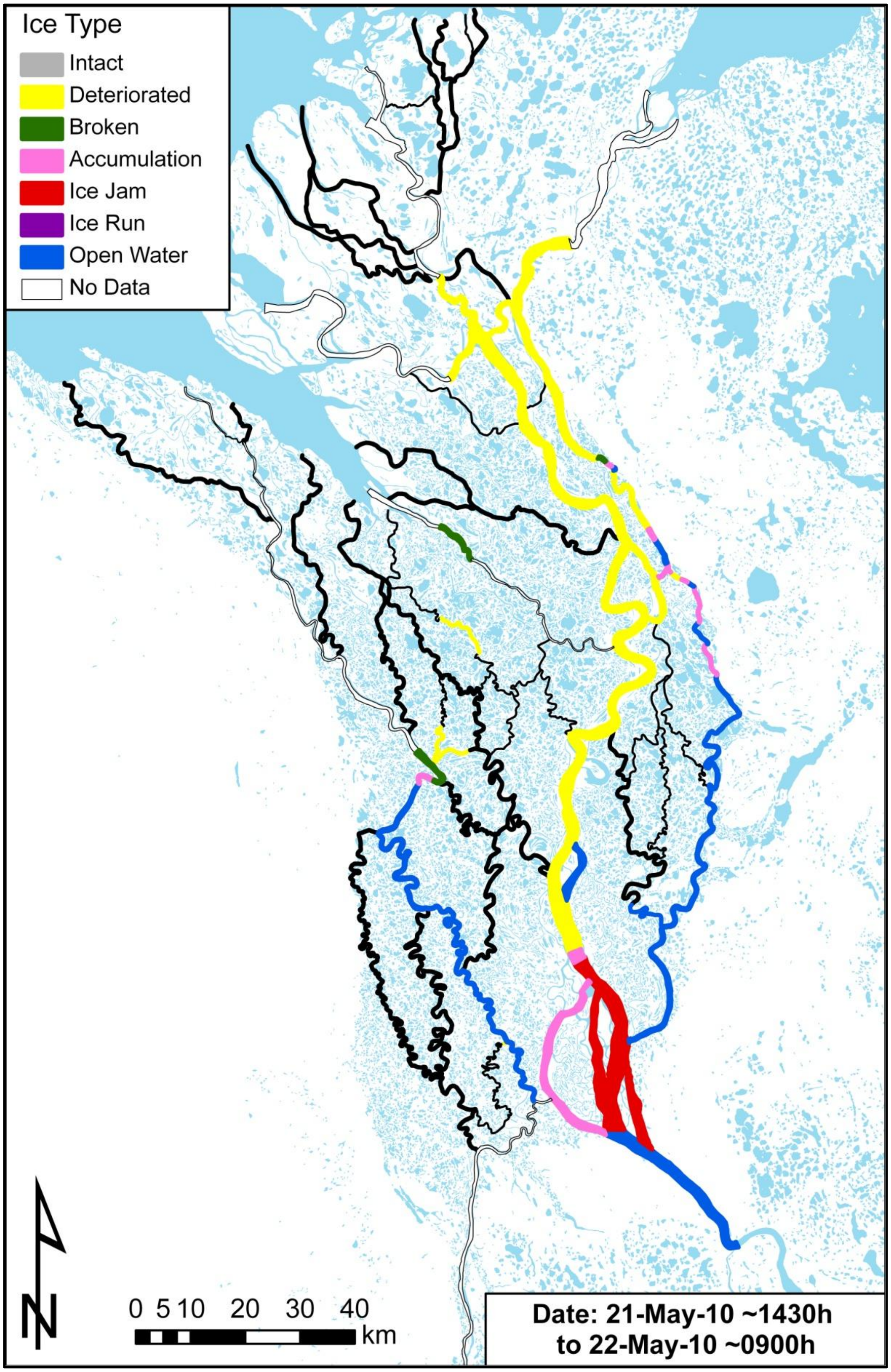

Figure 3.29 Map of 2010 breakup progression on 21-May-10. (data source: oblique photos).

Figure 3.30 Examples of lake-channel connections during the breakup period: (a) East Channel ice running from the along a side channel into a lake on 23-May-08 (UofA photo) and (b) erosion of East Channel bank with ice flowing into lake on 21-May-10 (UofA photo).

4.0 HEC-RAS Modeling of Primary Channels[13]

This chapter reports on the development and calibration of a steady, gradually varied flow hydraulic model used to calibrate geometry for the primary channels of the Mackenzie Delta using the U.S. Army Corps of Engineers Hydrologic Engineering Center River Analysis System (HEC-RAS). The objectives of this modeling effort and its application in further research are also explained. In addition, geometric data collected as part of IPY-SCARF is presented.

This hydraulic modeling effort was conducting in support of the development of the MDHM, a comprehensive one-dimensional network model, that is currently being developed for the Mackenzie Delta, which will be capable of incorporating the effects of ice jams, storm surges and off-channel storage (Nafziger *et al.*, 2009). Efforts to develop this model have been hindered by a lack of geometric data describing the Delta channels and almost no information on channel slope. Previous hydraulic modeling efforts (e.g. on the Peace River) have shown the importance of channel slope to accurate flow routing (Hicks, 1996). Therefore, the objective of this hydraulic modeling effort was the calibration of an analogous channel geometry of the primary network, capable of reproducing known water levels for known flow splits. An additional objective was the identification of areas or channels on which to focus additional data collection efforts, including manual flow measurements and channel geometry surveys.

[13] Components of this chapter were presented in the conference poster entitled, "Modelling the effects of ice on flow distributions in the Mackenzie Delta" by J. Morley, J. Nafziger, F. Hicks, P. Marsh, L. Lesack, S. Beltaos, J.J. van der Sanden, and T. Carter for the 16th Workshop on River Ice in Winnipeg, MB on September 18-21, 2011.

4.1 Previous Modeling of the Mackenzie Delta

Environmental Canada’s one-dimensional finite difference hydraulic model, ONE-D, was previously applied for the Mackenzie Delta by the WSC (Kerr and Miyagawa, 1996; Fassnacht, 1993b; Fassnacht, 1993a; Kerr, 1993b; Kerr, 1993a). That model routed inflow through 85 channel reaches (Fassnacht, 1997; Fassnacht, 1993a) to a downstream boundary on the Middle Channel below Langley Island (approximately *km* 245) (Fassnaucht, 1993a). Reports state that the model also included some provisions for storage effects (Kerr and Miyagawa, 1996), but do not detail what those were. That model was later enhanced to include sediment transport effects (Fassnacht, 1997).

Cross sections acquired before the ONE-D model was created (e.g. T. Blench & Associates Ltd., 1974; Lapointe, 1986), were not referenced to a geodetic datum. For the ONE-D model, representative cross sections at the upstream and downstream ends of each channel were measured for all but four reaches, and the intermediate geometry was estimated by interpolating between each of these cross-section pairs (Fassnacht, 1993a). While the cross section geometry acquired for the ONE-D model is available, it was not tied into a vertical datum with sufficient accuracy to be practically useful for determining channel slope. Therefore, these geometry data were of marginal usability for this study. However, the network of primary, secondary and tertiary channels chosen for the MDHM was based upon the channels used in the ONE-D model (Nafziger *et al.*, 2009). The MDMH has the potential to characterize the flow in the Mackenzie Delta more fully than previous models by including the effects of storm surges, storage and ice jams (Nafziger *et al.*, 2009), and potentially, more realistic channel gradients.

4.2 Description of Model used in this Study

HEC-RAS is a one-dimensional, gradually varied flow, steady-state hydraulic model. It also has unsteady flow modeling capabilities, but these were not relevant to this modeling effort. For steady state modeling in subcritical reaches, HEC-RAS computes water surface profiles based upon the standard-step method, working upstream from a user specified water surface elevation at the downstream boundary of channels, and solving the energy equation for a given geometry (Brunner, 2002):

$$Y_2 + Z_2 + \frac{\alpha_2 V_2^2}{2g} = Y_1 + Z_1 + \frac{\alpha_1 V_1^2}{2g} + h_e \qquad 4-1$$

where: Y_1, Y_2 = depth of water at cross section (m);

Z_1, Z_2 = elevation of the main channel inverts (m);

V_1, V_2 = average velocities (m/s) (total discharge/ total flow area);

α_1, α_2 = velocity weighting coefficient;

g = gravitational acceleration (m/s^2); and

h_e = energy head loss (m).

The head loss is calculated as a combination of frictional resistance and (empirical) expansion/contraction losses as defined by the following equation (Brunner, 2002):

$$h_e = L\bar{S}_f + C\left|\frac{\alpha_2 V_2^2}{2g} - \frac{\alpha_1 V_1^2}{2g}\right| \qquad 4-2$$

where: L = discharge weighted reach length (m);

$\bar{S}_f$ = representative friction slope between two sections; and

C = expansion or contraction loss coefficient.

As described in Section 4.3, a rectangular cross-section approximation with high banks was employed in this modeling effort and only low (in-bank) flows were modeled. As floodplain flows were not considered, and kinetic energy correction (α) was simply taken as one. Also, the weighted reach lengths (L), and the representative friction slopes ($\bar{S}_f$) were calculated using only channel area (i.e. not weighted to include overbank areas). Therefore, the friction slope between two sections (using a rectangular channel approximation) was calculated based upon the user specified Manning's roughness coefficient (*n*) for the channel and the application of the Manning's equation (Brunner, 2002):

$$Q = \frac{1}{n} A R^{2/3} S_f^{1/2} \qquad 4-3$$

where: Q = flow at cross-section(m^3/s);

n = Manning's roughness coefficient;

A = flow area of cross-section (m^2); and

R = hydraulic radius for channel (m) (*A*/wetted perimeter).

HEC-RAS computes water levels for one-dimensional steady flows in networks by applying the energy equation (Equation 4-1) from downstream boundaries to channel junctions. If the water surface elevation at a specific junction can be calculated from two downstream boundaries (i.e. from two downstream channels) junction water level on the main channel (i.e. the one with greater flow) are taken as the boundary condition to compute water levels upstream of that junction. This means that water level discontinuity was possible on the other channel. In this study, the objective was to test different channel slopes, to see which slope would best reproduce observed water surface profiles for known flow splits while also minimizing water level discontinuities at junctions.

4.3 Geometric Data used to Develop the HEC-RAS Model

4.3.1 Channel Geometry Data Collected During the Study Period

Figure 4.1 shows a map of the Delta with the locations of each of the cross-sections surveyed by Environment Canada in August 2007 and September 2008, on the Middle, East, West and West-Middle Connector Channels:

- 17 cross-sections were measured on the Middle Channel in the central Delta, as shown in Table 4.1.
- Four cross-sections were measured on the East Channel just downstream of the East-Middle Channel junction, as shown in Table 4.2.
- 11 cross-sections were measured on the West Channel, including four around the junction of the West-Middle Connector Channel and 7 surrounding Aklavik, as shown in Table 4.3.
- Two cross-sections were measured on the West-Middle Connector Channel, as shown in Table 4.4.
- Two cross-sections were measured on non- primary channels, as shown in Table 4.5.

Table 4.1 Cross-sections surveyed along the Middle Channel in 2007 and 2008. (Data Source: Environment Canada).

Cross Section	**Station** (km)	**Left Bank UTM Zone 8W** (NAD83)		**Right Bank UTM Zone 8W** (NAD83)		**Wetted Top Width** (m)	**CGG05 Water Level** (m)	**CGG05 Avg. Bed Elevation** (m)
SB17	24.2	537688	7498310	538946	7499436	1438	4.24	-5.52
SB16	45.5	527829	7515816	534098	7516088	1391	3.31	-0.55
SB15	62.2	527683	7530837	528446	7531415	780	2.07	-15.01
SB14	69.0	523144	7536192	524237	7536690	2518	1.99	-4.57
SB13	73.3	521677	7540249	524018	7541258	2340	1.86	-5.28
SB12	78.3	520192	7545265	522999	7546036	2711	1.63	-4.76
SB11	89.4	522930	7555674	524799	7555792	1684	1.39	-9.12
SB10	99.3	521989	7565609	523755	7565183	1739	1.25	-8.23
SB09	103.5	524003	7569530	524937	7568837	927	1.17	-16.54
SB08	104.6	524466	7570303	525616	7570006	941	1.19	-17.29
SB07	107.1	525252	7572114	526535	7572893	1352	1.16	-12.16
SB06	109.2	523515	7572916	525224	7574740	2396	1.12	-9.79
SB05	111.5	524811	7576190	525281	7575365	750	1.08	-23.88
SB04	114.9	528190	7576273	528579	7574787	1395	1.11	-10.06
SB03	118.9	531583	7577574	532581	7577402	751	1.00	-18.14
SB02	124.4	531506	7582894	532400	7582330	790	0.99	-17.38
SB01	133.0	538342	7587366	539231	7587464	696	0.89	-26.34

Table 4.2 Cross-sections surveyed along the East Channel in 2007 and 2008. (Data Source: Environment Canada).

Cross Section	**Station** (km)	**Left Bank UTM Zone 8W** (NAD83)		**Right Bank UTM Zone 8W** (NAD83)		**Wetted Top Width** (m)	**CGG05 Water Level** (m)	**CGG05 Avg. Bed Elevation** (m)
SB201	49.9	534277	7519853	534558	7518694	751	3.20	-0.55
SB202	53.0	536986	7521029	537204	7520518	425	3.10	0.81
SB203	56.9	540417	7522627	540767	7522273	427	2.89	0.75
SB204	61.3	541618	7526600	542179	7526674	420	2.71	0.24

Table 4.3 Cross-sections surveyed along the West Channel in 2007 and 2008. (Data Source: Environment Canada).

Cross Section	**Station** (km)	**Left Bank UTM Zone 8W** (NAD83)	**Right Bank UTM Zone 8W** (NAD83)	**Wetted Top Width** (m)	**CGG05 Water Level** (m)	**CGG05 Avg. Bed Elevation** (m)
SB107	52.8	514455 7502365	514761 7502259	272	3.66	-0.80
SB105	62.8	517173 7506766	517428 7506588	290	3.38	-3.64
SB104	66.8	517073 7510270	517286 7510266	157	3.27	-2.60
SB106	69.3	515005 7511209	515155 7511397	199	3.19	-1.62
SB307	174.3	495772 7566588	496250 7566410	194	-	-
SB306B	175.4	495730 7567632	496228 7567474	241	-	-
SB305	176.4	496890 7568296	496819 7567677	317	-	-
SB304	179.2	499485 7567168	499281 7566454	359	-	-
SB303	180.2	499845 7567298	500645 7566827	360	-	-
SB302	181.9	499373 7568156	499909 7568723	288	-	-
SB301	183.6	498244 7569541	499058 7569993	464	-	-

Table 4.4 Cross-sections surveyed along the West-Middle Connector Channel in 2007 and 2008. (Data Source: Environment Canada).

Cross Section	**Station** (km)	**Left Bank UTM Zone 8W** (NAD83)	**Right Bank UTM Zone 8W** (NAD83)	**Wetted Top Width** (m)	**CGG05 Water Level** (m)	**CGG05 Avg. Bed Elevation** (m)
SB103	66.9	518830 7508530	519003 7508161	321	3.24	0.39
SB102	70.6	518967 7510759	519847 7511004	790	3.18	0.41

Table 4.5 Additional cross-sections surveyed along non-primary channels 2007 and 2008. (Data Source: Environment Canada).

Cross Section	**Left Bank UTM Zone 8W** (NAD83)	**Right Bank UTM Zone 8W** (NAD83)	**Wetted Top Width** (m)	**CGG05 Water Level** (m)	**CGG05 Avg. Bed Elevation** (m)
SB101	525764 7503586	526020 7504626	740	3.50	1.48
SB108	515600 7504938	515658 7505117	94	3.38	2.95

The cross-sections measured in this study were not incorporated into the HEC-RAS model as they were relatively few in number and concentrated only in the upper Delta. Therefore, a rectangular cross-section approximation was assumed for this study.

4.3.2 Determining Channel Widths for the Rectangular Channel Approximation

A rectangular cross-section approximation has been shown to be a reliable estimate of geometry in previous hydraulic models (e.g. Hicks, 1996). For this study, top widths were measured at 500 m intervals along the primary channels using Geographic Information System (GIS) software and geo-referenced raster images of 2004 air photos obtained from the Northwest Territories Center for Geomatics (NWTCG) through the Mackenzie Valley Air Photo Project (Nafziger *et al.*, 2009; NWT Centre for Geomatics, 2007). Measured top widths were then smoothed to increase computational efficiency during modeling. Figures 4.2 to 4.8 show the top widths and smoothed widths used for each of the seven primary channels modeled, with key locations along each of the channels also identified. A total of 1,996 cross-sections over the 983 km of channel length modeled were used. The number of cross-sections along each channel is shown in Table 4.6.

Table 4.6 Number of rectangular cross-sections used in model along each of the primary channels.

Channel	Number of cross-sections in model
Middle Channel	587
East Channel	472
West Channel	564
West-Middle Connection Channel	60
Napoiak Channel	127
Neklek Channel	24
Reindeer Channel	132

4.4 Selection of Calibration and Validation Period

By necessity, geometry calibration must be done using non-complex flow scenarios, as otherwise backwater effects would distort the results. Based upon the flow measurement campaigns during the study period (as discussed in Chapter 2), an open water calibration period, two open water validation periods and one ice-affected period were chosen for modeling:

- Calibration Scenario - 2-Aug-08 to 12-Aug-08,
- Validation Scenario #1 - 14-Jun-07 to 20-Jun-07,
- Validation Scenario #2 - 4-Sep-09 to 17-Sep-09, and
- Winter Scenario - 13-Apr-09 to 24-Apr-09.

Each of the open water scenarios had the following four qualities:

1. Manual flow measurements were available, which allowed for the least number of assumptions regarding flow splits at channel junctions.

2. Flows were relatively steady over the measurement period, as confirmed by gauge levels that were relatively unchanging over the period (i.e. a runoff event was not occurring), as discussed in Section 2.3.2.

3. Backwater effects from storm surges (on the downstream water level boundary condition) were known to be minimal.

4. Surveyed water surface profiles level elevations were available along the primary channels, to allow comparison with modeled water surface.

The calibration scenario was selected from among the open water measurement campaigns, as this period had the most comprehensive manual flow measurements. Therefore, the least number of assumptions regarding flow distributions at channel junctions were necessary. The Winter Scenario was chosen as it is the campaign with a measurement at a gauging site without rating curve.

4.4.1 Selection of Flow Boundary Conditions

Assumptions were necessary to estimate flow distributions in the primary channels for each of the scenarios modeled. To do this, flow change locations, listed in Table 4.7, were selected based upon the available flow data. These flow change locations were consistent for each scenario and were situated at the junction of every primary channel and at the junctions of some of the larger secondary channels. If no flow data was available for distributaries or tributaries to a primary channel then the flow at those channel junctions was assumed zero (Q_a), and, thus, no flow change was assumed at that location. The sensitivity of assuming zero flow at specific junctions was tested and is discussed in Section 0.

A constant flow was assumed between each flow change location and the channel segments between these flow change locations were termed a reach. The location and name (named from upstream to downstream) of the reaches used are shown in Table 4.8, and mapped in Figure 4.9. Also shown in this table are the five gauging stations with rating curves, for which the average rating curve flow over the period (Q_r) was used to approximate the flow over the reach where the gauging station is located. The remainder of the flow assumptions were dependent upon the manually measured flows available for each scenario, based upon conservation of mass. As a constant flow was assumed over each reach, manual flow measurements at a specific location along a reach were assumed to apply over the entire reach, though manual measurements were not at the same location along a reach in each scenario. Specific flow assumptions for each of the scenarios modeled are described in the following section. A comprehensive list of all the resulting flows, for each reach, during each flow scenario, is shown in Appendix D. For simplicity, flows were rounded to the nearest cubic meter per second (m^3/s), although the WSC only reports flows to three significant figures.

Table 4.7 Location of flow changes along primary channels.

Channel	Flow change location (d/s of km)	Flow increase or decrease	Junction/Gauge
Middle Channel	0	↑	Inflow - 10LC014
	25	↓	Unnamed Secondary Channel A
	31.5	↓	Unnamed Secondary Channel B
	39	↓	Unnamed Secondary Channel C
	45	↑	Unnamed Secondary Channel A
	48.2	↓	East Channel
	59.5	↑	Unnamed Secondary Channel C
	62.5	↑	West-Middle Connector Channel
	82.5	↓	Aklavik Channel
	140.8	↓	Napoiak Channel
	221	↓	Neklek Channel
	223	↓	Reindeer Channel
	245	↓	Arvoknar Channel
	258.5	↓	Harry/Kuluarpak Channel
	281	↓	Kumak Channel
East Channel	48.2	↑	Confluence
	76.7	↓	Kalinek Channel
	117.7	↓	Unnamed Tertiary Channel
	232.2	↑	Neklek Channel
West Channel	0	↑	Inflow - 10MC002
	42.5	↓	Husky Channel
	64.8	↓	West-Middle Connector Channel
	162.5	↑	Husky Channel
West-Middle Connector Channel	64.8	↑	Confluence
	68.8	↑	Unnamed Secondary Channel B
Napoiak Channel	140.8	↑	Confluence
Neklek Channel	221	↑	Confluence
Reindeer Channel	223	↑	Confluence

Table 4.8 Defined reaches (with assumed constant flow) along the primary channels.

Channel	**d/s flow change station**	**u/s flow change station**	**Reach name**	**Assumed flow for all periods**	
				Type	**Gauge**
Middle Channel	0	25	M-1	$Q_{r\ (average)}$	10LC014
	25	31.5	M-2		
	31.5	39	M-3		
	39	45	M-4		
	45	48.2	M-5		
	48.2	59.5	M-6		
	59.5	62.5	M-7		
	62.5	82.5	M-8		
	82.5	140.8	M-9	$Q_{r\ (average)}$	10MC008
	140.8	221	M-10		
	221	223	M-11		
	223	245	M-12		
	245	258.5	M-13		
	258.5	281	M-14		
	281	293.5	M-15		
East Channel	48.2	76.7	E-1		
	76.7	117.7	E-2		
	117.7	232.2	E-3	$Q_{r\ (average)}$	10LC002
	232.2	284.2	E-4		
West Channel	0	42.5	W-1	$Q_{r\ (average)}$	10MC002
	42.5	64.8	W-2		
	64.8	162.5	W-3		
	162.5	282	W-4	$Q_{r\ (average)}$	10MC003
West-Middle Connector Channel	64.8	68.8	WM-1		
	68.8	94.8	WM-2		
Napoiak Channel	140.8	204.3	NP-1		
Neklek Channel	221	233	NL-1		
Reindeer Channel	223	289	RD-1		

4.4.1.1 Flow Assumptions for Open Water Calibration Scenario

Figure 4.10 shows the nodal diagram used to determine flows for each reach for the Open Water Calibration Scenario. Assumed flows are shown with a dashed line (Q_a) and manually measured flows (from Figure 2.28) are also shown. As flow was not measured along the Unnamed Secondary Channel A, the flow in this channel was assumed zero. Following from this assumption, and by assuming flow is conserved at *km* 48.2, flows in channels 'M-2' through 'M-5' were calculated. Flow along the Unnamed Secondary Channel C was calculated as the difference between flow in reach 'M-4' and 'M-5'. Flows 'M-7' and 'M-8' were calculated by assuming flow conservation at *km* 59.5 and 62.5, and *km* 68.8 along the West-Middle Connector Channel. The difference between the calculated flow (Q_c) for 'M-8' and the measured (rating curve) flow at 'M-9' was used to calculated the flow in the Aklavik Channel labeled 'D'.

On the East Channel, equal flows were assumed to leave the East Channel at *km* 76.7 and *km* 117.7. Based on this assumption, the flow along reach 'E-2' could be calculated. The remainder of flows for reaches on the East Channel were known, as they were manually measured or reported at a gauge with a rating curve. There were three manual measurements along reach 'W-2': 1,443 m^3/s, 1,384 m^3/s and 1,415 m^3/s at *km* 53, 58, and 58.5, respectively. As these measurements were taken over only 5.5 km and were all within only 60 m^3/s of each other (0.4% of the inflow), the average of these manual measurements was used for reach 'W-2', with the difference between 'W-1' and 'W-2' assumed to leave the West Channel at the Husky Channel (*km* 42.5). The manual flow measurement at *km* 68.5 was measured for reach ‘W-3’. As such, when flow was conserved at *km* 64.8, there was a 55 m^3/s (0.4% of the total Delta inflow) difference that was not accounted for once the manually measured loss to the West-Middle Connector Channel was subtracted. The flow difference between ‘W-3’ and ‘W-4’ was assumed to enter the West Channel via the Husky Channel at *km* 162.5.

During the calibration period, flows in the lower delta were measured at the gauging stations downstream from the Quadrapus (referred to as Quadrapus Flow Scenario A). As shown in the box outlined in Figure 4.10(b), the difference between the sum of the inflows and outflows at the Quadrapus was 93 m^3/s or 0.6% of the total Delta inflow, which was quite small considering potential errors in measurement and channels that are unaccounted for. As a result of this flow difference, the flow in the Neklek Channel (‘NL-1’) could be calculated in two ways. Flow conservation along the East Channel at *km* 232 yielded a flow of 3,499 m^3/s, whereas solving for ‘M-11’ and then ‘NL-1’ yielded a flow of 3,406 m^3/s. The average of these two values was used for modeling and the sensitivity was tested (as will be discussed in Section 0). Flow measurements on both the gauge channel and Middle Channel at *Mackenzie River (Outflow Middle Channel) below Langley Island* (10MC010) *(km* 245) were used to calculate the flow at ‘M-13’. The flow measured at *Mackenzie River at Kuluarpak Channel* (10LC021) was assumed to leave the Middle Channel at *km* 258.5, thus enabling ‘M-14’ to be calculated. The flow difference between the calculated flow along ‘M-14’ and the measured flow at *Mackenzie River (Kumak Channel) below Langley Island* (10LC019) (‘M-15’), left the Middle Channel at *km* 281.

4.4.1.2 Flow Assumptions for Validation Scenario #1

Figure 4.11 shows the nodal diagram used to calculate the flows for Validation Scenario #1. In addition to the assumption of zero flow at Unnamed Secondary Channel A, flow was assumed on Unnamed Secondary Channel B based on the average tendencies illustrated in Figure 2.41 (which shows the range of percentage of total Delta inflow for all manually measured flows during the open water season). Following this figure, flow to Unnamed Secondary Channel B was assumed as 7.1% of the average total Delta inflow during this period. The flow measured at *Peel River at Frog Creek* (10MC022) was used for reach 'W-2', and 50% of this was assumed to flow into the West-Middle Connector Channel ('MW-1') at *km* 64.8. This percentage was based on the percentage of flow observed in this channel during the calibration run, which was the only period for which both of these locations were manually measured. Flow was conserved at *km* 64.8 to calculate the flow along W-3. Based on these assumptions, flow at M-2 to M-8 and WM-2 were calculated using the same process as for the calibration run, which was also used to calculate the flows for the first three reaches of the East Channel.

During this validation period, flows in the lower delta were measured at the same locations as during the calibration period (Quadrapus Flow Scenario A), except flow was not measured at ('E-4'). Therefore, flow at 'E-4' was determined by first calculating flows 'M-10', 'M-11' and 'NL-1', and then conserving flow at each of the junctions. Flows 'M-12' to 'M-15' were determined using the same assumptions as were used for the calibration scenario.

4.4.1.3 Flow Assumptions for Validation Scenario #2

The nodal diagram used to calculate the flows for Validation Scenario #2 is shown in Figure 4.12. Zero flow in Unnamed Secondary Channel A was assumed and, as the flow entering the West-Middle Connector Channel and the flow towards Unnamed Secondary Channel B were both measured during this period, flows ‘M-2’ to ‘M-8’ were calculated in the same way as for the calibration run. The same assumption of equal flow leaving at *km* 76.7 and 117.7 along the East Channel was also used to calculate ‘E-2’. The flow along the West Channel from *km* 42.5 to 64.8 (‘W-2’) was calculated based on the assumption that 0.7% of the inflow left the West Channel at *km* 42.5. This number was based upon the two manual flow measurements at *Peel River at Frog Creek* (10MC022), where the percentage of flow leaving at *km* 42.5 ranged from 0.5 to 0.9%. The flow along ‘W-3’ was also based on this assumption and conservation of flow at *km* 64.8.

The flow assumptions through the Quadrapus for Validation Scenario #2 were different than the assumptions used for the calibration period, as measured flows location were close to the Quadrapus junction (Quadrapus Flow Scenario B). The difference between the sum of the inflows and outflows in the box shown in Figure 4.12 was 200 m^3/s (1.4% of the Delta inflow). Due to this difference, flow at ‘M-11’ can be calculated in two ways, by conserving flow at either *km* 221 or 223 The average of these two flow calculations was used for ‘M-11’. The flow measured in the Neklek Channel was used to calculate ‘E-4’, assuming no flow loss at *km* 232. The flow at ‘M-12’ was much lower (in terms of percentage of total Delta inflow), than that measured in Quadrapus Flow Scenario A (i.e. for the calibration scenario and Validation Scenario #1), Figure 2.41 could not be used to develop an estimate of the flow downstream of ‘M-12’. As a result, Table 4.9, which summarizes the two measurements on the gauge channel and Middle Channel at *Mackenzie River (Outflow Middle Channel) below Langley Island* (10MC010), was used. This resulted in the assumption that ~43% of the flow entering the junction at *km* 245 left the Middle Channel at ‘J’. The average percentage of Delta inflow, as shown in Figure 2.41 measured at *Mackenzie River at Kuluarpak Channel* (10LC021), was assumed to leave the Middle Channel at *km* 258.5. At *km* 281, the average percentage of inflow leaving the channel was also assumed, based on the two other measurements in 2007 and 2008. Thus, 2.1% of the inflow was assumed to leave the Middle Channel at *km* 281.

As a result of these assumptions, the flow in the downstream section of the Middle Channel was much lower for Calibration Scenario #2 than for the other two open water scenarios modeled. Graphs showing the modeled flows along each of the channels for all three of the open water modeling periods are shown in Figures 4.13 to 4.19. Appendix D also provides a comparison of the flows used in each period, both as magnitudes and percentages of total inflow to the Delta.

Table 4.9 Flows measured on the Middle and Gauge Channel at *Mackenzie River (Outflow Middle Channel) below Langley Island* (10MC010).

Date	Q_m on Middle Channel (m^3/s)	Q_m on Gauge Channel (m^3/s)	Percentage
05-Aug-08	5020	2127	42.4%
19-Jun-07	6280	2680	42.7%
	Average		42.5%

4.4.1.4 Flow Assumptions for Winter Scenario

As there was only was one manual flow measurement (that supplemented the rating curve gauging station data) during the Winter Scenario, there were insufficient flow measurements to determine flow along each of the primary channels in the same way as the open water scenarios. Therefore a different approach was employed. This involved estimating the flow in each of the channels based upon the average percent of total Delta inflow observed during the open water scenarios. Though flow distributions were different in the winter, the intention was to compare the modeled water surface produced using this estimation of flow, with the measured water levels and measured flow during the Winter Scenario.

Figure 4.20 and Table 4.10 show the average percent flow distribution in terms of total Delta inflow during the open water periods, based upon conservation of mass and the available flow measurements. The averages of the manual measurements (as presented in Figure 2.41) were used to determine this distribution, but only measurements from Quadrapus Flow Scenario A were used, as the difference in flow splits between the two scenarios were substantial and Quadrapus Flow

Scenario was only measured once during the study period.

Table 4.10 Average percent of inflow along each of the primary channel reaches during open water conditions. (Data source: the WSC).

Channel	**d/s flow change station** (km)	**u/s flow change station** (km)	**Reach name**	**Percent of inflow**
Middle Channel	0	25	M-1	93.0%
	25	31.5	M-2	93.0%
	31.5	39	M-3	85.9%
	39	45	M-4	56.3%
	45	48.2	M-5	56.3%
	48.2	59.5	M-6	52.0%
	59.5	62.5	M-7	81.6%
	62.5	82.5	M-8	92.6%
	82.5	140.8	M-9	78.8%
	140.8	221	M-10	74.5%
	221	223	M-11	50.2%
	223	245	M-12	30.4%
	245	258.5	M-13	17.4%
	258.5	281	M-14	15.9%
	281	293.5	M-15	13.9%
East Channel	48.2	76.7	E-1	4.3%
	76.7	117.7	E-2	3.0%
	117.7	232.2	E-3	1.6%
	232.2	284.2	E-4	26.4%
West Channel	0	42.5	W-1	7.0%
	42.5	64.8	W-2	6.7%
	64.8	162.5	W-3	4.4%
	162.5	282	W-4	5.1%
West-Middle Connector Channel	64.8	68.8	WM-1	3.9%
	68.8	94.8	WM-2	11.0%
Napoiak Channel	140.8	204.3	NP-1	4.3%
Neklek Channel	221	233	NL-1	24.6%
Reindeer Channel	223	289	RD-1	20%

The total delta inflow (of 3,517 m^3/s) for the Winter Scenario was multiplied by the percentages shown in Table 4.10 to yield the flows modeled for the Winter Scenario. A list of these calculated flows is shown in Appendix D. Ground-fast ice data could not be included in the Winter Scenario as observations of accumulations of groundfast ice were limited to the channel outlets past the downstream boundaries of the primary channels (as discussed in Section 3.1.2). Though smaller (secondary and tertiary) channels could be blocked by groundfast ice in the winter, this could not be accounted for.

4.4.2 Downstream Water Level Boundary Condition

An external downstream boundary condition was required for each channel during each scenario. The downstream boundary condition on the East Channel was assumed equal to the average water level recorded at the during each period, as this gauging station is only 1 km from the outlet of the East Channel into Kittigazuit Bay. The boundary conditions selected for each channel during the scenarios modeled is shown in Table 4.12. A downstream boundary condition that was the same chosen for the Middle, West, Reindeer and Napoiak Channels, and, as the average water level of the Beaufort Sea was not expected to be variable between the scenarios, this same downstream boundary condition was also chosen for each of the open water scenarios. The selection of this downstream boundary was based upon a linear extrapolation of the measured water levels recorded at the downstream gauges on the Middle Channel down to the outlet of the Middle Channel (*km* 293.5), as shown in Figure 4.21. The water level resulting from these extrapolations are shown in Table 4.12. The average of these extrapolations and the elevation recorded at *Mackenzie River (Kumak Channel) below Langley Island* (10LC019), was used as the downstream boundary condition for these channels. A downstream boundary of 0.48 m was used for Winter Scenario for all Channels. This is the average water level recorded at , because there were insufficient water levels available at the downstream gauges to extrapolate to the downstream boundary on the Middle Channel.

Table 4.11 Downstream boundary conditions for modeling scenarios. (Data source: the WSC).

Channel	**Elevation of downstream boundary condition** (m)			
	Calibration Scenario	**Validation Scenario #1**	**Validation Scenario #2**	**Winter Scenario**
Middle Channel	0.07			0.48
East Channel	0.02	0.11	0.01	0.48
West Channel	0.07			0.48
Napoiak Channel	0.07			0.48
Reindeer Channel	0.07			0.48

Table 4.12 Extrapolated elevation at the downstream outlet of the Middle Channel using the downstream gauges of the Middle Channel. (Data source: the WSC).

Extrapolation	**Calibration Scenario** (m)	**Validation Scenario #1** (m)	**Validation Scenario #2** (m)
Gauge 10LC019	0.18	0.15	0.05
Extrapolation using 10LC019 and 10MC010	0.13	0.03	-0.07
Extrapolation using 10LC019, 10MC010, 10MC008	0.08	0.06	0.13

4.4.3 Determination of Channel Roughness

An assumption of channel roughness was necessary, as geometry was the calibrated parameter in this modeling effort. The Manning's channel roughness (*n)* calibrated for the ONE-D model by the WSC ranged from 0.020 to 0.060, based upon reach location and time of year (Kerr, 1993b). Open water roughness values ranged from 0.020 to 0.050 and ice-affected roughness values ranged from 0.031 to 0.060 (Kerr, 1993b). However, information detailing the flow data used for calibration and the process for calibration of roughness for this ONE-D model was not available. Therefore, these roughness values were not used for this modeling effort as they could not be justified. Instead, a Manning's roughness coefficient (*n*) of 0.030 was estimated based upon both Chow (1959), which suggested a roughness coefficient for major streams ranging from 0.025 to 0.060, and a judgment of the physical roughness limit decided upon after visiting the study site. Given the necessity of estimating channel roughness, a sensitivity analysis was employed, as will be discussed.

The average ice thickness (of ~1 m) measured on the primary channels, as described in Section 3.1.1, was used to model the primary channels under winter conditions. Previous modeling efforts on the Mackenzie River upstream of the Delta (e.g. Hicks *et al.*, 1995) estimated a roughness for the underside of a mid-winter ice cover of 0.015. Based upon a similar ice cover forming in the Delta and using judgment, a Manning's *n* value of 0.015 for the underside of ice was selected for this modeling effort.

4.4.4 Measured Water Surface Profiles During Modeling Scenarios

Averages of the water levels reported at each of the gauges over the corresponding flow measurement periods were used for comparing the modeled water surface to observed water surface elevations, for each of the scenarios modeled. Plots of the water levels reported for a four week period centered on the midpoint of the calibration period are shown in Figure 4.22 for the (a) Middle, (b) East, (c) West, (d) Napoiak and (e) Reindeer Channels gauging station(s). Figures 4.23 to 4.25 show the same corresponding graphs for Validation Scenario #1 and #2 and the Winter Scenario, respectively. The symbols show the elevations used to compare with the modeled results and the corresponding values are summarized in Table 4.13. This table also shows the limited number of water levels that are available for the Winter Scenario. Some gauges only reported water levels for parts of these periods. In these cases, the average of the available water levels was used. In addition, as shown in Figures 4.23(a) and (e) and 4.24(a) and (b), water levels had to be extrapolated at some gauges when data were not available during the flow measurement period. If measurements were similar (within ~0.05 m) before and after the period, then the average of these water levels was used for comparison. The water level used for comparison at the *Mackenzie River at Confluence East Channel* (10LC015) for the Winter Scenario was recorded at the time of manual flow measurement and is shown in italics in the table.

On the West Channel, the water surface elevation at the two upstream gauges did not decrease in downstream direction, as expected. As shown in Figure 4.22(c), for the calibration period, the water level recorded at *Mackenzie River (Peel Channel) above Aklavik* (10MC003) at *km* 0 and *Peel River at Frog Creek* (10MC022) at *km* 53 had the same magnitude. For Validation Scenario #1, the water level reported at *Peel River at Frog Creek* (10MC022) at *km* 53 was ~1.5 m higher than the measurement at *Mackenzie River (Peel Channel) above Aklavik* (10MC003), as shown in Figure 4.23(c).

Table 4.13	Table of average water levels recorded at gauging station during the modeling scenarios. (Data source: the WSC).

Channel	**Station Number**	**Station at WL measurement** (km)	**Average water level** (m)			
			Calibration Scenario	**Validation Scenario #1**	**Validation Scenario #2**	**Winter Scenario**
Middle Channel	10LC014	0.0	4.53	6.67	4.65	3.39
	10LC015	48.2	3.00	4.48	3.34	*3.35*
	10MC008	110.5	1.53	2.58	1.53	
	10MC010	245.0	0.45	0.77	0.69	
	10LC019	285.0	0.18	0.15	0.05	
East Channel	10LC015	52.2	3.00	4.48	3.34	*3.35*
	10LC002	144.2	1.29	2.14	1.19	0.83
	10LC012	232.2	0.48	0.88	0.50	
	10LC013	283.2	0.11	0.01	0.02	0.48
West Channel	10MC002	0.0	6.61	5.64	6.05	3.97
	10MC022	53.0	6.49	7.13		
	10MC003	173.0	1.27	1.93	1.10	0.57
Napoiak Channel	10MC023	188.8	0.62	0.91	0.24	0.65
Reindeer Channel	10MC011	276.5	0.25	0.30	0.14	0.72

4.4.5 Available Water Surface and Bed Elevations along Middle, East and West Channels

In addition to water surface elevation recorded by WSC at gauging stations, water surface and bed elevations along the primary channels are available from different sources. A plot of these measured bed and water surface elevations along the Middle, East and West Channels, which was used to help estimate the initial channel slope of each of these channels, is presented in Figures 4.26 to 4.28, respectively. There are six types of data shown on these graphs:

1. The water surface elevations at the time of cross-sections surveys, during the study period (as described in Section 4.3.1), are shown at their respective locations. The average water level slope calculated from the cross-section measured along the Middle Channel is 0.00003.
2. The mean bed elevations from each of the cross-sections from the same surveys are also plotted.
3. Water levels taken from National Topographic Series (NTS) maps, where the contour lines intersected the Mackenzie and Peel Rivers, are presented, though they could not be referenced to the CGG05 datum. As the slope of the channels in the Delta is mild, these contours only intersected the channel upstream of the channel inflow boundaries.
4. Digital elevation model (DEM) centerline water surface elevations, which were provided by NWTCG (NWT Centre for Geomatics, 2007), show the water surface elevation on the day of measurement to the nearest meter, as the reflectance of water does not allow for greater resolution. The overall water surface slope suggested by these DEM data is 0.00002, which is very similar to that found based on the surveyed cross-sections for this study.
5. DEM bank elevation is also shown and was extracted by masking areas outside of the banks of the Middle and East Channel (Data source: J. Nafziger, UofA). As a result, the DEM bank elevations range by ~5 m at each location.
6. The water surface profiles during both a high water level and lower water level open water day were plotted to demonstrate the range in water level

elevations expected at each gauging station during the summer months.

On the Middle Channel, water surface elevation measurements show a possible water surface slope break between *km* 30 and *km* 80. The water surface slope changes from a steeper (though still hydraulically mild) slope to a flatter slope. A similar water level slope break is evident on the East Channel, but was not observed on the West Channel though limited water surface elevation data was available (along the West Channel). Previous studies by Lapointe (1984) have also suggested a slope change in this area on the Middle Channel.

4.4.6 Geometry Calibration Results

The geometry calibration process involved adjusting the channel bed slope and bed elevation until the computed water surface profile matched the observed water levels for the input flow distribution and water level discontinuities at channel junctions were minimized. This involved a systematic iterative approach, which started by assuming reasonable values of channel roughness (section 4.???) and adjusting the elevation of the bed using the water surface slopes observed in Figures 4.26 to 4.28, with a slope break around *km* 48.2 along the Middle Channel. However, this geometry did not reproduce water levels at both the upstream and downstream gauge locations for the Calibration Scenario. A constant slope was also investigated for each channel, but no combinations of slope and elevation were found that could reproduce water levels at both the upstream and downstream of each channel. Only by introducing sills (i.e. bed discontinuities) at certain channel junctions could the observed water surface profiles be reasonably matched. The bed profile and resulting computed water levels obtained for the final calibration run, are shown in Figures 4.29 to 4.35, for the Middle, East, West, West-Middle Connector, Napoiak, Neklek and Reindeer Channels, respectively. The calibrated bed slope and downstream bed elevation for each channel is summarized in Table 4.14. A flatter slope was found on the distributaries compared to the Middle Channel.

The objective of this study was to produce an analogous channel geometry that effectively reproduced known water level profiles for known flow distributions. However, because channel roughness was also unknown, the calibrated geometry is not necessarily an exact representation of the actual channel geometry. In terms of the validity of the large bed discontinuities required to achieve a successful geometry calibration (up to 10 m), it should be noted that large large bed discontinuities have actually been observed in the Delta, including large scour holes on the East Channel (up to 30 m deep) (Beltaos *et al.*, 2011; Inkratas *et al*., 2009; Gharabaghi *et al*., 2009). Lapointe *et a*l. (1984) also noted that large thalweg irregularities have been observed on many of the Delta channels. As a result, the discontinuities in the calibrated geometry are not considered unrealistic. However, it is important to keep in mind that this calibrated geometry is linked to the assumed channel roughnesses and, therefore, other combinations of channel geometry and channel roughness could also reproduce the observed water surface profiles comparably well. However, insufficient data is available to optimize this the calibration; in particular, for the Reindeer and Napoiak Channels, since only one known water surface elevation is available for each.

Table 4.14 Calibrated bed slope and downstream elevations for the reaches on each channel.

Channel	d/s flow change station (km)	u/s flow change station (km)	Reach name	Slope	d/s bed elevation (m)
Middle Channel	0	25	M-1	0.000060	
	25	31.5	M-2		
	31.5	39	M-3		
	39	45	M-4		
	45	48.2	M-5		
	48.2	59.5	M-6		
	59.5	62.5	M-7		
	62.5	82.5	M-8		
	82.5	140.8	M-9		
	140.8	221	M-10		-18.15
	221	223	M-11	0.000025	
	223	245	M-12		
	245	258.5	M-13		
	258.5	281	M-14		
	281	293.5	M-15		-11.8
East Channel	48.2	76.7	E-1	0.000029	
	76.7	117.7	E-2		
	117.7	232.2	E-3		
	232.2	284.2	E-4		-7.4
West Channel	0	42.5	W-1	0.000030	
	42.5	64.8	W-2		
	64.8	162.5	W-3		
	162.5	282	W-4		-7.5
West-Middle Connector Channel	64.8	68.8	WM-1	0.000300	
	68.8	94.8	WM-2		-1
Napoiak Channel	140.8	204.3	NP-1	0.000010	-3.7
Neklek Channel	221	233	NL-1	0.000010	-13
Reindeer Channel	223	289	RD-1	0.000025	-9.5

For the calibration period, the average (absolute value) difference between the computed and modeled water surface elevations was 0.24 m, and ranged up to 1.26 m, with the water level at *Peel River at Frog Creek* (10MC022) having the largest difference. If the water level difference at 10MC022 is not included, the average difference is 0.16 m, and ranges up to 0.75 m. The discontinuities at junctions were each less than 0.05 m.

4.4.7 Results for Open Water Validation Periods

The calibrated bed geometry was validated for the two remaining open water cases and the resulting computed water surface elevations are in Appendix E. The average difference between the observed and computed water levels was 0.50 m for Validation Scenario #1. The range was up to 1.2 m and was once again highest at *Peel River at Frog Creek* (10MC022). Excluding that site, the average difference is 0.44 m and ranged up to 0.88 m. For Validation Scenario #2, the average difference between the modeled and observed water surface was 0.25 m, and ranged up to 0.75 m. A water level at *Peel River at Frog Creek* (10MC022) was not available for this scenario.

Water surface discontinuities at the junctions of channels occurred in both of the open water validation runs. For Validation Scenario #1, water level discontinuities ranged from -2.06 m to 0.7 m, while the range for Validation Scenario #2 was between -0.48 m and 1.20 m. For both validations periods, the greatest discontinuities were at the junctions closest to the downstream boundaries (i.e. the Napoiak Channel junction, the Reindeer Channel junction and the Neklek Channel junction).

Given the lack of geometric and hydrometric data available, the open water results were encouraging. Overall, if the water level measurements at *Peel River at Frog Creek* (10MC022) were excluded, all of the modeled water surfaces were within 1 m of the measured water surface. However the water surface slope in the Delta is quite flat, so this difference is still significant. Additionally, large water surface discontinuities, ranging up to 2.2 m, at channel junctions were observed. Before assessing the overall value of this calibrated channel geometry for open water scenarios, a sensitivity analysis was first conducted.

4.4.8 Results for Ice-Affected Period

HEC-RAS did not produce a modeled water surface profile using the inputted geometry and flow assumptions. The reason for this is unknown, but it could because the depth of flow is less than the thickness of ice in some locations. In reality, it is possible that large portions of some channels cross-sections were blocked by groundfast ice in the winter months, but as the actual cross-section geometries were unknown this could not be accounted for. In addition, flow distributions are different during the winter months, which were also not accounted for in this model run. As a result, validation of the calibrated open water geometry was not possible for a simple ice-affected scenario.

4.5 Open Water Sensitivity Analysis

To test the effect of each assumption, one variable at a time was changed and the model was run for the calibration and validation scenarios. The assumptions tested for sensitivity included flow distributions, channel bed roughness and downstream boundary conditions.

4.5.1 Sensitivity of Model Result to Flow Assumptions

The first flow assumption was that flow in Unnamed Secondary Channel A was equal to zero. Based on channel width and depth the maximum possible flow during on this channel open water conditions was anticipated to be 30% of the total Delta inflow. The model was run with 10%, 20% and 30% of the inflow leaving the Middle Channel at *km* 25 and returned at *km* 45, with corresponding decreases in the flows in reaches ‘M-2’, ‘M-3’, and ‘M-4’. The modeled water levels remained the same for all downstream cross-sections, but the upstream water levels decreased a maximum of 0.04 m at the upstream boundary of the Middle Channel for each 10% increase in flow attributed to Unnamed Secondary Channel A. Therefore, the assumption of zero flow in Unnamed Secondary Channel A, had a minimal effect on modeled water surface profile generated in this modeled effort.

Another flow assumption on the Middle Channel was that the difference between the flow deduced by conservation of mass at *km* 62.5 (downstream of the Turtle) and the rating curve flow at *km* 110.5 was lost to the Aklavik Channel at *km* 82.5. This assumption was made as this is the only secondary or tertiary channel between these two stations. However, this flow loss is quite substantial, ranging from 9% to 16% of the total Delta inflow and no flow measurements are documented on the Aklavik Channel to suggest or confirm that it carries such a substantial flow. Therefore, the sensitivity of the model to this assumption was tested by assuming the flow was lost gradually between *km* 62.5 and *km* 110.5 to five channels that were equally spaced along the Middle Channel and each had equal flow. This had negligible effects on the water surface profile generated and water levels on the Middle Channel changed by up to 0.02 m.

As flow measurements during the calibration and validation periods suggested two different flow distributions at the Quadrapus (Quadrapus Flow Scenario A and B), the sensitivity of these flows was tested by adopting the opposite flow scenario than that which was used for calibration and validation. For the calibration run and Validation Scenario #1, this involved adopting Quadrapus Flow Scenario B and changing flows for 'M-10' to 'M-15' and for 'NK-1', 'RD-1' and 'E-4'. Validation Scenario #2 was also run for with the flow distribution for Quadrapus Flow Scenario #1. The substantial water level changes that resulted are summarized in Table 4.15. Water surface discontinuities that ranged up to 3.0 m were also observed at junctions. Clearly, the flow split through the Quadrapus had a large effect on modeled water levels upstream. As a result, measured flow on each leg of the Quadrapus during the same timeframe as measurements at all nearby gauging sites are recommended.

Table 4.15 Maximum water level change observed as a result of applying the opposite Quadrapus Flow Distribution State used for calibration or validation.

Channel	**Approximate Maximum Change in Water Level** (m)		
	Calibration Scenario	**Validation Scenario #1**	**Validation Scenario #2**
Middle Channel	-0.7	-0.8	0.6
East Channel	0.4	0.6	-0.5
Reindeer Channel	0.6	1.0	-0.6
Neklek Channel	0.4	0.7	-0.4

4.5.2 Sensitivity of Model Results to Channel Roughness

A channel Manning's roughness coefficient of 0.030 was selected for all channels modeled and the sensitivity of increasing and decreasing this value by 0.010 was tested. This change dramatically affected upstream water levels, such that at *km* 0 on the Middle Channel the modeled water surface increased by 1.5 to 2.5 m (dependent on the flow scenario) when the roughness was increased by 0.010. The water level decreased by the same amount when the Manning's roughness coefficient was lowered by 0.010. The most pronounced effect was for Validation Scenario #1, likely because the total Delta inflow was highest during this period. Although the range of Manning's *n* both calibrated in the ONE-D model of the delta (Kerr, 1993b) and suggested by Chow (1959) is broader than the range tested in this sensitivity analysis, the range tested for this sensitivity analysis still resulted in significant water levels changes. Evidently, the modeled water surface is sensitive to changes in channel Manning's n. However, it is likely that a different geometry could be calibrated for each channel roughness value within a reasonable range. The calibrated bed slope and elevation found in this modeling effort only reproduced observed water surface elevations if the roughness coefficient is equal to 0.030.

4.5.3 Sensitivity of Model Results to Changes in Downstream Boundary Condition

The sensitivity of the East Channel downstream boundary condition was not tested, as it was measured at a gauging station. For the rest of the channels, the sensitivity of the modeled water surface to changes in the downstream boundary conditions was tested, using the range of possible downstream boundary conditions shown in Table 4.12. Each of the open water scenarios was run with the boundary condition for each of the channel set at -0.07 m and 0.18 m. The effects of this change on water levels generated for the Middle Channel ranged up to 0.03m at *Mackenzie River at Arctic Red River* (10LC014), but were larger closer to the downstream boundary. From this analysis it was determined that changes in the downstream boundary condition had a minimal effect on modeled water surface profile generated in this modeled effort.

4.5.4 Summary of Sensitivity Analysis

Overall the modeled water surface elevation using the calibrated geometry was most sensitive to changes in assumed flow splits close to the downstream boundary. Further flow measurements would be helpful for further calibration and validation. In particular, measurements in the area of the Quadrapus during the same timeframe as measurements at the *Mackenzie River (Reindeer Channel) at Ellice Island* (10MC011), *Mackenzie River (Middle Channel) at Tununuk Bay* (10LC012) and *Mackenzie River (Outflow Middle Channel) below Langley Island* (10MC010) are recommended. The model was also sensitive to changes in Manning's *n*. Although there are likely many combinations of calibrated bed slope, bed elevation and Manning's n that could reproduce observed water levels for the known flow splits, the analogous channel geometry found in this modeling effort only successfully reproduces flow water levels when a Manning's n of 0.030 is used.

4.6 Summary of Geometry Calibration Results

An analogous channel geometry for the primary channels was calibrated using HEC-RAS. This geometry produced a modeled water surface during open water conditions that was an average 0.24 m from the observed water surface elevation. In the two validation periods, this average difference between observed and modeled water levels ranged from 0.25 m to 0.50 m. Although some of the differences between observed and modeled water levels were substantial (up to 1.2 m), it is suggested that the channel geometry shown in Table 4.14 be incorporated into the MDHM as an initial input geometry. Additional changes to this geometry are anticipated as more data becomes available.

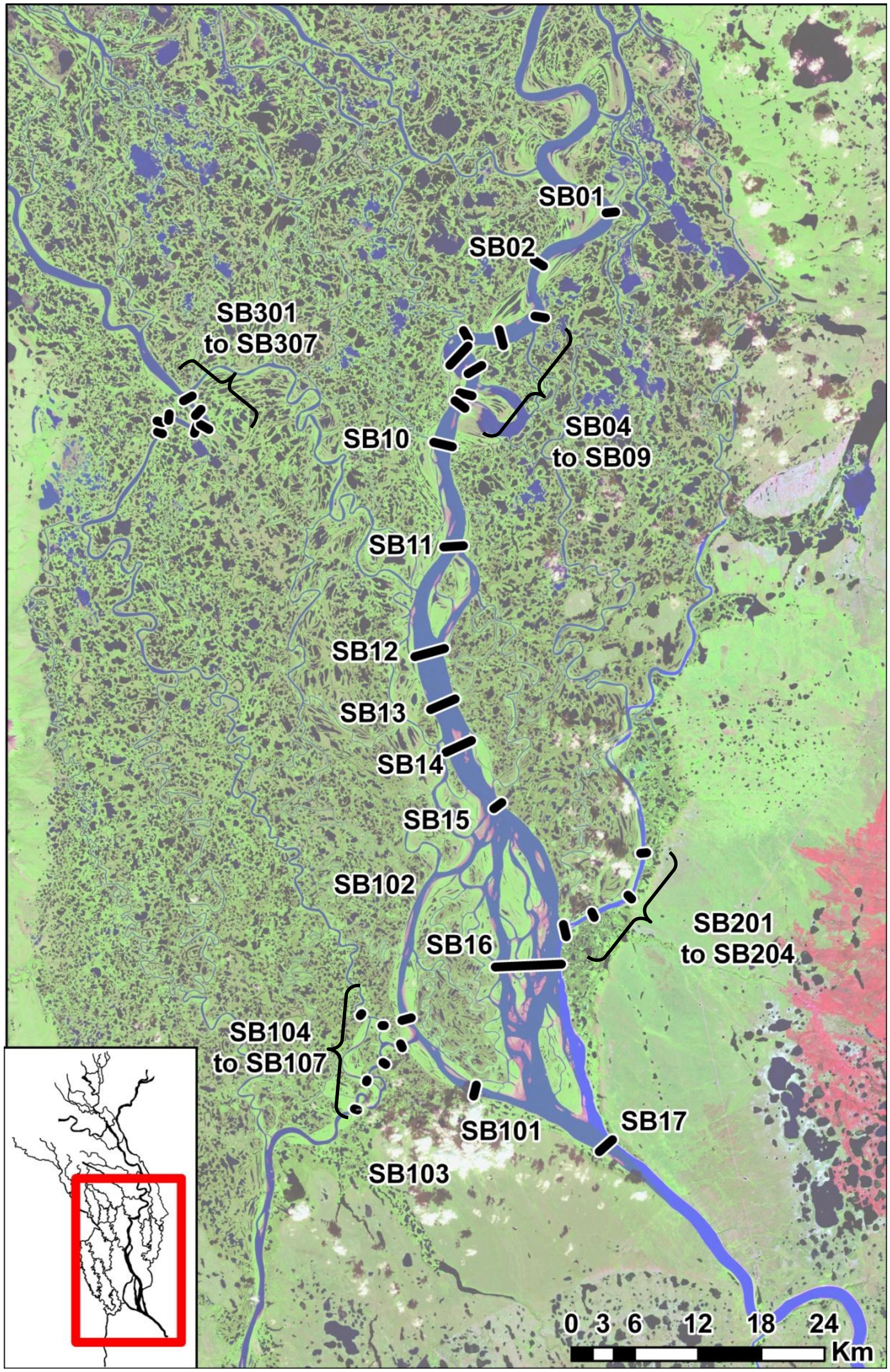

Figure 4.1 Location of cross-section measured in 2007 and 2008.
(Data source: Environment Canada).

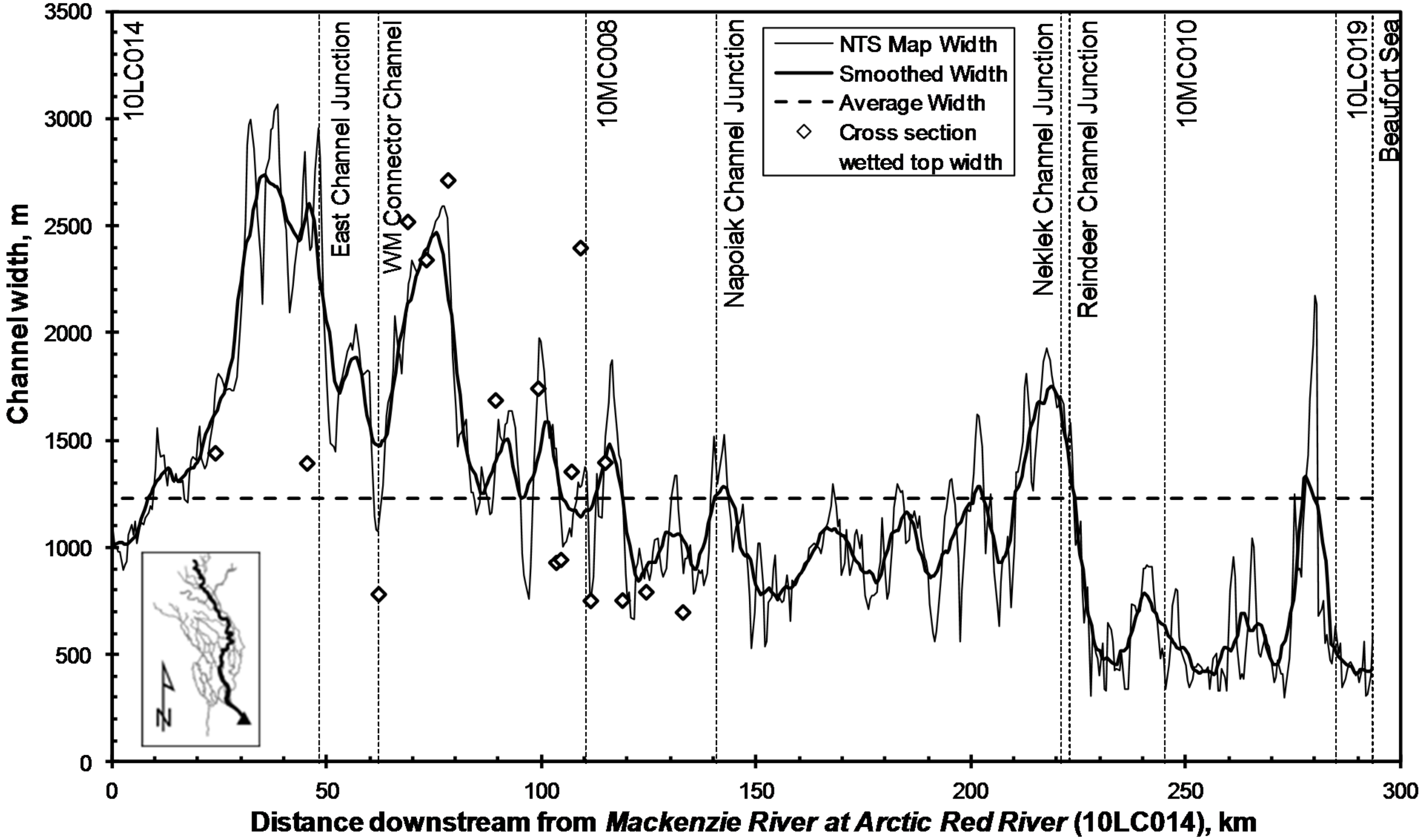

Figure 4.2 Smoothed and un-smoothed top widths of the Middle Channel of the Mackenzie Delta. (Data Source: Env. Canada).

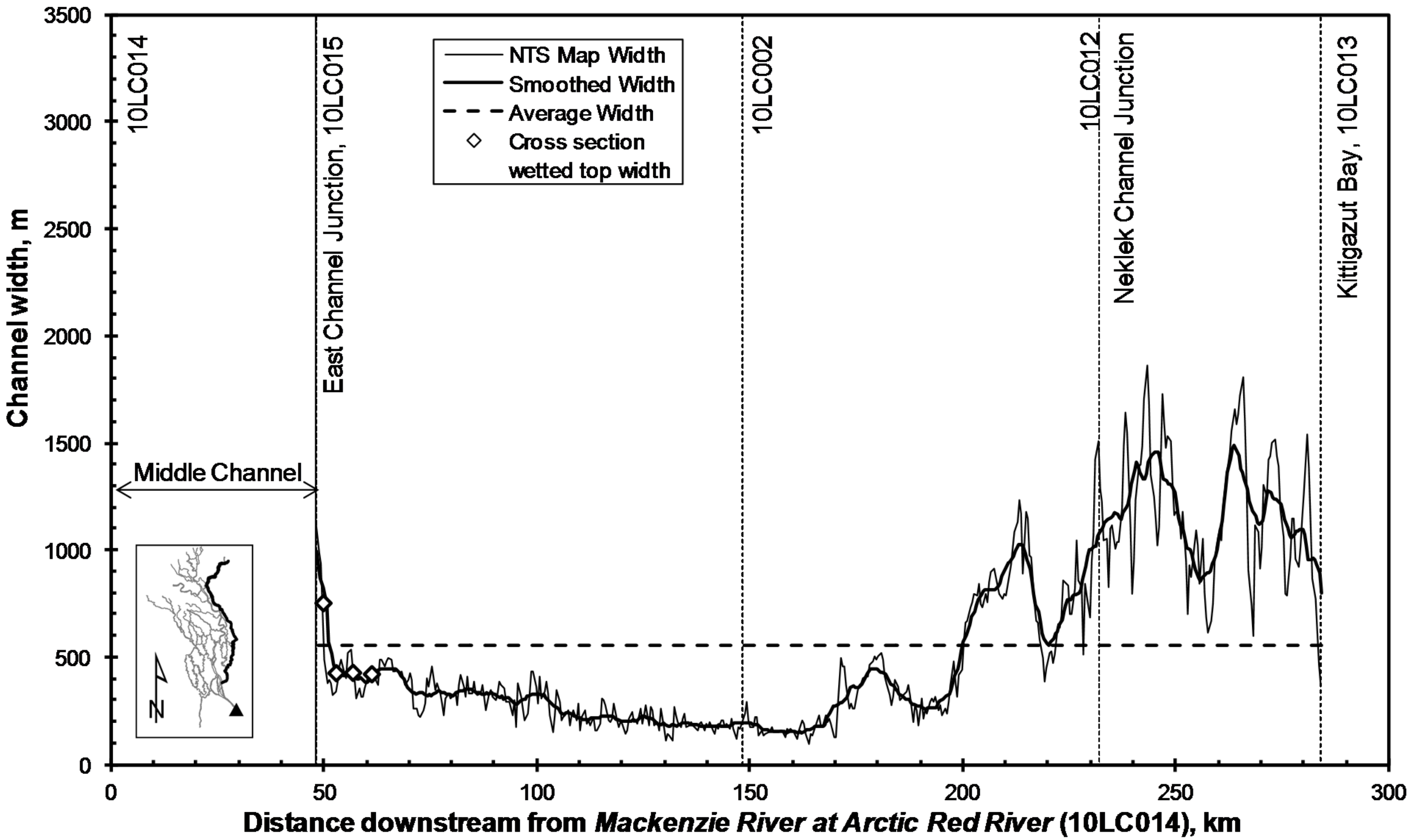

Figure 4.3 Smoothed and un-smoothed top widths of the East Channel of the Mackenzie Delta. (Data Source: Env. Canada).

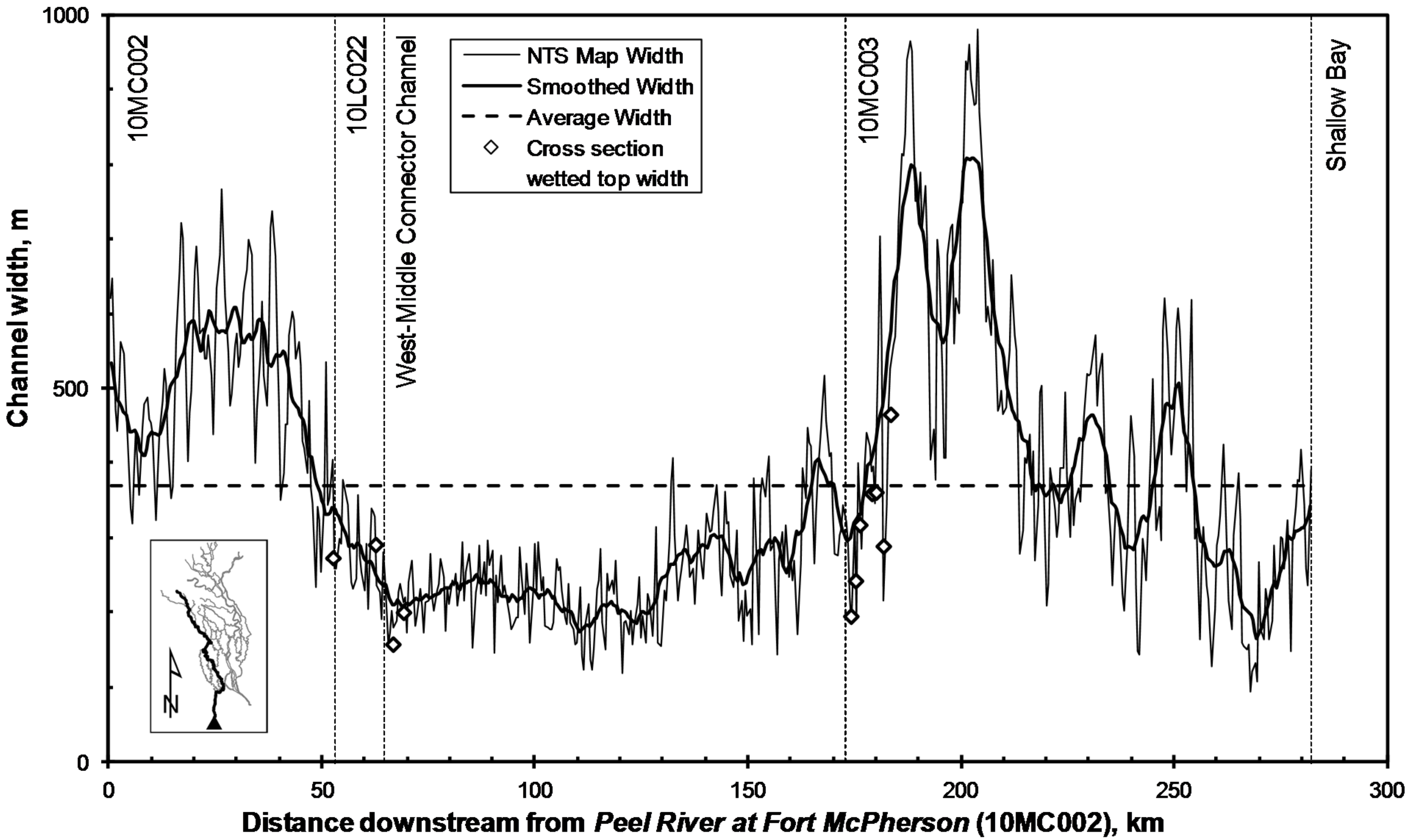

Figure 4.4 Smoothed and un-smoothed top widths of the West Channel of the Mackenzie Delta. (Data Source: Env. Canada).

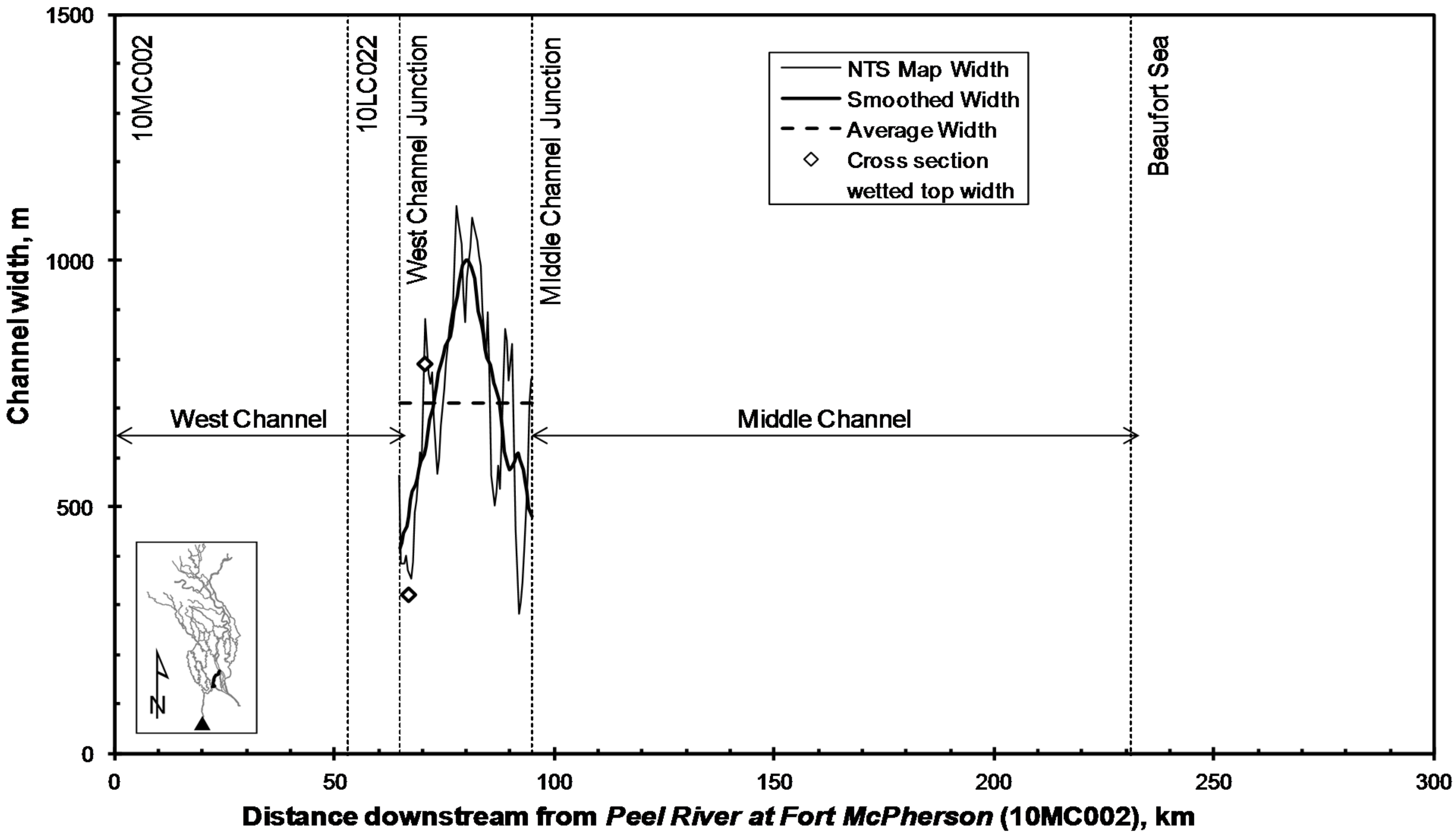

Figure 4.5 Smoothed and un-smoothed top widths of the West-Middle Connector Channel of the Mackenzie Delta. (Data Source: Env. Canada).

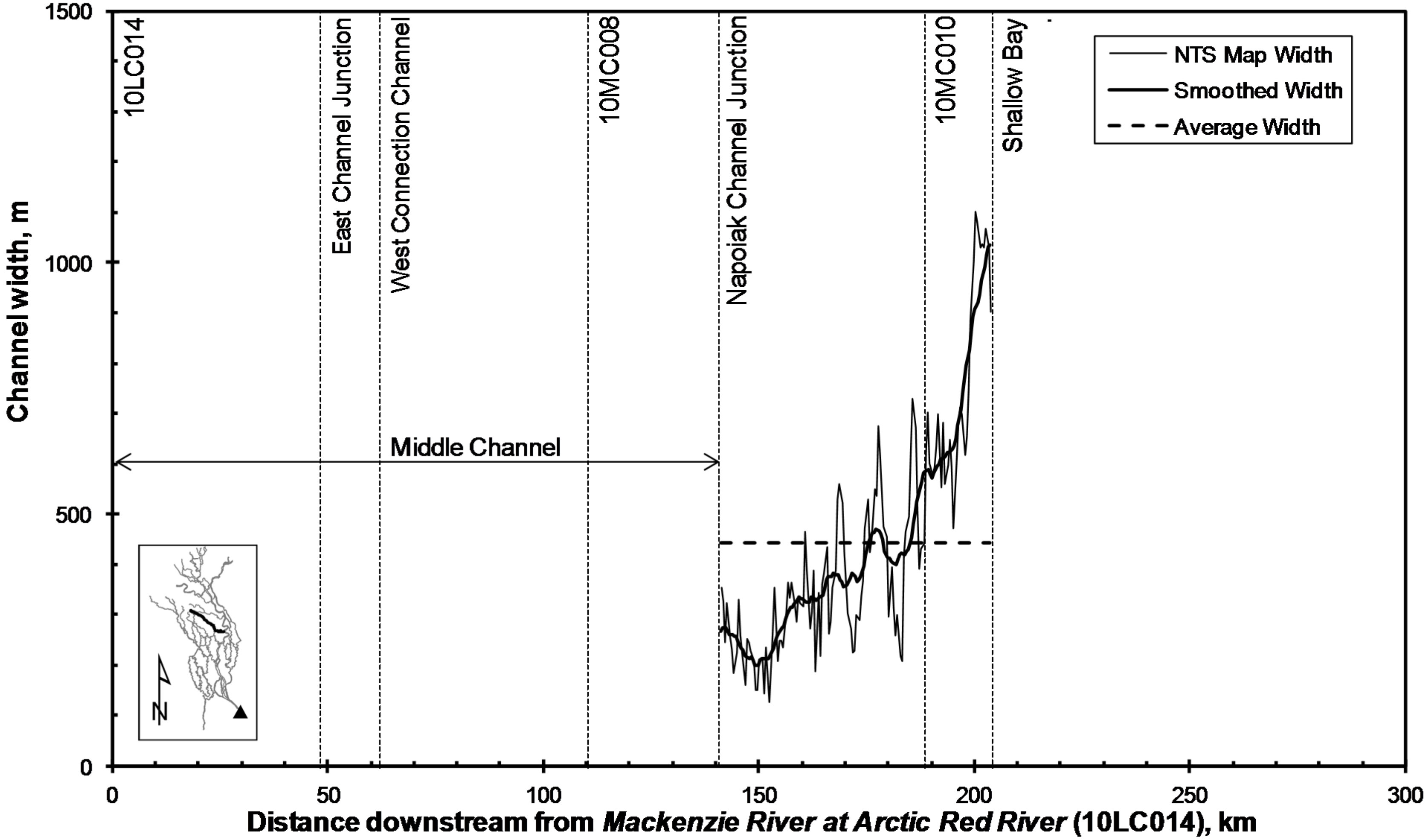

Figure 4.6 Smoothed and un-smoothed top widths of the Napoiak Channel of the Mackenzie Delta. (Data Source: Env. Canada).

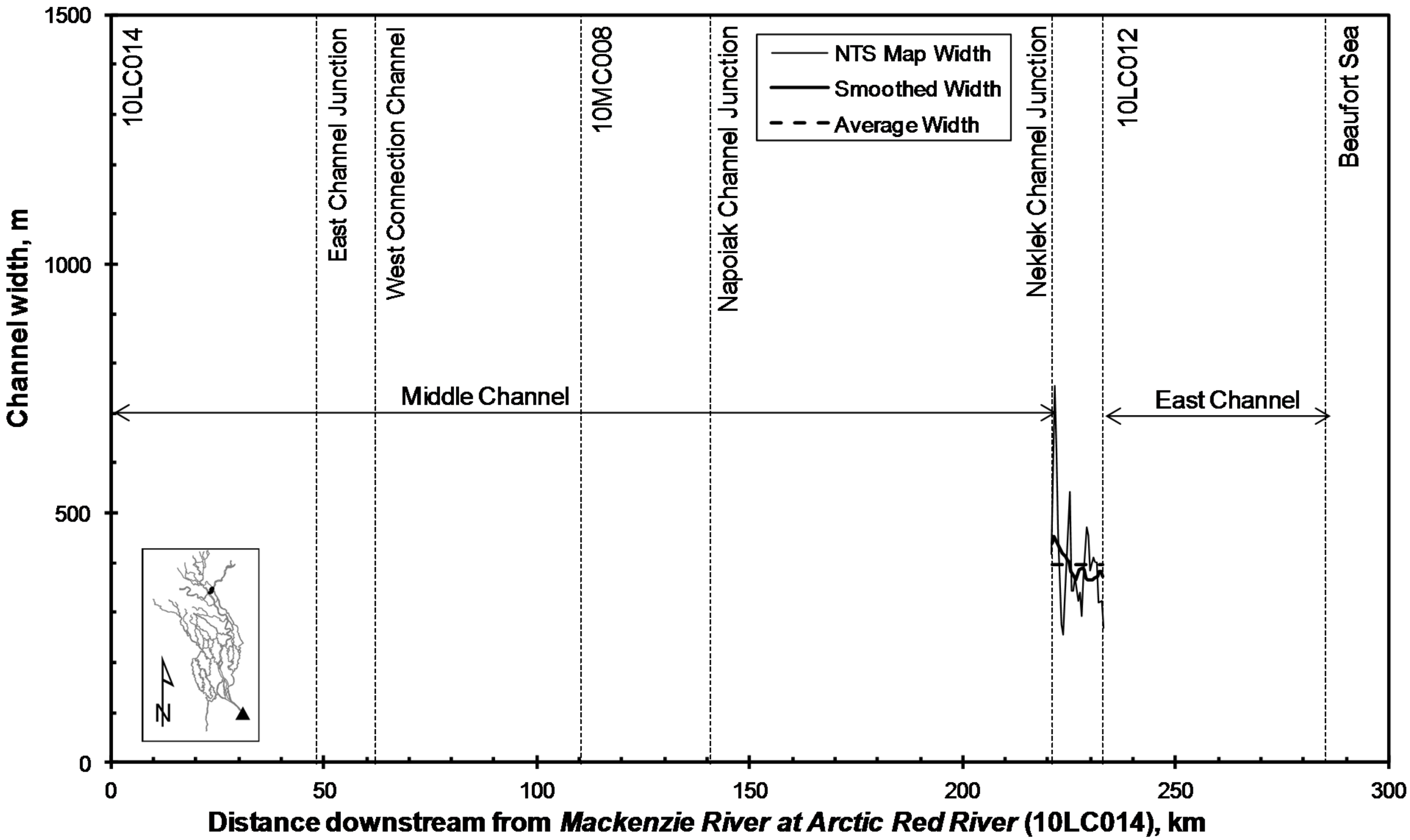

Figure 4.7 Smoothed and un-smoothed top widths of the Neklek Channel of the Mackenzie Delta. (Data Source: Env. Canada).

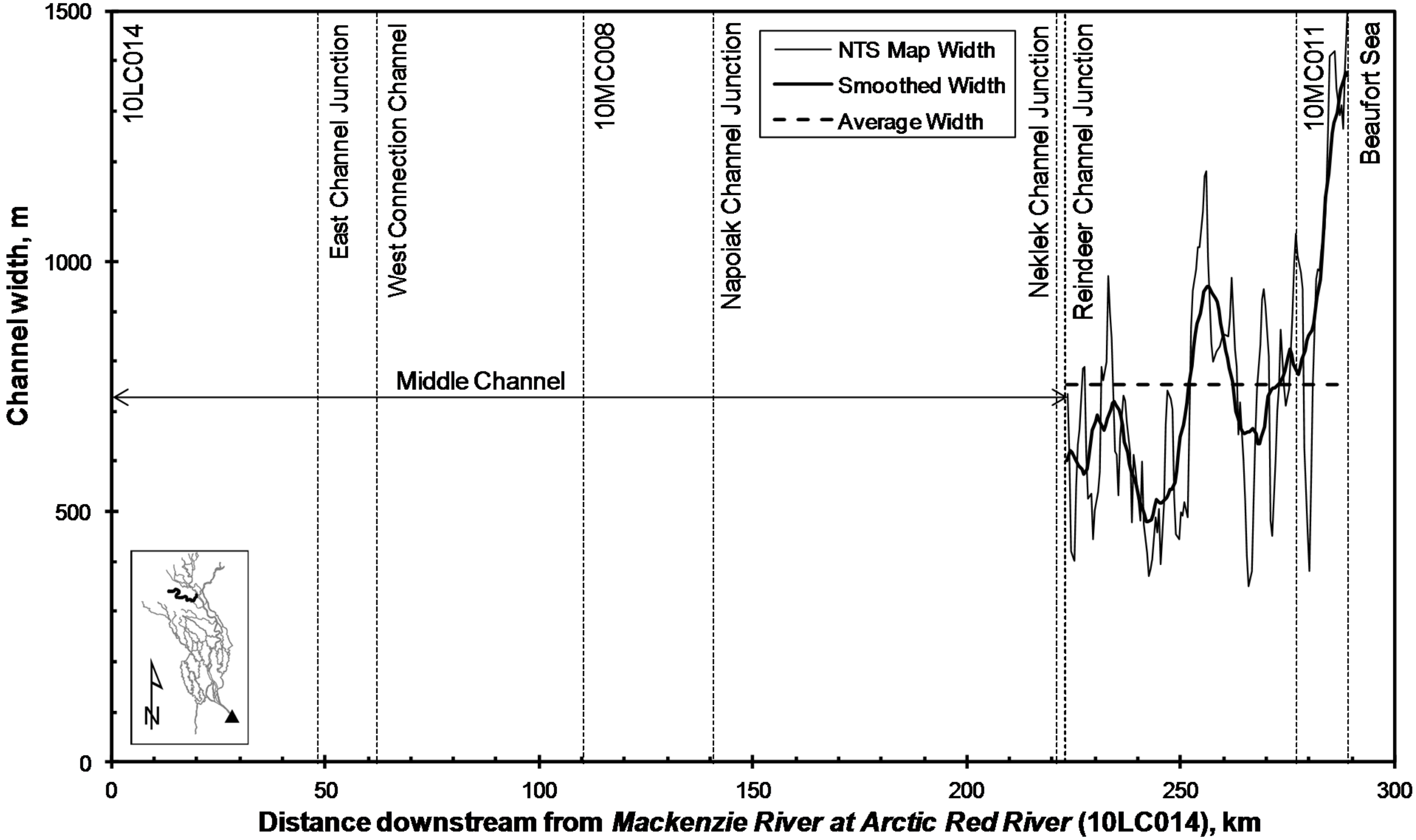

Figure 4.8 Smoothed and un-smoothed top widths of the Reindeer Channel of the Mackenzie Delta. (Data Source: Env. Canada).

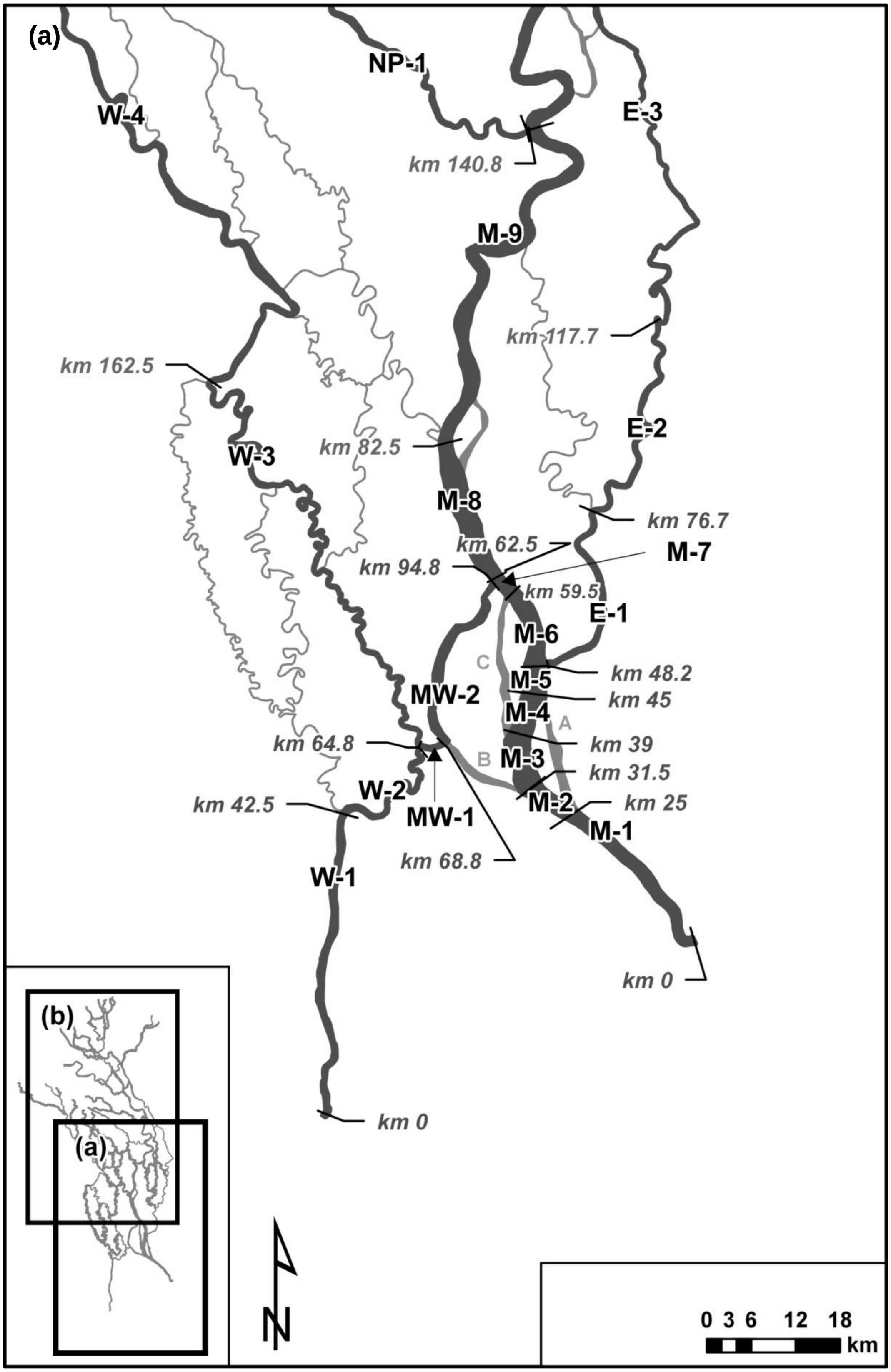

Figure 4.9 Flow change locations and reach names for the primary channels in the (a) upper Delta and (b) lower Delta.

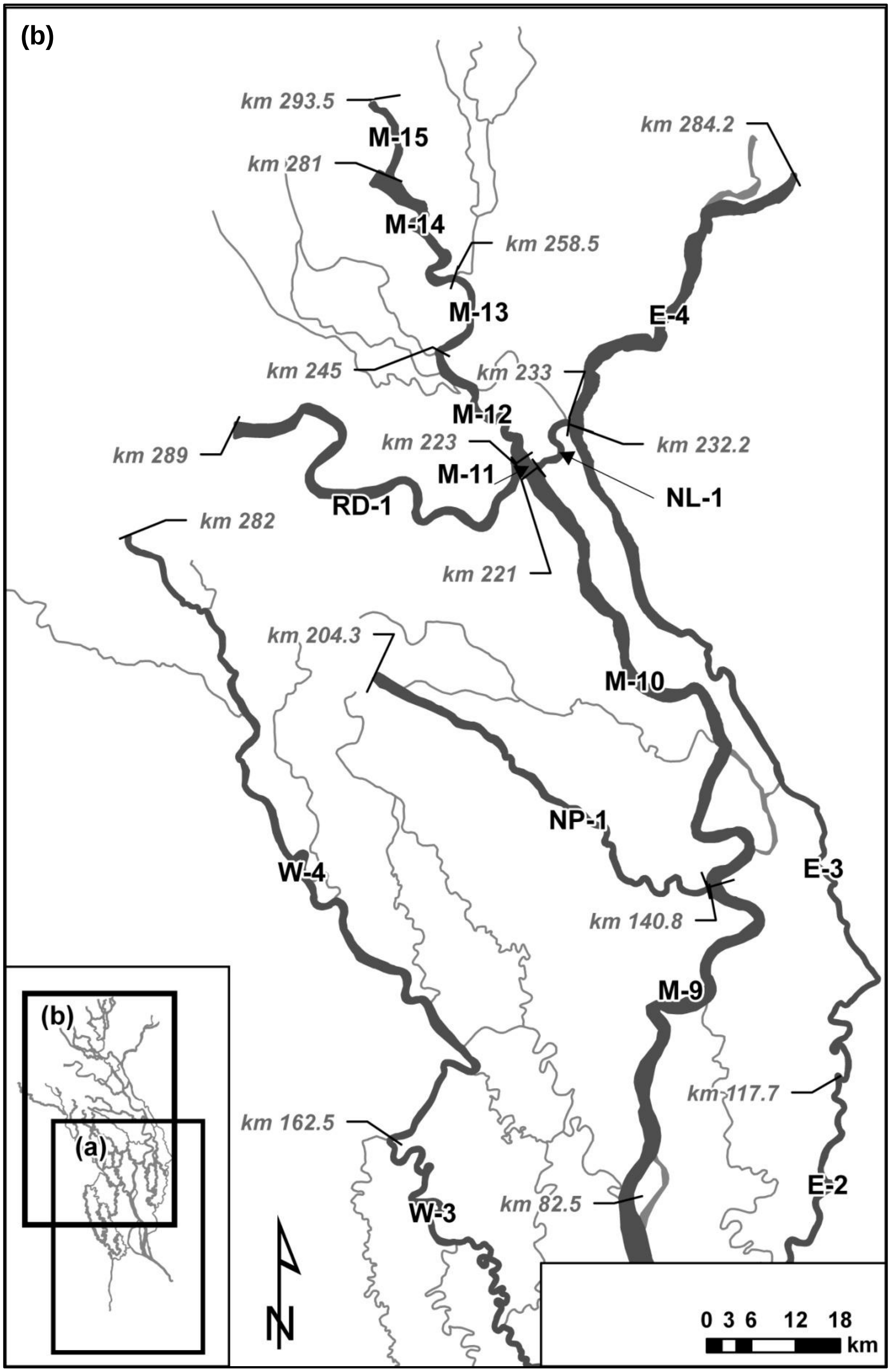

Figure 4.9 continued Flow change locations and reach names for the primary channels in the (a) upper Delta and (b) lower Delta.

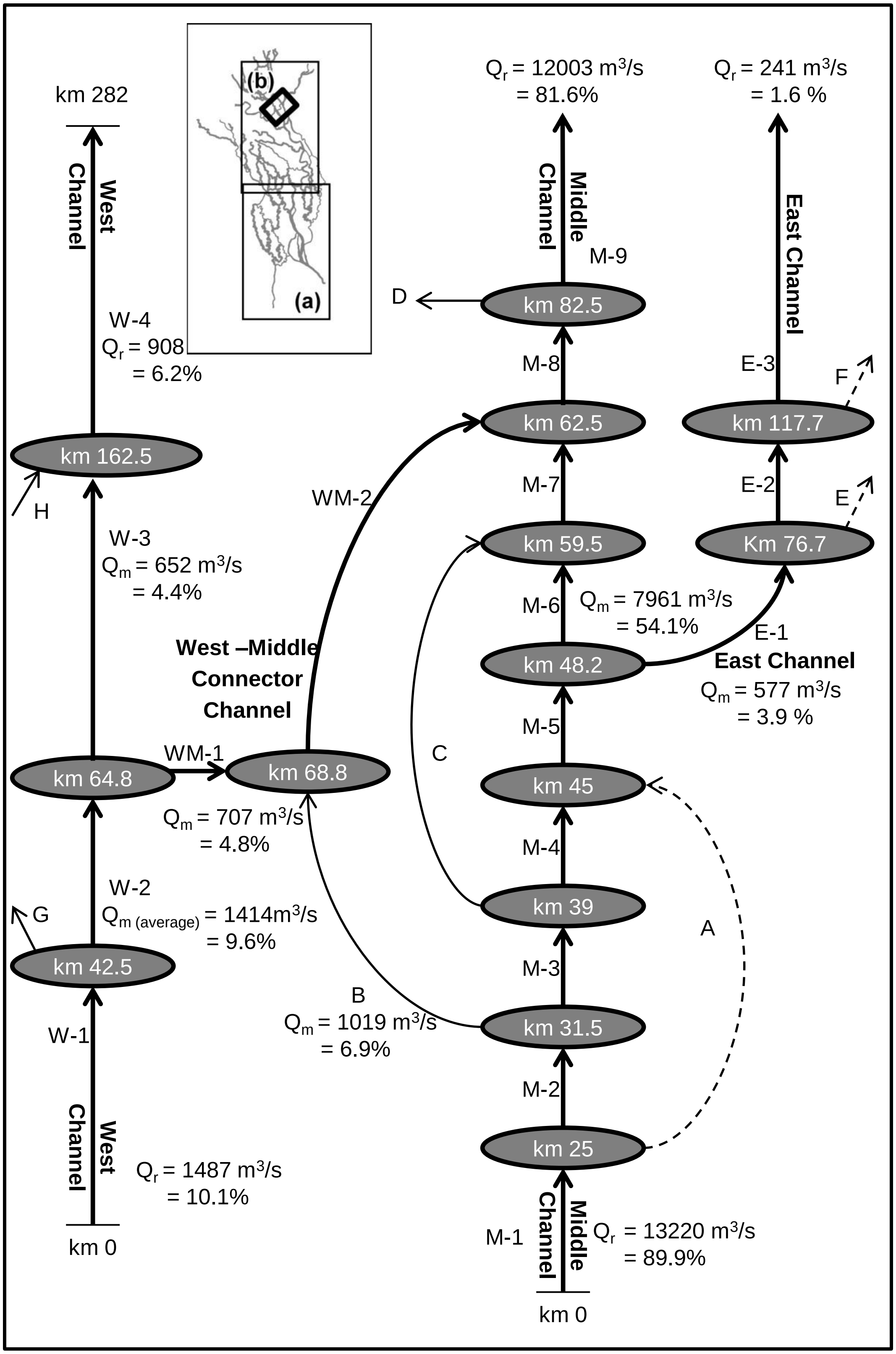

Figure 4.10 Nodal diagram of flow for the Calibration Scenario from 2-Aug-08 to 12-Aug-08 for (a) the upper delta and (b) the lower delta. (Data source: the WSC).

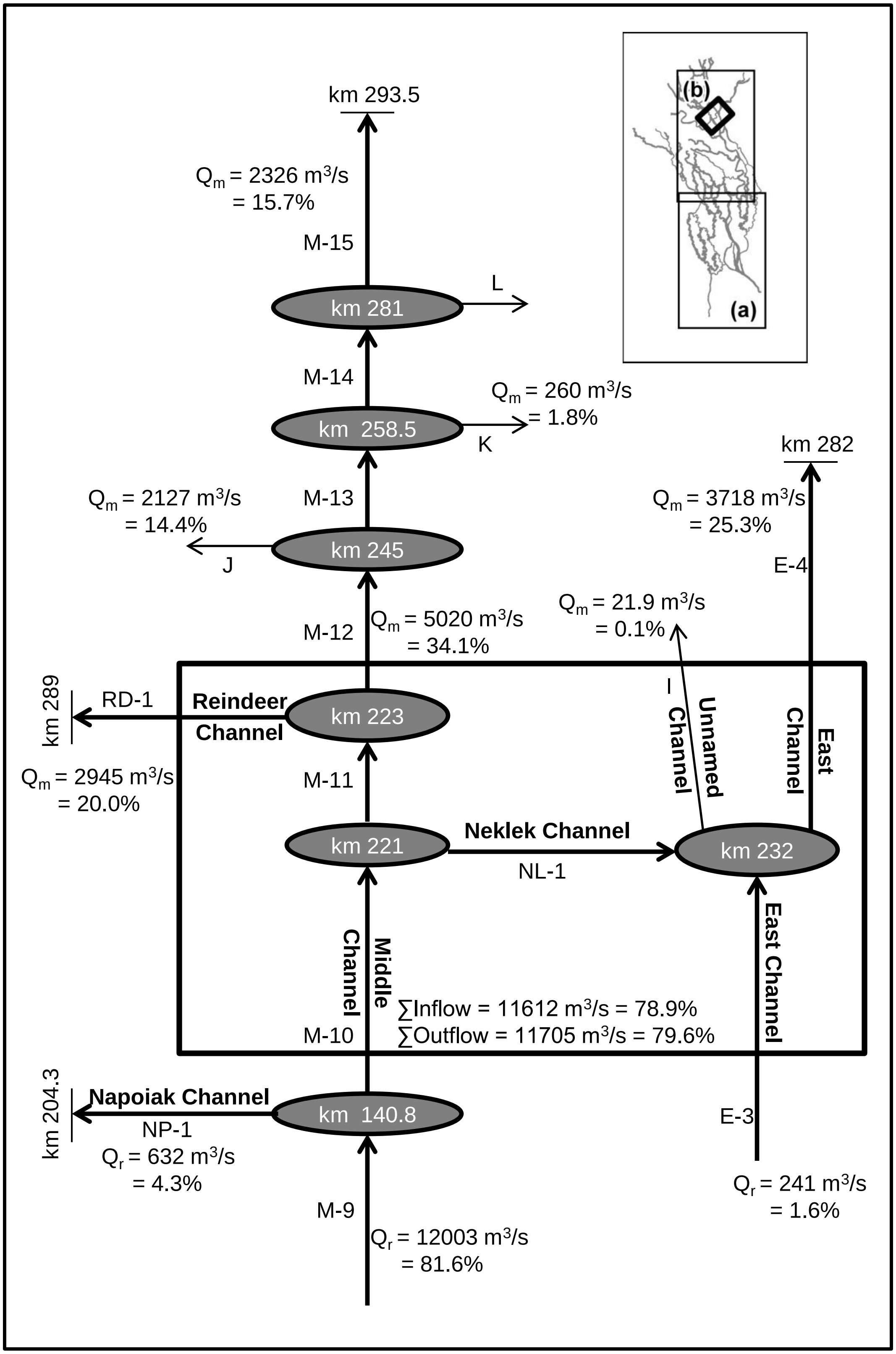

Figure 4.10 continued — Nodal diagram of flow for the Calibration Scenario from 2-Aug-08 to 12-Aug-08 for (a) the upper delta and (b) the lower delta. (Data source: the WSC).

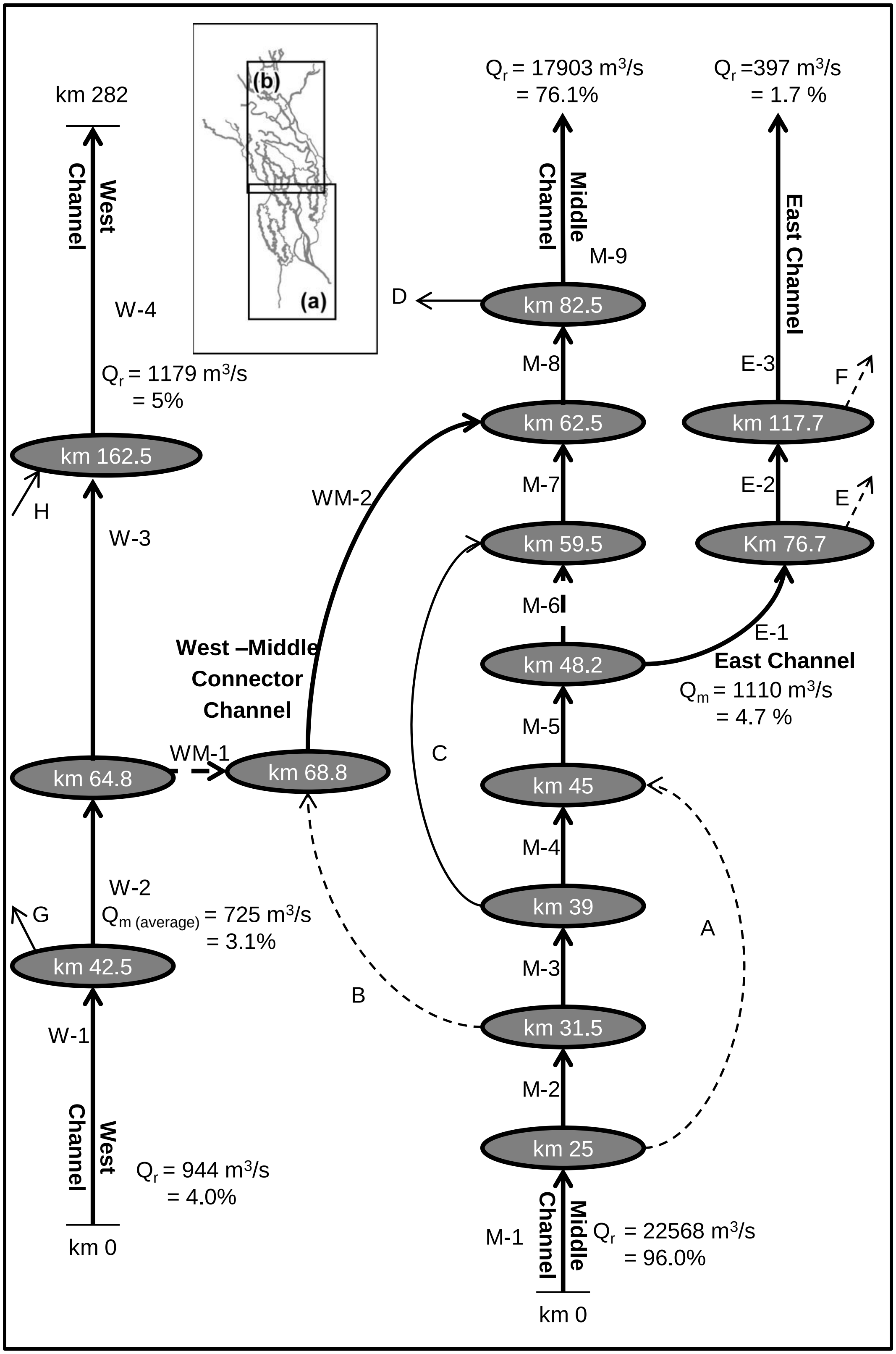

Figure 4.11 Nodal diagram of flow for Validation Scenario #1 from 14-Jun-07 to 20-Jun-07 for (a) the upper delta and (b) the lower delta. (Data source: the WSC).

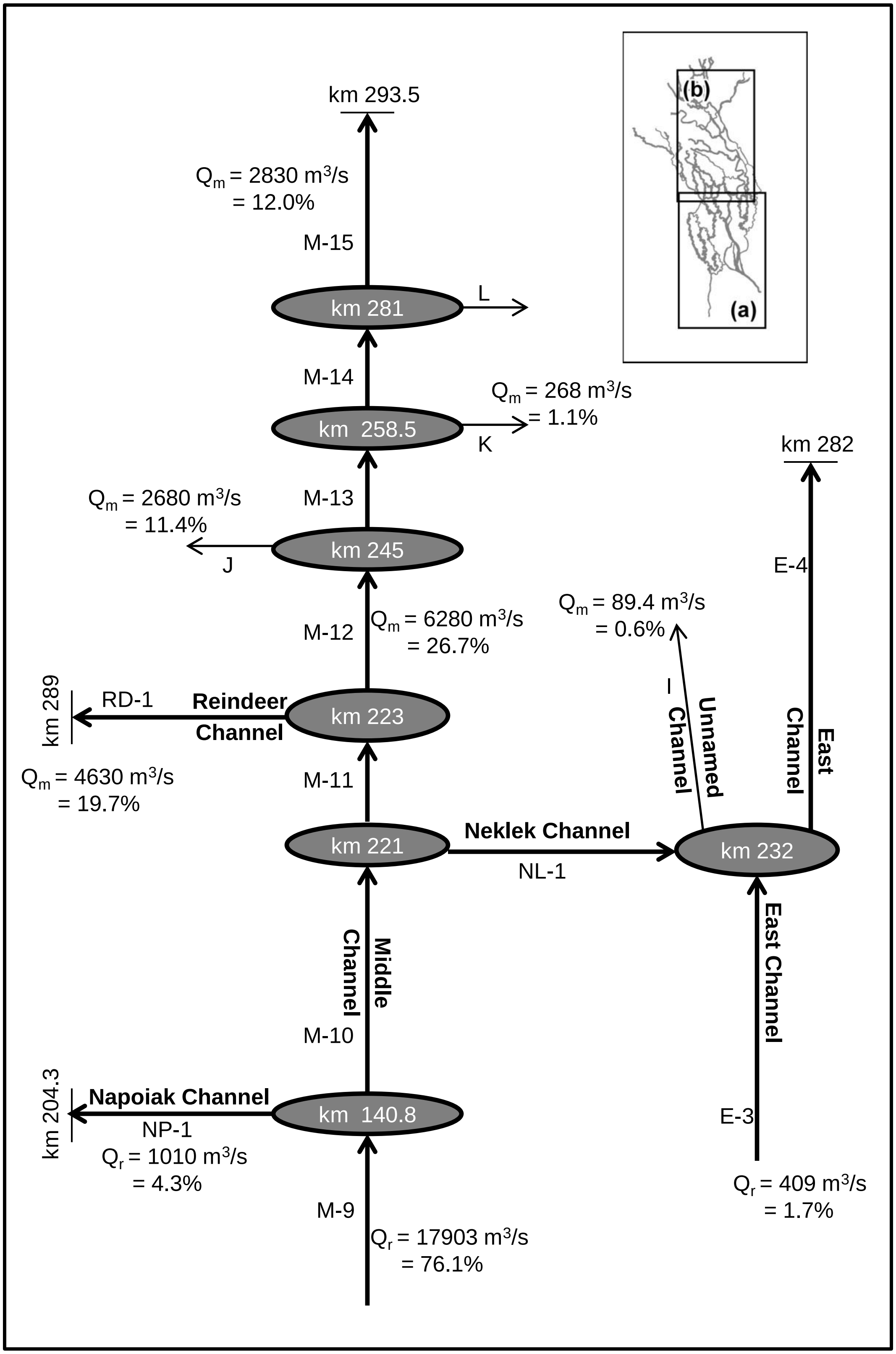

Figure 4.11 continued Nodal diagram of flow for Validation Scenario #1 from 14-Jun-07 to 20-Jun-07 for (a) the upper delta and (b) the lower delta. (Data source: the WSC).

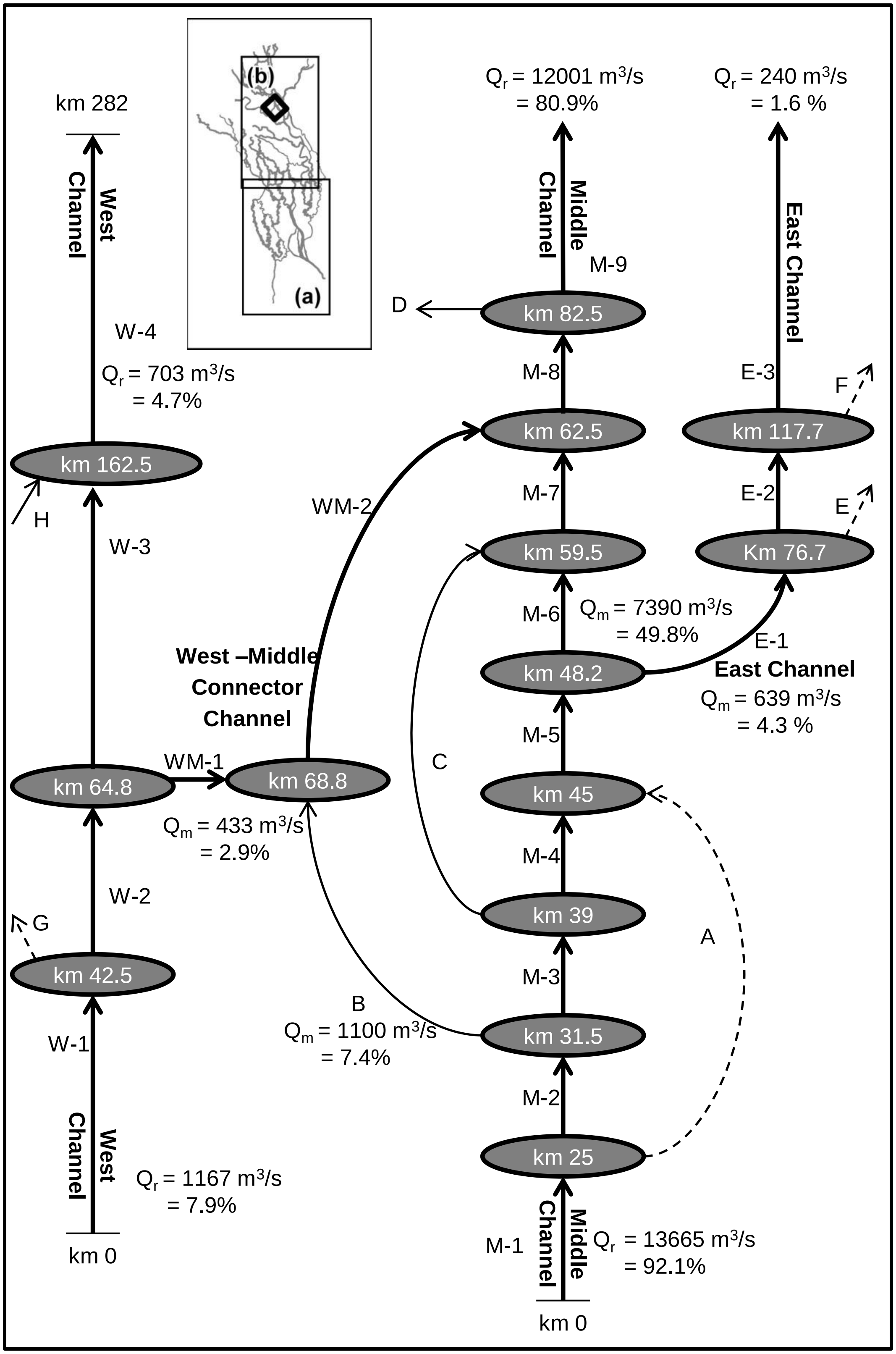

Figure 4.12 Nodal diagram of flow for Validation Scenario #2 from 4-Sept-09 to 20-Sep-09 for (a) the upper delta and (b) the lower delta. (Data source: the WSC).

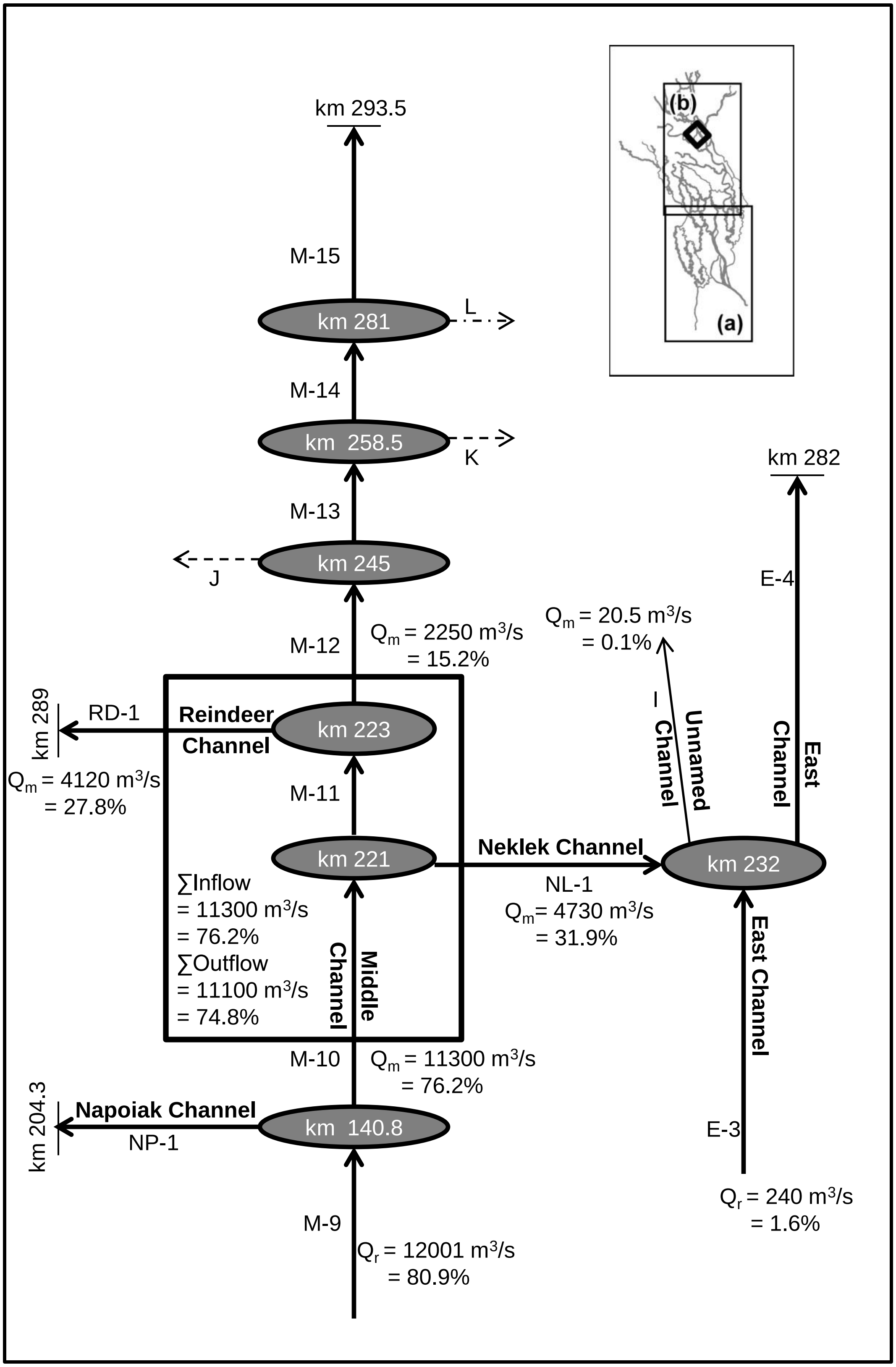

Figure 4.12 continued — Nodal diagram of flow for Validation Scenario #2 from 4-Sept-09 to 20-Sep-09 for (a) the upper delta and (b) the lower delta. (Data source: the WSC).

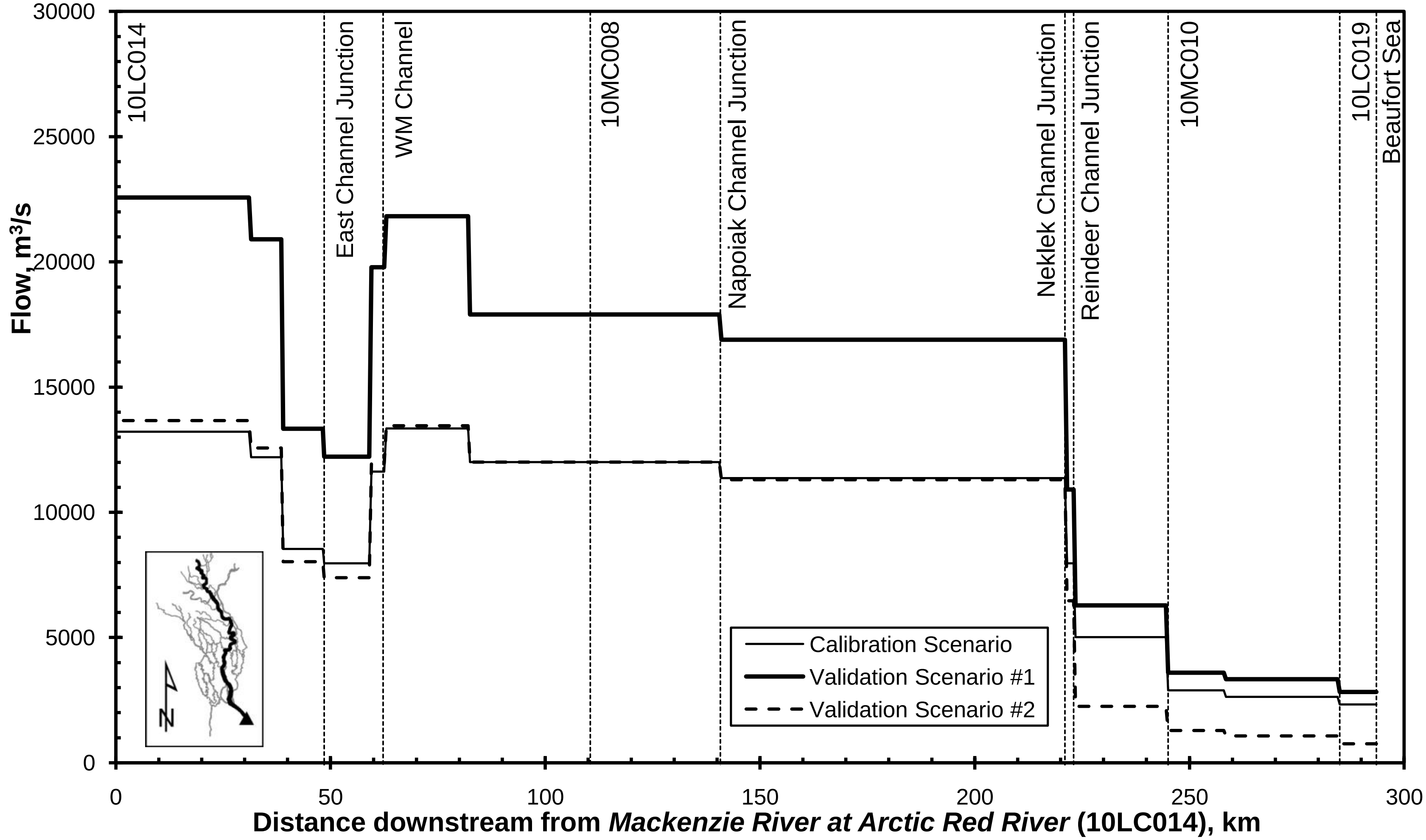

Figure 4.13 Flows used as model input for the Middle Channel for the calibration and validation periods.

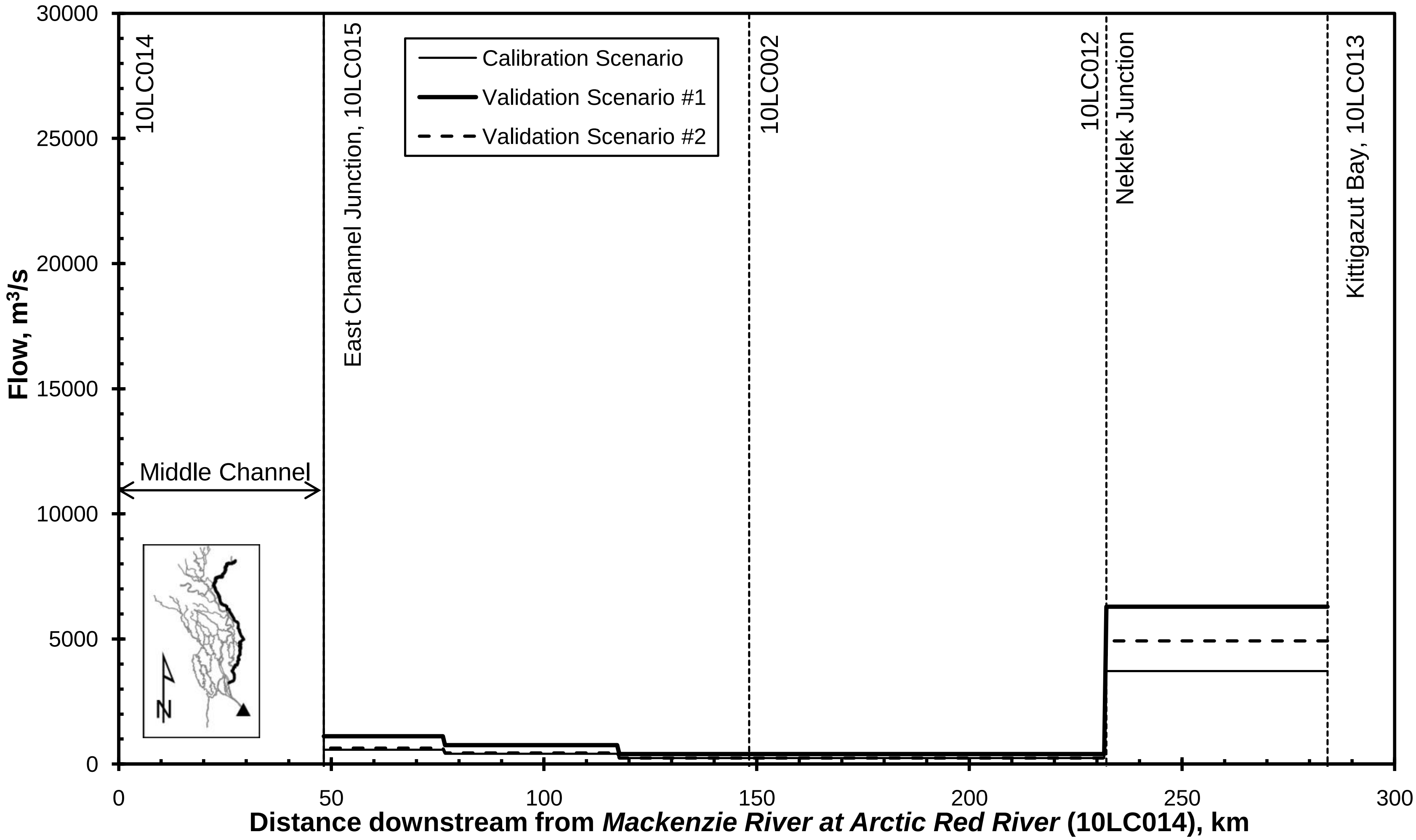

Figure 4.14 Flows used as model input for the East Channel for the calibration and validation periods.

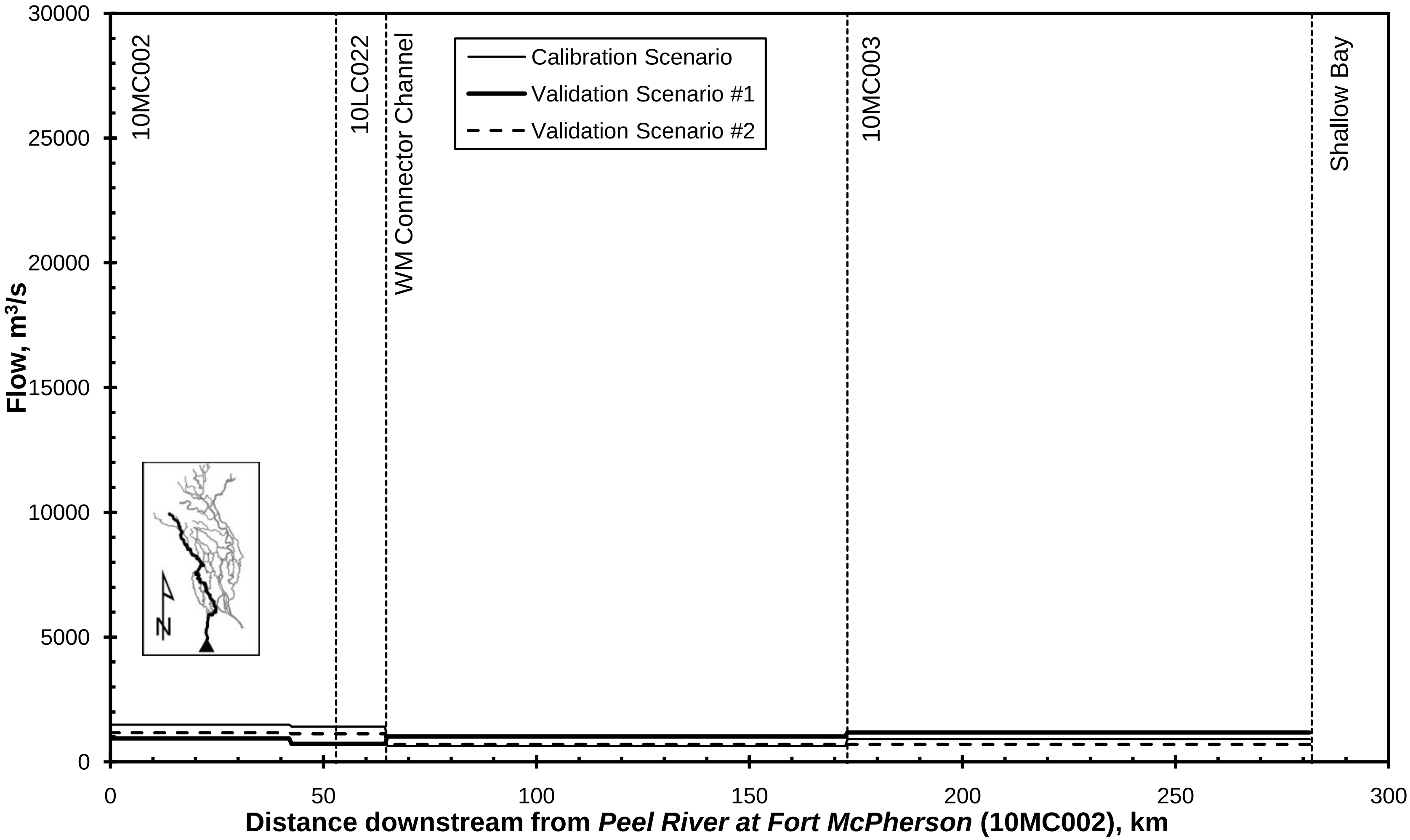

Figure 4.15 Flows used as model input for the West Channel for the calibration and validation periods.

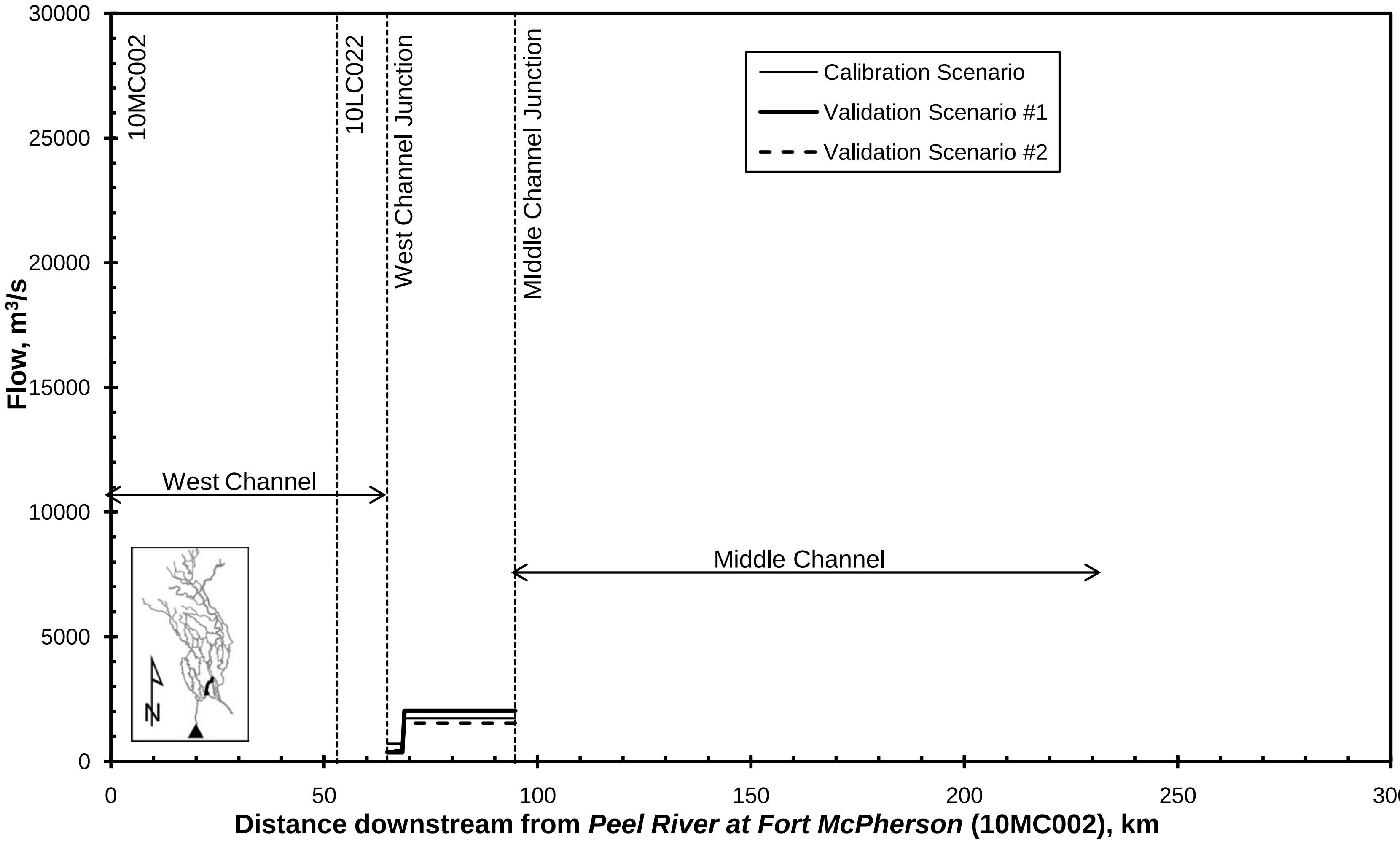

Figure 4.16 Flows used as model input for the West-Middle Connector Channel for the calibration and validation periods.

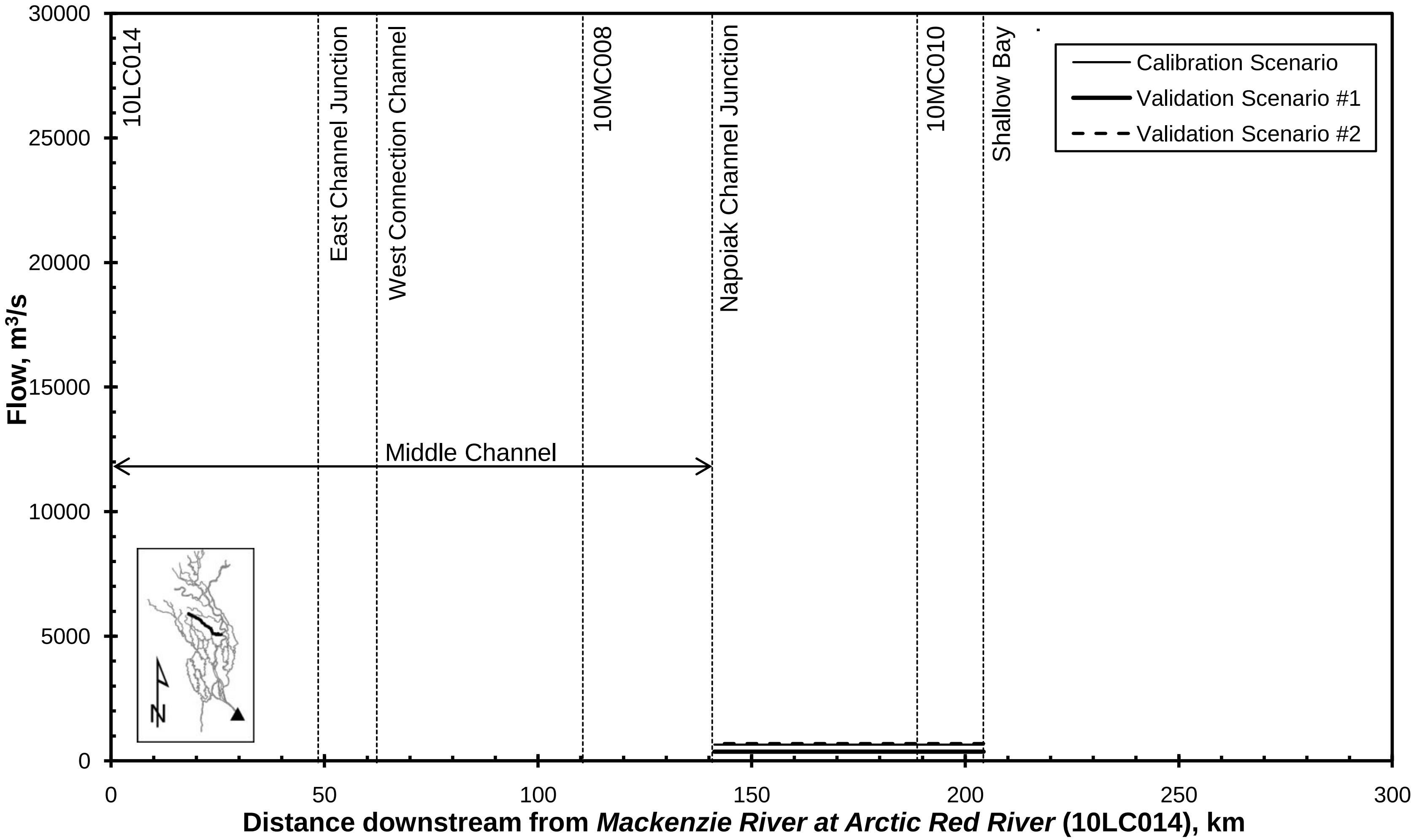

Figure 4.17 Flows used as model input for the Napoiak Channel for the calibration and validation periods.

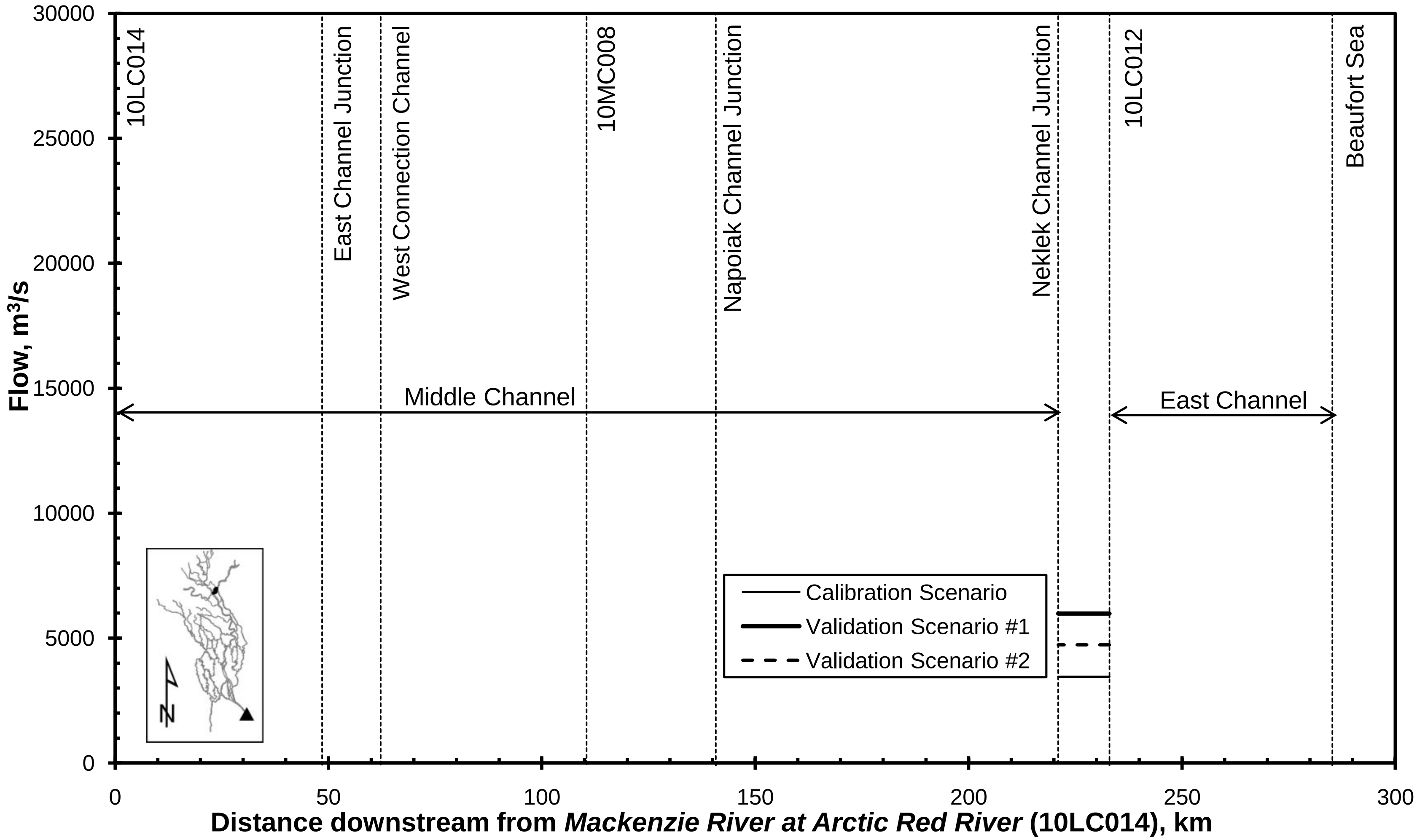

Figure 4.18 Flows used as model input for the Neklek Channel for the calibration and validation periods.

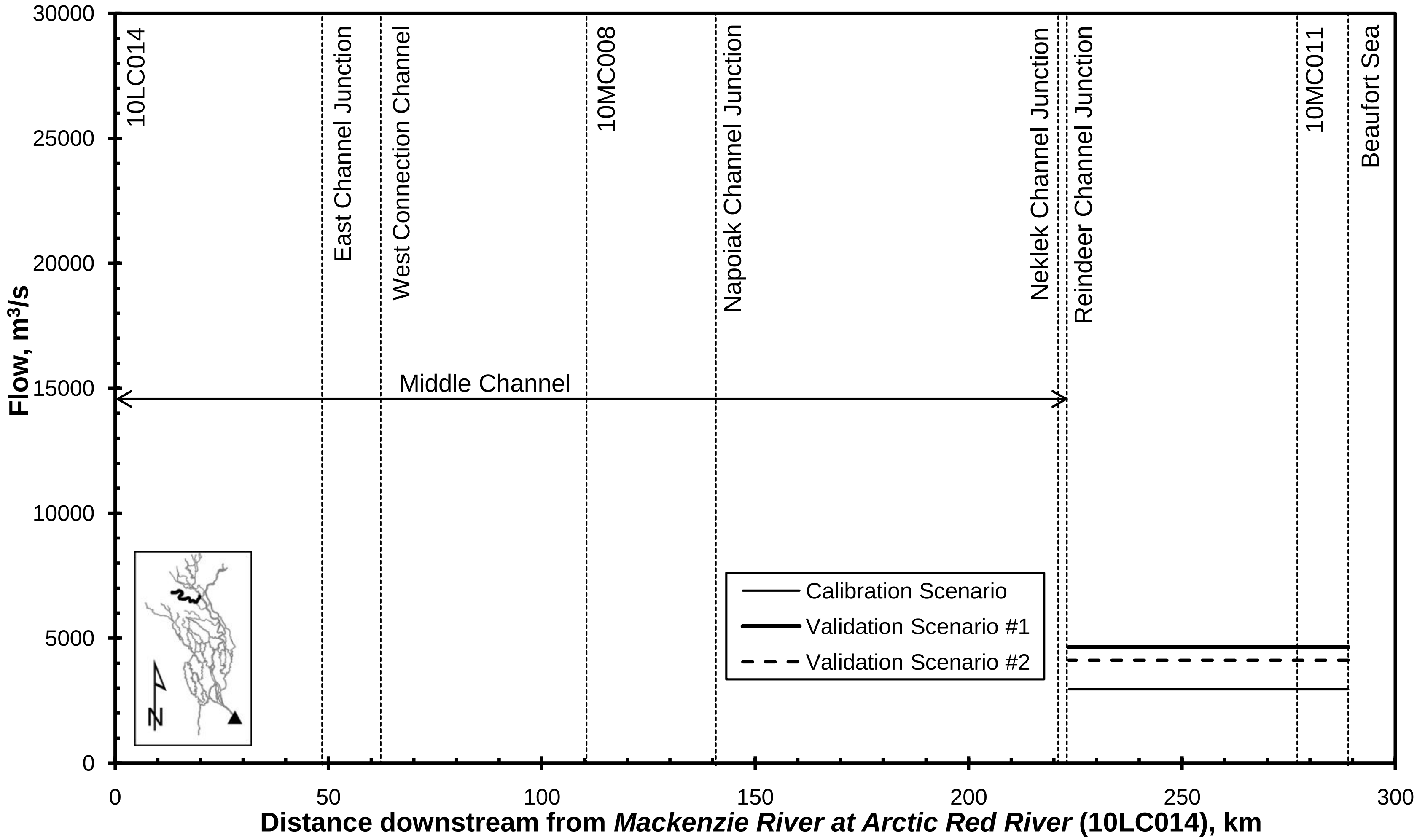

Figure 4.19 Flows used as model input for the Reindeer Channel for the calibration and validation periods.

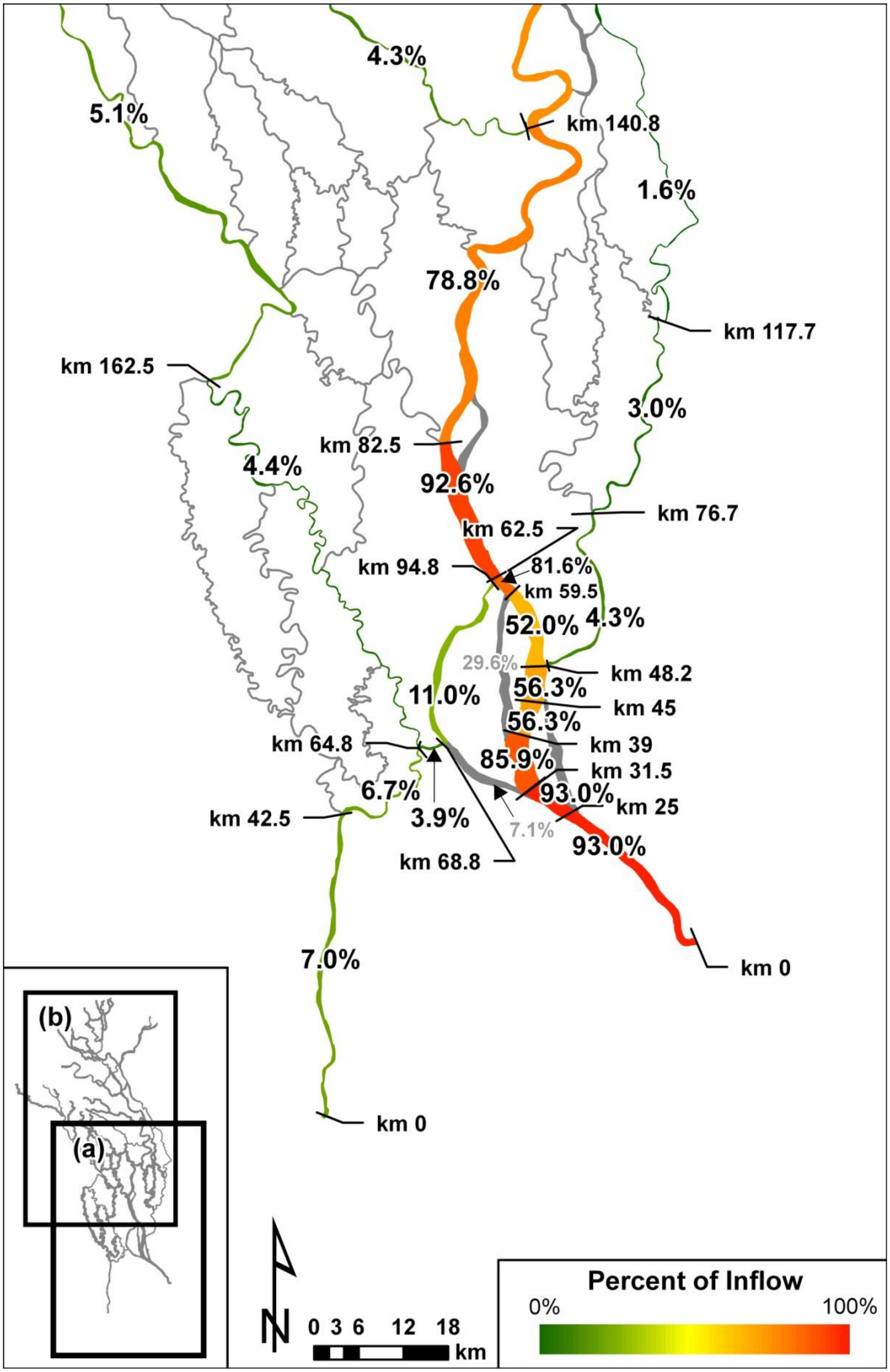

Figure 4.20 Average percent of inflow during open water conditions along each reach of the primary channels in (a) the upper Delta and (b) the lower Delta. (Data source: the WSC).

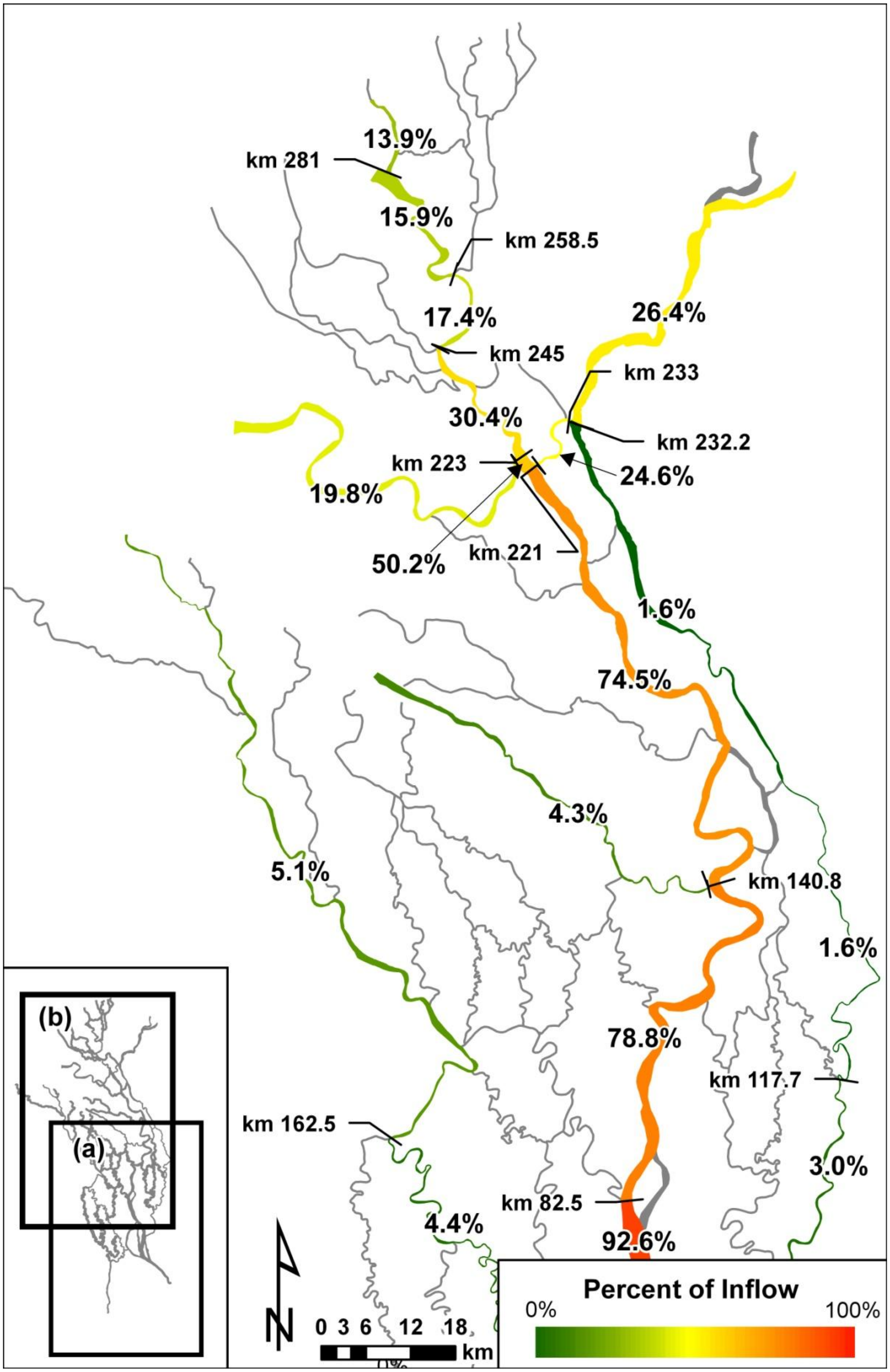

Figure 4.20 continued Average percent of inflow during open water conditions along each reach of the primary channels in (a) the upper Delta and (b) the lower Delta.(Data source: the WSC).

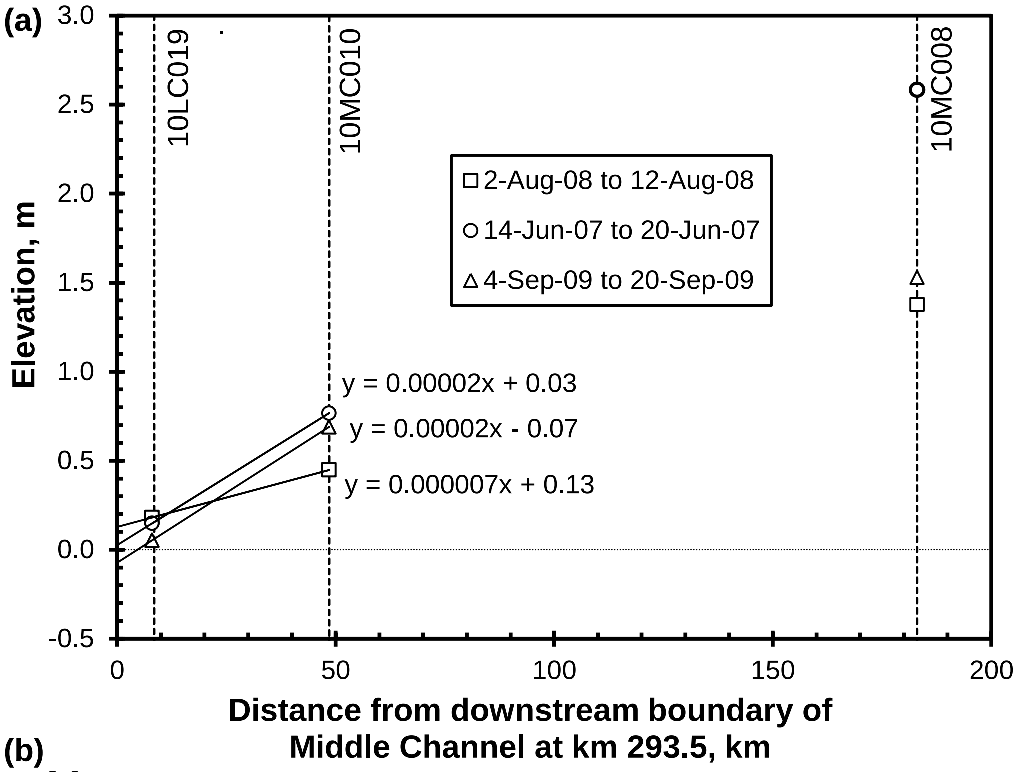

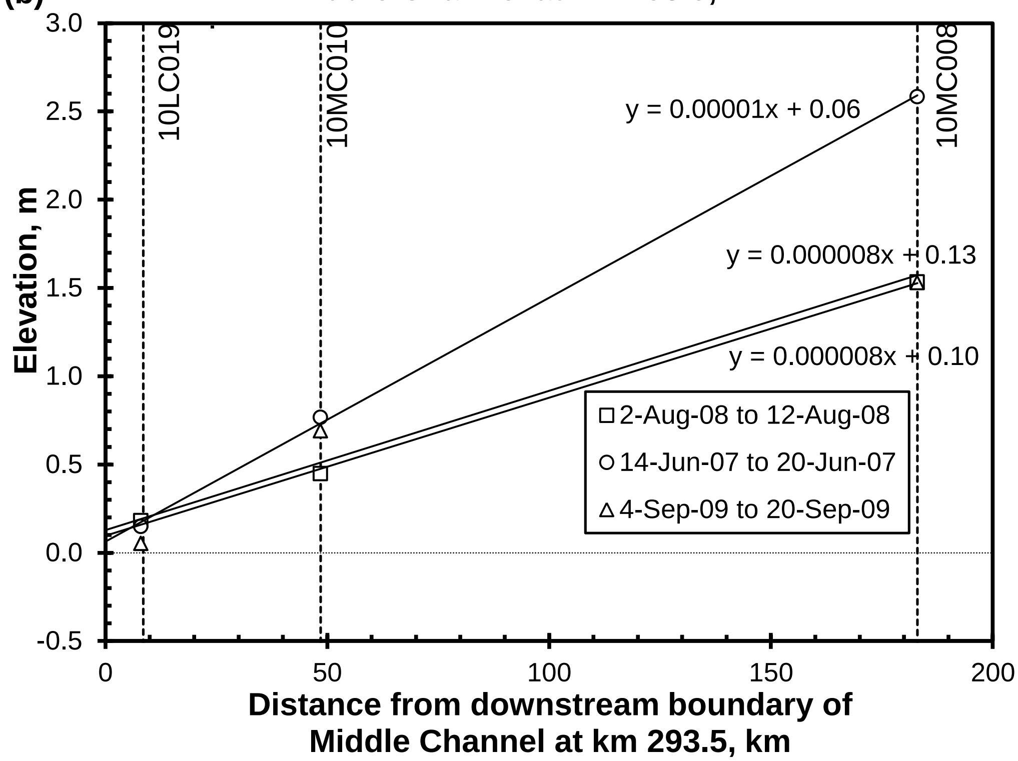

Figure 4.21 Extrapolation of downstream boundary condition for the Middle Channel of the Mackenzie Delta using (a) water levels recorded at three downstream gauge stations and (b) water levels recorded at two downstream gauge stations. (Data source: the WSC).

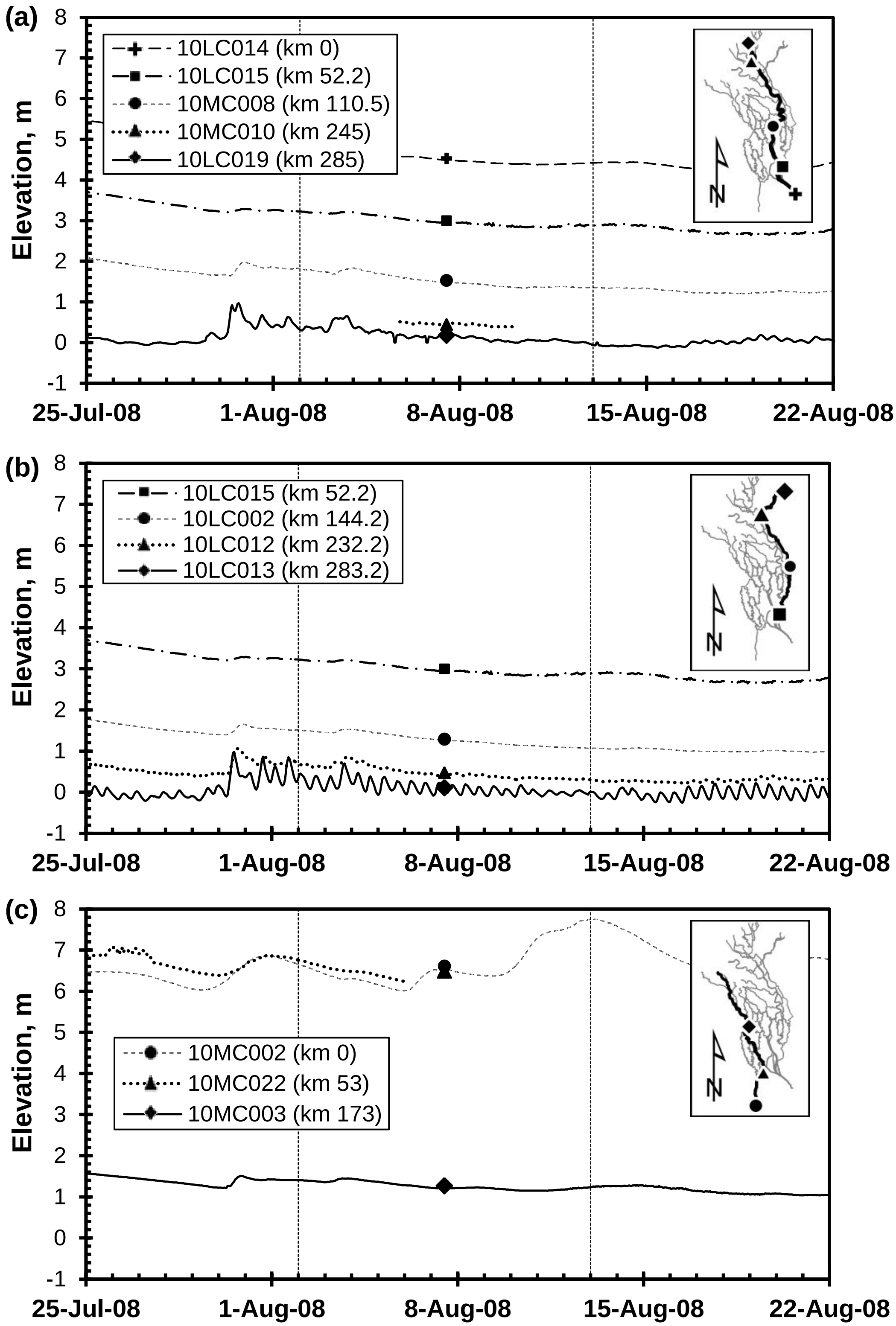

Figure 4.22 Water levels at gauges along the (a) Middle Channel (b) East Channel (c) West Channel (d) Napoiak Channel and (e) Reindeer Channel for the Calibration Scenario. (Data source: the WSC).

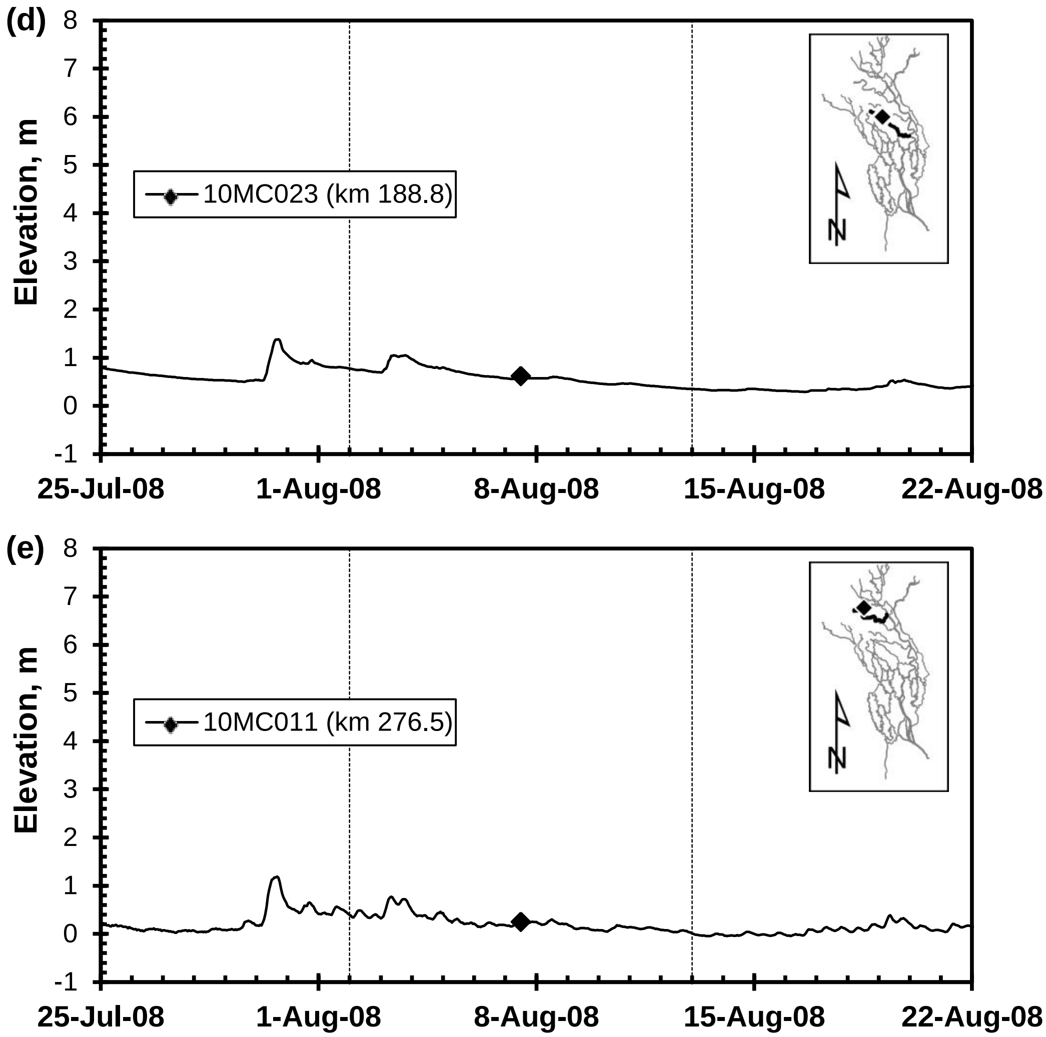

Figure 4.22 continued Water levels at gauges along the (a) Middle Channel (b) East Channel (c) West Channel (d) Napoiak Channel and (e) Reindeer Channel the Calibration Scenario.
(Data source: the WSC).

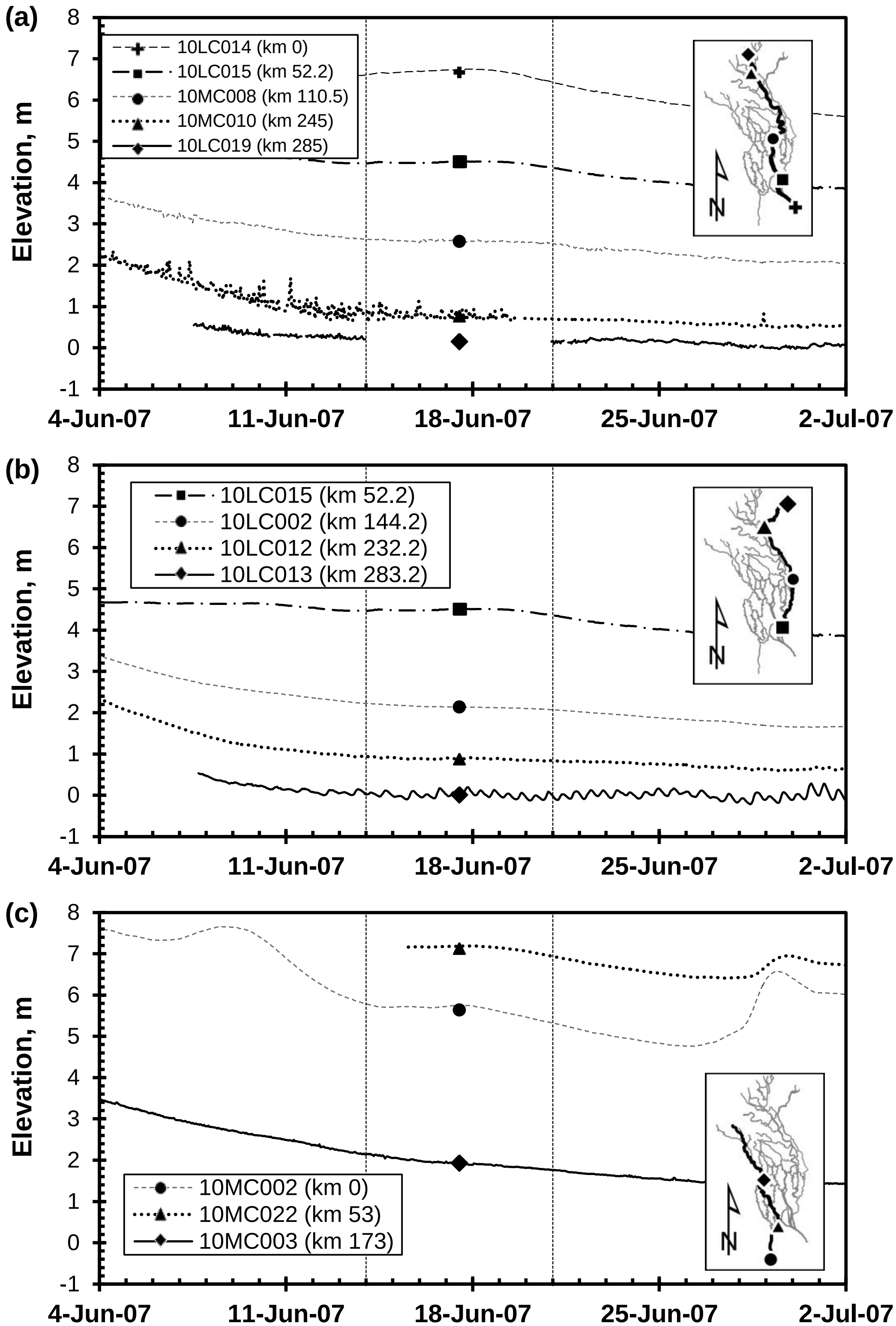

Figure 4.23 Water levels at gauges along the (a) Middle Channel (b) East Channel (c) West Channel (d) Napoiak Channel and (e) Reindeer Channel for Validation Scenario #1. (Data source: the WSC).

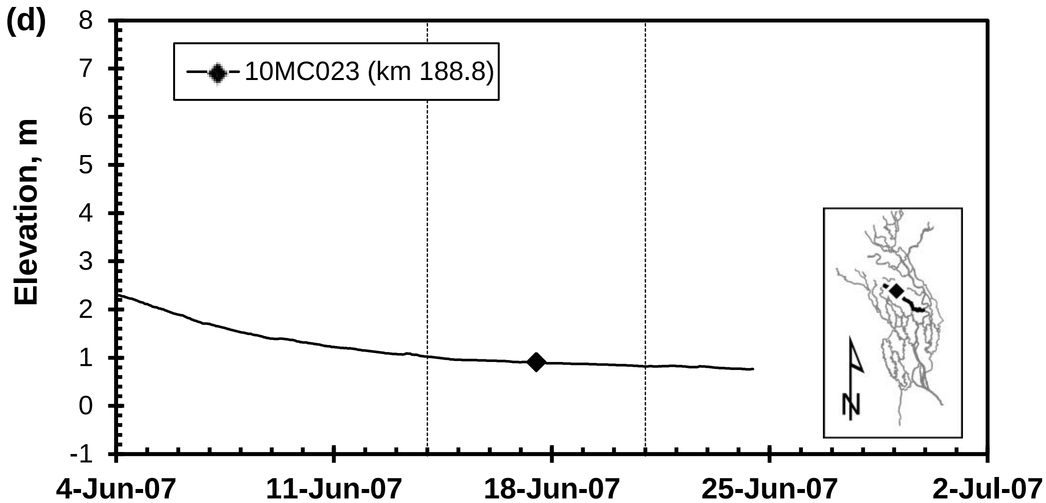

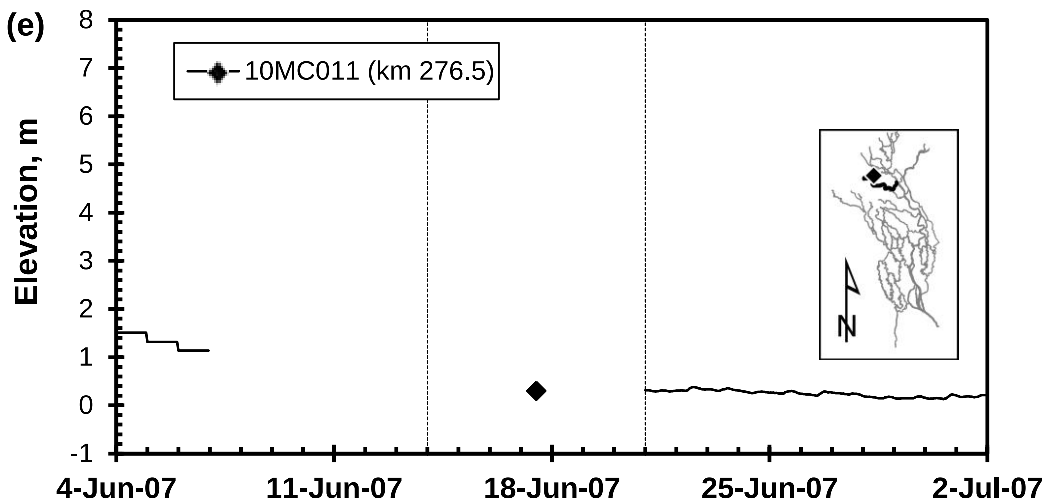

Figure 4.23 continued Water levels at gauges along the (a) Middle Channel (b) East Channel (c) West Channel (d) Napoiak Channel and (e) Reindeer Channel for Validation Scenario #1. (Data source: the WSC).

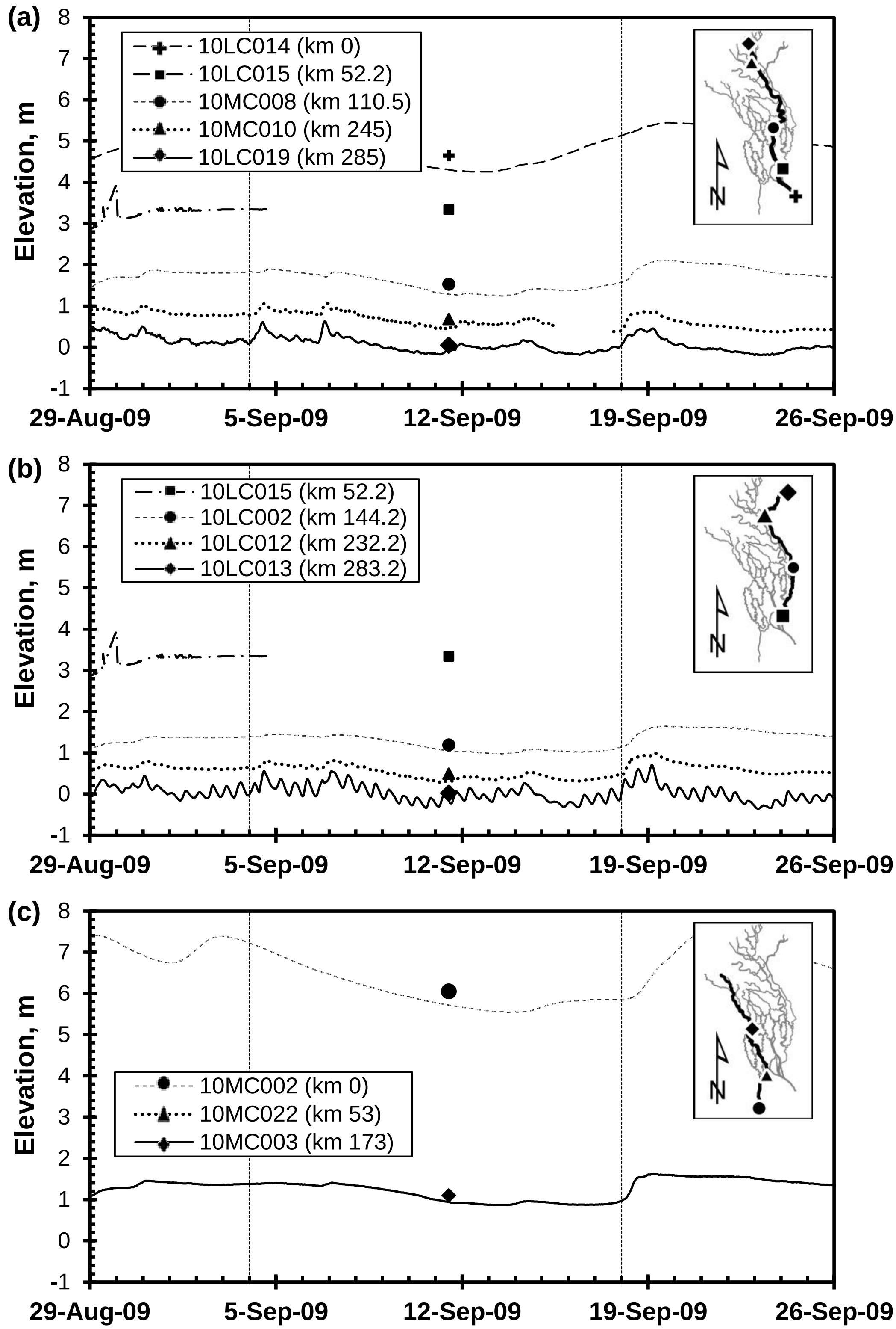

Figure 4.24 Water levels at gauges along the (a) Middle Channel (b) East Channel (c) West Channel (d) Napoiak Channel and (e) Reindeer Channel for Validation Scenario #2. (Data source: the WSC).

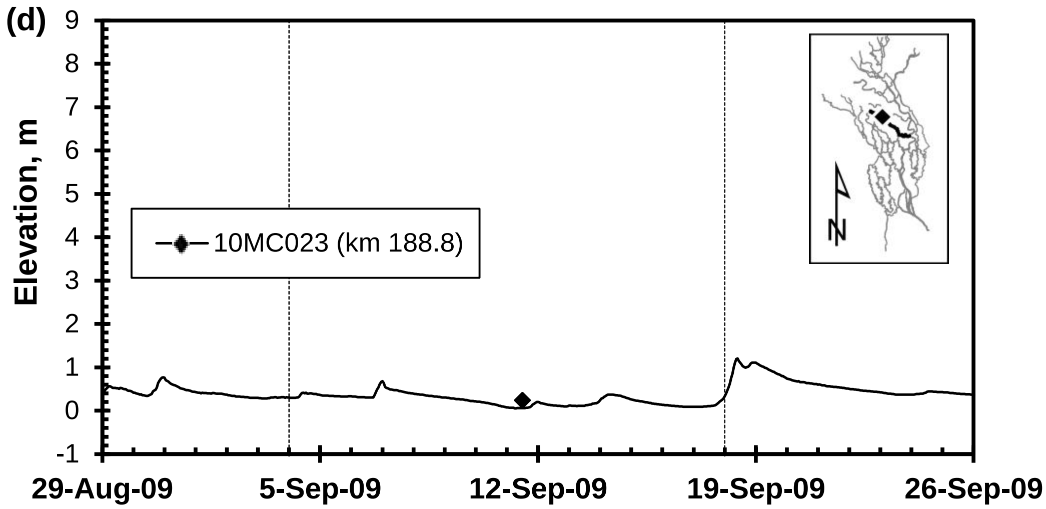

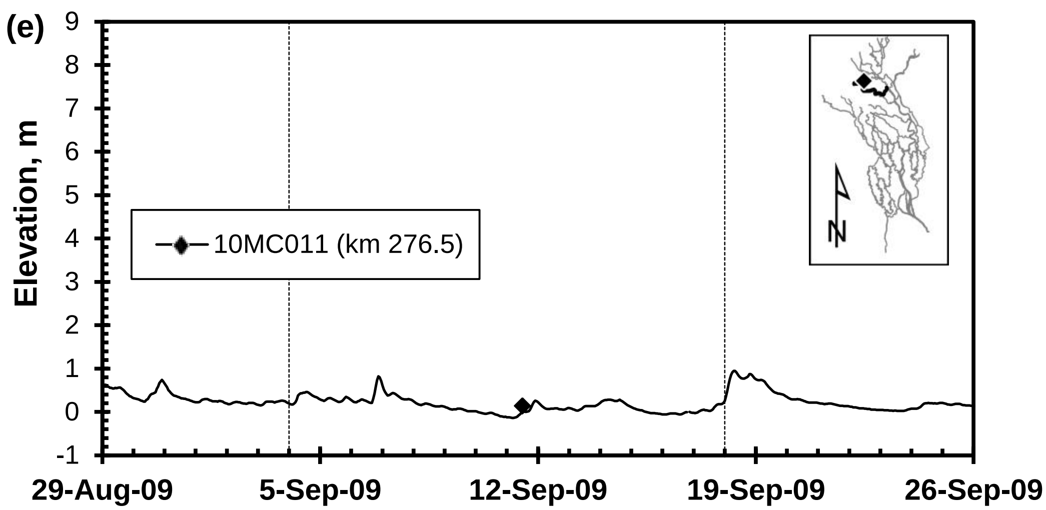

Figure 4.24 continued — Water levels at gauges along the (a) Middle Channel (b) East Channel (c) West Channel (d) Napoiak Channel and (e) Reindeer Channel for Validation Scenario #2. (Data source: the WSC).

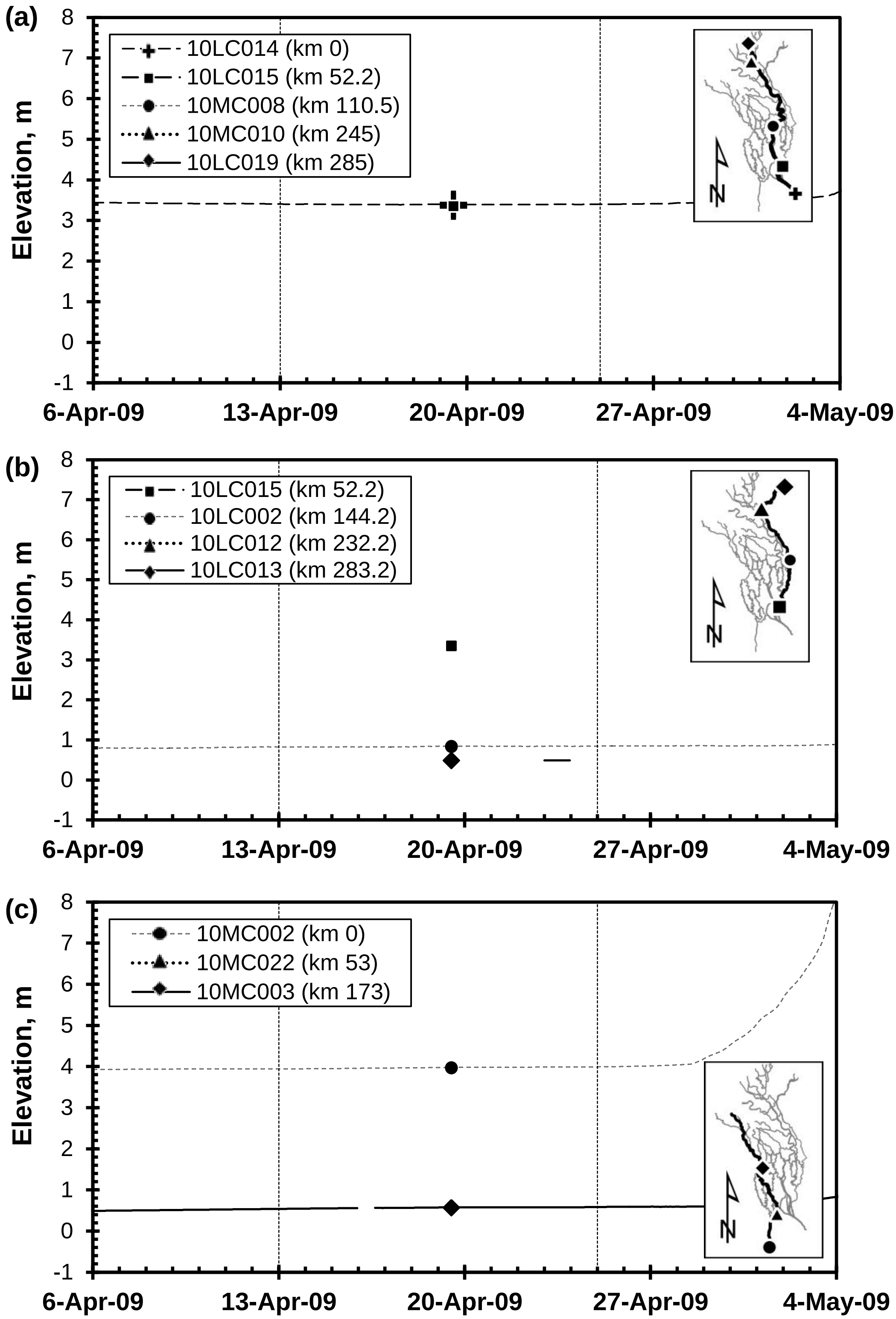

Figure 4.25 Water levels at station along the (a) Middle Channel (b) East Channel (c) West Channel (d) Napoiak Channel and (f) Reindeer Channel for the Winter Scenario.
(Data source: the WSC).

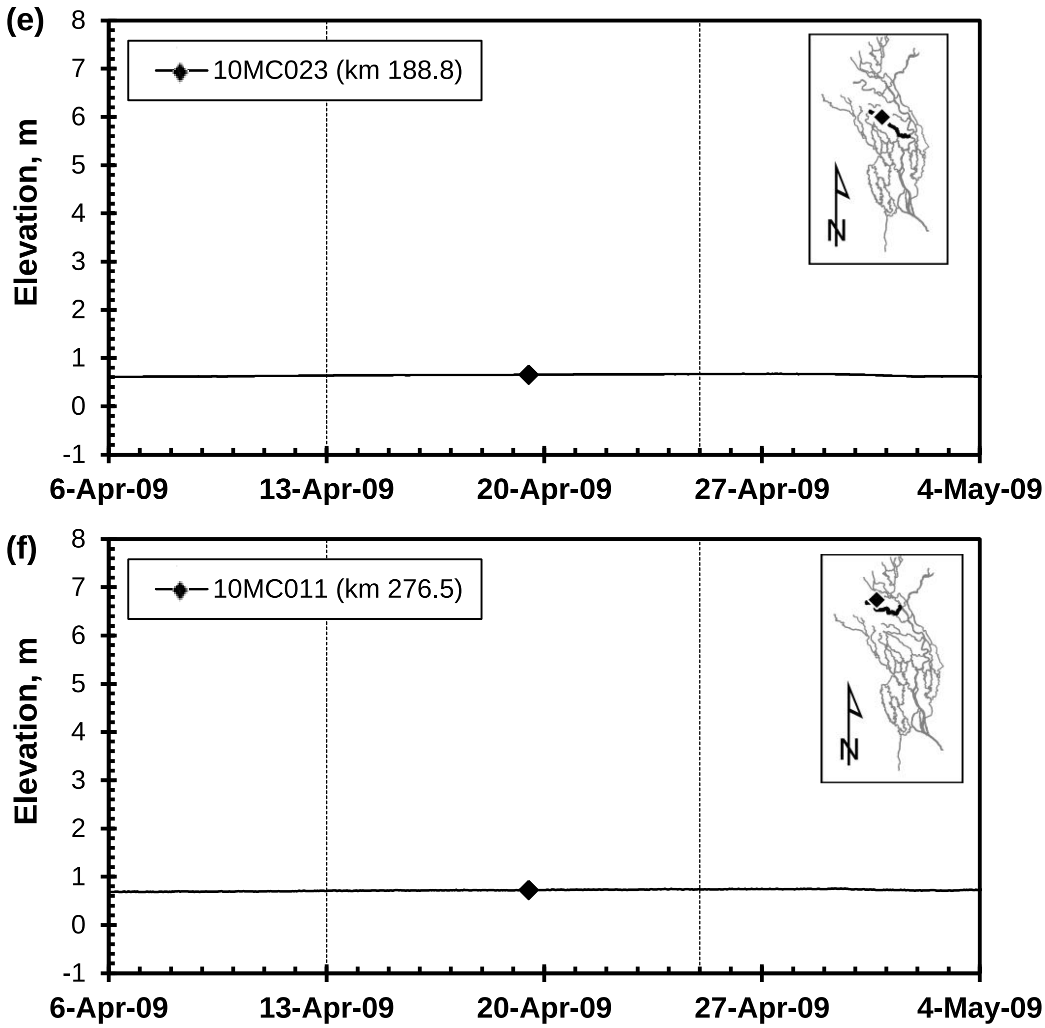

Figure 4.25 continued Water levels at station along the (a) Middle Channel (b) East Channel (c) West Channel (d) Napoiak Channel and (f) Reindeer Channel for the Winter Scenario. (Data source: the WSC).

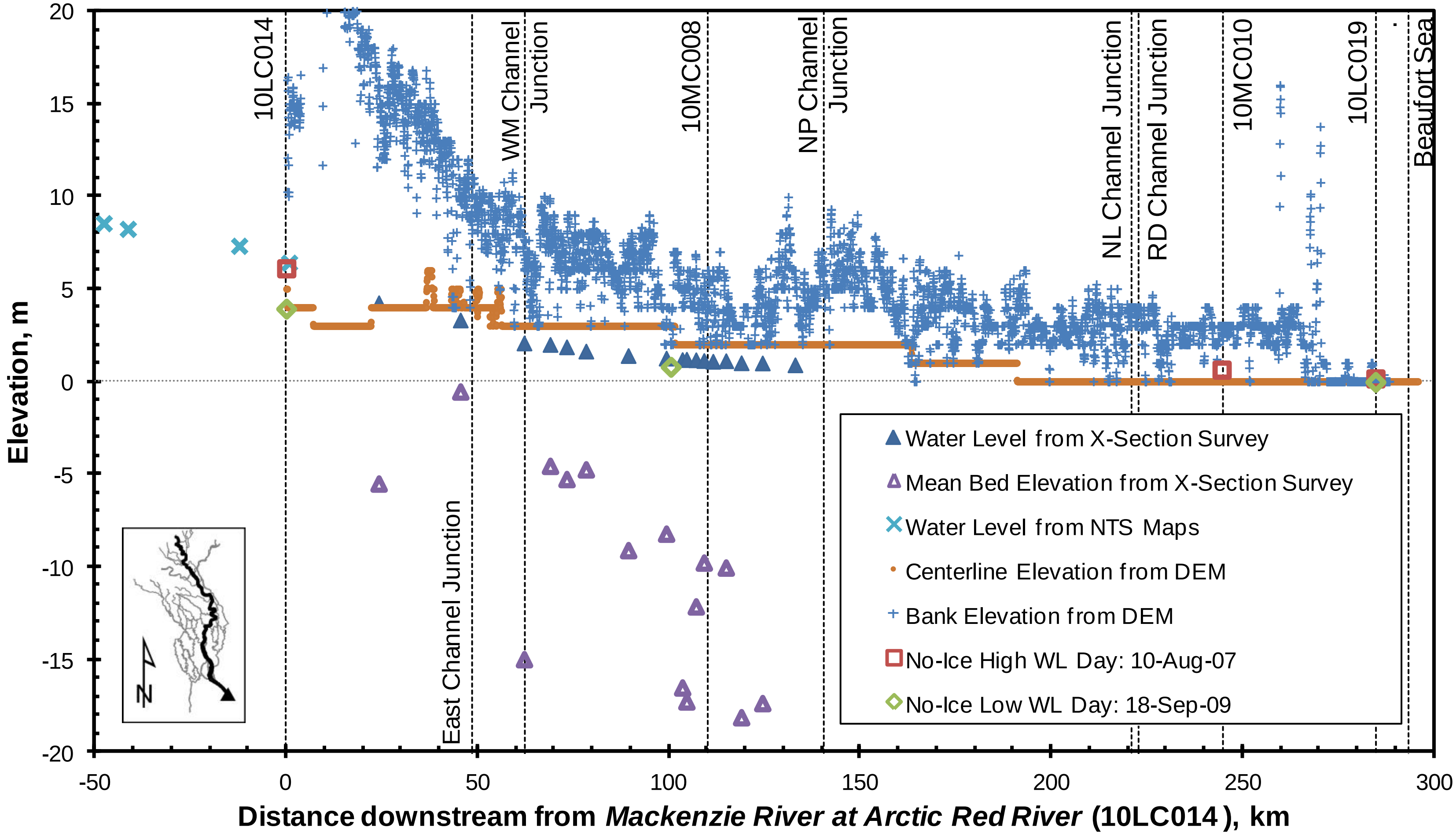

Figure 4.26 Plot showing measured elevations along the Middle Channel of the Mackenzie Delta. (Data source: the WSC, Environment Canada and NWTCG)

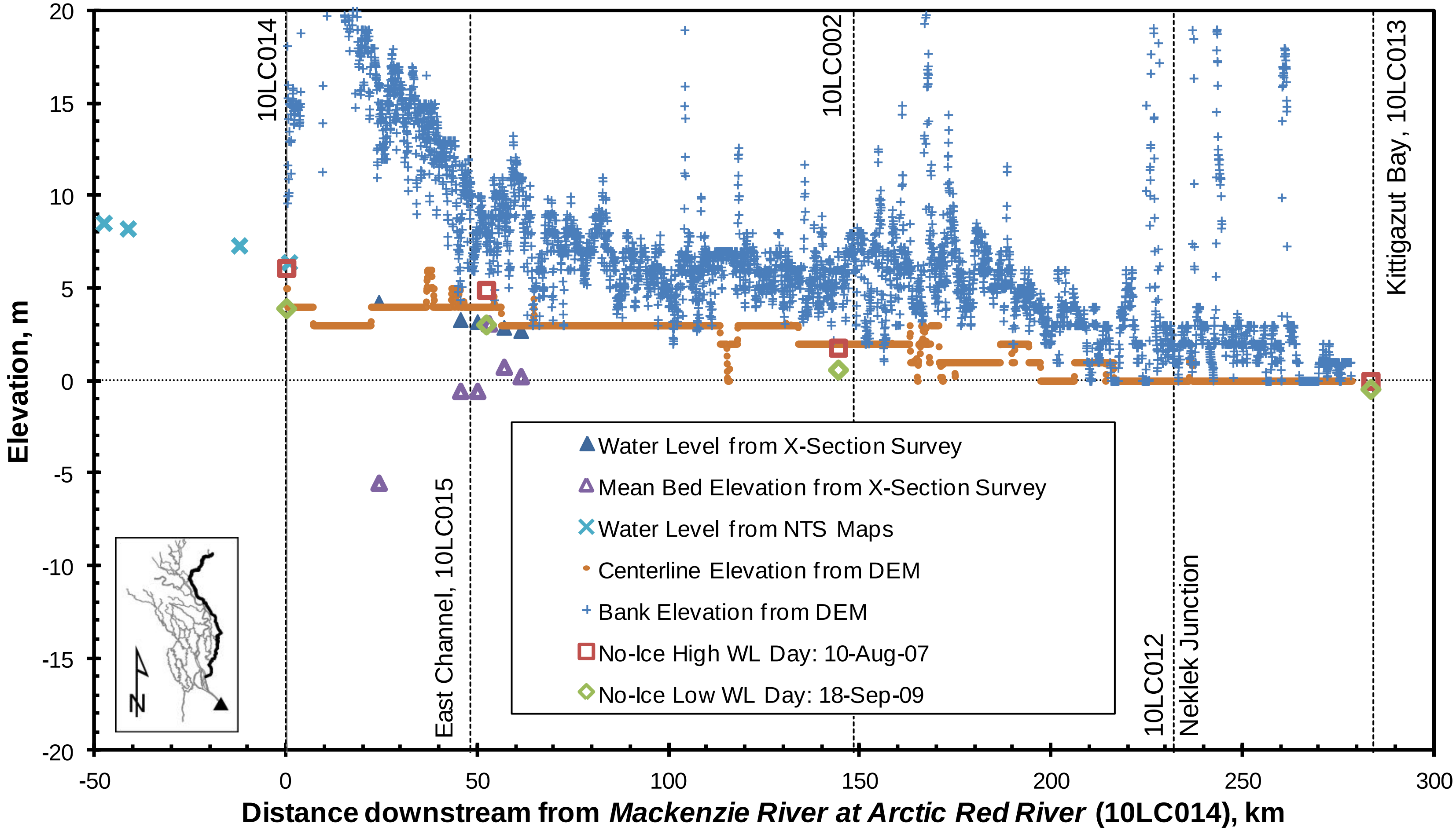

Figure 4.27 Plot showing measured elevations along the East Channel of the Mackenzie Delta. (Data source: the WSC, Environment Canada and NWTCG)

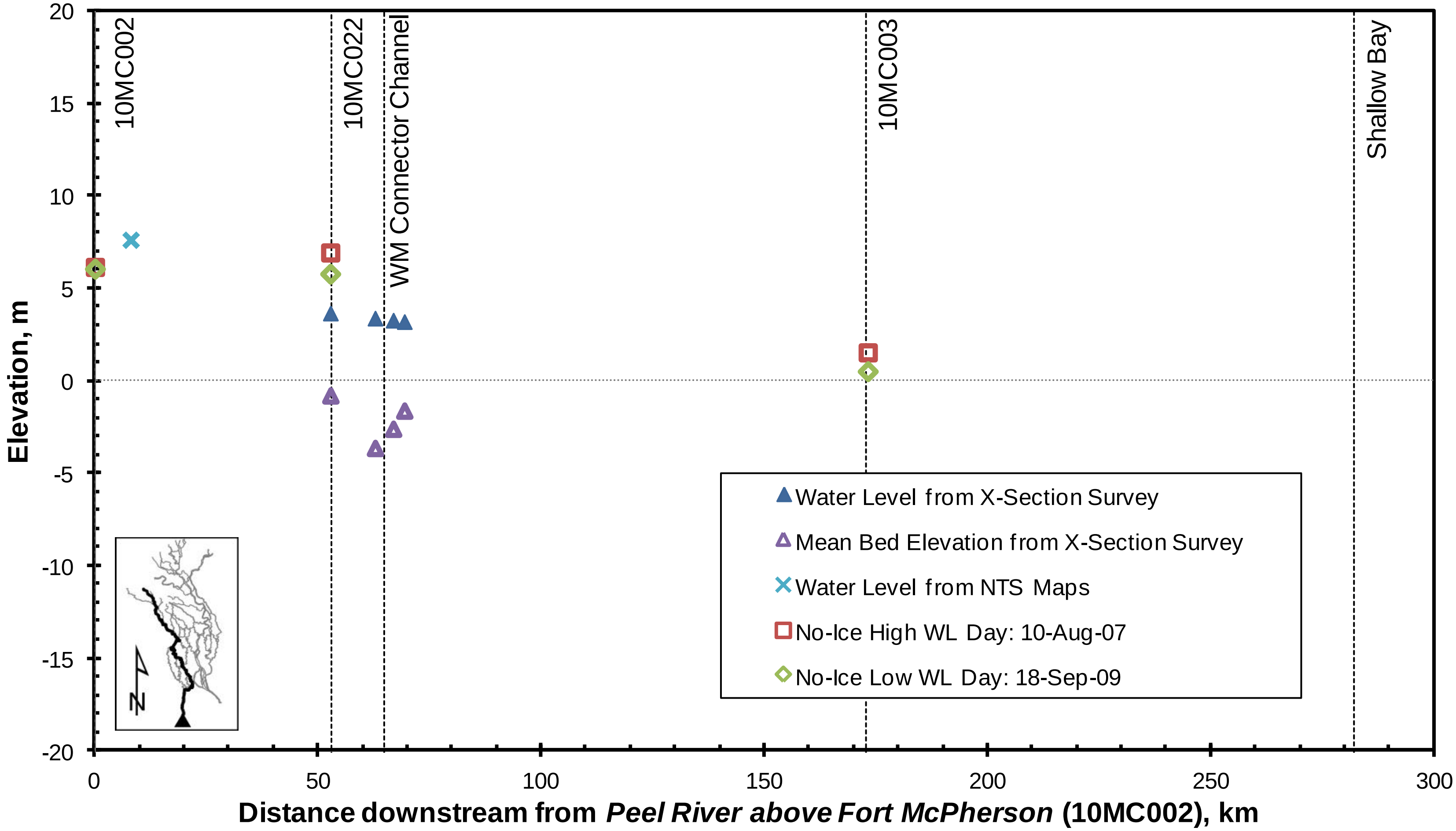

Figure 4.28 Plot showing measured elevations along the West Channel of the Mackenzie Delta. (Data source: the WSC, Environment Canada and NWTCG)

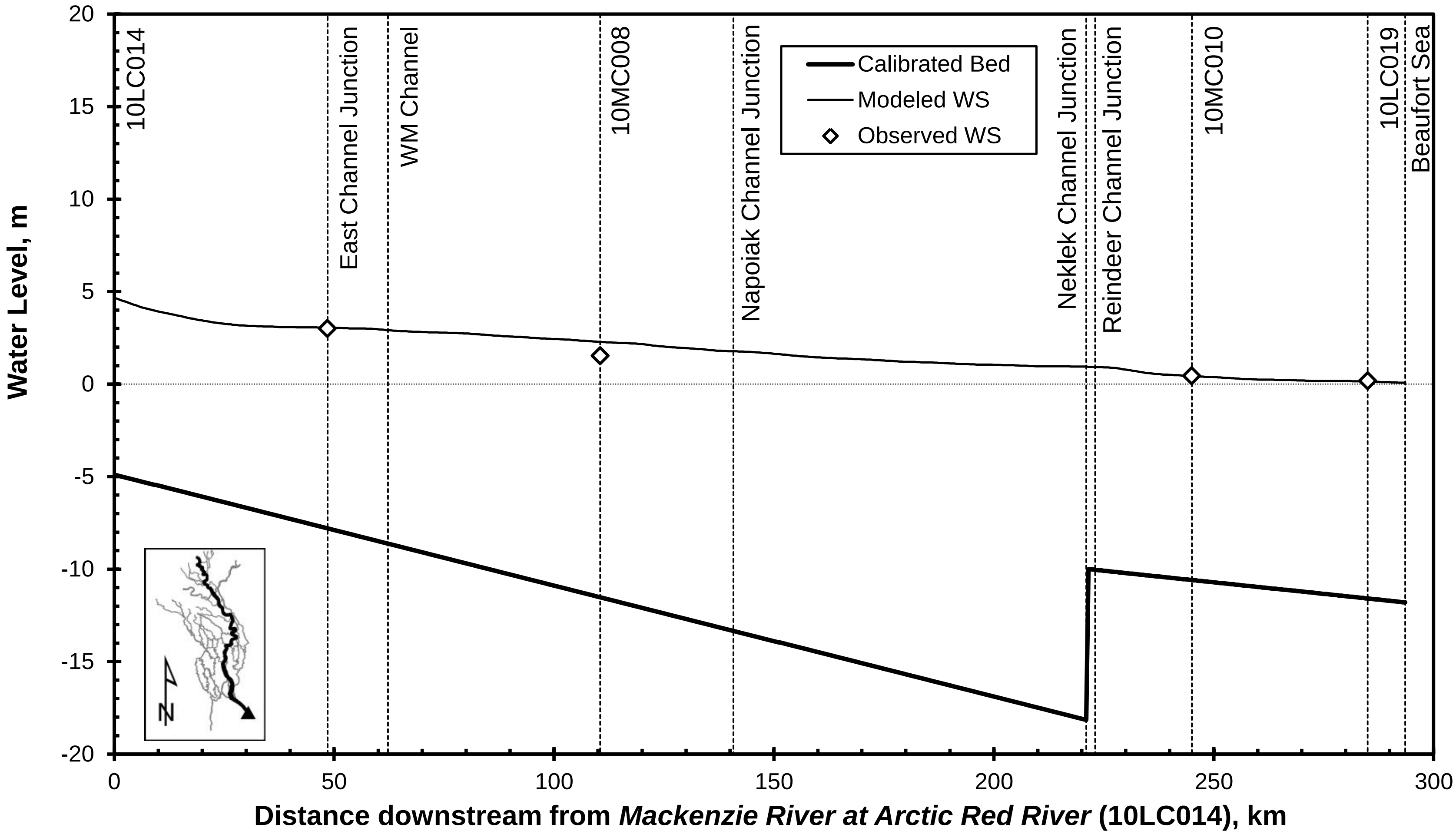

Figure 4.29 Calibrated bed geometry and modeled water surface profile for Calibration Scenario from 2-Aug-08 to 12-Aug-08 along the Middle Channel.

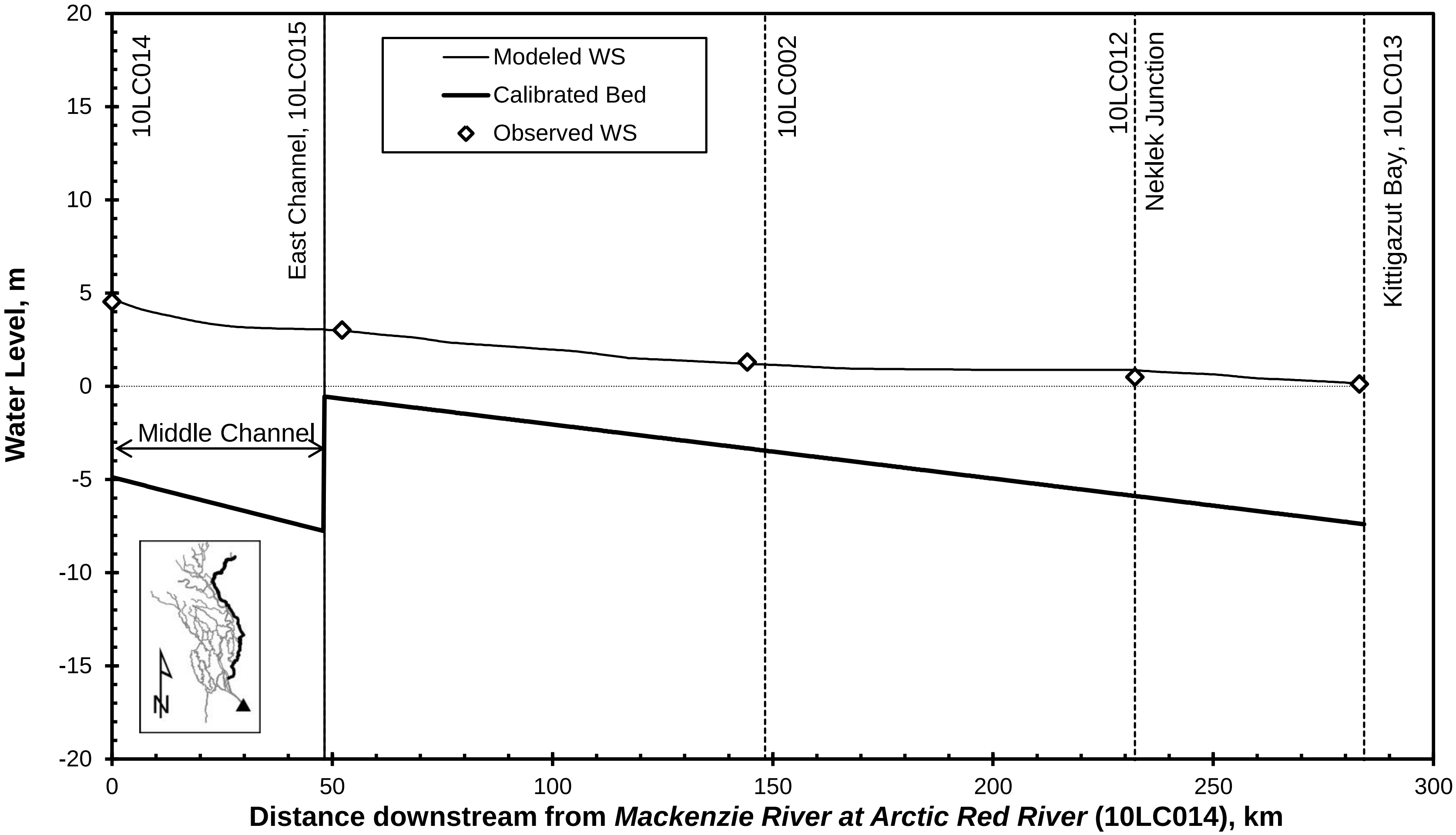

Figure 4.30 Calibrated bed geometry and modeled water surface profile for Calibration Scenario from 2-Aug-08 to 12-Aug-08 along the East Channel.

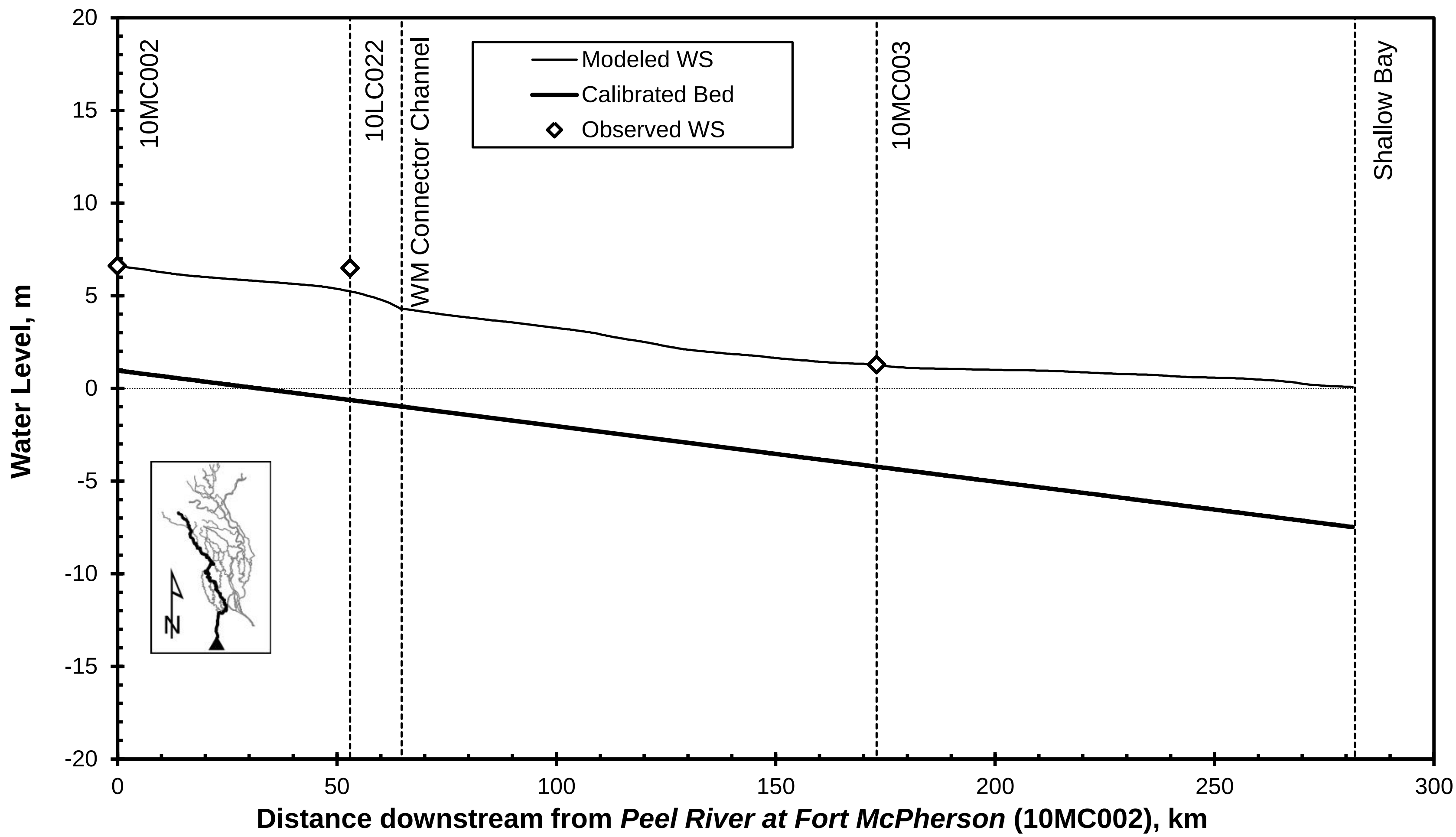

Figure 4.31 Calibrated bed geometry and modeled water surface profile for Calibration Scenario from 2-Aug-08 to 12-Aug-08 along the West Channel.

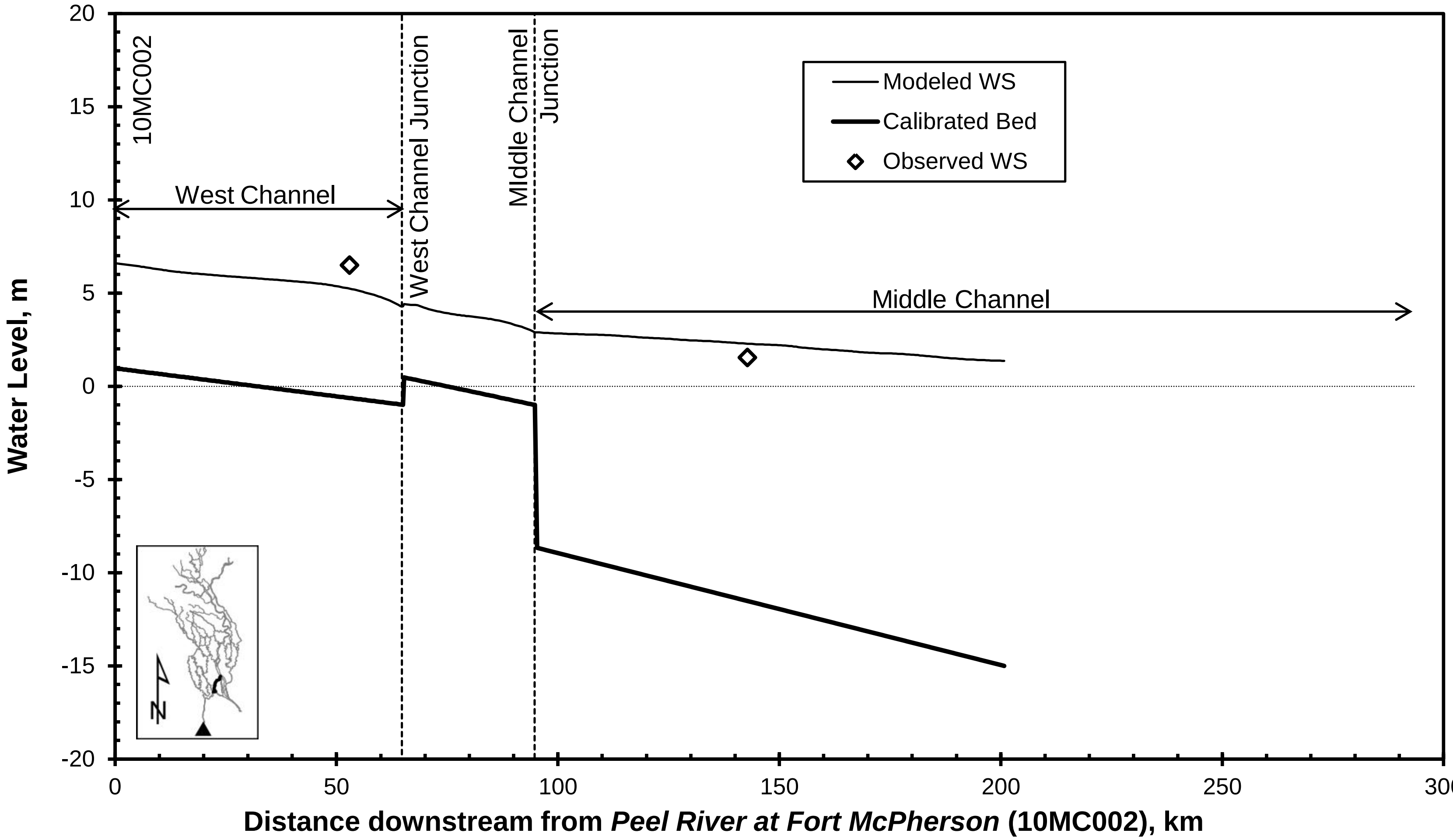

Figure 4.32 Calibrated bed geometry and modeled water surface profile for Calibration Scenario from 2-Aug-08 to 12-Aug-08 along the West-Middle Connector Channel.

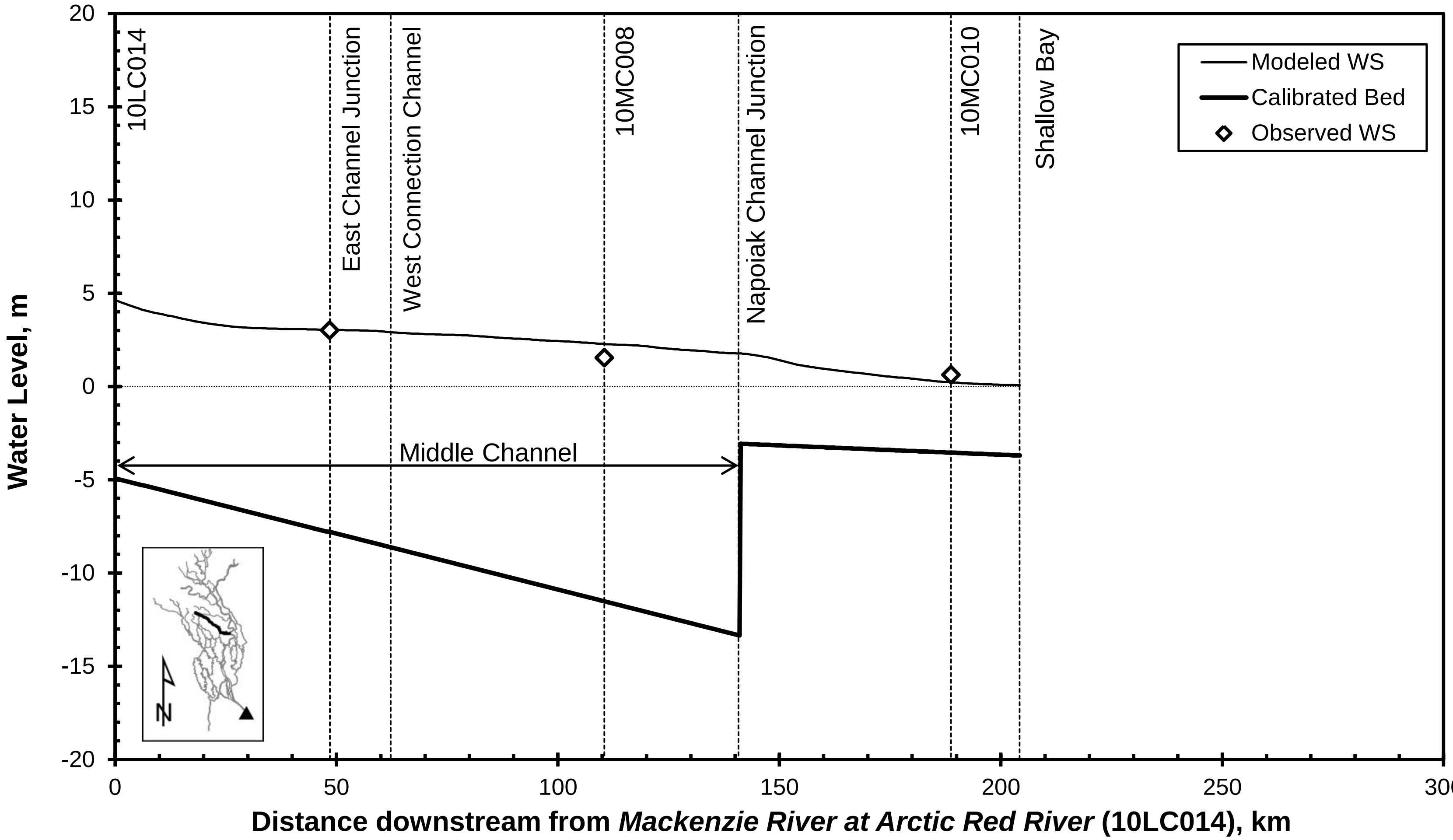

Figure 4.33 Calibrated bed geometry and modeled water surface profile for Calibration Scenario from 2-Aug-08 to 12-Aug-08 along the Napoiak Channel.

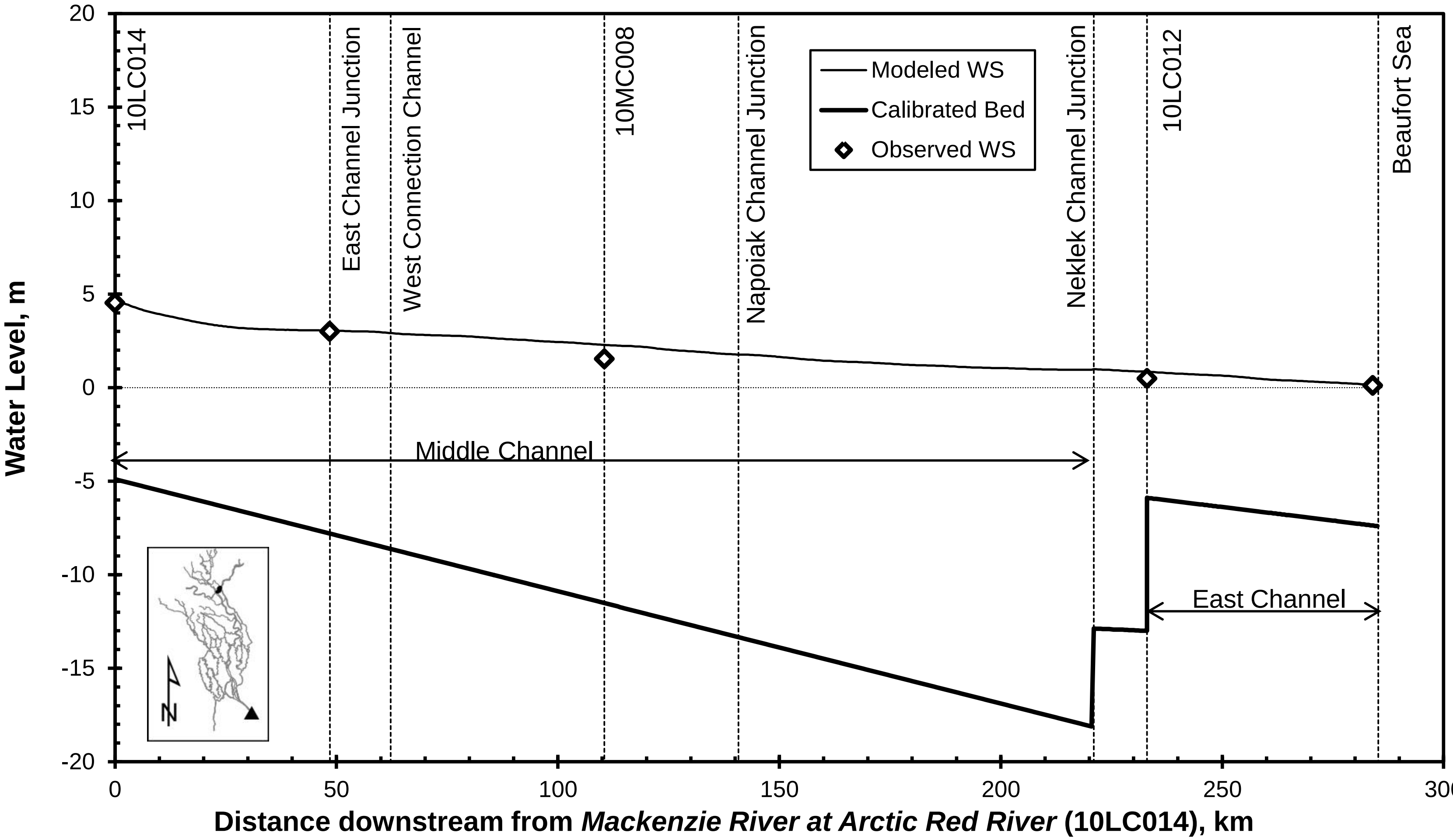

Figure 4.34 Calibrated bed geometry and modeled water surface profile for Calibration Scenario from 2-Aug-08 to 12-Aug-08 along the Neklek Channel.

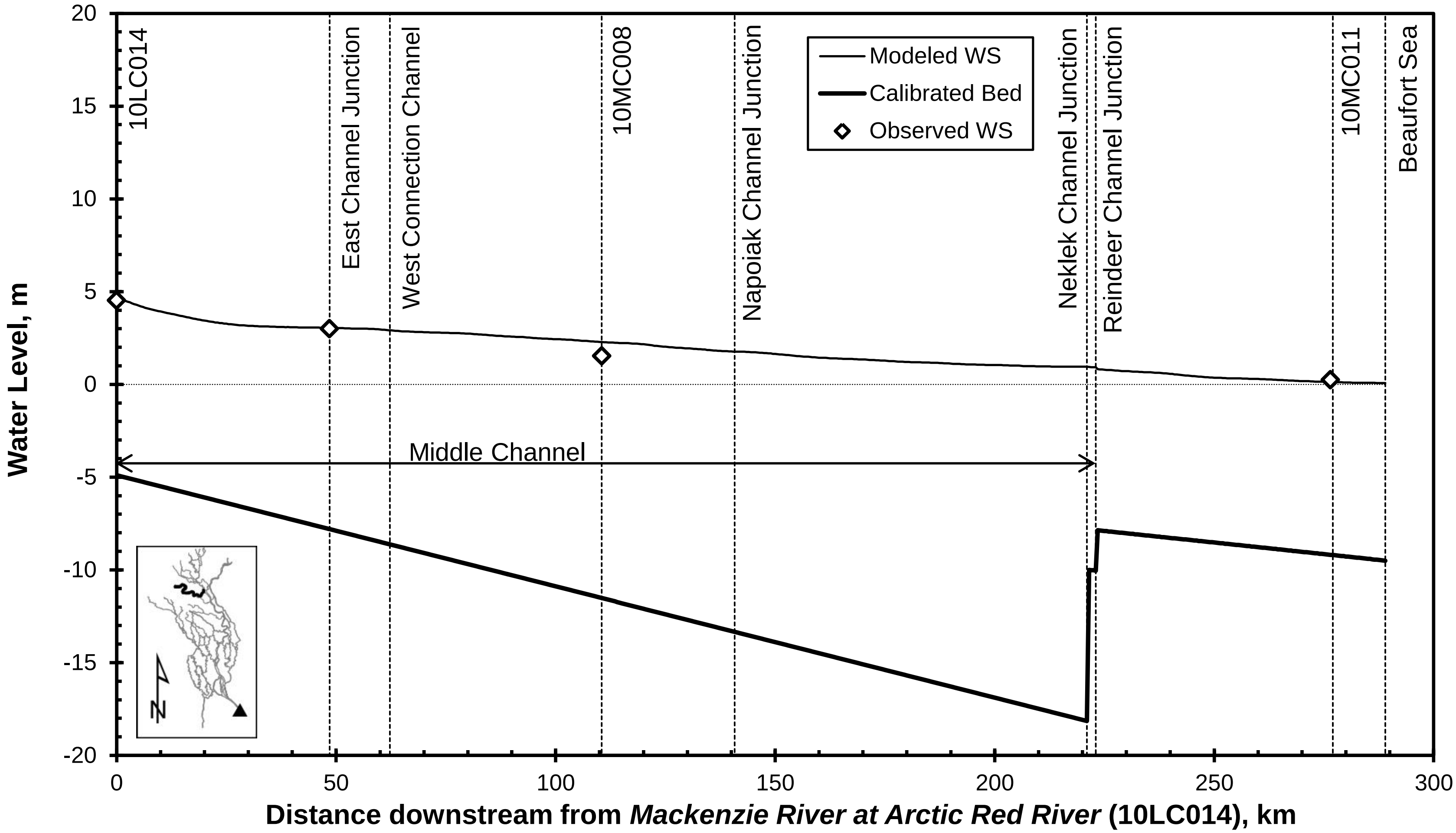

Figure 4.35 Calibrated bed geometry and modeled water surface profile for Calibration Scenario from 2-Aug-08 to 12-Aug-08 along the Reindeer Channel.

5.0 Summary and Recommendations

This study was part of a larger project (entitled IPY-SCARF) aimed at quantifying the water and nutrient fluxes towards the Beaufort Sea. In support of this project, two objectives were pursued in this study. First, the available data describing the Delta geometry, ice processes and flow distributions, with particular emphasis on the data collected as part of IPY-SCARF, was collated. Using this data, hydraulic modeling was used to calibrate an analogous channel geometry that can be used as input to the MDHM, which is a one-dimensional network model of the Delta that is currently being developed, but has been limited by a lack of geometric information (Nafziger *et al.*, 2009).

As part of the IPY-SCARF collaboration, WSC increased flow and water levels measurements at gauging stations in the Delta. This included upgrading gauging stations to report flow during the winter months, and measuring flow near each gauging station manually. Using this data, both manually measured and rating curve flows were compared to the average inflows to the Delta, which was assumed as the sum of the flow at the *Mackenzie River at Arctic Red River* (10LC014) and the *Peel River above Fort McPherson* (10MC002). Overall, it was found that on average ~95% of the inflow comes from the Mackenzie River, but the Peel River contributes a lower percentage (~3%) in the winter than in the summer months (~7%). From the flow record during the study period, it was found that the Middle Channel at *Mackenzie River (Middle Channel) below Raymond Channel* (10MC008) has, on average, ~10% greater percentage of inflow during the winter months than in the summer months. The mid-Delta gauges on the East and West Channel had ~ 1% less of the inflow in the winter than in the summer months, which suggested that flow in smaller channels may be blocked during winter and, therefore, a larger percentage of flow routes through the Middle Channel.

There were twenty one measurement campaigns during the study period that represent the most comprehensive data on flow distribution in the Delta to date. Maps were produced showing the flow distribution during five periods when manual measurements were available at stations without rating curves. Four of these maps were for open water conditions, while one was for ice-affected conditions in winter. During open water, flows measurements in the Turtle area were consistent between measurements periods (within ~2% of the inflow). However, in the Quadrapus, the same consistency was not evident and measurements in different periods varied by up to ~15% of the inflow. Additional flow measurements in the Quadrapus area are recommended to facilitate a better understanding of the implications and possible cause of such variations in flow distribution. Manual flow measurements during winter are also suggested as only one winter flow measurement is available on the East Channel just downstream of the Middle Channel. Although, the consistency of this flow split during winter could not be assessed, this measurement was of similar magnitude to that measured in summer, but nearly four times greater (in terms of percentage of total Delta inflow). This suggests that flow distributions may be drastically different in winter than in summer, possibly due to ice effects.

The lakes of the Mackenzie Delta are reliant upon water levels in the Delta channels for replenishment of both water and nutrients (Marsh, 1986; Marsh and Hey, 1988). The annual hydrographs during the study period, between 2006 and 2010, show that annual peak water levels at nearly all gauging stations occur during spring breakup. During this time, ice jams cause a backwater affect that leads to water levels that are much higher than those caused by high flows during the summer months.

Winter field data collection as part of IPY-SCARF included measurements of mid-winter ice thicknesses. An average ice thickness of ~1m thick was measured on the primary channels in the Delta, with non-ground fast ice thickness measurements ranging from ~0.4 m to ~2.0 m. The ice thickness measurements on the Middle and East Channels did not show the same tendency towards increased ice thickness with increased latitude as previously found in studies by Anderson and Anderson (1974). Future efforts by IPY-SCARF partners will include analysis of GPR transects to yield supplemental ice thickness data.

Breakup events were also monitored between 2006 and 2010, including documentation with 23,714 oblique photos taken by IPY-SCARF partners during aerial reconnaissance flights. From these photos, ice conditions on specific days during breakup were mapped and a sequence of events during breakup was deduced. Several consistent patterns in the formation and release of ice jams were evident over the five years of study. An ice jam with the toe located between *km* 60 and 80 in the Middle Channel, occurred in four of the five years studied. Breakup in the fifth year (2007) was mostly thermal and no ice jams were documented. An ice jam in the East Channel with the toe between *km* 60 and 71 was also observed in all but one of the four years when ice jams formed in the Middle Channel. Although small ice jams and accumulations were common in the West Channel and at other locations on the East Channel, the locations lacked consistency. Overall, as breakup progressed, ice deteriorated first in the smaller channels with ice remaining intact longer in the Middle Channel.

With the exception of the water levels reported at *Peel River at Frog Creek* (10MC022) and *Mackenzie River at Confluence East Channel* (10LC015),which are located just upstream of the most frequent jamming locations, peak water levels occurred first at the upstream gauges and then at the mid-Delta gauges. In addition to oblique photos documenting breakup, NRCan produced a post-processed satellite imagery product for the Delta showing ice and flood conditions at one to five day intervals during breakup in 2008 (van der Sanden and Drouin, 2011b; van der Sanden and Drouin, 2011a). It was found that the conditions indicated in the maps agreed well with oblique photos.

In this study, a one-dimensional hydraulic model was used to calibrate slope and channel elevation for the primary channels, using a rectangular cross-section approximation. This hydraulic modeling effort involved the adjustment of channel bed slope and elevation until computed water surface profiles matched recorded water levels for known flow splits. The model was calibrated for open water conditions using the flows measured between 2-Aug-08 to 12-Aug-08; and some assumptions were required as flow splits were not measured at all junctions. The calibrated bed slopes for the primary channels ranged from 0.00001 to 0.00030. For the calibration scenario, the average (absolute value) difference between computed and modeled water surface elevations was 0.24 m. For the two validations periods this difference ranged from 0.26 m to 0.50 m, with the greatest water levels difference found at *Peel River at Frog Creek* (10MC022). Overall, the calibrated geometry was successful in reproducing water levels observed during open water conditions. However, the calibrated geometry did not successively reproduce winter water surface elevations, as the model would not run due to a lack of flow information during ice covered conditions.

It was found that the modeled water surface elevations during summer were sensitive to changes in flow, particularly those closer to the downstream boundary. Additional flow measurement in the area of the Quadrapus are recommended, as measurements during this study period indicated a considerable variability in flow splits, in terms of the percentage of total Delta inflow. Measurements of both water surface and channel slope along the length of each of the primary channels is also recommended. In addition, the calibrated geometry was sensitive to changes in Manning's *n*. The slope and elevation calibrated in this modeling effort only reproduced measured water surface profiles if a Manning's n value of 0.030 was used. Until more flow and geometric cross-sections are measured in order to calibrate Manning's n, the calibrated bed slope found in this hydraulic modeling effort is suggested as input for the MDHM for the open water scenario.

6.0 References

Anderson, J. C. and Anderson, R. J. (1974). Winter Distribution of Flow in the Mackenzie Delta, N.W.T. Progress Report.

Bélanger, M. (2010). Overflow on the Mackenzie Delta Sea Ice Surface and the Hydraulics of Strudel Flows. (MSc, University of Alberta, Department of Civil and Environmental Engineering).

Beltaos, S., Carter, T., and Prowse, T. (2011). Morphology and genesis of deep scour holes in the Mackenzie Delta. Canadian Journal of Civil Engineering, 38(6). 638-649. doi:10.1139/l11-034.

Beltaos, S. and Carter, T. (2009). Field studies of ice breakup and jamming in the Mackenzie Delta. Proceedings of the 15th Workshop on the Hydraulics of Ice Covered Rivers, 2009, 266-283.

Bigras, S. C. (1990). Hydrological regime of lakes in the Mackenzie Delta, Northwest Territories, Canada. Arctic & Alpine Research, 22(2). 163-174.

Brunner, G. C. (2010). HEC-RAS River Analysis System User's Manual Version 4.1. CPD-68. US Army Corps of Engineers, Institute for Water Resources. Davis, CA.

Brunner, G. W. (2002). HEC-RAS, River Analysis System Hydraulic Reference Manual. CPD-69. US Army Corps of Engineers, Institute for Water Resources. Davis, CA.

Carmack, E. C., Macdonald, R. W., and Jasper, S. (2004). Phytoplankton productivity on the Canadian Shelf of the Beaufort Sea. Marine Ecology Progress Series, 27737-50.

Chow, V.T. (1959). Open Channel Hydraulics. McGraw Hill Book Co. New York. 680 pp.

Drouin, H. and van der Sanden, J. J. (2011). Groundfast Ice Mapping – Mackenzie Delta 2010. Natural Resources Canada / Canada Centre for Remote Sensing. Ottawa, ON.

Emmerton, C. A., Lesack, L. F. W., and Marsh, P. (2007). Lake abundance, potential water storage, and habitat distribution in the Mackenzie River Delta, western Canadian Arctic. Water Resources Research, 43(5). doi:10.1029/2006WR005139.

Emmerton, C. A., Lesack, L. F. W., and Vincent, W. F. (2008). Mackenzie River nutrient delivery to the Arctic Ocean and effects of the Mackenzie Delta during open water conditions. Global Biogeochemical Cycles, 22(1). doi:10.1029/2006GB002856.

Fassnacht, S. (1993a). 1992 channel cross-sections for Mackenzie Delta hydraulic model. IWD-NWT NOGAP Project C10.3. Inland Waters Directorate, Environment Canada. Yellowknife, NWT.

Fassnacht, S. (1993b). Mack Delta - Flow distribution analyses by S. Fassnacht. Mack Delta Worknote 27. Environment Canada. Yellowknife, NWT.

Fassnacht, S. (1994). Mackenzie Delta channel stability investigations at: Niglintgak Island and East Channel Swimming Point. WT-NWT NOGAP Project 11.6. Inland Waters Directorate, Environment Canada. Yellowknife, NWT.

Fassnacht, S. (1997). A multi-channel suspended sediment transport model for the Mackenzie Delta, Northwest Territories. Journal of Hydrology, 197128-145.

Gharabaghi, B., Inkratas, C., Beltaos, S., and Krishnappan, B. (2007). Modelling of three-dimensional flow velocities in a deep hole in the East Channel of the Mackenzie Delta, Northwest Territories. Canadian Journal of Civil Engineering, 34(10). 1312-1323. doi:10.1139/l07-054.

Goulding, H. L. (2008). Spatial and temporal patterns and hydroclimatic controls of river ice break-up in the Mackenzie Delta, NWT. (MSc, University of Victoria, Department of Geography).

Goulding, H. L., Prowse, T. D., and Beltaos, S. (2009). Spatial and temporal patterns of break-up and ice-jam flooding in the Mackenzie Delta, NWT. Hydrological Processes, 23, 2654-2670, DOI: 10.1002/hyp.7251.

Hicks, F. E. (1996). Hydraulic flood routing with minimal channel data: Peace River, Canada. Canadian Journal of Civil Engineering, 23(2). 524-535.

Hicks, F. E.,Chen, X.and Andres, D., (1995) “Effects of Ice on the Hydraulics of the Mackenzie River at the Outlet of Great Slave Lake, NWT: A Case Study”, Canadian Journal of Civil Engineering, 22(1). 43-54.

Inkratas, C., Gharabaghi, B., Beltaos, S., and Krishnappan, B. (2009). 3D modelling of ice-covered flows in the vicinity of a deep hole in the East Channel of the Mackenzie Delta, N.W.T. Canadian Journal of Civil Engineering, 36(5). 791-800. doi:10.1139/L09-031.

Kerr, J. (1993a). Mack Delta - 1-D Model - Water-Level Gage-to-Geodetic conversions. Mack Delta Worknote 44. Environment Canada. Yellowknife, NWT.

Kerr, J. (1993b). Mack Delta- 1-D Model - 1982-88 Calibration & Resulting Hydrographs & Profiles. Mack Delta Worknote 50. Environment Canada. Yellowknife, NWT.

Kerr, J. and Miyagawa, R. (1996). 1-D Hydrodynamic Modelling for Mackenzie Delta. Internal report MHM94-2. Environment Canada. Yellowknife, NWT.

Lapointe, M. F. (1984). Patterns and processes of channel change, Mackenzie Delta, NWT. 1983-84 Progress Report. Northern Hydrology Section, Surface Water Division, NHRI, Environment Canada. Ottawa, ON.

Lapointe, M. F. (1986). Mackenzie Delta channel dynamics: miscellaneous data. Cold Regions Section, Surface Water Division, NHRI, Environment Canada. Ottawa, ON.

Lesack, L. and Marsh, P. (2007). Lengthening plus shortening of river-to-lake connection times in the Mackenzie River Delta respectively via two global change mechanisms along the arctic coast. Geophysical Research Letters, 34(23).

Mackay, J. R. (1963). The Mackenzie Delta Area, N.W.T. Miscellaneous report (Geological Survey of Canada), 23. Rodger Duhamel, Queen's Printer and Controller of Stationary. Ottawa, ON.

Mackenzie River Basin Board (MRBB). (2010). Understanding the Basin. Retrieved January 25, 2012, from http://www.mrbb.ca/information/9/index.html

Marsh, P. (1986). Modelling Water Levels for a Lake in the Mackenzie Delta. Proceedings of the Cold Regions Hydrology Symposium, 1986, 23-29.

Marsh, P. and Hey, M. (1988). Mackenzie River Water Levels and Flooding of Delta Lakes. NHRI Contribution #88013. National Hydrology Research Institute, Environment Canada. Saskatoon, SK.

Marsh, P., Lesack, L., and Roberts, A. (1993). The environmental efforts of Ice Jam Flooding on Lakes in the Mackenzie Delta. Proceedings of the Workshop on Environmental Aspects of River Ice, TD Prowse (Editor). 1993, 358-381.

Marsh, P. and Hey, M. (1989). The flooding hydrology of Mackenzie Delta Lakes near Inuvik, N.W.T., Canada. Arctic, 42(1). 41-49.

Nafziger, J., Hicks, F., Andrishak, R., Marsh, P., and Lesack, L. (2009).

Hydraulic Model of River Flow and Storage Effects in the Mackenzie Delta, Canada. Proceedings of the 17th International North Research Basins Symposium and Workshop, 2009, 1-8.

NWT Centre for Geomatics. (2007). Mackenzie Valley Air Photo Project 2004 Retrieved January 31, 2012, from http://www.gnwtgeomatics.nt.ca/RemoteSensing/avhrr/MackenzieValleyPhotos.asp

Pelletier, P. M. (1988). Uncertainties in the single determination of river discharge: a literature review. Canadian Journal of Civil Engineering, 15834-850.

Pelletier, P. M. (1990). A review of techniques used by Canada and other northern countries for measurement and computation of streamflow under ice conditions. Nordic Hydrology, 21317-340.

Rouse, W. R., Douglas, M. S. V., Hecky, R. E., Hershey, A. E., Kling, G. W., Lesack, L., et al. (1997). Effects of climate change on the freshwaters of arctic and subarctic North America. Hydrological Processes, 11(8). 873-902.

Stevens, C., Moorman, B., Solomon, S., and Hugenholtz, C. (2009). Mapping subsurface conditions within the near-shore zone of an Arctic delta using ground penetrating radar. Cold Regions Science and Technology, 56(1). 30-38.

T. Blench & Associates Ltd. (1974). Channel geometry and flow data: Mackenzie Delta - Lower Delta. Prepared for the Northern Engineering Services Company Ltd. Submitted by T. Blench and Associates Ltd. Consulting Hydraulic Engineers.

Terroux, A., Sherstone, D., Kent, T., Anderson, J., Bigras, S., and Kriwoken, L. (1981). Ice regime of the Lower Mackenzie River and Mackenzie Delta. The National Hydrology Research Institute, Environment Canada. Hull, Quebec.

Traynor, S. and Dallimore, S. (1992). Geological investigations of proposed pipeline channel crossings in the vicinity of Taglu and Niglintgak Islands, Mackenzie Delta, NWT. Environmental Studies Research Funds report no. 116. Ottawa.

van der Sanden, J. J. and Drouin, H. (2011a). Spring 2008 Flood Condition, Mackenzie River Delta, Northwest Territories, Canada. GIS ready map series. Ottawa, ON. National Resources Canada.

van der Sanden, J. J. and Drouin, H. (2011b). Spring 2008 Ice Cover Condition, Mackenzie River Delta, Northwest Territories, Canada. Ottawa, ON.

National Resources Canada.

Véronneau, M. (2006). Demystifying the vertical datum in Canada: A case study in the Mackenzie Delta. Natural Resources Canada. Ottawa, ON.

Walker, J. and Wang, D. (1997). Measurement of flow under ice covers in North America ,, Journal of Hydraulic Engineering, 123(11). 1037-1040.

Woo, M. and Thorne, R. (2003). Streamflow in the Mackenzie Basin, Canada. Arctic, 56(4). 328-340.

Appendix A. List of Contact Information and Contributions of IPY-SCARF Partners

This appendix lists the contributions of IPY-SCARF partners to this study. Contact names and affiliations are listed, along with the data that were provided.

Environment Canada:

- P. Marsh, S. Beltaos, T. Carter, and M. Russell, National Water Resources Institute:
    - Oblique photos from in breakup 2007 and 2008.
    - Cross sections in 2007 and 2008, as presented in Section 4.3.1.
    - Water levels during breakup in 2008
- R. Piling, R. Wedel, A. Pippy, G. Lennie and L. Greenland, the Water Survey of Canada:
    - Unpublished hourly water levels WSC gauging stations, as graphed in Appendix B and included in the attached CD.
    - Manual flow measurements at gauging stations as discussed in Chapter 2.
    - Ice thickness measurements at WSC stations, as presented in Section 3.1.1.
    - Mackenzie Basin High Water Reports over the study period from 2006 to 2010.

Natural Resource Canada:

- J. J. van der Sanden and H. Drouin, Canada Centre for Remote Sensing,:
    - Ice thickness measurements as discussed in Section 3.1.1.
    - GPR transects during winter of 2010, as discussed in Section 3.1.1
    - Groundfast Ice Mapping Product (Drouin and van der Sanden, 2011) as discussed in Section 3.1.2.

- Breakup Ice Cover Mapping Product (van der Sanden and Drouin, 2011b) presented in Section 3.2.2.
- Breakup Flood Condition Mapping Product (van der Sanden and Drouin, 2011a) presented in Section 3.2.2.
- Oblique photos from breakup in 2008.

- S. Solomon and D. Forbes, Bedford Institute of Oceanography:
    - Oblique photos from breakup in 2008.
    - Outer Delta Flooding and Breakup reports over the study period from 2006 to 2010.
- G. Lintern, Natural Resources Canada:
    - Oblique photos from breakup in 2009
- R. Bowen, Natural Resources Canada:
    - Oblique photos from breakup in 2009

Simon Fraser University:

- L. Lesack, J. Gareis and L. Duma, Departments of Geography and Biological Sciences:
    - Oblique photos from breakup in 2008, 2009 and 2010.

University of Alberta:

- F. Hicks, J. Nafziger and M. Belanger and J. Morley, Department of Civil and Environmental Engineering:
    - Oblique photos from breakup in 2007 to 2010

Additional Contributor - Aurora Research Institute:

- R. Ross, Aurora Research Institute:
    - Oblique photos from breakup in 2010

Appendix B. Water Level Hydrographs at Gauging Stations Operated by the WSC

This appendix contains plots of the hourly, daily and manually measured on at WSC gauges during the study period from 2006 to 2010. Tables of the flow and water levels recorded at each gauge are on the CD provided. In total there are fourteen stations that report water level in the Mackenzie Delta including the two stations upstream on the Peel and Mackenzie Rivers:

- Figure B.1 Water levels from 2006 to 2010 at the WSC gauge *Mackenzie River (East Channel) at Inuvik* (10LC002).
- Figure B.2 Water levels from 2006 to 2010 at the WSC gauge *Mackenzie River (Middle Channel) at Tununuk Bay* (10LC012).
- Figure B.3 Water levels from 2006 to 2010 at the WSC gauge .
- Figure B.4 Water levels from 2006 to 2010 at the WSC gauge *Mackenzie River at Arctic Red River* (10LC014).
- Figure B.5 Water levels from 2006 to 2010 at the WSC gauge *Mackenzie River at Confluence East Channel* (10LC015).
- Figure B.6 Water levels from 2006 to 2010 at the WSC gauge *Mackenzie River (Kumak Channel) below Langley Island* (10LC019).
- Figure B.7 Water levels from 2006 to 2010 at the WSC gauge *Big Lake at Taglu Island* (10LC020).
- Figure B.8 Water levels from 2006 to 2010 at the WSC gauge *Mackenzie River at Kuluarpak Channel* (10LC021).
- Figure B.9 Water levels from 2006 to 2010 at the WSC gauge *Peel River above Fort McPherson* (10MC002).

- Figure B.10 Water levels from 2006 to 2010 at the WSC gauge *Mackenzie River (Peel Channel) above Aklavik* (10MC003).
- Figure B.11 Water levels from 2006 to 2010 at the WSC gauge *Mackenzie River (Middle Channel) below Raymond Channel* (10MC008).
- Figure B.12 Water levels from 2006 to 2010 at the WSC gauge *Mackenzie River (Outflow Middle Channel) below Langley Island* (10MC010).
- Figure B.13 Water levels from 2006 to 2010 at the WSC gauge *Mackenzie River (Reindeer Channel) at Ellice Island* (10MC011).
- Figure B.14 Water levels from 2006 to 2010 at the WSC gauge *Peel River at Frog Creek* (10MC022).
- Figure B.15 Water levels from 2006 to 2010 at the WSC gauge *Mackenzie River (Napoiak Channel) above Shallow Bay* (10MC023).

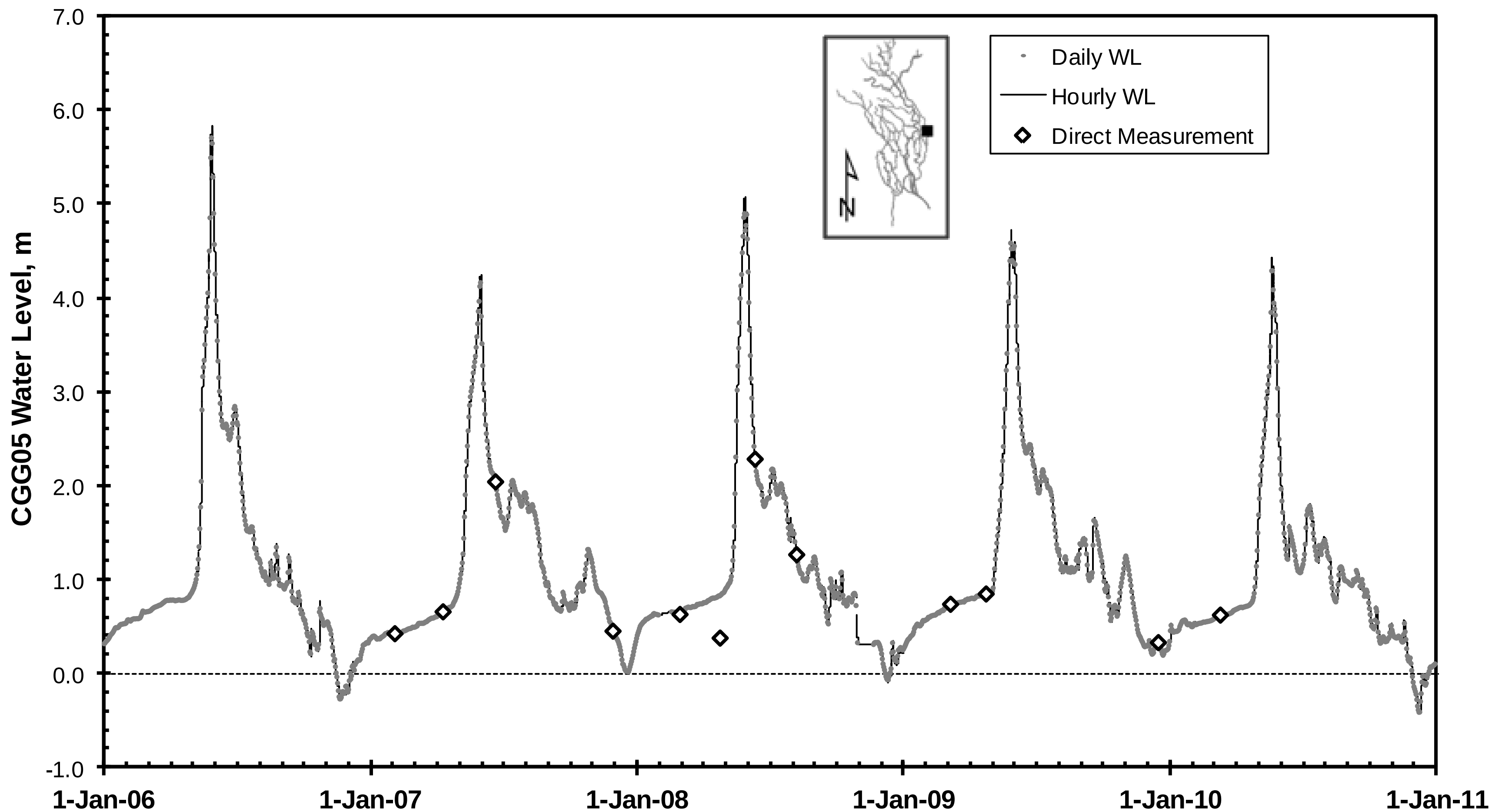

Figure B.1 Water levels from 2006 to 2010 at the WSC gauge *Mackenzie River (East Channel) at Inuvik* (10LC002). (Data source: the WSC).

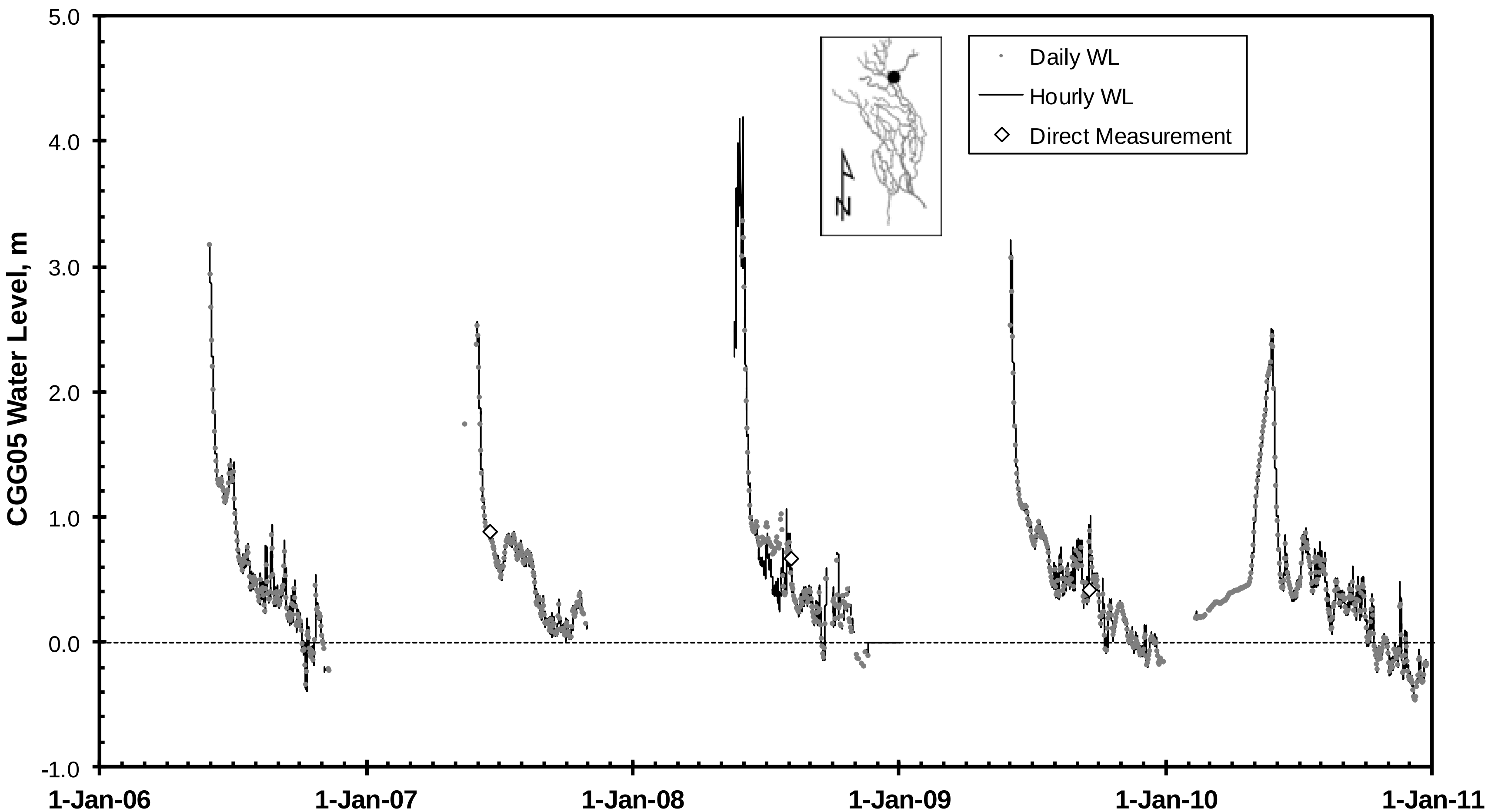

Figure B.2 Water levels from 2006 to 2010 at the WSC gauge *Mackenzie River (Middle Channel) at Tununuk Point* (10LC012). (Data source: the WSC).

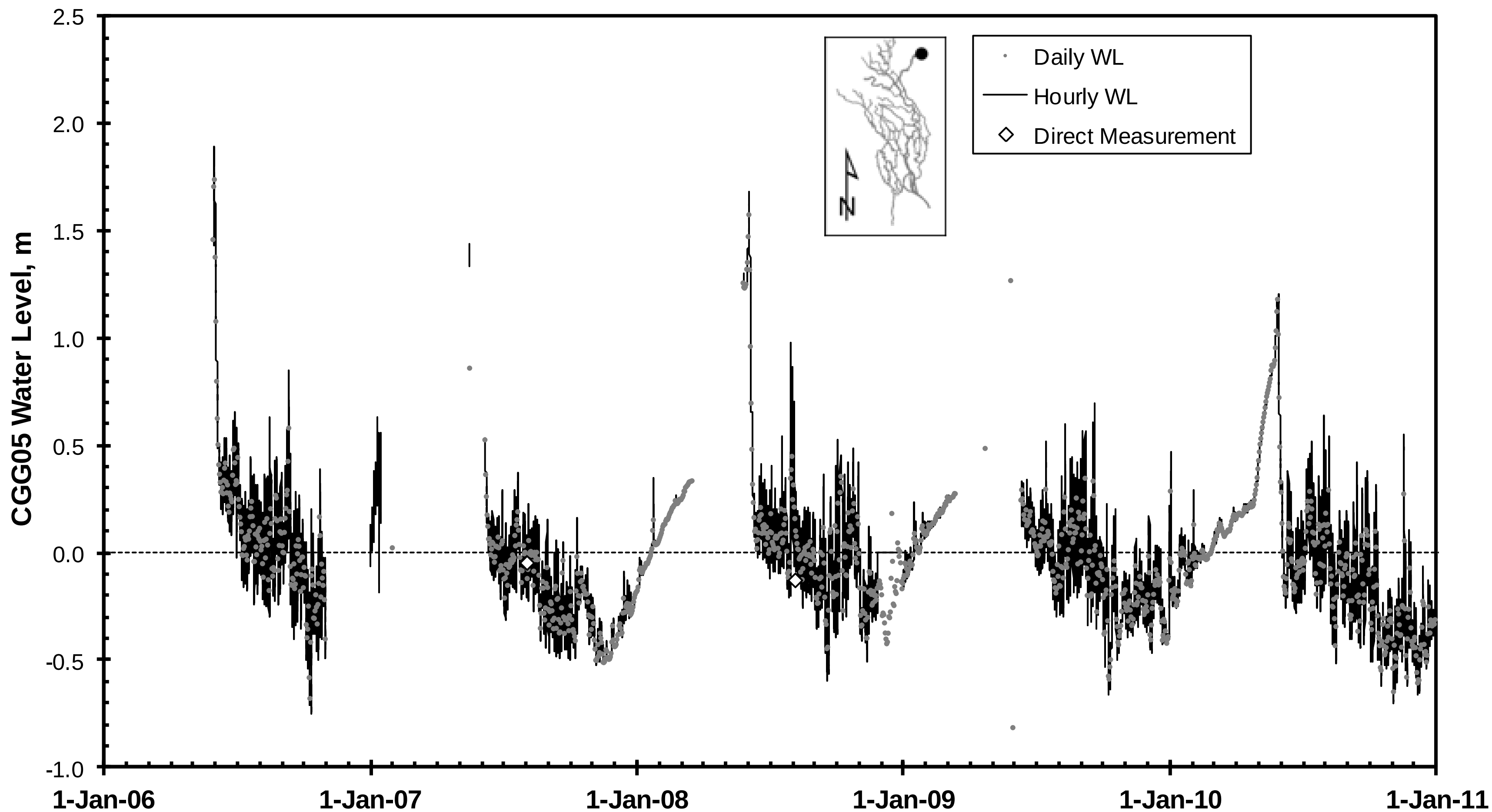

Figure B.3 Water levels from 2006 to 2010 at the WSC gauge *Mackenzie River (East Channel) above Kittigazuit Bay* (10LC013). (Data source: the WSC).

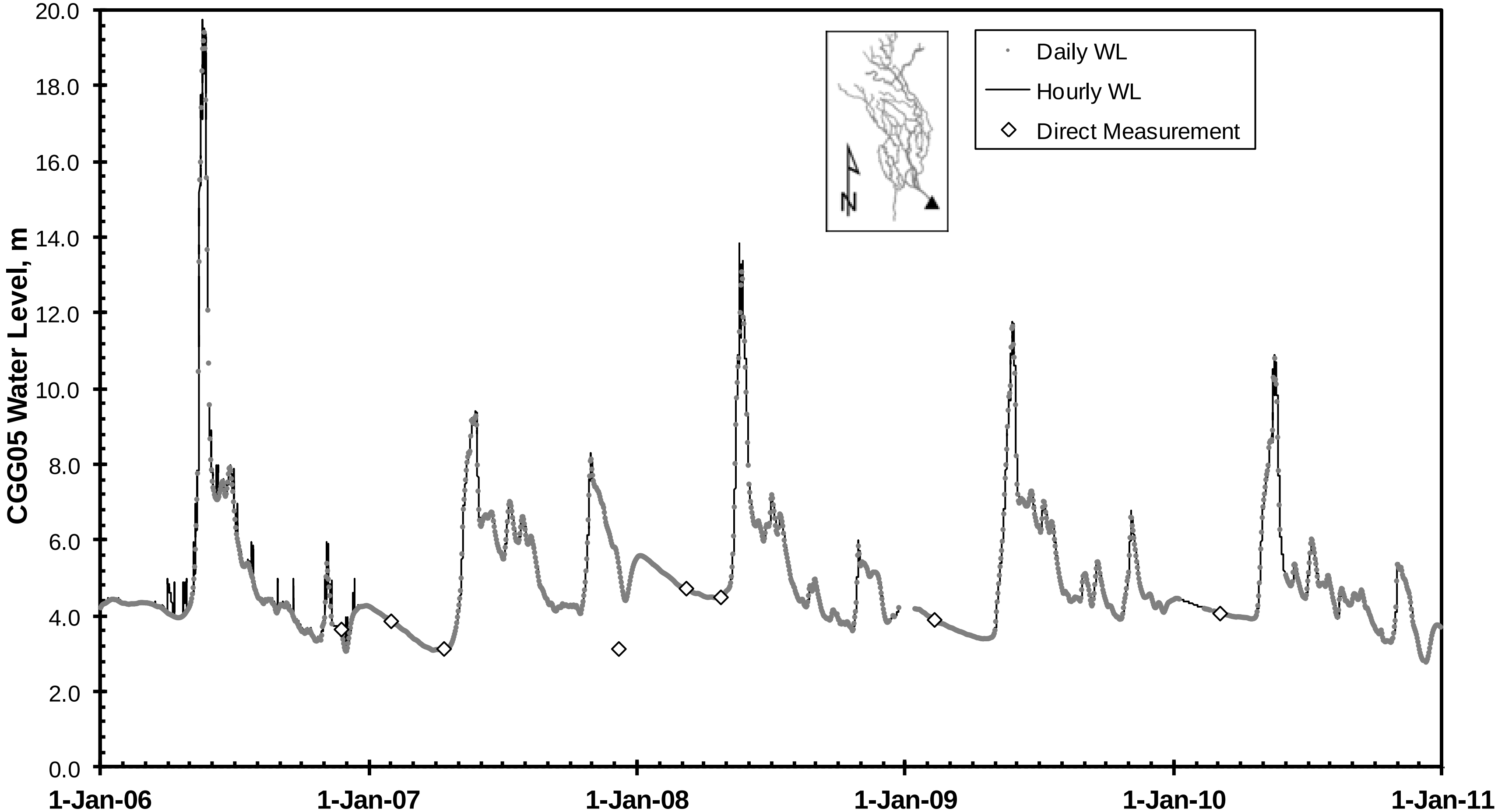

Figure B.4 Water levels from 2006 to 2010 at the WSC gauge *Mackenzie River at Arctic Red River* (10LC014). (Data source: the WSC).

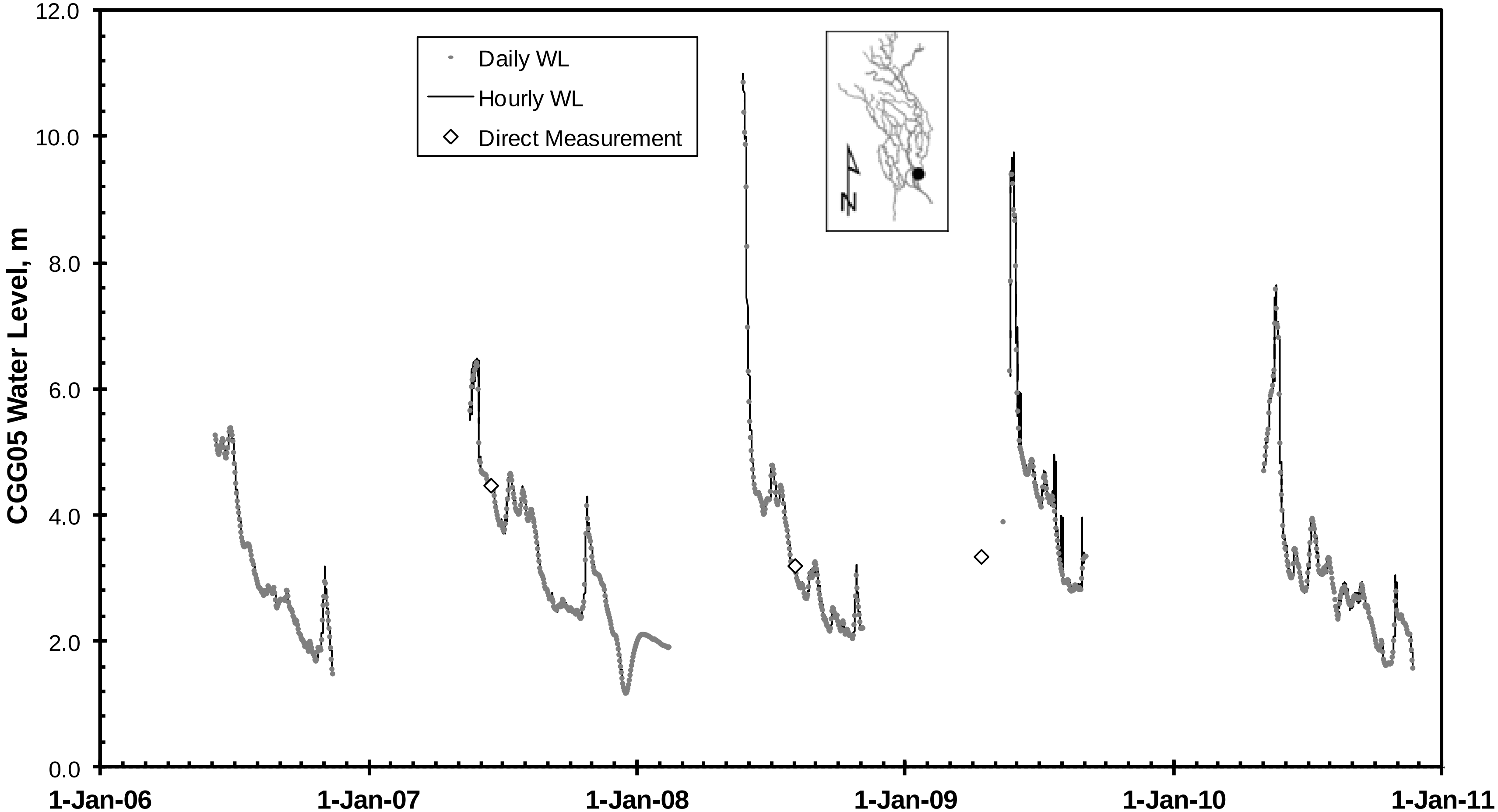

Figure B.5 Water levels from 2006 to 2010 at the WSC gauge *Mackenzie River at Confluence East Channel* (10LC015). (Data source: the WSC).

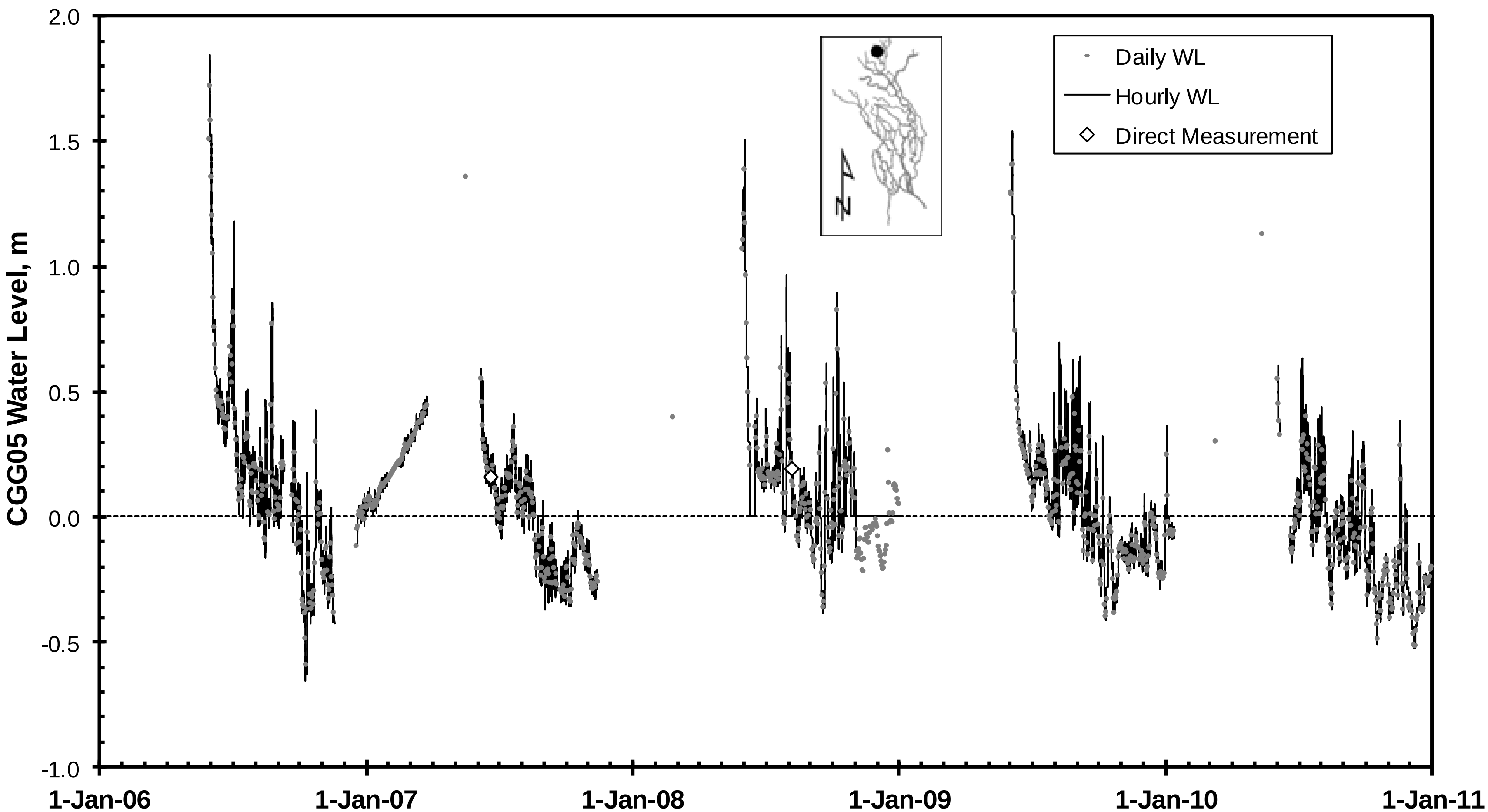

Figure B.6 Water levels from 2006 to 2010 at the WSC gauge *Mackenzie River (Kumak Channel) below Langley Island* (10LC019). (Data source: the WSC).

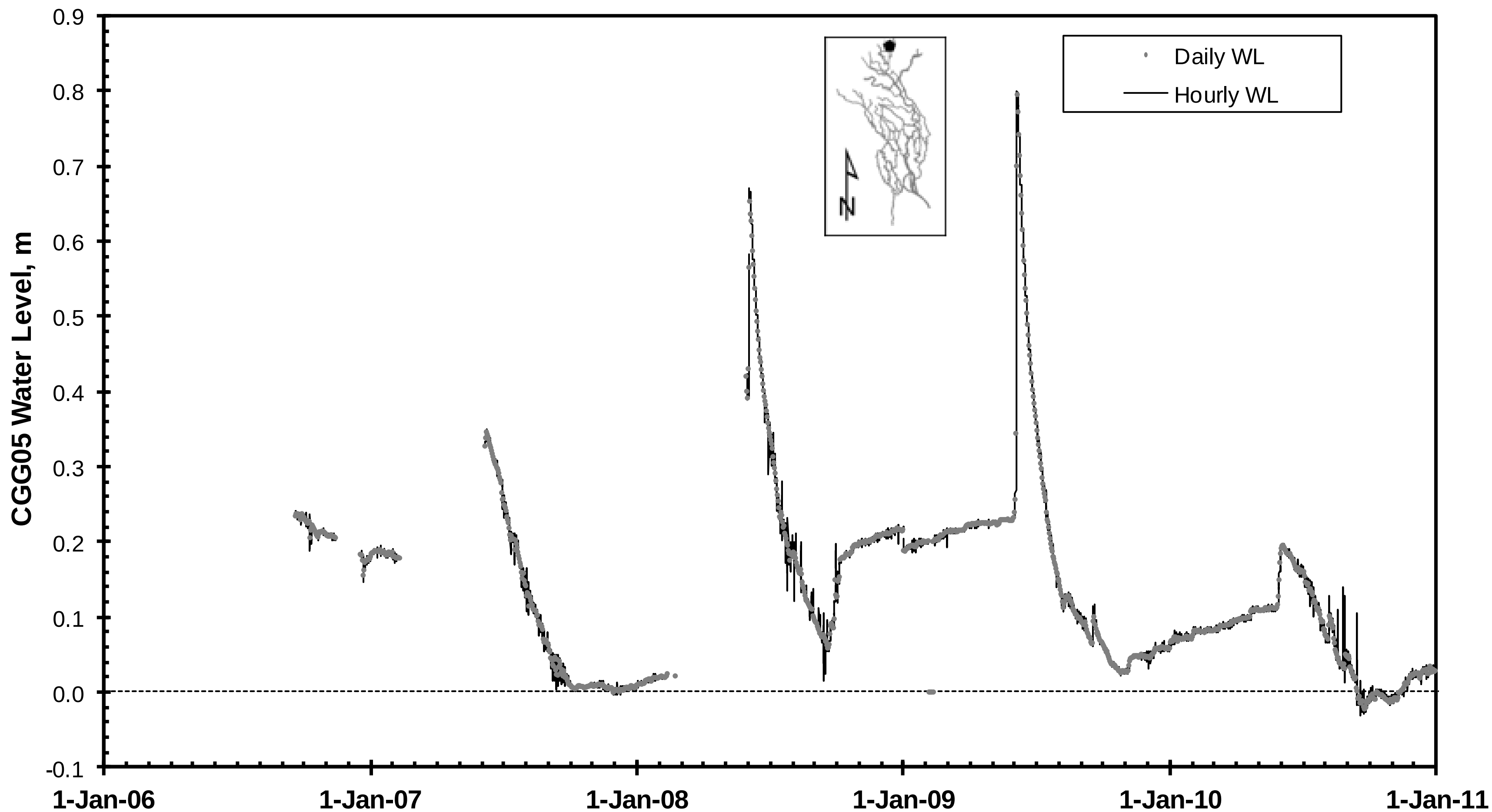

Figure B.7 Water levels from 2006 to 2010 at the WSC gauge *Big Lake at Taglu Island* (10LC020). (Data source: the WSC).

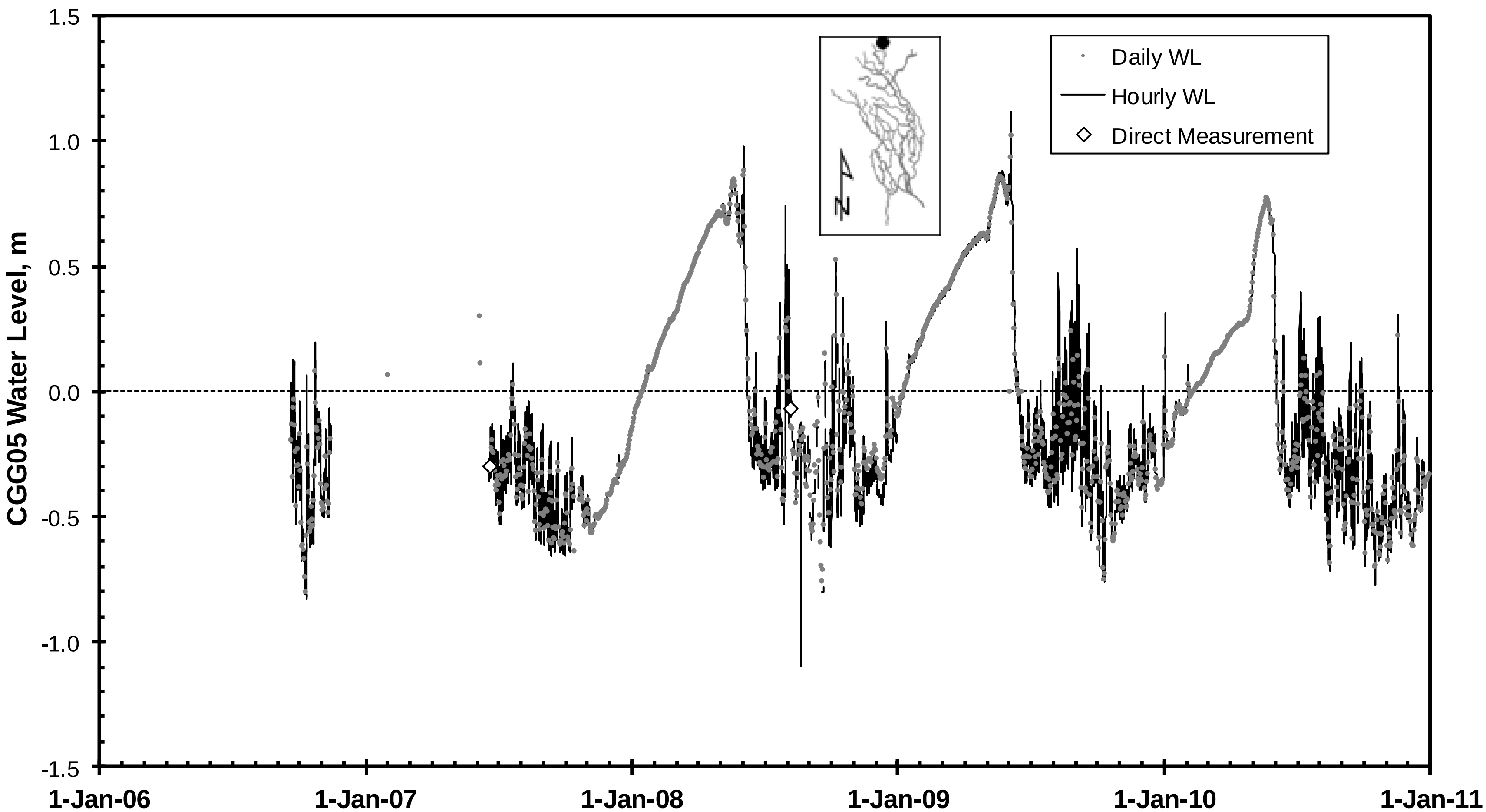

Figure B.8 Water levels from 2006 to 2010 at the WSC gauge *Mackenzie River at Kuluarpak Channel* (10LC021). (Data source: the WSC).

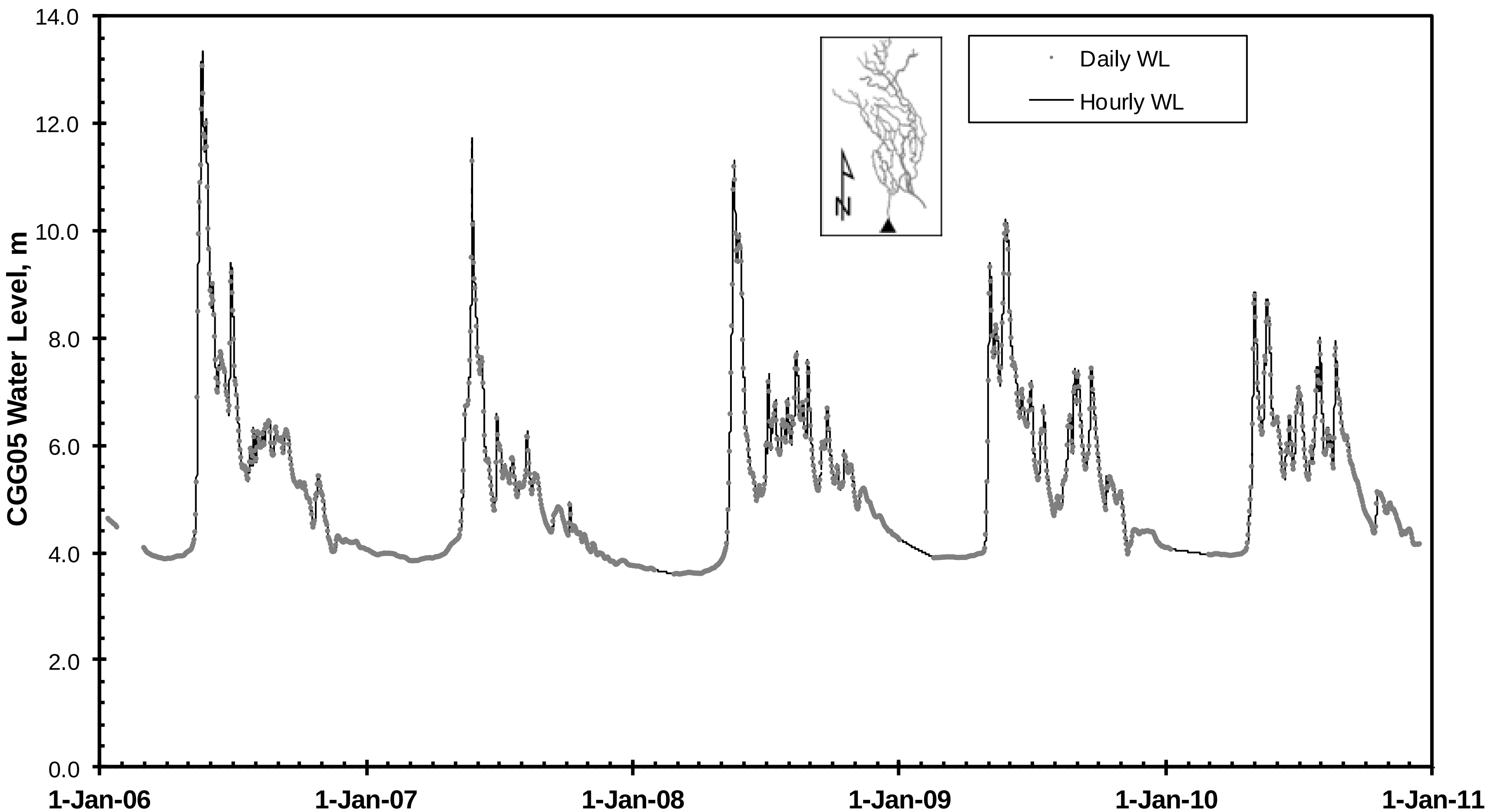

Figure B.9 Water levels from 2006 to 2010 at the WSC gauge *Peel River above Fort McPherson* (10MC002). (Data source: the WSC).

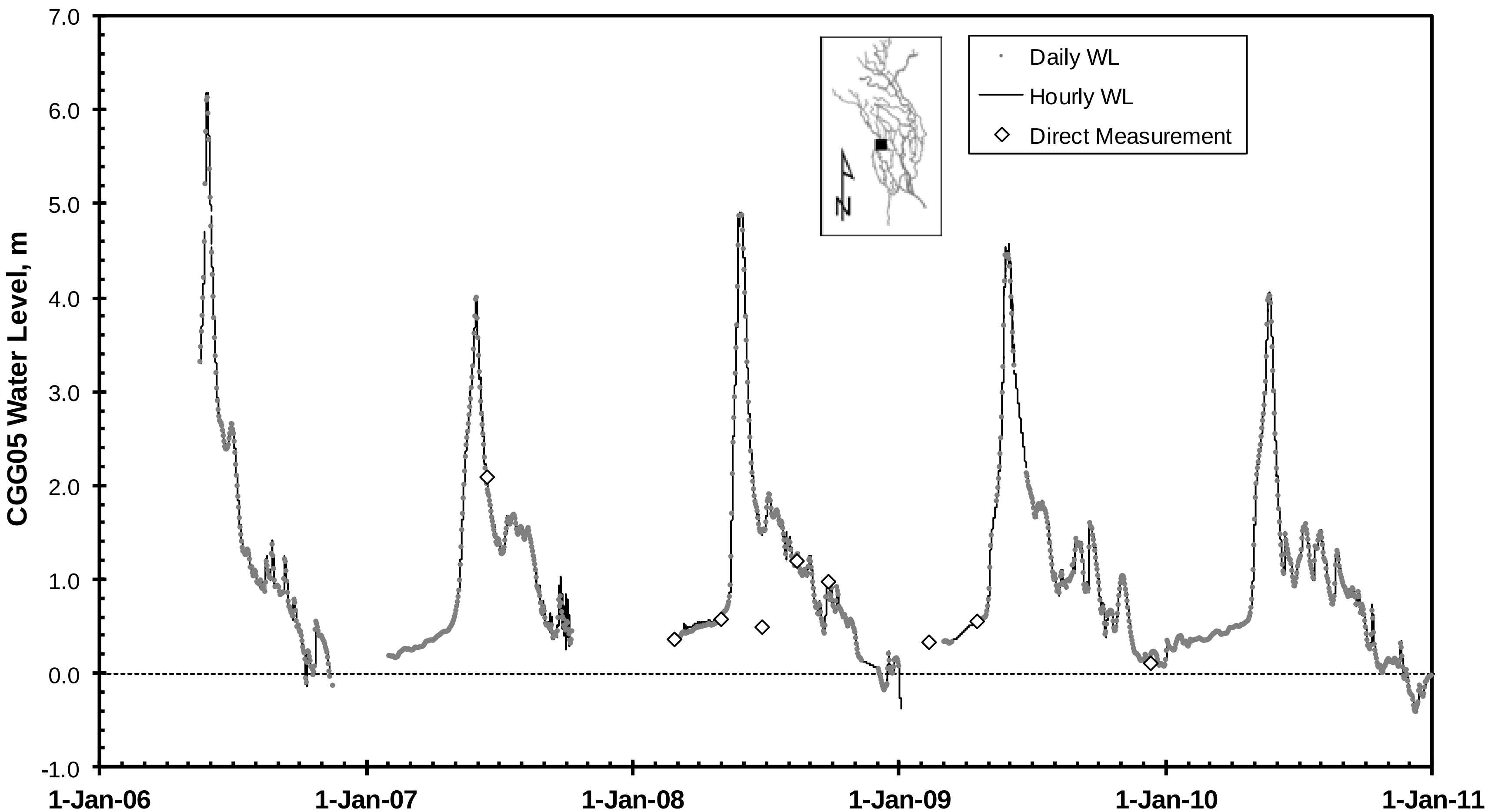

Figure B.10 Water levels from 2006 to 2010 at the WSC gauge *Mackenzie River (Peel Channel) above Aklavik* (10MC003). (Data source: the WSC).

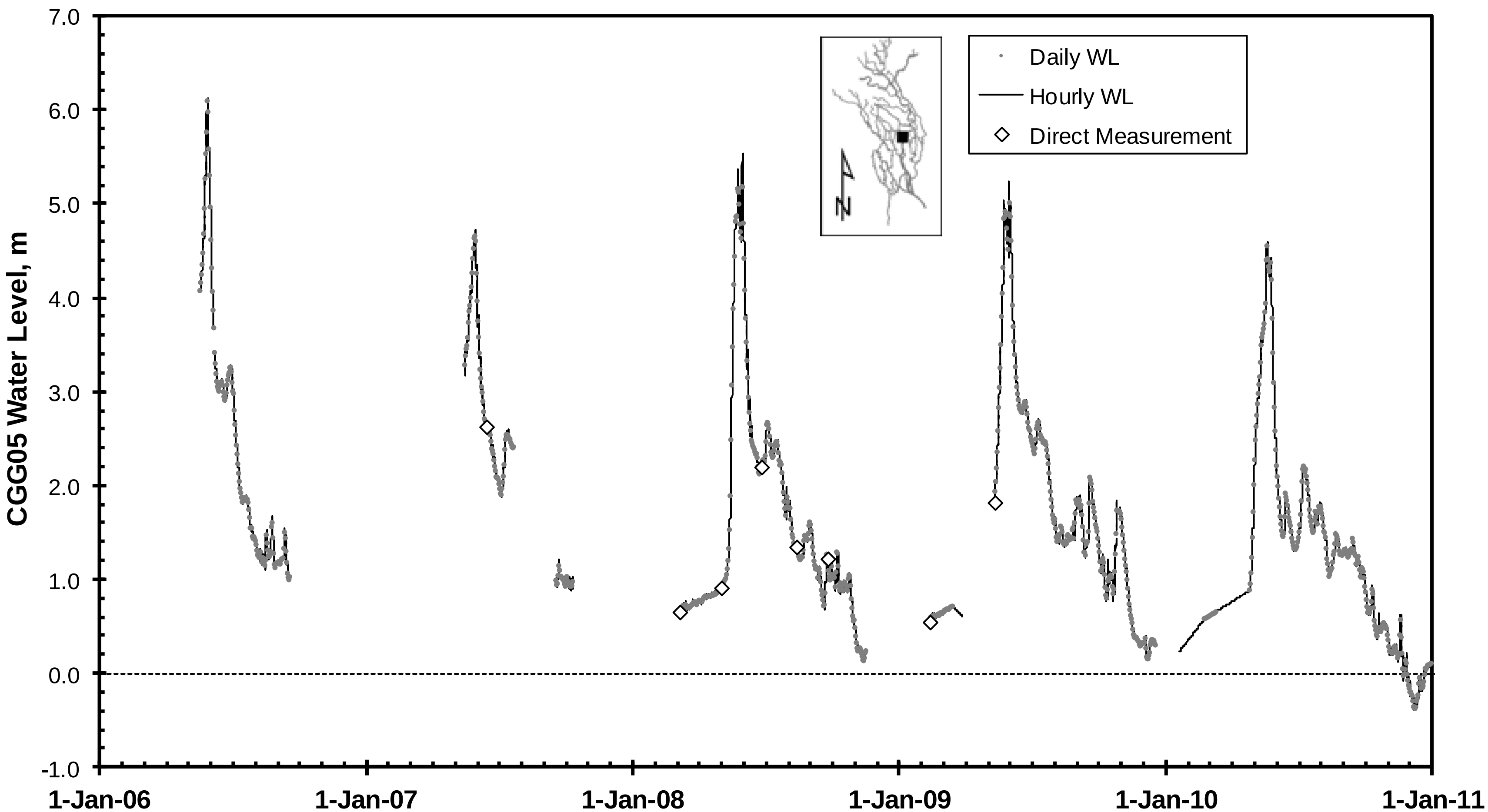

Figure B.11 Water levels from 2006 to 2010 at the WSC gauge *Mackenzie River (Middle Channel) below Raymond Channel* (10MC008). (Data source: the WSC).

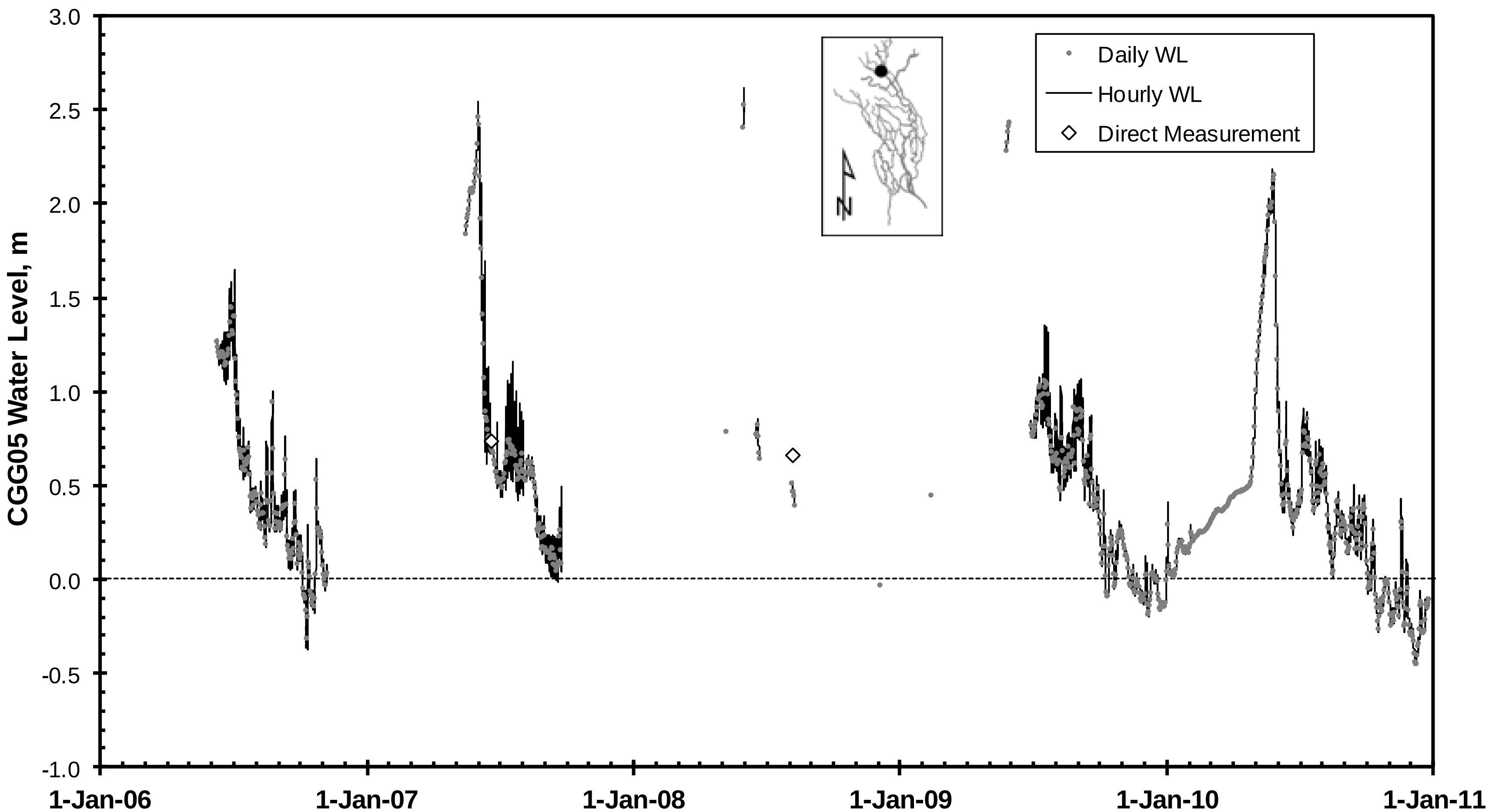

Figure B.12 Water levels from 2006 to 2010 at the WSC gauge *Mackenzie River (Outflow Middle Channel) below Langley Island* (10MC010). (Data source: the WSC).

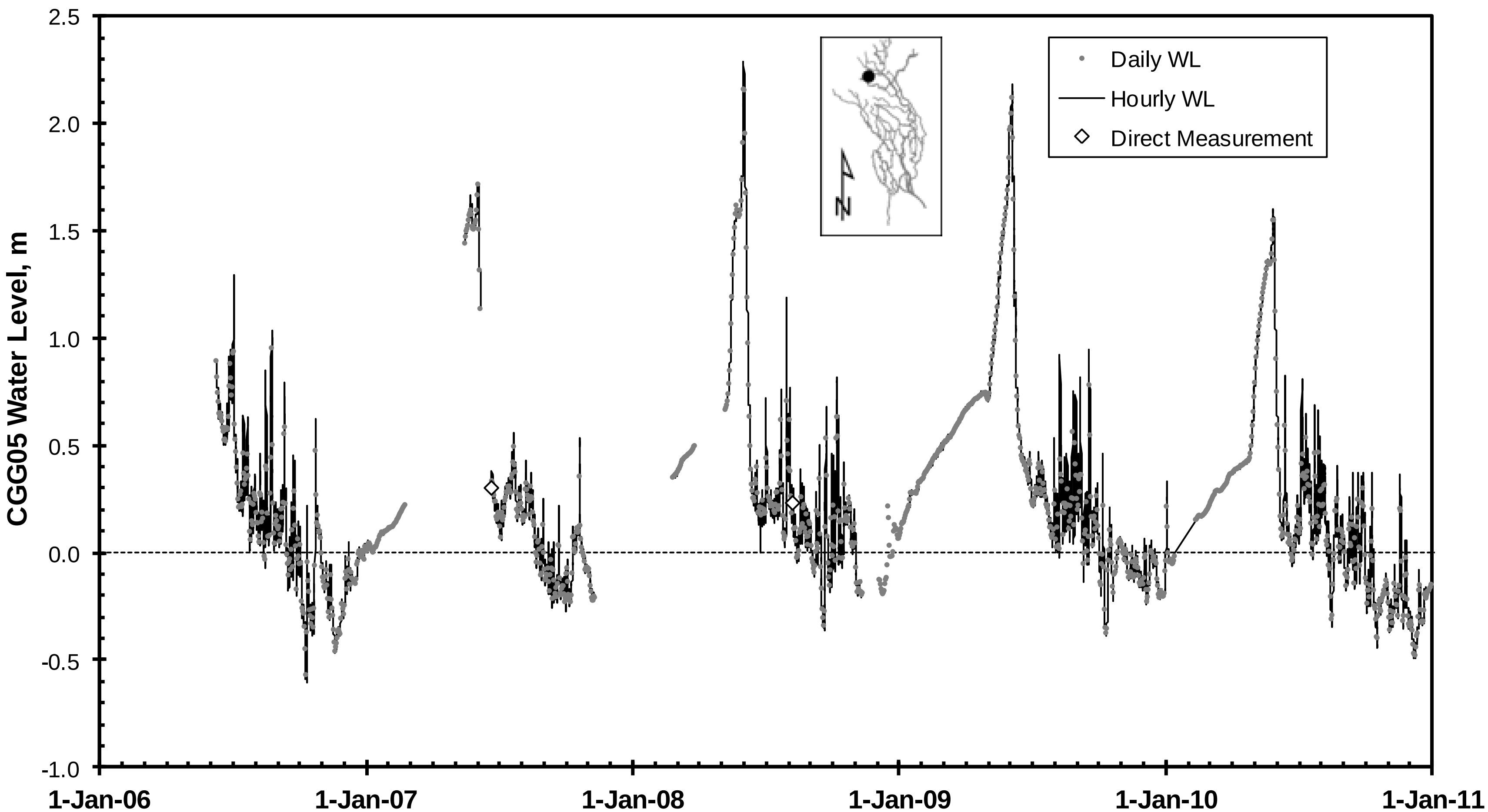

Figure B.13 Water levels from 2006 to 2010 at the WSC gauge *Mackenzie River (Reindeer Channel) at Ellice Island* (10MC011). (Data source: the WSC).

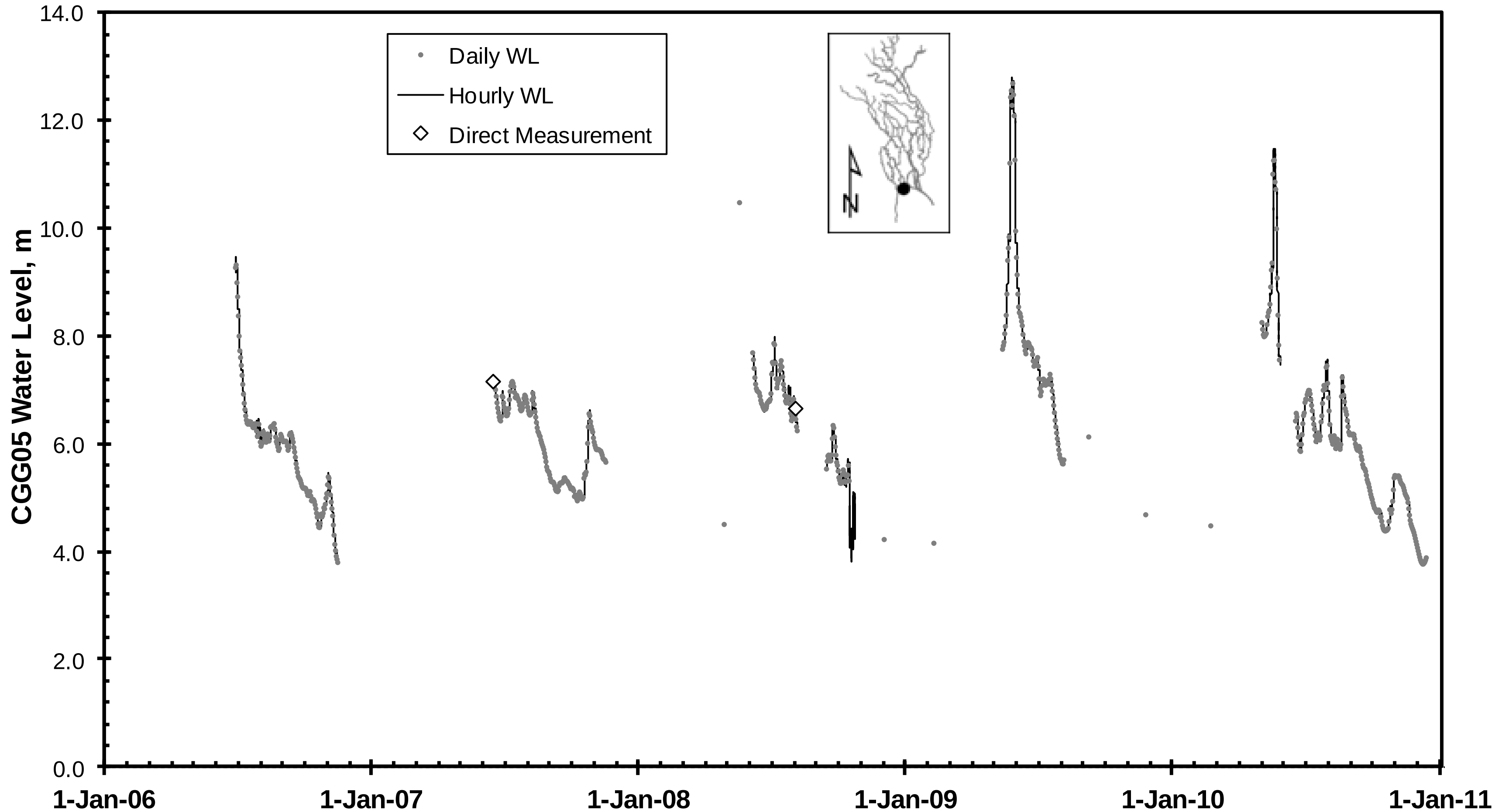

Figure B.14 Water levels from 2006 to 2010 at the WSC gauge *Peel River at Frog Creek* (10MC022). (Data source: the WSC).

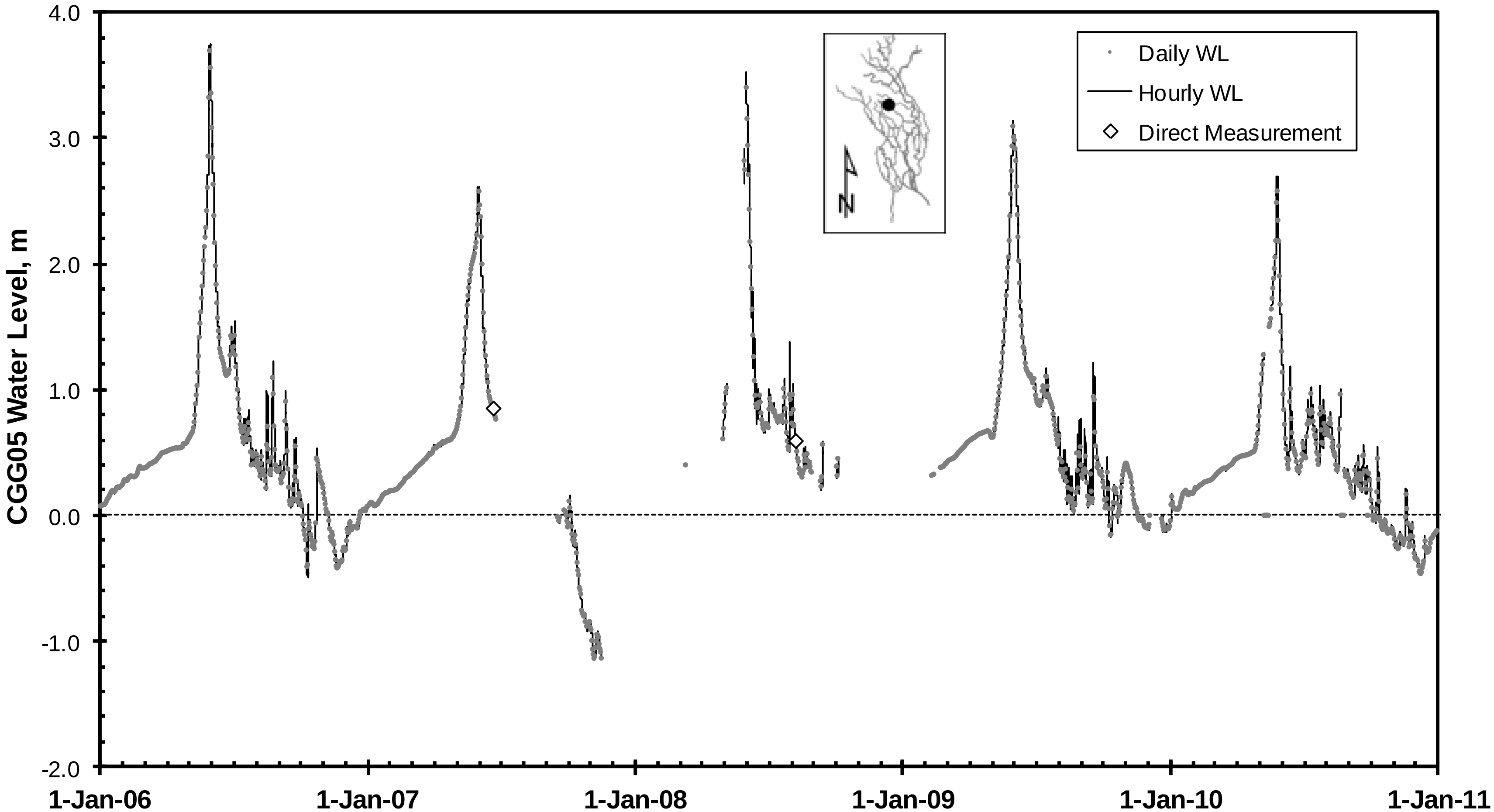

Figure B.15 Water levels from 2006 to 2010 at the WSC gauge *Mackenzie River (Napoiak Channel) above Shallow Bay* (10MC023). (Data source: the WSC).

Appendix C. Direct Manual Flow Measurements at Gauging Stations Operated by the WSC

This Appendix contains the direct manual water level and flow measurements that were obtained at each station in the Mackenzie Delta between 2007 and 2009 by the WSC. Elevations are shown to CGG05 datum. There are no measurements at *Big Lake at Taglu Island* (10LC020). The flow measurements at *Peel River above Fort McPherson* (10MC002) were unavailable. In addition, spreadsheets with all available hourly and daily data at each gauge over the study period are provided on the attached CD.

Table C.1(a) WSC direct manual water level and flow measurements at each of the station in the Mackenzie Delta.

Station Number	Date and Time	CGG05 Elevation (m)	Discharge (m^3/s)	Notes
10LC002	3-Feb-07 14:40	0.421	30.8	
	10-Apr-07 16:25	0.654	17.2	
	21-Jun-07 17:07	2.038	409	
	29-Nov-07 16:24	0.448	77.9	
	29-Feb-08 14:39	0.626	47.9	
	24-Apr-08 14:45	0.374	27.8	
	11-Jun-08 15:37	2.280	431	NW wind (Backwater)
	7-Aug-08 15:18	1.262	209	
	28-Nov-08 15:39		48.4	
	6-Mar-09 15:10	0.734	17.46	
	24-Apr-09 9:45	0.844	15	
	16-Dec-09 15:06	0.326	44.129	
	11-Mar-10 16:18	0.619	38.724	
10LC012	18-Jun-07 20:03	0.887	89.4	
	4-Aug-08 16:45	0.672	21.7	
	17-Sep-09 11:59	0.422	20.5	
10LC013	2-Aug-07 17:24	-0.045	4040	
	4-Aug-08 15:15	-0.126	3718	
10LC014	23-Nov-06 20:54	3.659	2973	
	30-Jan-07 14:27	3.875	3778	
	12-Apr-07 14:19	3.144	3551	
	6-Dec-07 15:25	3.143	4072	
	7-Mar-08 14:40	4.739	4008	
	23-Apr-08 15:15	4.508	3869	
	8-Feb-09 15:00	3.911	4094	
	5-May-09 12:53		6550	
	17-Dec-09 16:08		3854	
	4-Mar-10 14:05	4.079	4450	
10LC015	15-Jun-07 16:55	4.475	1110	
	2-Aug-08 20:45	3.201	577	
	13-Apr-09 13:10	3.346	639	
10LC019	19-Jun-07 20:37	0.162	2830	
	5-Aug-08 13:55	0.195	2326	
10LC021	19-Jun-07 17:08	-0.296	268	
	5-Aug-08 11:05	-0.066	260	

Table C.1(b). WSC direct manual water level and flow measurements at each of the station in the Mackenzie Delta (continued).

Station Number	Date and Time	CGG05 Elevation (m)	Discharge (m^3/s)	Notes
10MC003	14-Jun-07 17:22	2.098	1190	
	26-Feb-08 14:15	0.370	218	
	30-Apr-08 14:45	0.584	196	
	25-Jun-08 19:30	0.500	860	
	12-Aug-08 12:00	1.204	973	
	24-Sep-08 16:08	0.984	846	
	9-Feb-09 14:40	0.339	137	
	16-Apr-09 14:10	0.561	189.2	
	10-Dec-09 13:50	0.115	139	
10MC008	14-Jun-07 13:09	2.629	16900	
	5-Mar-08 13:25	0.656	3960	
	1-May-08 14:15	0.913	3876	
	25-Jun-08 15:00	2.200	16200	
	12-Aug-08 15:00	1.349	13000	
	24-Sep-08 13:05	1.223	10200	
	11-Feb-09 14:36	0.549	3990	
	11-May-09 14:30	1.822	8402	
	19-Jan-10 14:24		4434	
10MC010	19-Jun-07 11:49	0.740	6280	Middle Channel
	19-Jun-07 12:25	0.732	2680	Gauge Channel
	5-Aug-08 15:40	0.665	5020	Middle Channel
	5-Aug-08 16:10	-0.745	2127	Gauge Channel
10MC011	20-Jun-07 13:14	0.305	4630	
	6-Aug-08 11:45	0.235	2945	
10MC022	15-Jun-07 14:39	7.164	725	
	2-Aug-08 14:15	6.663	1443	
10MC023	20-Jun-07 18:56	0.856	1010	
	6-Aug-08 15:30	0.597	632	

Appendix D. Summary of Flows Used for Open Water Modeling Effort

This appendix shows a table of the flows used for modeling in HEC-RAS based upon the assumptions outlined in Section 4.4.1. For the open water scenarios, the type of flow is shown (assumed, calculated or measured). The percentage of total delta inflow is also shown for each of the open water scenarios.

Table D.1(a). Summary of flow used the flow scenarios modelled.

Reach name	d/s flow change station (km)	u/s flow change station (km)	Flow (m^3/s)							Percent of Total Delta Inflow		
			Calibration Scenario		Validation Scenario #1		Validation Scenario #2		Winter Scenario	Calibration Scenario	Validation Scenario #1	Validation Scenario #2
			14707	Q_r	23512	Q_r	14832	Q_r	3517	14707	23512	14832
M-1	0	25	13220	Q_r	22568	Q_r	13665	Q_r	3271	89.9%	96.0%	92.1%
M-2	25	31.5	13220	Q_c	22568	Q_c	13665	Q_c	3271	89.9%	96.0%	92.1%
M-3	31.5	39	12201	Q_c	20899	Q_c	12565	Q_c	3021	83.0%	88.9%	84.7%
M-4	39	45	8538	Q_c	13336	Q_c	8029	Q_c	1980	58.1%	56.7%	54.1%
M-5	45	48.2	8538	Q_c	13336	Q_c	8029	Q_c	1980	58.1%	56.7%	54.1%
M-6	48.2	59.5	7961	Q_m	12226	Q_a	7390	Q_m	1829	54.1%	52.0%	49.8%
M-7	59.5	62.5	11624	Q_c	19789	Q_c	11926	Q_c	2870	79.0%	84.2%	80.4%
M-8	62.5	82.5	13350	Q_c	21820	Q_c	13459	Q_c	3257	90.8%	92.8%	90.7%
M-9	82.5	140.8	12003	Q_r	17903	Q_r	12001	Q_r	2771	81.6%	76.1%	80.9%
M-10	140.8	221	11371	Q_c	16893	Q_c	11300	Q_m	2620	77.3%	71.8%	76.2%
M-11	221	223	7965	Q_c	10910	Q_c	6470	$Q_{c\ (avg.)}$	1766	54.2%	46.4%	43.6%
M-12	223	245	5020	Q_m	6280	Q_m	2250	Q_m	1069	34.1%	26.7%	15.2%
M-13	245	258.5	2893	Q_c	3600	Q_c	1293	Q_c	612	19.7%	15.3%	8.7%
M-14	258.5	281	2633	Q_c	3332	Q_c	1071	Q_c	559	17.9%	14.2%	7.2%
M-15	281	293.5	2326	Q_m	2830	Q_m	760	Q_c	489	15.8%	12.0%	5.1%

Table D.1(b). Summary of flow used the flow scenarios modelled.

Reach name	d/s flow change station (km)	u/s flow change station (km)	Flow (m^3/s)							Percent of Total Delta Inflow		
			Calibration Scenario		Validation Scenario #1		Validation Scenario #2		Winter Scenario	Calibration Scenario	Validation Scenario #1	Validation Scenario #2
E-1	48.2	76.7	577	Q_m	1110	Q_m	639	Q_m	151	3.9%	4.7%	4.3%
E-2	76.7	117.7	409	Q_c	754	Q_c	440	Q_c	104	2.8%	3.2%	3.0%
E-3	117.7	232.2	241	Q_r	397	Q_r	240	Q_r	56	1.6%	1.7%	1.6%
E-4	232.2	284.2	3718	Q_m	6291	Q_c	4950	Q_c	928	25.3%	26.8%	33.4%
W-1	0	42.5	1487	Q_r	944	Q_r	1167	Q_r	246	10.1%	4.0%	7.9%
W-2	42.5	64.8	1414	$Q_{m\ (avg.)}$	725	Q_m	1059	Q_c	236	9.6%	3.1%	7.1%
W-3	64.8	162.5	652	Q_m	363	Q_c	626	Q_c	155	4.4%	1.5%	4.2%
W-4	162.5	282	908	Q_r	1179	Q_r	703	Q_r	179	6.2%	5.0%	4.7%
WM-1	64.8	68.8	707	Q_m	362	Q_a	433	Q_m	137	4.8%	1.5%	2.9%
WM-2	68.8	94.8	1726	Q_c	2031	Q_c	1533	Q_c	387	11.7%	8.6%	10.3%
NP-1	140.8	204.3	632	Q_m	1010	Q_m	701	Q_c	151	4.3%	4.3%	4.7%
NL-1	221	233	3452	$Q_{c\ (avg.)}$	5983	Q_c	4730	Q_m	863	23.5%	25.4%	31.9%
RD-1	223	289	2945	Q_m	4630	Q_m	4120	Q_m	700	20.0%	19.7%	27.8%

Table D.1(c). Summary of flow used the flow scenarios modelled.

Reach	Flow (m3/s)						Percent of Total Delta Inflow		
	Calibration Scenario		Validation Scenario #1		Validation Scenario #2		Calibration Scenario	Validation Scenario #1	Validation Scenario #2
A	0	Q_a	0	Q_a	0	Q_a	0.0%	0.0%	0.0%
B	1019	Q_m	1669	Q_a	1100	Q_m	6.9%	7.1%	7.4%
C	3663	Q_c	7563	Q_c	4536	Q_c	24.9%	32.2%	30.6%
D	1347	Q_c	3917	Q_c	1458	Q_c	9.2%	16.7%	9.8%
E	168	Q_a	356	Q_a	199	Q_a	1.1%	1.5%	1.3%
F	168	Q_a	357	Q_a	200	Q_a	1.1%	1.5%	1.3%
G	73	Q_c	219	Q_c	108	Q_a	0.5%	0.9%	0.7%
H	256	Q_c	816	Q_c	77	Q_c	1.7%	3.5%	0.5%
I	21.9	Q_m	89.4	Q_m	20.5	Q_m	0.1%	0.4%	0.1%
J	2127	Q_m	2680	Q_m	957	Q_a	14.5%	11.4%	6.5%
K	260	Q_m	268	Q_m	222	Q_a	1.8%	1.1%	1.5%
L	307	Q_c	502	Q_c	311	Q_a	2.1%	2.1%	2.1%

Appendix E. Modeled Water Surface for Open Water Validations Periods

This appendix shows figures of the modeled water surface for both of the open water validation periods:

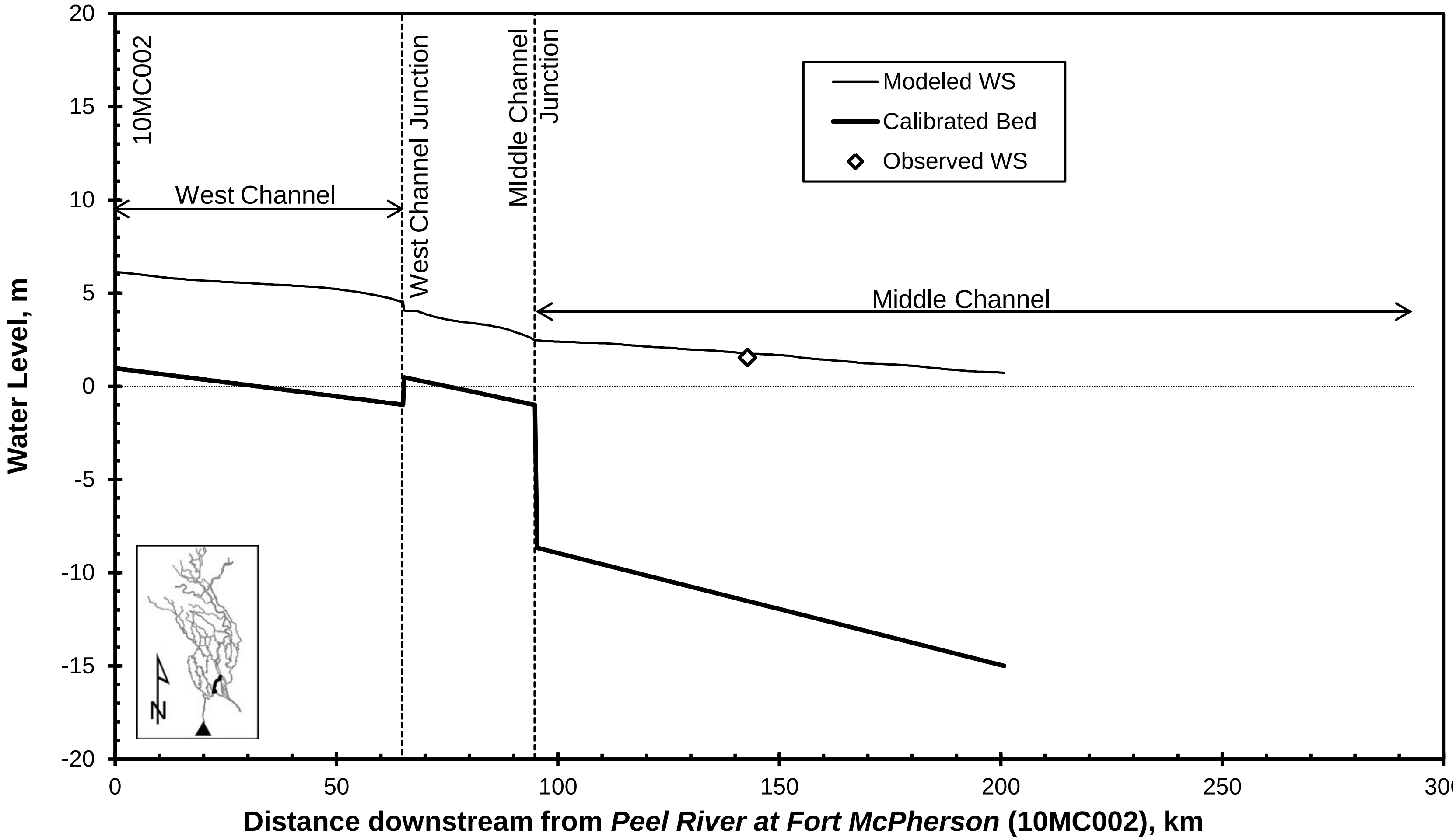

Figure E.11 Modeled water surface for Validation Scenario #2 from 4-Sep-09 to 17-Sep-09 along the West-Middle Connector Channel using calibrated bed slope and elevation.

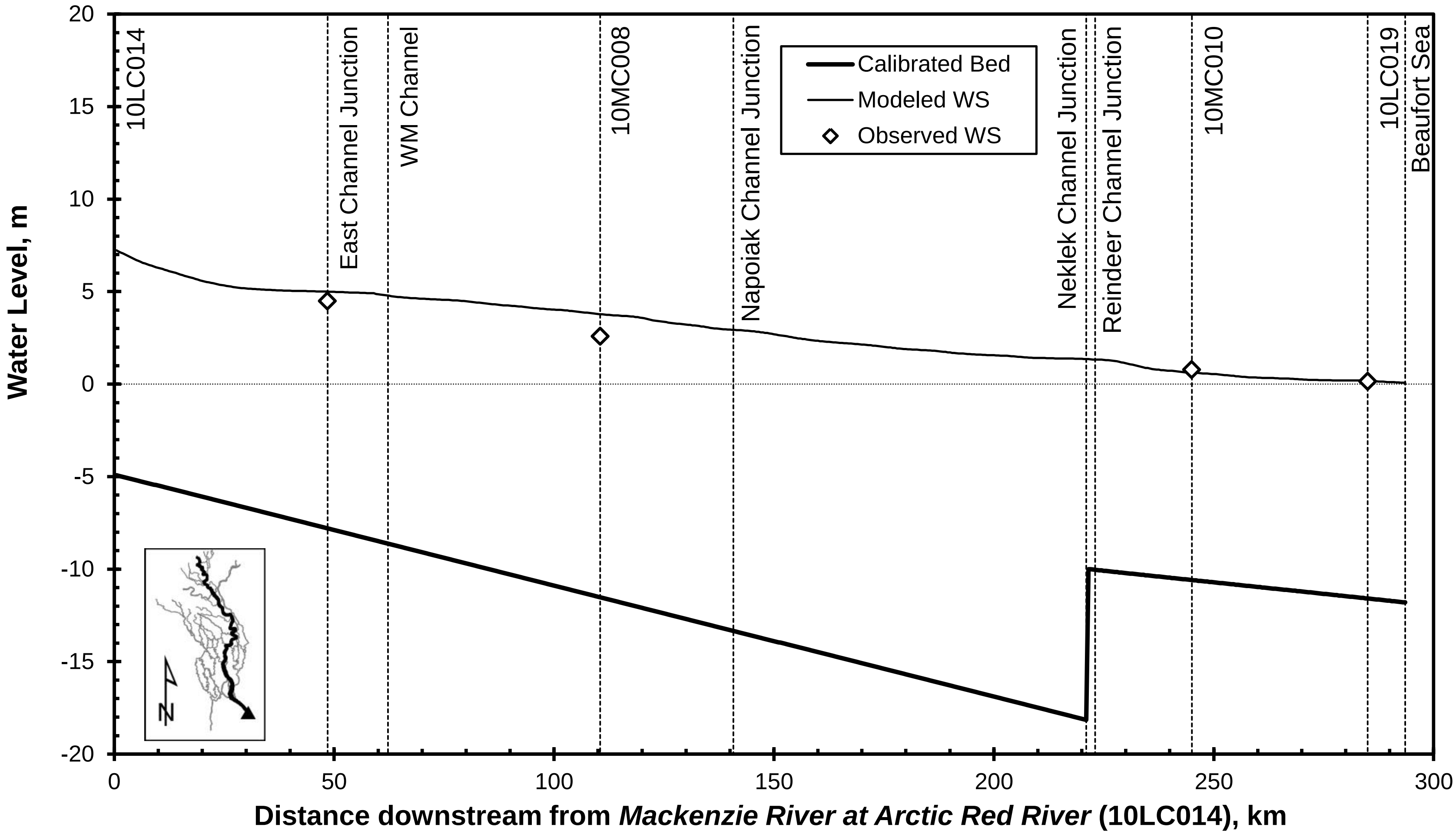

Figure E.1 Modeled water surface for Validation Scenario #1 from 14-Jun-07 to 20-Jun-07 along the Middle Channel using calibrated bed slope and elevation.

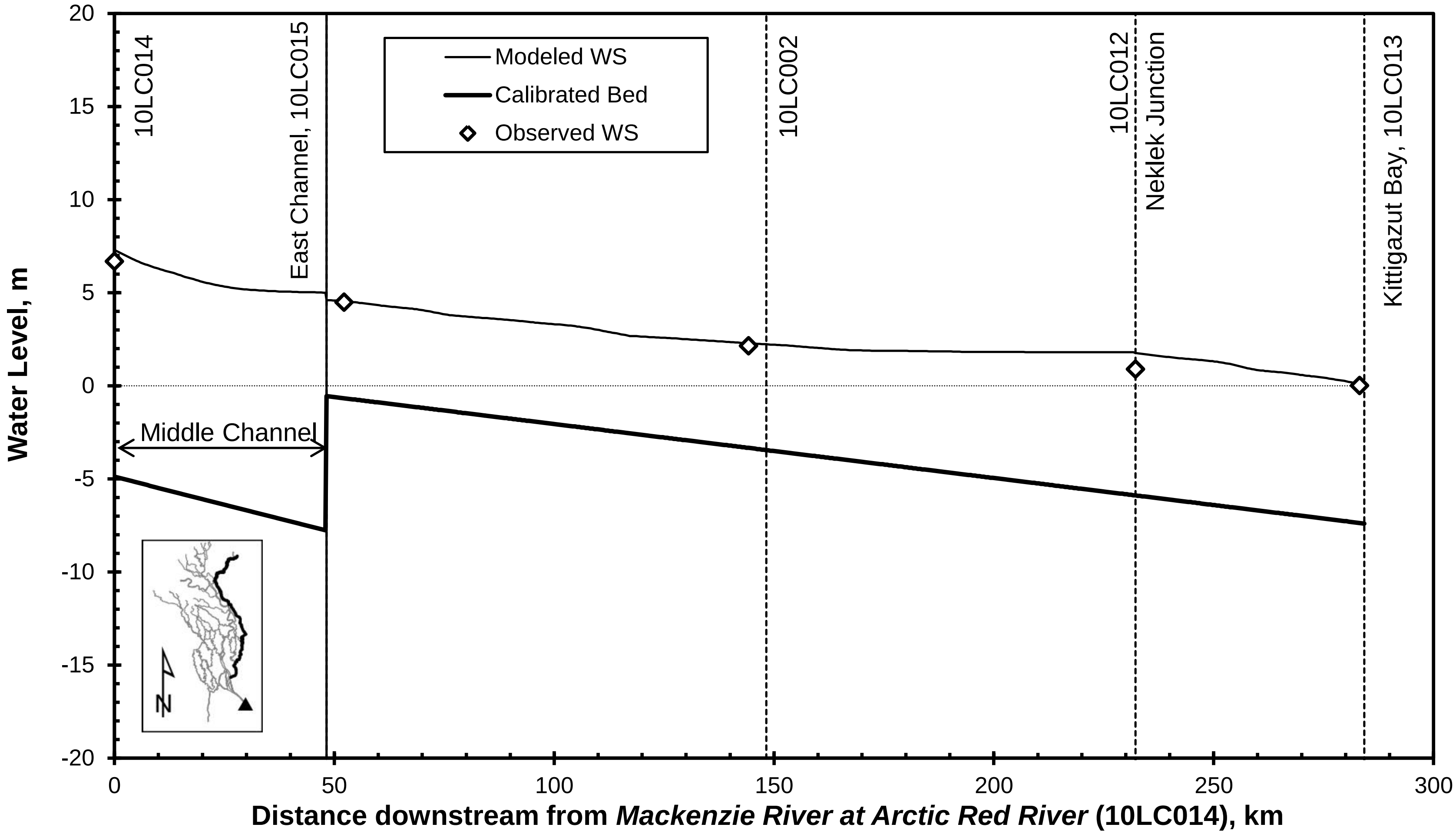

Figure E.2 Modeled water surface for Validation Scenario #1 from 14-Jun-07 to 20-Jun-07 along the East Channel using calibrated bed slope and elevation.

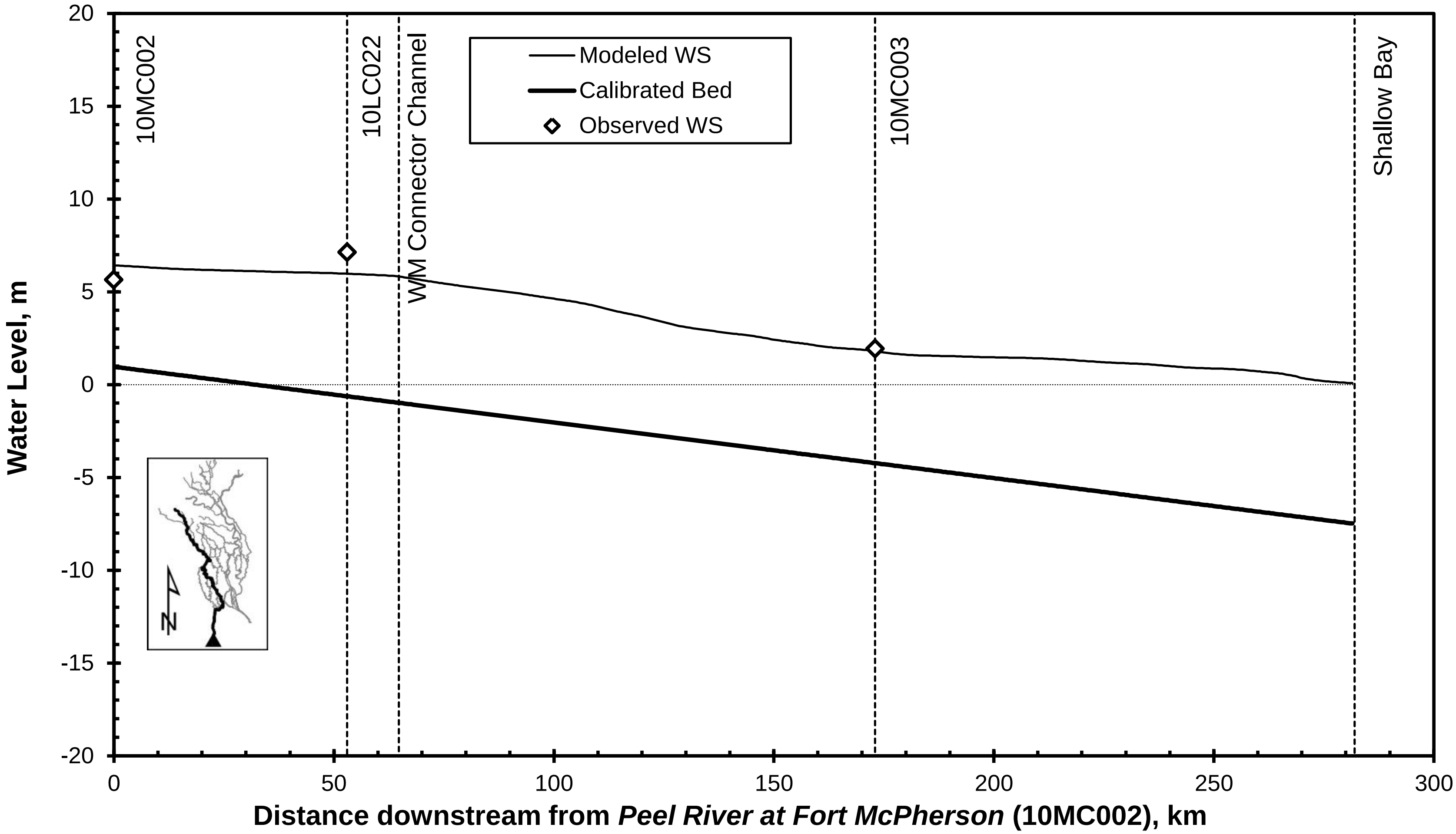

Figure E.3 Modeled water surface for Validation Scenario #1 from 14-Jun-07 to 20-Jun-07 along the East Channel using calibrated bed slope and elevation.

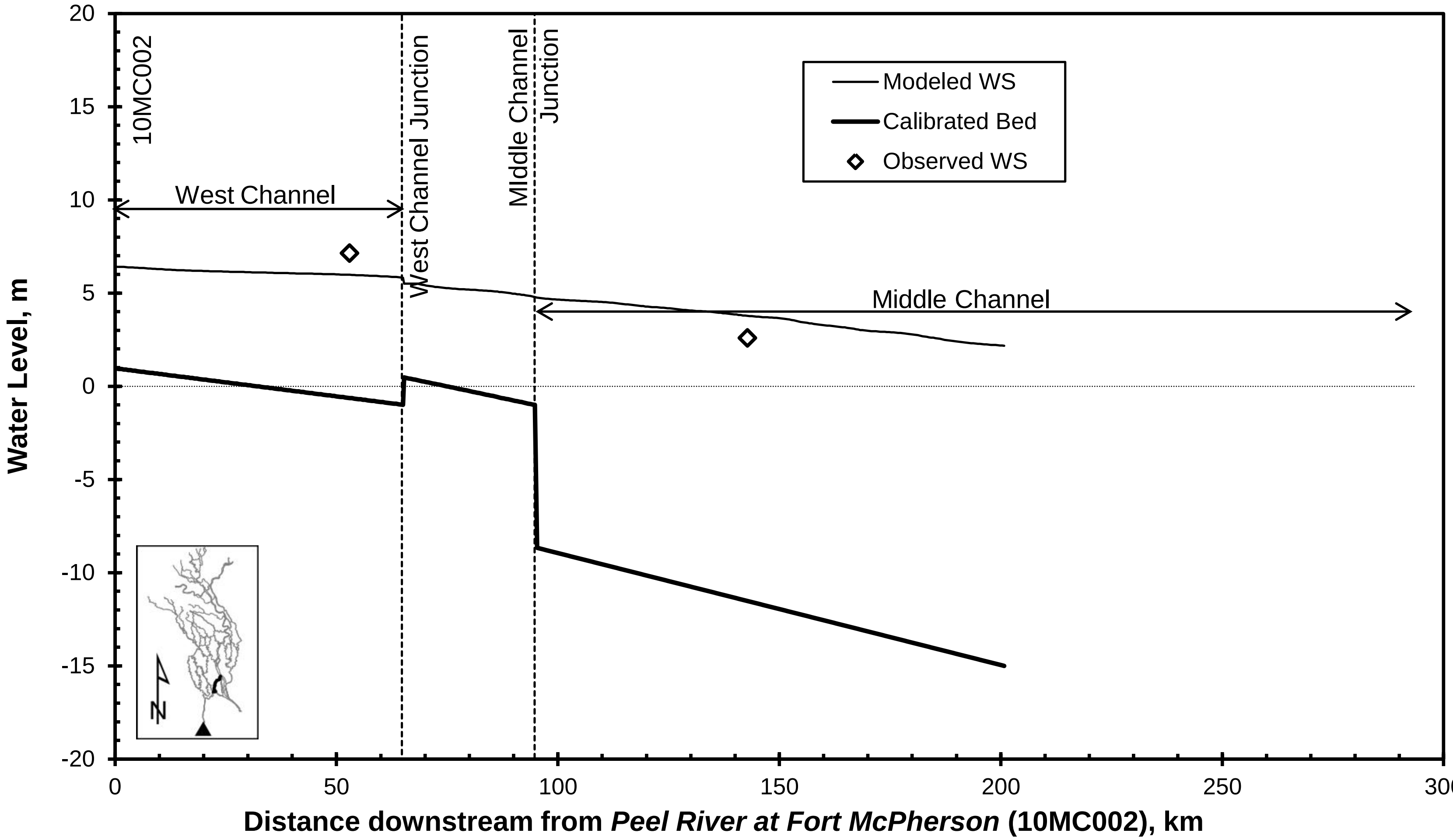

Figure E.4 Modeled water surface for Validation Scenario #1 from 14-Jun-07 to 20-Jun-07 along the West-Middle Connector Channel using calibrated bed slope and elevation.

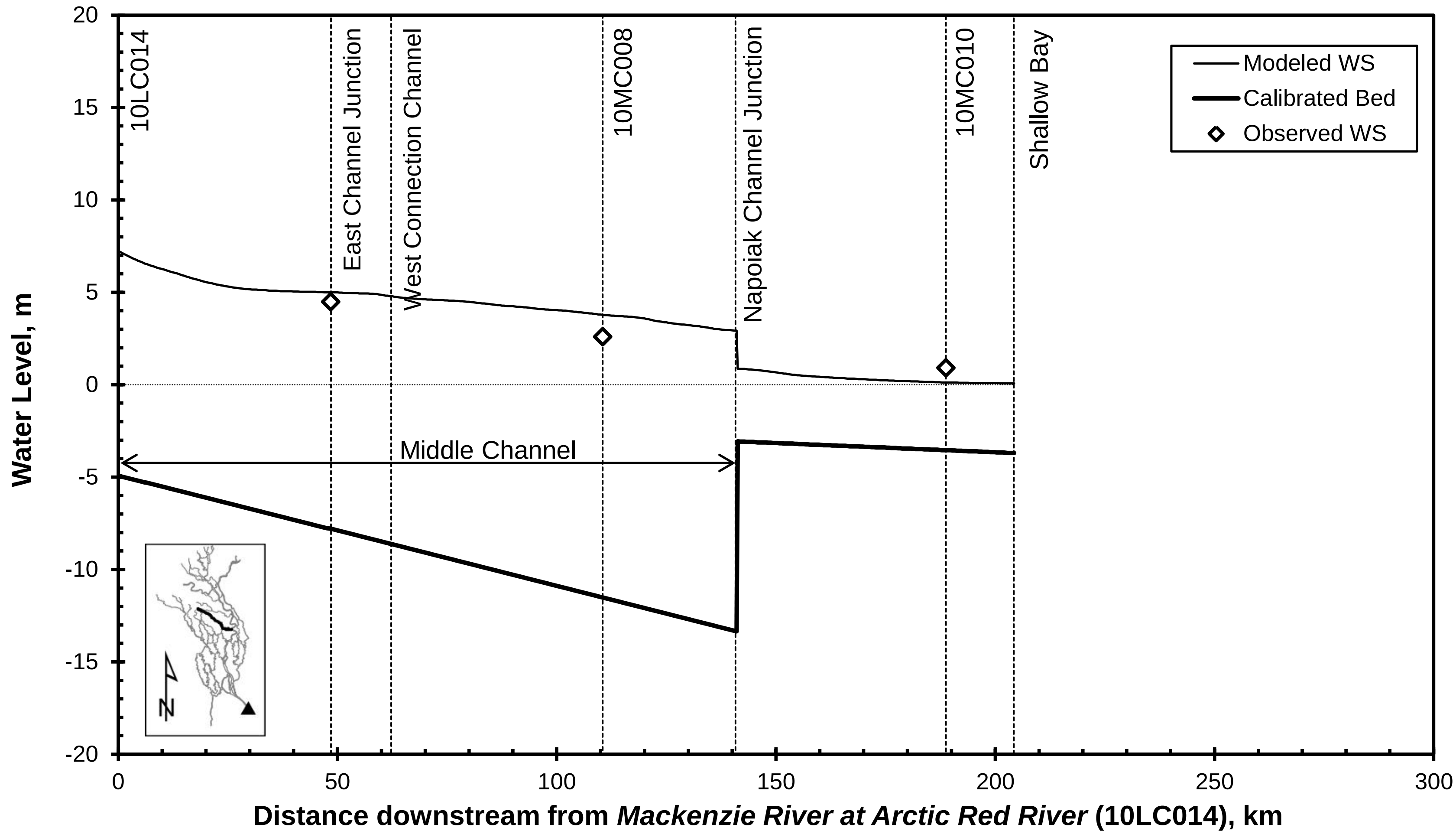

Figure E.5 Modeled water surface for Validation Scenario #1 from 14-Jun-07 to 20-Jun-07 along the Napoiak Channel using calibrated bed slope and elevation.

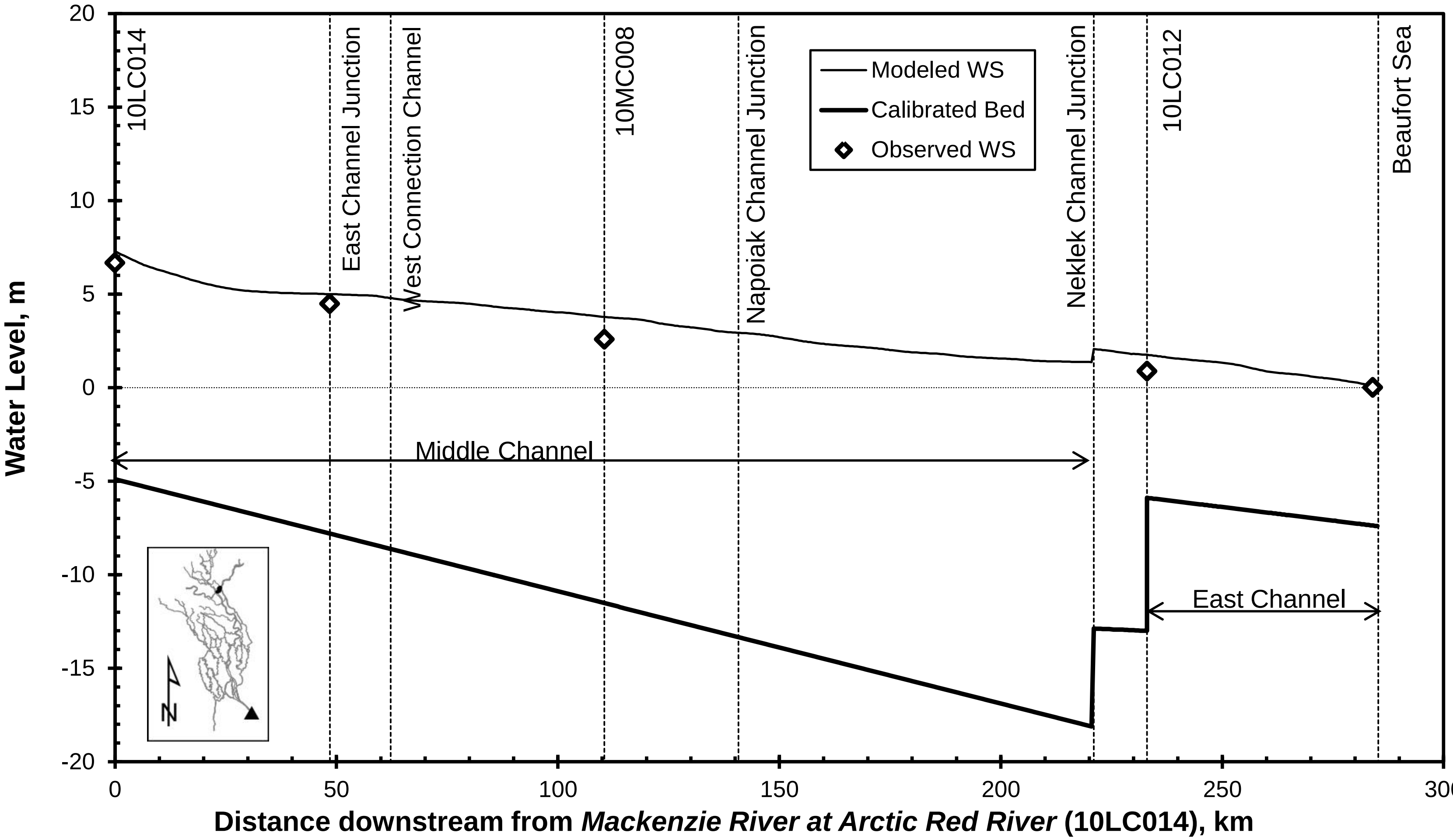

Figure E.6 Modeled water surface for Validation Scenario #1 from 14-Jun-07 to 20-Jun-07 along the Neklek Channel using calibrated bed slope and elevation.

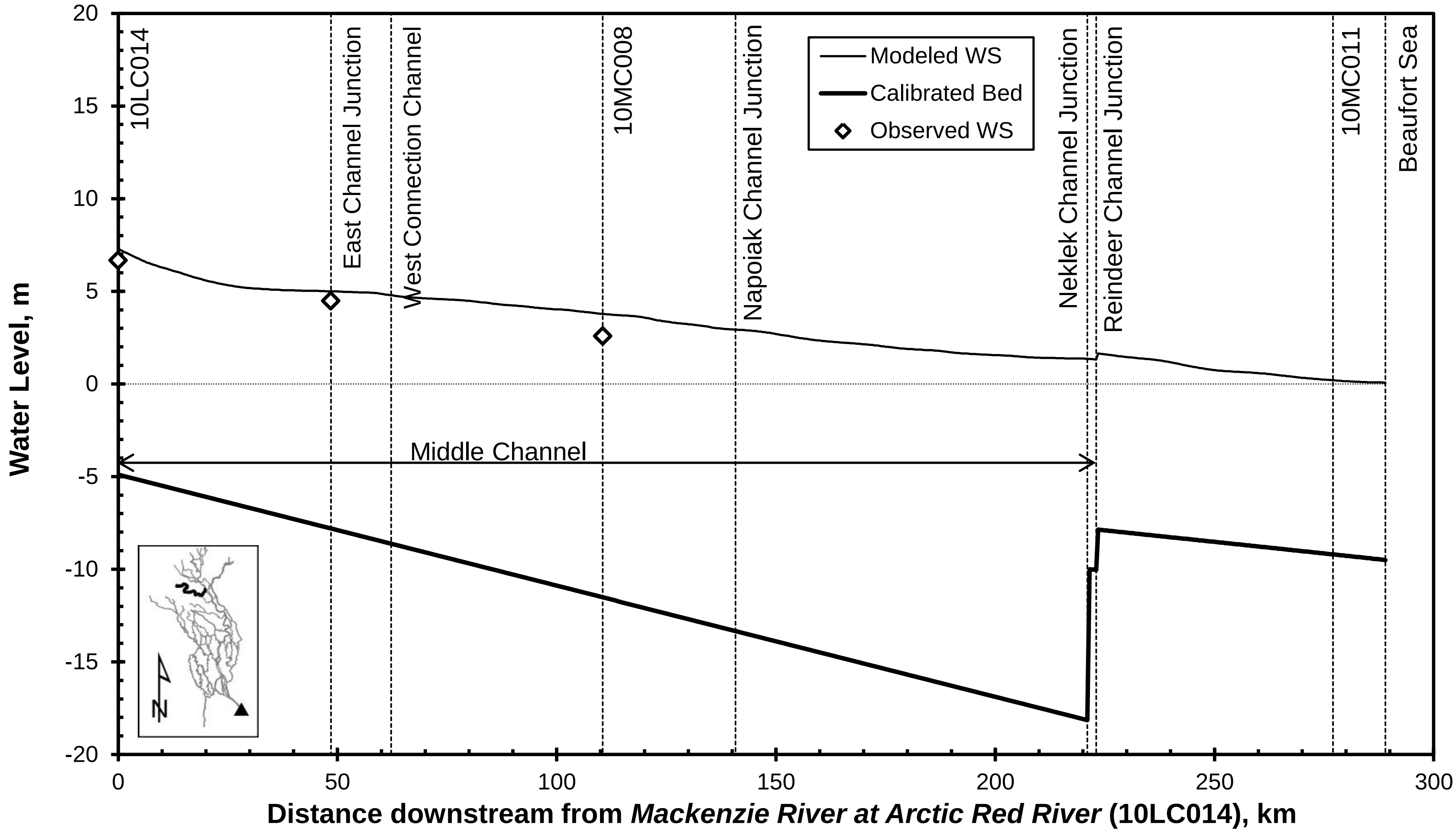

Figure E.7 Modeled water surface for Validation Scenario #1 from 14-Jun-07 to 20-Jun-07 along the Reindeer Channel using calibrated bed slope and elevation.

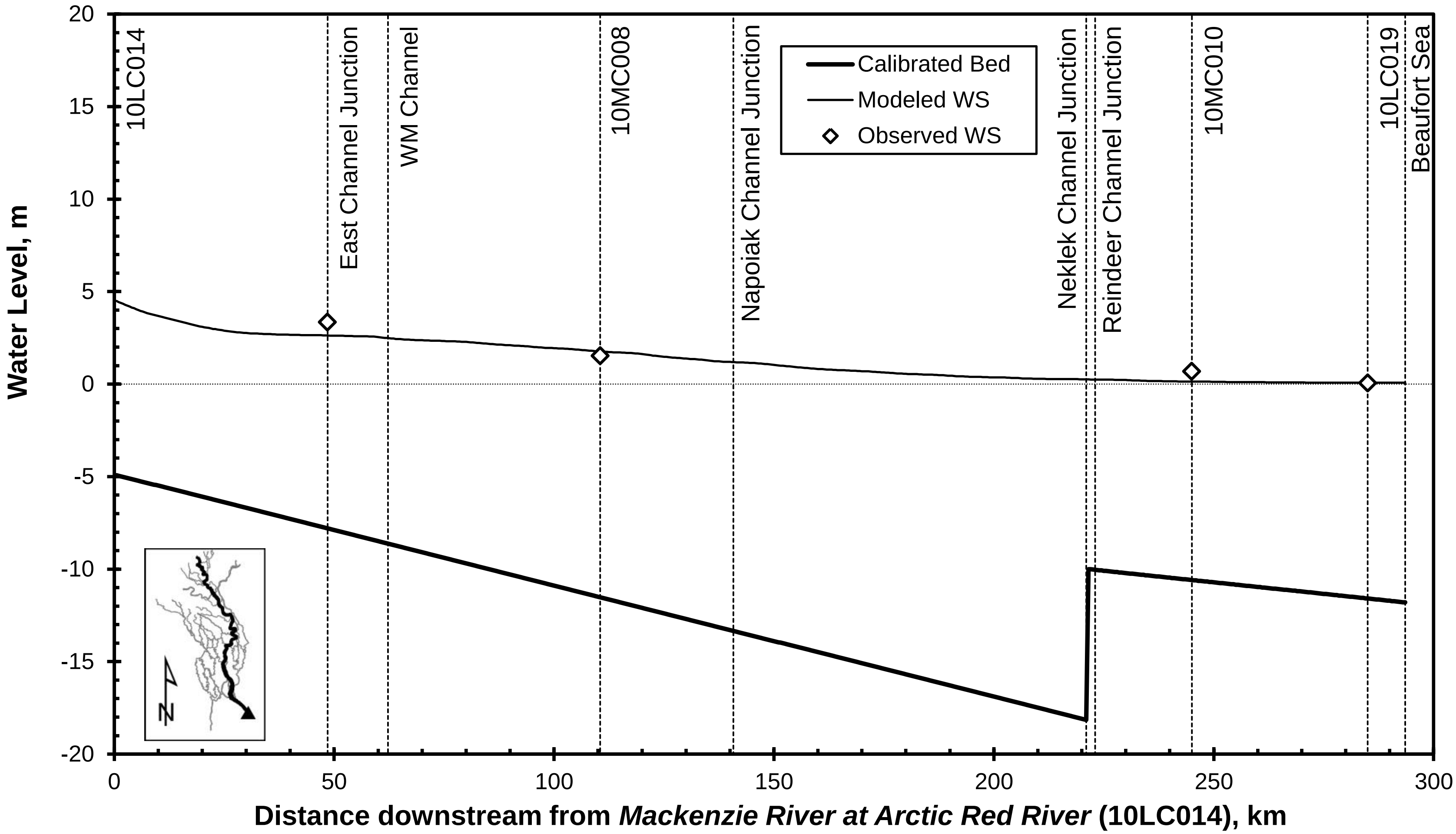

Figure E.8 Modeled water surface for Validation Scenario #2 from 4-Sep-09 to 17-Sep-09 along the Middle Channel using calibrated bed slope and elevation.

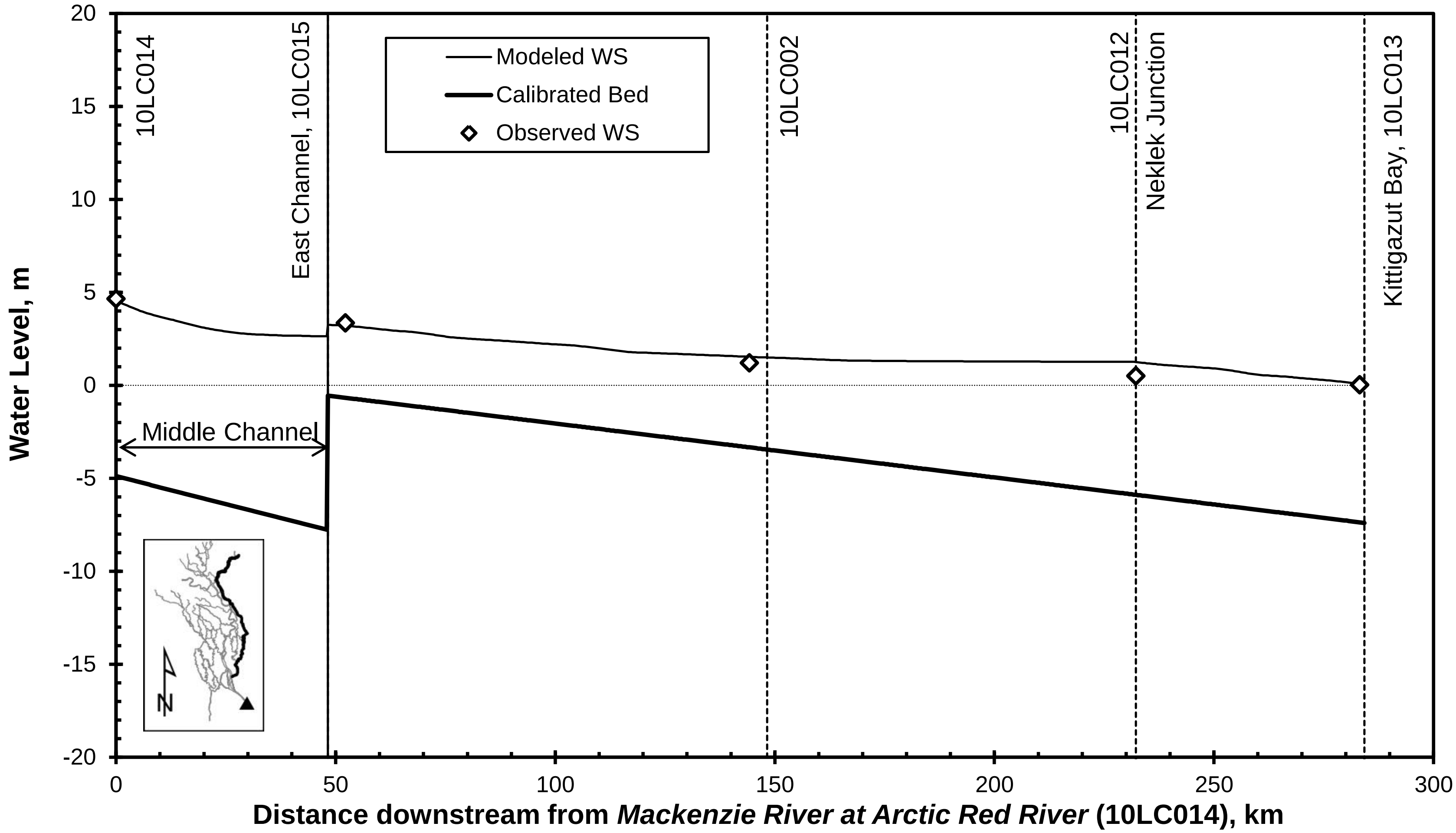

Figure E.9 Modeled water surface for Validation Scenario #2 from 4-Sep-09 to 17-Sep-09 along the East Channel using calibrated bed slope and elevation.

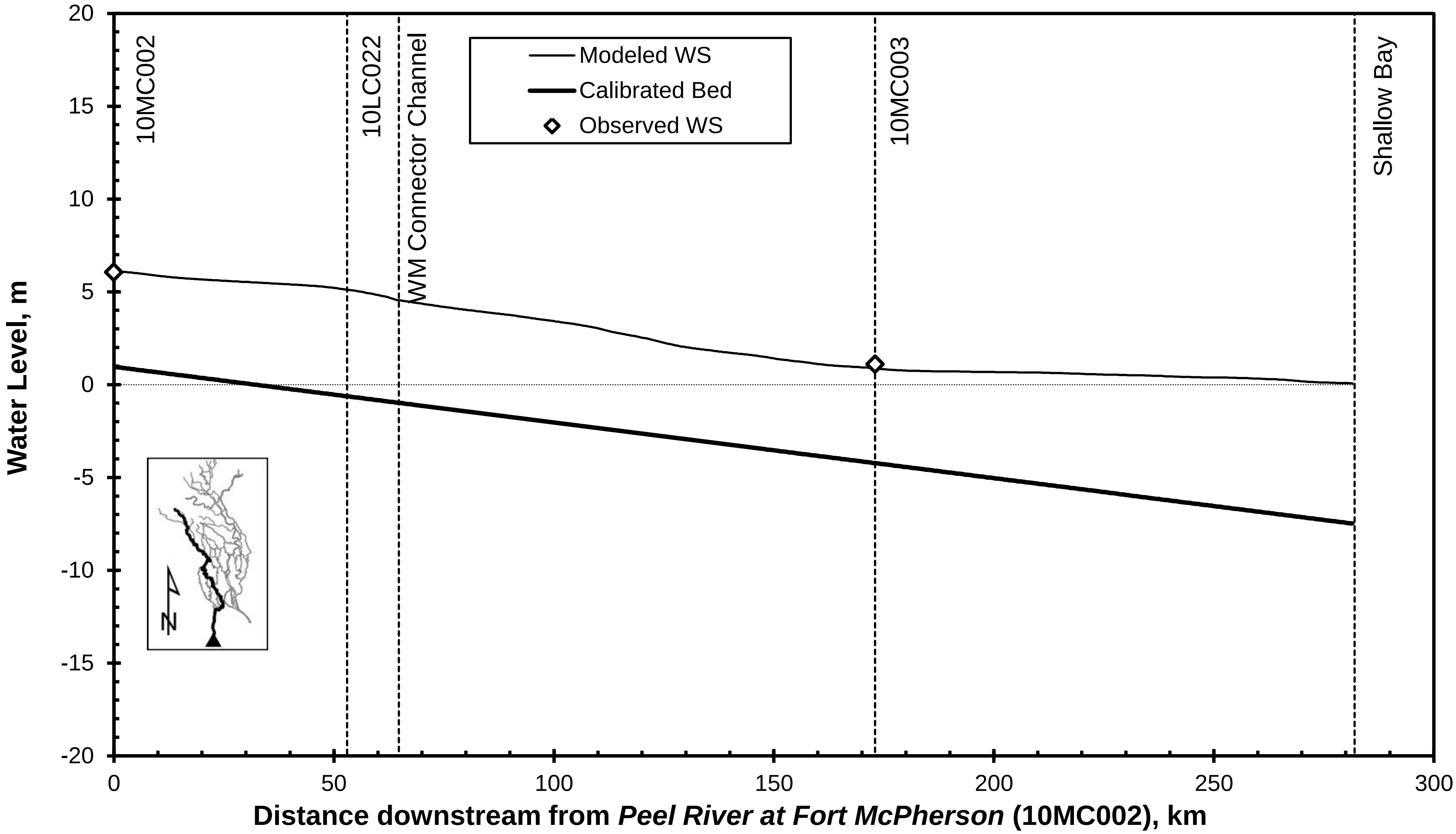

Figure E.10 Modeled water surface for Validation Scenario #2 from 4-Sep-09 to 17-Sep-09 along the West Channel using calibrated bed slope and elevation.

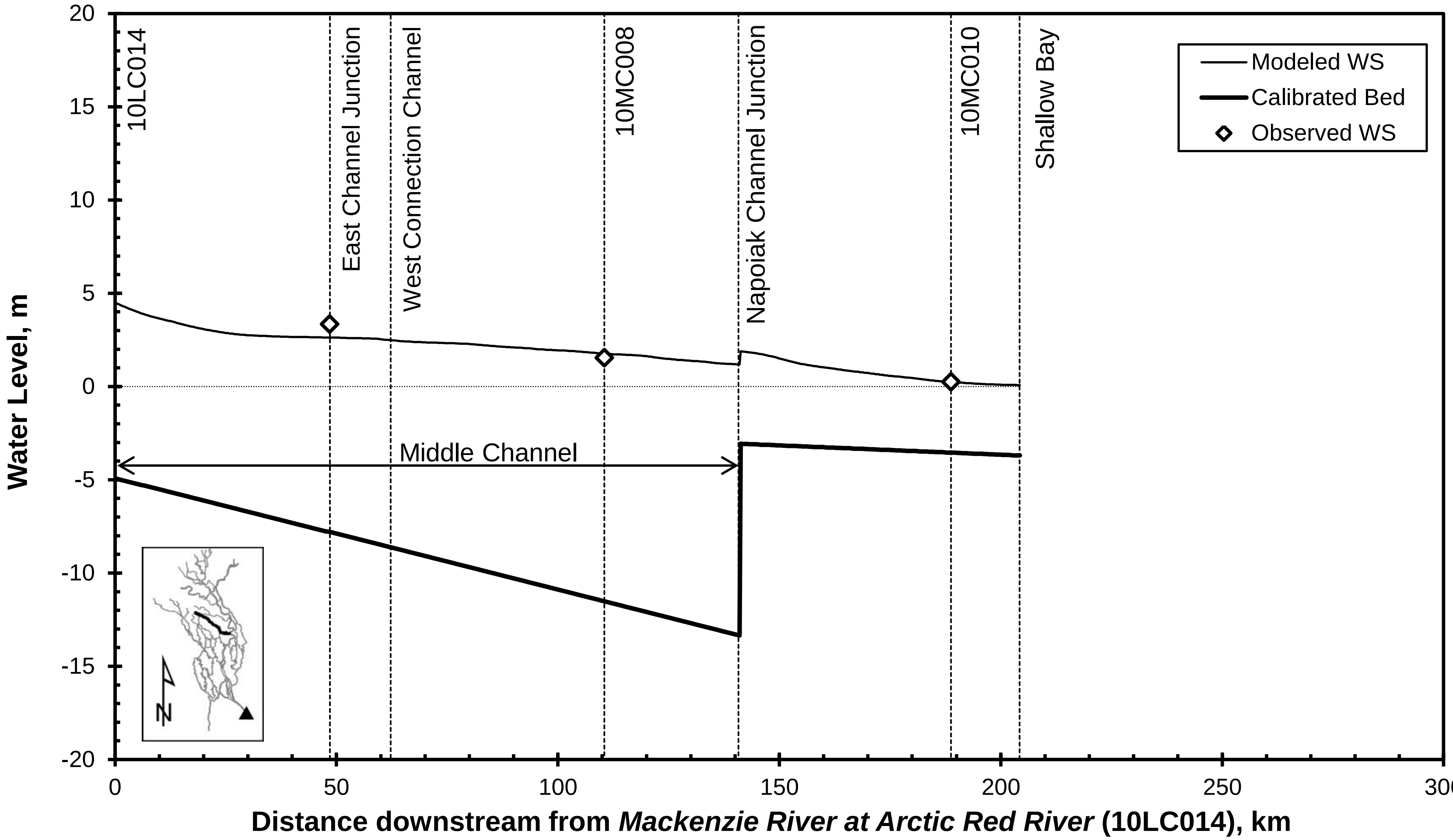

Figure E.12 Modeled water surface for Validation Scenario #2 from 4-Sep-09 to 17-Sep-09 along the Napoiak Channel using calibrated bed slope and elevation.

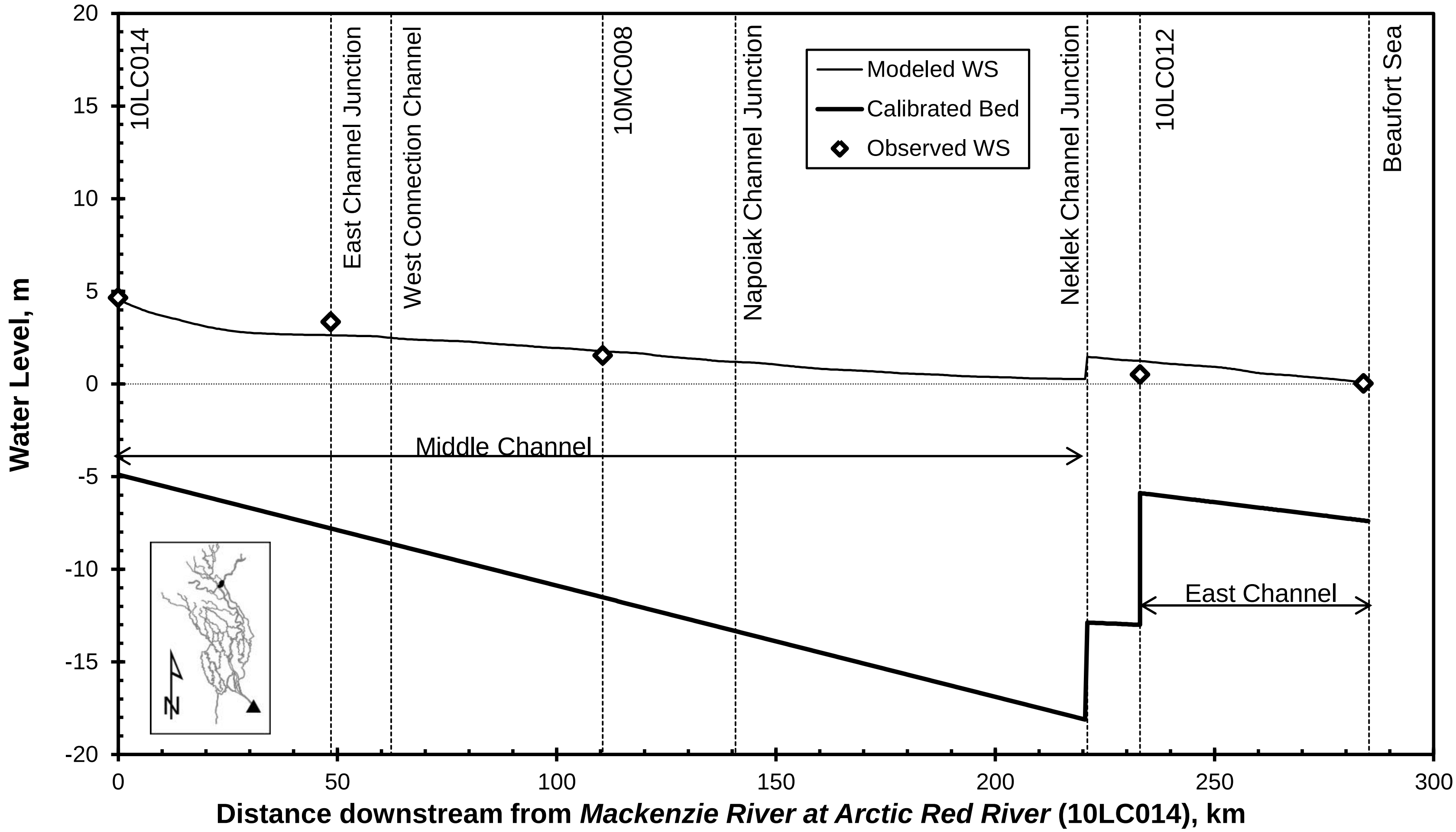

Figure E.13 Modeled water surface for Validation Scenario #2 from 4-Sep-09 to 17-Sep-09 along the Neklek Channel using calibrated bed slope and elevation.

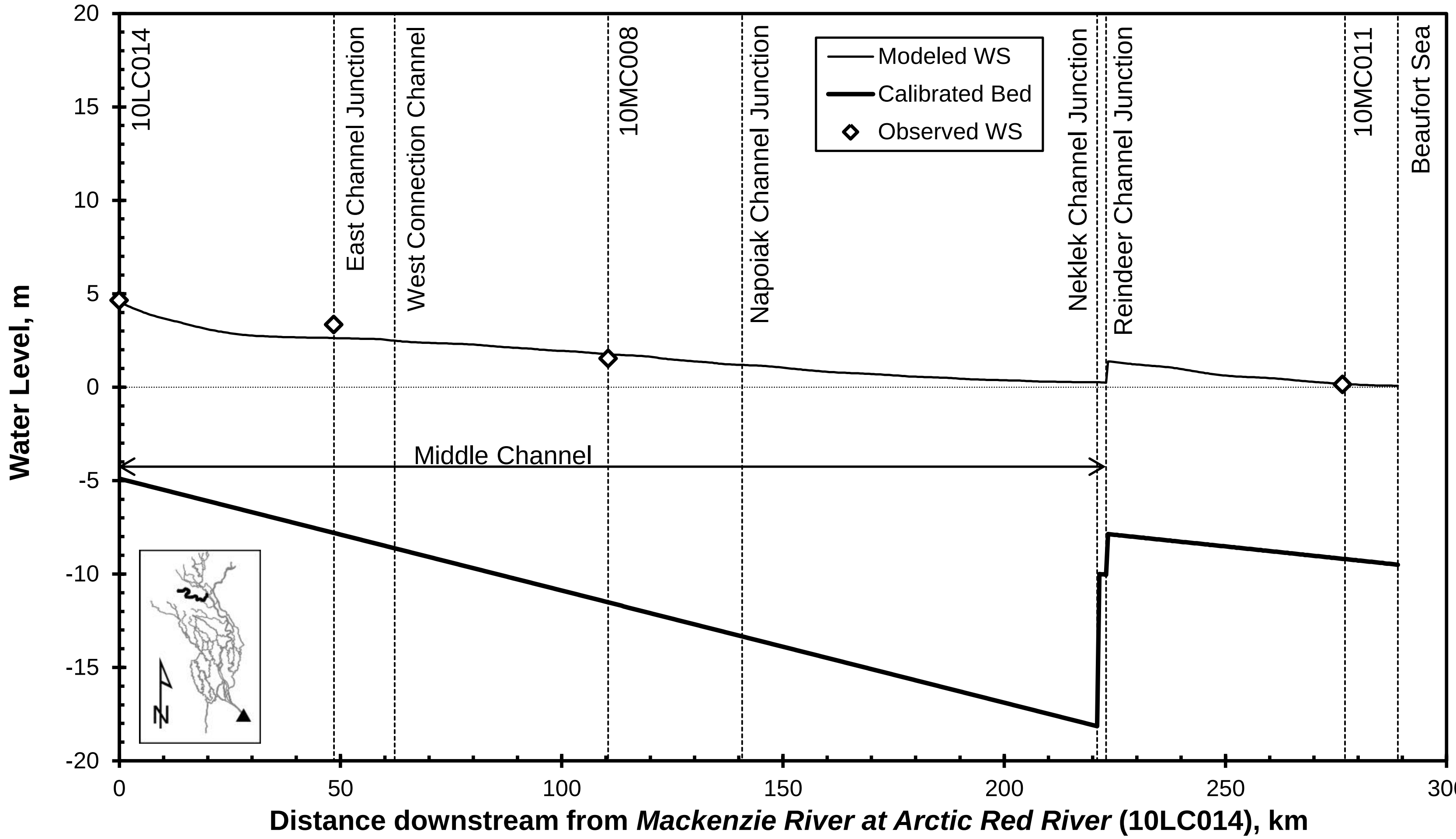

Figure E.14 Modeled water surface for Validation Scenario #2 from 4-Sep-09 to 17-Sep-09 along the Reindeer Channel using calibrated bed slope and elevation.